

**Electrochemical Strategies for the Generation
and Utilization of Alkoxy Radicals
and
Alkene Functionalization**

Deepak Mishra

**This thesis is submitted for the degree of
Doctor of Philosophy (PhD)
at Cardiff University**



October 2021

SUMMARY

This thesis describes the exploration and development of electrochemical methods for the generation and utilization of alkoxy radicals and alkene functionalization.

Chapter 1 introduces the basic concepts of synthetic organic electrochemistry and also discusses some advanced analytical techniques employed in electrochemistry.

Chapter 2 describes the manganese – catalyzed electrochemical deconstructive chlorination of cycloalkanols. After the initial proof-of-concept for the direct generation of alkoxy radicals by using tertiary alcohols (1-phenylcyclopropan-1-ol and 1-phenylcyclobutan-1-ol), mediated electrolysis is demonstrated using catalytic quantities of manganese^(II) salts as a pre-catalyst to access active manganese^(III) species, electrochemically. In total, 40 examples of various β and γ chlorinated ketones are reported. This transformation provides an advantage over other methods by excluding the necessity for chemical oxidant for the turning over of the catalyst.

Chapter 3 addresses the limitation encountered in the preceding chapter. By leveraging the concept of Proton Coupled Electron Transfer (PCET), generation of alkoxy radical is achieved. Various triarylamine (Ar_3N) are used as redox mediators for the homogeneous electron transfer to deconstructively synthesize distally brominated ketones starting from cycloalkanols. Furthermore, a single-pass continuous flow electrochemical scale-up is demonstrated at 10 mmol scale which showcases the efficient and robust scalability of the electrochemical process.

And finally, chapter 4 discusses the electrochemical functionalization of alkenes. In the first part of the chapter, an interesting electrochemical trifluoromethylation of acrylamide is explored using Langlois's reagent as a trifluoromethyl source. The second part of the chapter builds on a serendipitous discovery for the oxidative *Z*-selective (sp^2)-H chlorination of acrylamides. The *Z*-selectivity is confirmed by x-ray crystallography and a radical clock experiment was employed to probe the mechanism of the transformation.

Acknowledgements

To start with, I would like to thank my supervisor, Louis Morrill for giving me an opportunity to work in his laboratories at Cardiff university. Louis, you have been a great source of motivation and inspiration to me. I sincerely thank you for your patience, guidance, and continued support for the last three years. I still remember your proposition “would you be interested in doing synthetic organic electrochemistry”? I had little or no knowledge about it back then but still said yes! That actually was one of the better decisions of my life. I would also like to thank Duncan Browne for all his support and guidance. The GMs are not the same without you Duncan. Within the Cardiff chemistry department, I would like to thank Robert Jenkins and Simon Waller for their help with regards to NMR and mass spectrometry experiments and maintenance.

I would like to thank many group members for their support.

Benjamin Allen – You are one of the excellent chemists I have come across. At times I used to think, is there anything this guy doesn't know? Thank you for introducing me to the electrochemistry and to Brooklynn 99. The latter kept me in the good mood to pursue the former. I have learnt a great deal from you. I wish you all the very best for your future endeavours.

Shyam Basak – Shyam you are the very definition of calm and composed. Your phenomenal knowledge, level-headedness, your wise approach to life were immediately missed when you left. I still remember those days of total madness from 7 to 11 and repeat. Thank you for always being there for me from chemistry to crazy parties. I know you will be absolutely amazing in your new role at Oxford.

Alex Seastram – Well Alex, three years felt like three months mate. I couldn't have asked for a better labmate to start this amazing journey with. Your ability to draw reaction mechanisms without missing a single step is still very impressive, even after three years. Your organizational skills are literally unattainable at least by me. I have realized this that, you can actually draw structures on chemdraw using keyboard faster than I could by using mice. Thank you very much for all the help and support, I can't make enough curries for you to thank you for teaching me CVs to proofreading my chapters. I wish you

very best for your future. I am sure you will absolutely smash anything you'll decide to do.

Kurt Polidano and Ben RB – Thank you Kurt for sharing your impeccable powerpoints and movies (meaning Star Wars). I hope I will see you soon sitting across the poker table. Ben RB – Your remarkable ability to draw mechanisms and talk at the same time still reminds me of those days. Thank you for helping me during difficult times with your wisdom and positive approach. I wish you both very best of luck.

Tom McBride – You are a flow wizard and an amazing person. Thank you for your help with the flow electrochemistry.

William Nicholson – You are great guy and very helpful to everyone. Thanks for your help with the vacuum distillation which I almost never wanted to do. Hopefully, I will see you around in your next trip to Himalayas. Keep climbing.

Roderick Stark – Your knowledge of chemistry is on completely another level. I was always impressed by your formal talks and problem-solving skills. I wish you very best.

Andrew Jones – You are a one stop solution to all the palladium and nickel related questions. Honestly, your level of expertise and knowledge in organometallics and ligand systems are completely on different level. Thank you very much for your help. Wish you all the very best. Go XEC!

Matthew William – “Matt the Machine” you have the ability to smash out any sort of project in weeks. Your punctuality and dedication are there for everyone to see and admire and emulate. Thanks for being a good listener and helping me to vent out. I have enjoyed all the interesting conversations. Keep'em smashing!

Daniel Latham and Albara Elgehani – Thank you both for organizing various group activities and bringing everyone together during the difficult times. Wish you both great successes ahead.

Mubarak Dambatta – Mub you are a charismatic personality. There have been many occasions where you selflessly offered your help and I sincerely thank you for that. I wish you all the best in your write-up period. Hopefully I will invite you soon for a lunch.

James Harnedy – You are an amazing chemist! Perfect mixture of knowledge, hunger and drive to achieve more. Your consistency and strive for perfection are something I am really very impressed with, and I have learnt a lot from you during a small span of time. Your efforts and contribution to the chlorination project was outstanding. I can already see an electrochemical star in the making. Thank you for all your help and support in various projects and proofreading and deleting my excessive commas 😊. It has been a pleasure working with you! And yes, TB is flying saucer!

I would also like to thank **Betty, Salma, Abdulbari, Luke, and Hussain** for all the great discussions and help at various stages of my PhD. I wish you all best of luck in your chemical journeys.

Renan Galaverna – I wish I had a chance to know you better. Whatever conversation I had with you were quite interesting. You almost made me to go to the gym with you. I wish you very best!

Last but not the least, special thanks to **CHEMY-PGR, services, safety, and stores** for all your hard work and efforts in making sure the department is safe for working during the COVID-19 hit duration. Without your efforts working in the labs would have been impossible.

Outside the lab, I would like to thank **Roberto Golovic**, we became friends over arguments! I have learnt many things from you and also picked up the habit of complaining as often as I can for any and all issues I may have. I hope Montenegro is treating you well.

List of Abbreviations

1,4-CHD	1,4-cyclohexadiene
Ac	Acetyl
AC	Alternating current
acac	Acetyl acetate
ACE	Alternating current electrolysis
AcOH	Acetic acid
ADP	Adenosine diphosphate
Ar	Aryl
BA	Brønsted acid
BDD	Boron doped diamond
BDFE	Bond Dissociation Free Energy
BZT	Benzothiazole
CCE	Constant current electrolysis
CE	Counter electrode
CPE	Constant potential electrolysis
CV	Cyclic voltammetry
d.r.	Diastereomeric ratio
DC	Direct Current
DCE	Dichloroethane
DCM	Dichloromethane
dibm	Diisobutylmethane
DMAP	4-(Dimethylamino) pyridine
DMF	Dimethyl formamide
DMPO	5,5-dimethyl-1-pyrroline- <i>N</i> -oxide
DMSO	Dimethyl sulfoxide
$E_{1/2}$	Half wave potential
$E_{p/2}$	Half peak potential
E_{pa}	Anodic peak potential
E_{pc}	Cathodic peak potential
ESR	Electron Spin Resonance
FGM	Functional group migration

GC	Glassy Carbon
HAT	Hydrogen Atom Transfer
HFIP	111,333-hexafluoroisopropanol
HRMS	High resolution mass spectrometry
I _{pa}	Anodic peak current
I _{pc}	Cathodic peak current
LA	Lewis acid
LMCT	Ligand to Metal Charge Transfer
LTA	Lead tetraoxide
MeCN	Acetonitrile
MeOH	Methanol
Mes-Acr	Mesityl acridinium
<i>n</i> -Bu	Butyl
NMR	Nuclear Magnetic Resonance
PCET	Proton Coupled Electron Transfer
Ph	Phenyl
PMP	<i>para</i> -Methoxyphenyl
Pt	Platinum
PT	Proton transfer
<i>p</i> -TsOH	<i>para</i> -toluene sulfonic acid
RE	Reference electrode
RM	Redox mediator
RVC	Reticulated vitreous carbon
SCE	Saturated calomel electrode
SET	Single Electron Transfer
SOMO	Singly Occupied Molecular Orbital
TBAB	Tetrabutylammonium bromide
TBAOAc	Tetrabutylammonium acetate
TBDPS	<i>tert</i> -Butyl diphenylsilyl
TBS	<i>tert</i> -Butyl dimethylsilane
<i>t</i> -Bu	<i>tert</i> -Butyl
TFA	Trifluoroacetic acid
TFE	Trifluoroethanol

THF	Tetrahydrofuran
TM	Transition metal
TMP	22,66 tetramethyl pyrrolidine
UV	Ultraviolet
WE	Working electrode

List of Publications

1. Manganese-Catalyzed Electrochemical Deconstructive Chlorination of Cycloalkanols via Alkoxy Radicals
Benjamin D. W. Allen,[†] Mishra Deepak Hareram,[†] Alex C. Seastram, Tom McBride, Thomas Wirth, Duncan L. Browne*, Louis C. Morrill*, *Org. Lett.*, **2019**, 21, 9241–9246 (First co-author)
2. Electrochemical Oxidative Z-selective C(sp²)-H Chlorination of Acrylamides
James Harnedy,[†] Mishra Deepak Hareram,[†] Graham J. Tizzard,^b Simon J. Colesb and Louis C. Morrill*, *Chem. Commun.*, **2021**, 57, 12643-12646 (First co-author)
3. Electrochemical Deconstructive Bromination of Cycloalkanols via Alkoxy Radicals enabled by Proton Coupled Electron Transfer (PCET)
Mishra Deepak Hareram, Albara Elgehani, Andrew C. Jones, James Harnedy, Alex Seastram, Matthew Burns and Louis C. Morrill (*in preparation*)

This PhD is dedicated to my parents, my brother, my sister-in-law, and my niece (Alisha this is for you)....

These three years would not have been possible without your unconditional support.

It is by logic we prove

but

It is intuition by which we discover

Table of Contents

Chapter 1: Introduction

1.1.	Introduction.....	2
1.2.	Electrochemical Set Up for Organic Synthesis.....	3
1.2.1.	Power Supply	4
1.2.2.	Solvents.....	4
1.2.3.	Electrolyte.....	5
1.2.4.	Electrode Material	5
1.2.5.	Divided vs Undivided Cell	6
1.2.6.	Constant Potential vs Constant Current Electrolysis	7
1.3.	Direct and Mediated Electrolysis	8
1.4.	Cyclic Voltammetry	12
1.5.	Electrosynthesis in Action	14
1.6.	Aims and Objectives	18
1.7.	References	19

Chapter 2: Manganese-Catalyzed Electrochemical Deconstructive Chlorination of Cycloalkanols *via* Alkoxy Radicals

2.	Preface	24
2.1.	Introduction	25
2.1.1.	Methods of Generation of Alkoxy Radicals	26
2.1.1.1.	Traditional Methods for the Generation of Alkoxy Radicals	27
2.1.1.2.	Transition metals for the Generation of Alkoxy Radicals.....	29
2.1.1.3.	Photoredox Methods for the Generation of Alkoxy Radicals	33
2.1.1.4.	Electrochemical Methods for the Generation of Alkoxy Radicals.....	36

2.2.	Aims and Objectives	39
2.3.	Results and Discussion.....	40
2.3.1.	Electrochemical β -scission of 1-phenylcyclopropan-1-ol.....	40
2.3.1.1.	Direct electrolysis	40
2.3.1.2.	Mediated Electrolysis.....	44
2.3.2.	Electrochemical β -scission of 1-phenylcyclobutan-1-ol	46
2.3.3.	Manganese Catalyzed Electrochemical Deconstructive Chlorination of Cycloalkanols	48
2.3.4.	Optimization of Substrates with Electron Releasing Substituents	51
2.3.5.	Substrate scope.....	52
2.3.6.	Flow Electrochemistry – Scale up	58
2.3.7.	Mechanistic Studies.....	59
2.3.8.	Limitations	60
2.3.9.	Plausible Mechanism	61
2.4.	Future Work.....	63
2.5.	Summary	64
2.6.	References	64

Chapter 3: Application of Proton-Coupled Electron Transfer (PCET) in the Generation and Utilization of Alkoxy Radicals

3.	Preface	71
3.1.	Introduction	72
3.1.1.	Definition and Thermochemistry of PCET	73
3.1.2.	Exploitation of PCET in the Generation of Alkoxy Radicals.....	75
3.2.	Aims and Objectives	83
3.3.	Results and Discussions.....	85

3.3.1. Electrochemical Deconstructive Bromination of Cycloalkanols via Alkoxy Radicals Enabled by PCET	85
3.3.1.1. Direct Electrolysis	85
3.3.1.2. Mediated Electrolysis	87
3.3.1.3. Optimized Conditions	95
3.3.1.4. Substrate Scope	97
3.3.1.5. Flow Electrochemical Scale Up	103
3.3.1.6. Mechanistic Studies	105
3.3.2. Electrochemical Remote Functionalization of C(sp ³)-H Bond via Alkoxy Radical Induced 1,5 - Hydrogen Atom Transfer (HAT) and Functional Group Migration enabled by Proton Coupled Electron Transfer (PCET)	108
3.3.2.1. Introduction.....	108
3.3.2.2. Results and Discussions	110
3.3.2.3. Plausible Mechanism.....	111
3.4. Future Work.....	113
3.4.1. Electrochemical Deconstructive Functionalization via PCET.....	113
3.4.2. Electrochemical Remote Functionalization of C(sp ³)-H Bond via Alkoxy Radical Induced 1,5 - Hydrogen Atom Transfer (HAT)	113
3.5. Summary	114
3.6. References	115

Chapter 4: Electrochemical Functionalization of Alkenes

4. Preface.	119
4.1. Introduction	120
4.1.1. Transition metal catalyzed alkene functionalization	120
4.1.1.1. Iron catalyzed alkene functionalization	121
4.1.1.2. Copper catalyzed alkene functionalization	123
4.1.1.3. Transition metal catalyzed Hydrogen Atom Transfer (HAT)	125
4.1.2. Photochemical Methods of Alkene Functionalization.....	128

4.1.2.1. Dual Photoredox Strategy	128
4.1.2.2. Photochemical “Docking-Migration” Strategy	130
4.1.3. Electrochemical Methods of Alkene Functionalization	133
4.2. Aims and Objectives	138
4.3. Results and discussion	138
4.3.1. Electrochemical trifluoromethylation of alkenes.....	138
4.3.2. Electrochemical oxidative Z-selective C(sp ²)-H chlorination of acrylamides	147
4.3.2.1. Introduction	147
4.3.2.2. Substrate Scope	151
4.3.2.3. Mechanistic Studies	154
4.3.2.4. Future Work	158
4.4. Summary.....	159
4.5. References.....	159

Chapter 5: Experimental – Manganese-Catalyzed Electrochemical Deconstructive Chlorination of Cycloalkanols *via* Alkoxy Radicals

5. Experimental and Characterization Data	168
5.1. General Procedures – Substrate Synthesis	168
5.1.1. General Procedure A – Synthesis of Cyclopropanols via Kulinkovich Reaction	168
5.1.2. General Procedure B – Generation and Addition of Grignard Reagents to Cycloalkanones.....	168
5.1.3. General Procedure C – Addition of Commercially-Available Grignard Reagents to Cycloalkanones.....	169
5.1.4. General Procedure D – Generation and Addition of Organolithium Reagents to Cycloalkanones.....	170
5.1.5. General Procedure E – Synthesis of Substituted Cyclobutanones	170
5.1.6. General Procedure F – Synthesis of Benzo-fused Cyclobutanols via Benzyne	171
5.2. Characterization of Substrates.....	172
5.3. General Procedures – Electrochemical Deconstructive-Chlorination of Cycloalkanols.	194

5.3.1.	General Procedure G – Standard Procedure	194
5.3.2.	General Procedure H – Syringe Pump Addition of Substrate	195
5.4.	Characterization of Products.....	196
5.5.	References	210

Chapter 6: Experimental – Electrochemical Deconstructive Bromination of Cycloalkanols *via* Alkoxy Radicals Enabled by Proton Coupled Electron Transfer (PCET)

6.	Experimental and Characterization Data	216
6.1.	General Procedures – Substrate Synthesis (PCET-Bromination).....	216
6.1.1.	General Procedure A – Generation and Addition of Organolithium Reagents to Cycloalkanones.....	216
6.2.	Characterization of Substrates.....	216
6.3.	Synthesis of Redox Mediators	227
6.4.	Cyclic Voltammetry	229
6.4.1.	Cyclic Voltammogram of Substrates	230
6.4.2.	Cyclic Voltammetry of Redox Mediators	234
6.4.	General Procedure for Electrochemical Deconstructive Bromination of Cycloalkanols	236
6.4.1.	Characterization of Products.....	237
6.5.	Experimental for Flow Electrochemical Scale Up	245
6.5.1.	Recirculating Flow	246
6.5.2.	Single Pass Flow	247
6.6.	Substrate Synthesis (PCET-HAT-FG Migration)	248
6.7.	Electrochemical Reaction (PCET-HAT-FG Migration)	250
6.8.	References	251

Chapter 7: Experimental – Electrochemical Alkene Functionalization

7.	Experimental and Characterization Data	257
7.1	Substrate Synthesis (Electrochemical Alkene Trifluoromethylation)	257
7.2	Electrochemical Reaction (Electrochemical Alkene Trifluoromethylation)	259
7.3	X-ray: Oxytrifluoromethylated Product 8 (Electrochemical Alkene Trifluoromethylation) 260	
7.4	Substrate Synthesis (Electrochemical oxidative Z-selective C(sp ²)-H chlorination of acrylamide	272
7.5.	Electrochemical Reactions (Electrochemical oxidative Z-selective C(sp ²)-H chlorination of acrylamide	280
7.6.	X-ray: Z-Chlorinated Product 9 (Electrochemical oxidative Z-selective C(sp ²)-H chlorination of acrylamide	285
7.7.	References	295

Chapter 1: Introduction

1.1. Introduction

Movement of electrons from an occupied molecular orbital to an unoccupied molecular orbital of a molecule or compound is the hallmark of any chemical reaction. Electrochemistry offers a precise control over such electron movements to bring about the desired transformation.

The use of electricity in organic chemistry to generate highly reactive intermediates (radicals and ionic radicals) has seen tremendous growth in the last two decades.¹ As such, the field of organic electrochemistry now has a strong literature foundation with a plethora of examples demonstrating the electrochemical generation of highly reactive species. Many examples exist including, but not limited to, the generation of selenides,^{2,3} nitrenes⁴ and isocyanides⁵. There have also been important developments in C-H functionalizations,^{6,7} mild conditions for oxidations,⁸ fluorinations,⁹ decarboxylations,¹⁰ functionalization of arenes,^{11,12} coupling reactions,¹³ heterocycle formations¹⁴ and natural product syntheses^{15,16} employing electrochemistry.

Synthetic organic electrochemistry provides a greener and safer alternative for organic transformations. It can be used to replace toxic or dangerous oxidizing or reducing agents, reduce energy consumption, and also can be used for the *in-situ* generation and utilization of unstable and hazardous reagents.¹⁷ In addition, scaleup technologies have also been developed with which the synthesis of desired compounds can be scaled up with ease.¹⁸

Historically, electro-organic synthesis can be traced back over 200 years when Alexander Volta reported the first ever electric battery by stacking different conducting substances in a form of pile, in the year 1799.¹⁹ Approximately 30 years later, Michael Faraday made ground-breaking discoveries in understanding the nature and effects of electricity by establishing the various laws of electrolysis (Faraday's Laws of Electrolysis).²⁰

The first ever electro-organic synthesis was performed by Faraday in 1834 by electrolyzing acetic acid in aqueous medium to form ethane by anodic decarboxylation. The method was then perfected by Hermann Kolbe who studied the decarboxylation of

fatty acids and half-esters of dicarboxylic acids and established the practical basis of electro-organic synthesis.²¹

The development of the potentiostat in 1942 allowed reactions to be carried out under constant potential, which was a significant improvement allowing for the carrying out of reactions under precise control.²² A major development in the science of electrochemistry came with the invention of polarography and cyclic voltammetry.^{23,24} These electroanalytical technologies remain to this day an indispensable set of techniques in an electrochemist's arsenal.

However, possibly the greatest drawback of electro-organic synthesis limiting its industrial application remains the lack of standardized equipment, which can result in issues with the reproducibility of electrochemical reactions. IKA's Electrasyn is one of the very few standardized commercially available instruments designed to tackle reproducibility issues in the field and is being tested and accepted by the electrochemists across industry and academia.

1.2. Electrochemical Set Up for Organic Synthesis

In a typical electrochemical setup, a power source (i.e., battery, potentiostat) is required to deliver power to an electrochemical cell. The substrate is dissolved in a solvent of choice, which interacts with the electrode material suspended in an electrochemical cell. An electrolyte is often used to improve the conductivity of the organic solvents. Depending upon the type of transformation being carried out, a choice can be made between an undivided or divided cell.²⁵ And finally, to run an electrochemical reaction a user has two choices: constant current electrolysis (CCE) also called galvanostatic or constant potential electrolysis (CPE) also called potentiostatic.

The following sub-sections will discuss the above constituents briefly

1.2.1. Power Supply

Historically, DC is used in electro-organic synthesis which is delivered by a potentiostat. When using DC, the polarities of the electrodes are fixed. However, during a paired electrolysis, the electrogenerated species at one electrode must travel to the other electrode for the desired reaction to occur. Due to the slow mass transfer of intermediates, short lived species may decompose before reaching the other electrode. This challenge can be solved by employing an alternating current electrolysis (ACE), where the frequency of the applied current can be tuned as per the requirement (figure 1.1).²⁶⁻²⁹

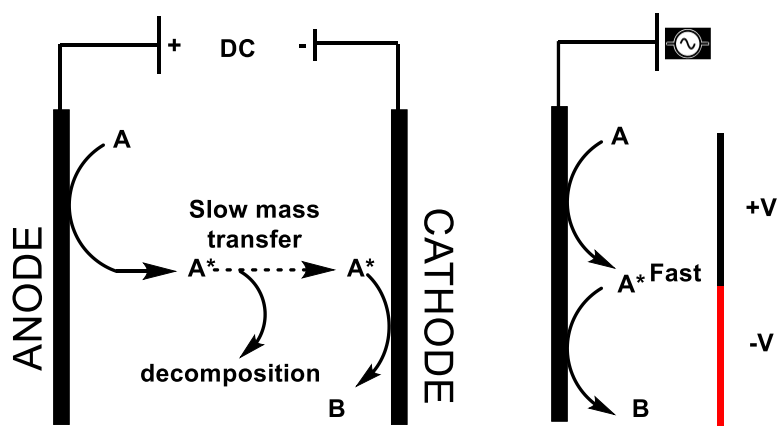


Figure 1.1 – Schematic presentation of direct current and alternating current electrolysis

1.2.2. Solvents

The solvent must dissolve the reagents and electrolyte and should be sufficiently stable under electrochemical conditions. Some important factors to consider while selecting solvents are as follows, the exploitable potential range of the solvents, proton activity, dielectric constant, accessible temperature, toxicity etc. Trifluoroacetic acid (TFA), acetic acid, water, methanol, 1,1,1,3,3,3-hexafluoroisopropanol (HFIP) are the most common polar protic solvents. Acetonitrile (MeCN), dimethylformamide (DMF), dimethyl sulfoxide (DMSO) are some of the popular choices for polar aprotic solvents.^{25,30}

1.2.3. Electrolyte

Electrolyte improves conductivity of an organic solvent by providing a source of positive and negative ions which carry charge through the solution and reduce the resistance.

Inorganic electrolytes such as LiClO_4 , NaClO_4 , NaCl etc., can be used in water, methanol, MeCN or DMF. Whereas organic electrolyte composed of ammonium cations (R_4N^+) along with suitable counter ions (ClO_4^- , BF_4^- , PF_6^- , OTs^-) are usually preferred for various other organic solvents.^{25,31}

1.2.4. Electrode Material

As the electron transfer takes place between the electrode and solution-electrolyte phase, deciding upon an appropriate electrode material could be one of the instrumental choices influencing the outcome of an electrochemical reaction.

For carrying out electrolysis, usually there are three different types of electrodes. Firstly, there is the working electrode (WE) where the reaction of interest happens. Depending upon the type of reaction, if an oxidative reaction is desired then the WE will be the anode and the cathode is the WE for a reductive process. The counter electrode (also known as auxiliary electrode) (CE) is used to close the circuit in the electrochemical cell. It is worth pointing out here that in organic synthesis, when paired electrolysis is carried out, both the electrodes function as WE. The reference electrode (RE) is an electrode which has a stable and well-known electrode potential, and it is used as a point of reference in the electrochemical cell for the potential control and measurement. A RE is usually employed for electroanalytical experiments and constant potential experiments, where the precise measurement of potential is essential. At preparative scale, a RE can be excluded.

An ideal electrode material should be inexpensive, non-toxic, stable to a wide range of temperatures, pressures, and solvents. The material should be easily transformed into desired shapes such as rods, discs, wires, foams and meshes.

From an organic synthesis point of view, where in almost all cases organic solvents (which result in high resistance) are used, electrodes with high surface area are advantageous. For example, use of Reticulated Vitreous Carbon (RVC) or carbon felt can be used as higher currents can be applied.^{32,33}

One of the factors to be considered while choosing an electrode material is the overpotentials. The overpotential is the difference between the theoretical cell voltage and the actual cell voltage that's necessary to induce electrolysis. Generally, materials with large oxygen overpotential are used for the anode and materials with a large hydrogen overpotential are used for the cathode.³⁴

In an oxidative electrolysis, platinum, carbon-based materials such as graphite, glassy carbon, RVC, Boron Doped Diamond (BDD) etc., are preferred. Whereas in reductive electrolysis where the cathode is the working electrode (WE), a sacrificial electrode can be used (Mg, Al, Zn, Fe, Ni, Sn, Pb, Cu etc.) as anode.

1.2.5. Divided vs Undivided Cell

Depending upon the type of species generated in the electrolysis and their stability, choice of a suitable electrolytic cell could be a deciding factor in the outcome of the reaction under study. Commonly two different types of cells are used in electro-organic synthesis.^{25,35} (a) divided cell and (b) undivided cell.

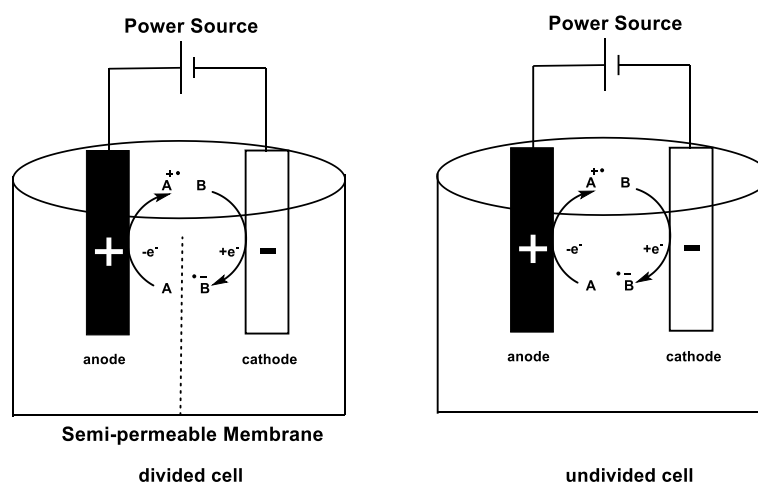


Figure 1.2 – Schematic presentation of divided and undivided electrolytic cell

In a divided cell, cathodic and anodic chambers are separated by a semipermeable membrane. A divided cell is used when the electrogenerated species must be protected from the activity of the counter electrode. This setup is usually complex, and the voltages are higher due to the increased distance between the electrodes.

On the other hand, in an undivided cell both the electrodes are in the same chamber.

An undivided cell offers a much simpler setup. By balancing the reaction at the counter electrode, a desired reaction can be carried out using an undivided cell.³⁵

1.2.6. Constant Potential vs Constant Current Electrolysis

A constant voltage is applied between the anode and the cathode in a constant potential electrolysis. This mode is usually preferred when a precise voltage is required. Often a prior knowledge of redox potentials of substrates is required which can be obtained by employing cyclic voltammetry (CV). Constant voltage reactions are less prone to form side products. The magnitude of the current flow depends on the overall resistance of an electrochemical cell – a high resistance in the cell will lead to low current and a slow reaction or the reactions may not go to full conversion (figure 1.3). The graphs here depict the variations in current and potential in constant potential and constant current electrolysis respectively and are based on experimental observations.

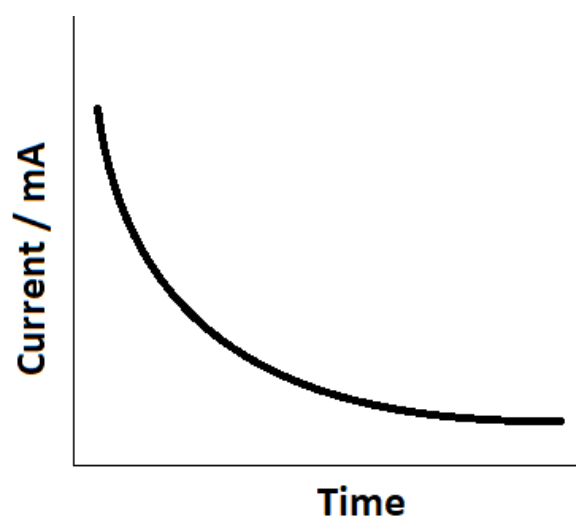


Figure 1.3 – Current vs time graph in constant potential electrolysis

On the other hand, in constant current electrolysis a constant magnitude of current is maintained over the period of reaction (figure 1.4). There is no control over the voltage and as the redox active species deplete over the course of a reaction the observed potential increases. Therefore, the potential range of constant current reaction must be carefully monitored and controlled to avoid undesired redox processes which could lead to formation of undesired products or decomposition of starting materials.³⁶

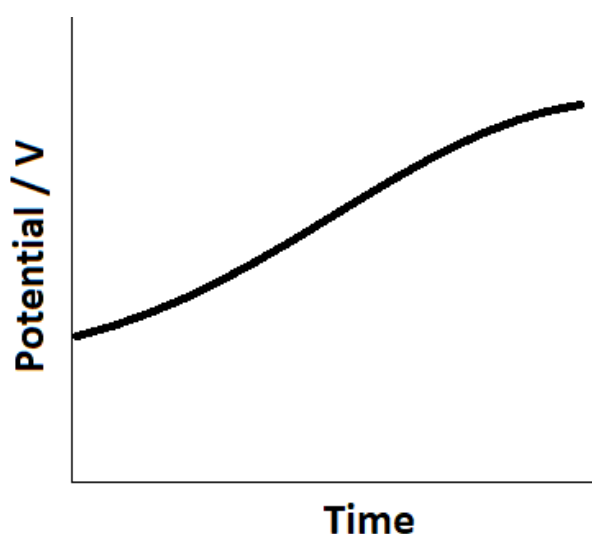


Figure 1.4 – Potential vs time graph in constant current electrolysis

1.3. Direct and Mediated Electrolysis

The electron transfer to and from an electrode is a heterogeneous process and at times can be inefficient in a given system. When electron transfer happens directly from the surface of the electrode to the substrate the event is referred to as direct electrolysis. Direct electrochemical reactions may suffer from inherent disadvantages due to the heterogeneous nature of electron transfer. Direct electrolysis can result in the passivation of the electrodes rendering electron transfer inefficient, which may negatively influence the levels of selectivity and conversion.

The above challenges associated with the direct electrolysis can be circumvented by employing redox mediators to carry out the desired electron transfer. This methodology is referred to as indirect electrolysis.^{35,37} By using catalytic quantities of a redox active substance (mediator),³⁸ the heterogeneous electron transfer process can be shifted to a homogeneous process. In such cases, the mediator interacts with the electrodes to furnish an electrogenerated species which moves back into the bulk solution and can interact homogeneously with the substrate (figure 1.5).

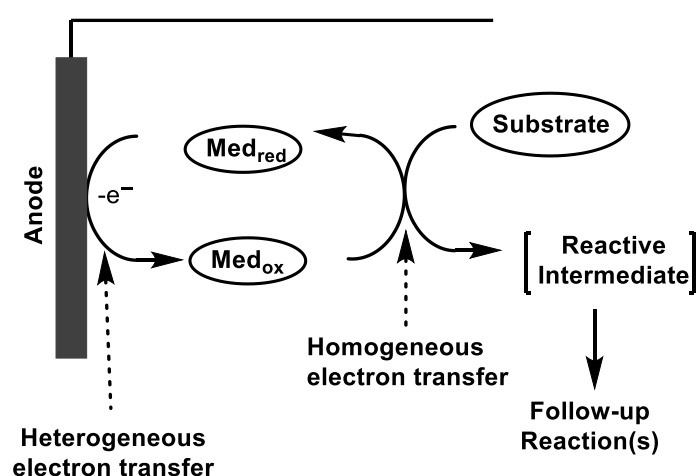


Figure 1.5 – Schematic representation of mediated electrolysis

An ideal redox mediator must have a redox potential lower than that of the substrate in the case of oxidative electrolysis and higher in the case of reductive electrolysis. A redox mediator must be stable in both oxidation states for a considerable time and most importantly a fast and reversible electron transfer between the electrode and mediator as well as between the mediator and substrate is also highly desirable.

Based on the nature of interaction between the redox mediator and the substrate, electron transfer can be distinguished into two types. When the electron transfer happens without any bond formation between the mediator and the substrate, it is called an outer-sphere electron transfer or non-bonded electron transfer. Whereas, if there is an initial bond formation between the activated mediator and the substrate followed by a bond cleavage, this is known as an inner-sphere electron transfer (figure 1.6).

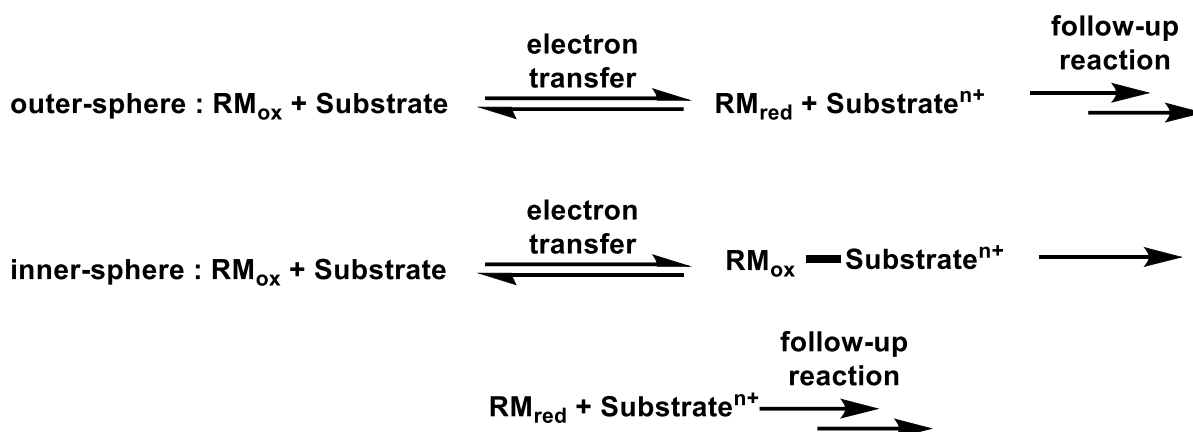
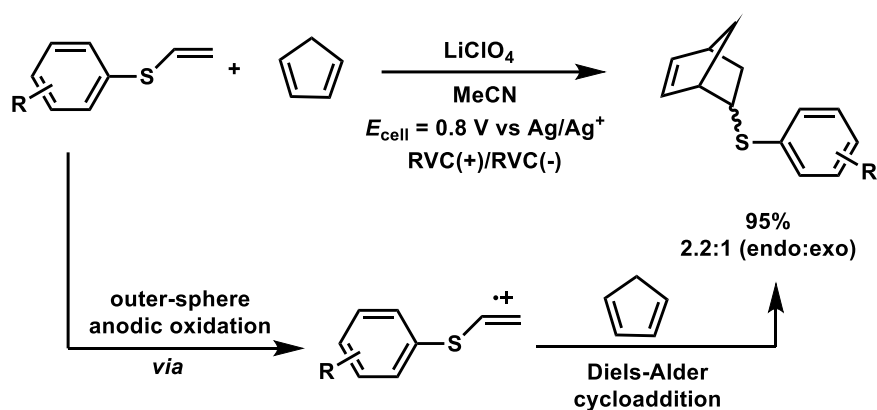


Figure - 1.6 – Schematic representation of the different types of electron transfer

Bauld and co-workers reported a Diels-Alder cycloaddition between the aryl vinyl sulfides and cyclopentadiene by electrochemical oxidation and triarylammonium salts.^{38a} This is one of the direct examples of the outer-sphere and inner-sphere electron transfer mechanism.

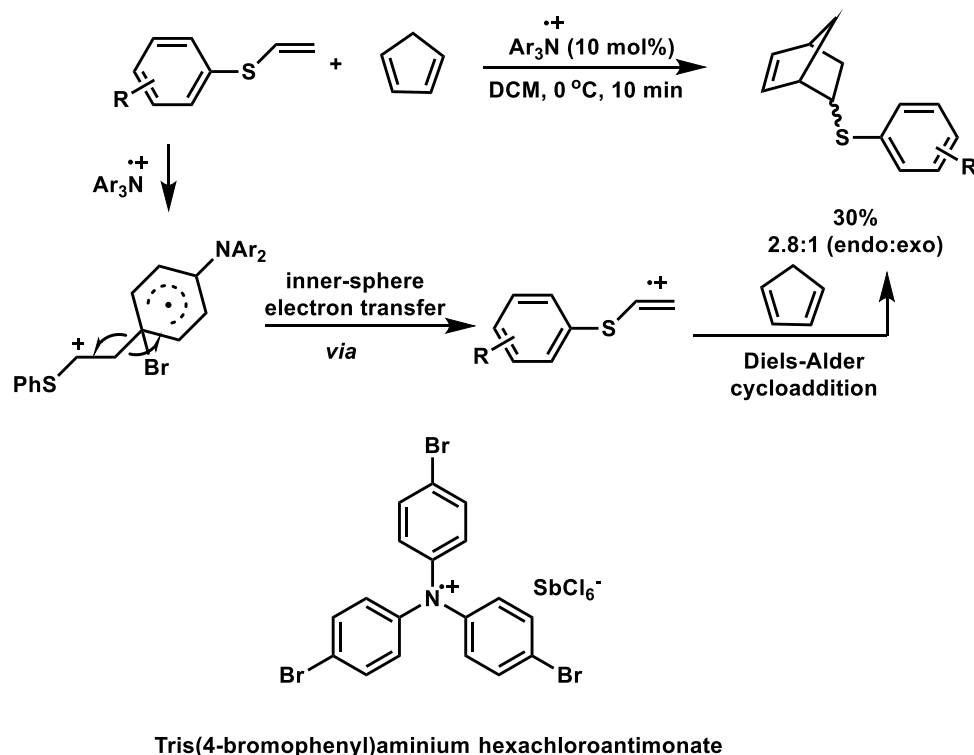
Bauld and co-workers observed the formation of a cycloaddition product when the aryl vinyl sulfide was electrolysed in the presence of cyclopentadiene (scheme 1.1).



Scheme 1.1 – outer-sphere electron transfer

This outer-sphere electron transfer happens between the aryl vinyl sulfide and the anode without the formation of any direct bond.

On the other hand Bauld and co-authors observed that when the same reaction was performed with the triarylamminium salt (tris(4-bromophenyl)aminium hexachloroantimonate) as an oxidant, the same cycloaddition product was formed (scheme 1.2).



Scheme 1.2 – inner-sphere electron transfer

This inner-sphere electron transfer starts with the formation of a bond between the aryl vinyl sulfide and the triarylamminium salt which upon subsequent homolysis generates the radical cation intermediate of the aryl vinyl sulfide and regenerates the triarylamminium salt.

The role of a redox mediator in electrochemistry is comparable to that of a photocatalyst in photoredox catalysis. Both the redox mediator and a photocatalyst are used as electron transfer agents. A redox mediator is activated by applying a suitable potential to the electrochemical cell whereas a photocatalyst is excited by irradiating with light (visible or ultraviolet) of suitable frequency (figure 1.7).

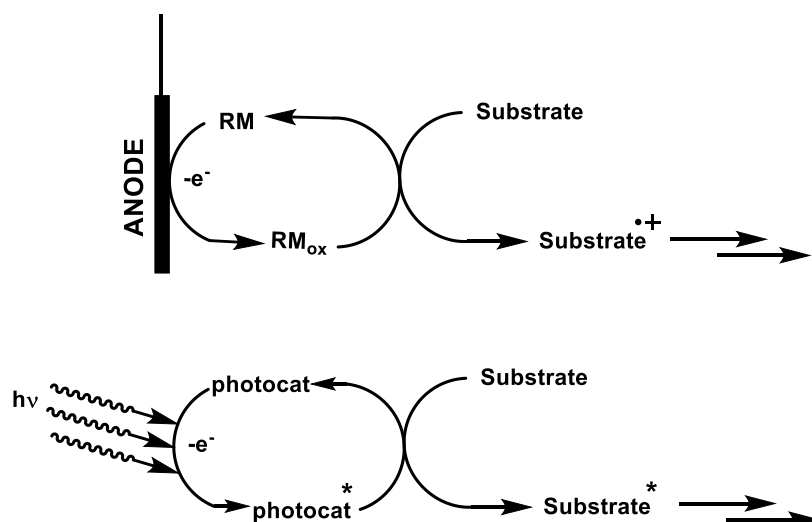


Figure 1.7 – Electron transfer in electrochemistry and photochemistry

A wide variety of redox mediators are available from the organic (triarylamines, TEMPO, DDQ, triarylimidazoles) to metal salts such as $\text{Cr}(\text{IV/III})$, $\text{Fe}(\text{III/II})$, $\text{Co}(\text{III/II})$, $\text{Mn}(\text{III/II})$ etc.^{39–42}

Chapter 3 of this thesis discusses the application of triaryamine redox mediators as an aid in electrosynthesis.

1.4. Cyclic Voltammetry

Cyclic voltammetry is an electroanalytical technique for measuring the current response of a redox active substance in an appropriate solution to a linearly cycled potential sweep between two or more values. This is a useful method to understand the mechanism and kinetics of electron-transfer reactions.^{43,44}

Cyclic voltammetry uses a three-electrode system comprised of a working electrode (WE), a reference electrode (RE) and a counter electrode (CE). WE material is usually glassy carbon disc; and that of the CE is platinum wire. The RE should have a well-defined electrode potential, such as Ag metal and AgNO_3 solution (the AgNO_3 reference electrode is employed for CVs measured and shown in this thesis). The RE draws negligible current and hence its composition is unchanged during the measurement. The RE is used as a means of replication of results, however they are not rigorously accurate. To overcome this, an internal standard is used whose redox potentials are well defined.

Figure 1.8 depicts a typical voltammogram of an electrochemically reversible one-electron redox process. A sweep from left to right is called the oxidative scan and the reverse sweep is called the reductive scan. The current response reaches peak maximum at point **c** (anodic peak current (i_{pa}) for oxidation at the anodic peak potential (E_{pa})). As the redox active species depletes with increase in the diffuse double layer, the current response decreases linearly **d**. In the reductive scan a negative potential is applied which reduces the oxidized species accumulated at the electrode surface.

For a reversible process the magnitude of anodic peak current (i_{pa}) and cathodic peak current (i_{pc}) at the anodic and cathodic peak potentials (E_{pa} and E_{pc}) should be equal.

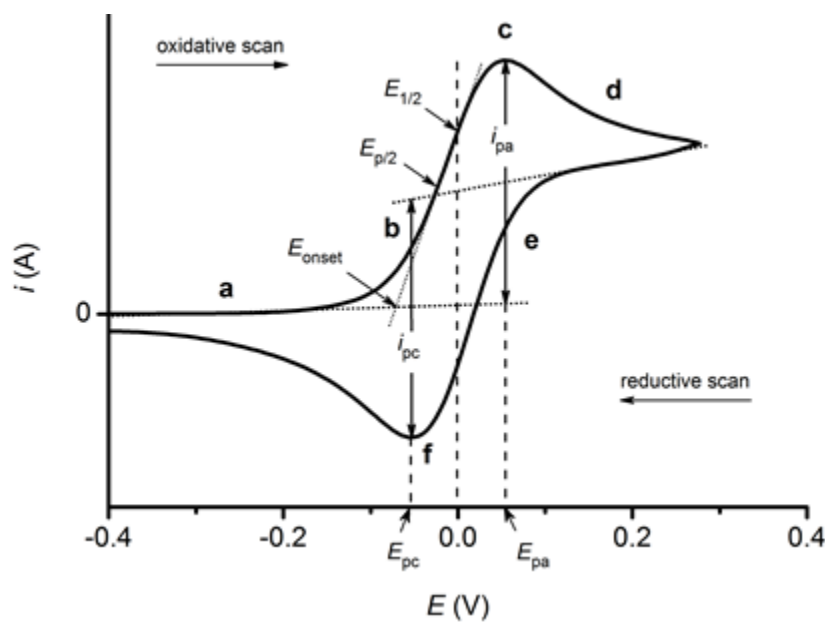


Figure 1.8 – Cyclic voltammogram of an electrochemically-reversible one-electron redox process (figure produced with permission from ossila.com)

In a cyclic voltammogram containing a feature that has a forward and reverse wave, half wave potential ($E_{1/2}$) is defined as the potential exactly in the middle of the two peaks **c** and **f**. Whereas, half peak potential ($E_{p/2}$) is the potential where the current is exactly half

of the peak current (i_{pa}). $E_{1/2}$ usually is used for a reversible or a quasi-reversible processes and $E_{p/2}$ is for irreversible processes.

CV studies were employed in this thesis to study the formation of an $Mn^{(III)} - Cl$ species which was necessary to identify the redox active species (**chapter 2**). In **chapter 3**, with the help of CV plots, suitable redox mediators were selected as electron transfer agents to induce a Proton Coupled Electron Transfer (PCET) process. And finally in **chapter 4**, CV plots helped in the proposal of a plausible mechanism for the oxidative chlorination of acrylamides based on the observed potentials.

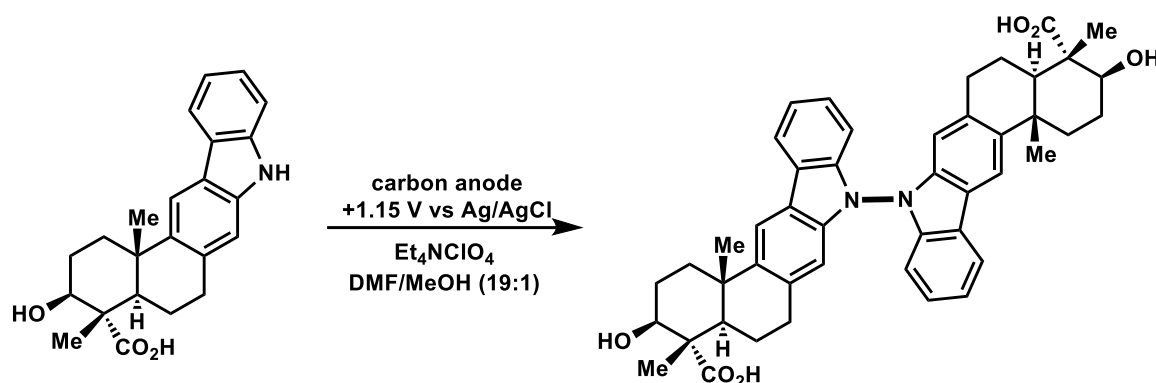
Hence, cyclic voltammetry is an indispensable electroanalytical technique for synthetic chemists.

1.5. Electrosynthesis in Action

An eminent late pioneering electrochemist Manuel Baizer foresaw the arrival of the electro-organic synthesis in 1986 when he wrote:⁴⁵ “In the last 50 years and particularly in the last twenty-six, organic electrochemical synthesis has ceased to be a laboratory curiosity, a methodology to be tried when all else fails, a procedure that involves mysterious black boxes and dials and wires. This science and technology are now well developed although not mature.”

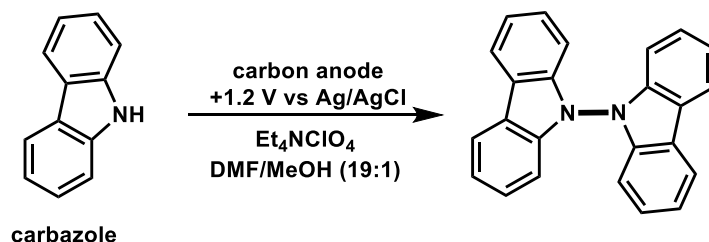
He would have been surely impressed by the progress that have been made into the science of electro-organic synthesis. The field is now somewhat mature since Baizer first penned his article.

Baran and co-workers reported a unique method of electrochemical dimerization of carbazoles and carbolines. The advantage of electrochemistry to precisely dial-in a required potential for the selective oxidative dimerization reaction was exploited (scheme 1.1).⁴⁶

*Scheme 1.3 – Electrochemical dimerization of carbazoles*

After exhausting the known classical chemical transformations, such as KMnO₄ oxidation,⁴⁷ deprotonation with LDA etc,⁴⁸ the authors envisaged an electrochemical oxidation method to induce the required dimerization based on the seminal work by Ambrose and co-workers.⁴⁹ Ambrose and co-workers while investigating the radical reaction pathways of carbazoles under electro-oxidative conditions found that, when the electrolysis of carbazoles was conducted in the presence of 2,4,6-trimethylpyridine, *N-N* coupled product was obtained.

Building on the seminal report by Ambrose and co-workers, in their optimization studies on a readily available carbazole, Baran and co-workers trialled various electrochemical conditions. They discovered that potentials over 1.6 V resulted in the decomposition of the carbazole. However, when the potential of 1.2 V was dialled, formation of the *N-N* dimerized product was observed (scheme 1.2).

*Scheme 1.4 – Optimization of N-N dimerization*

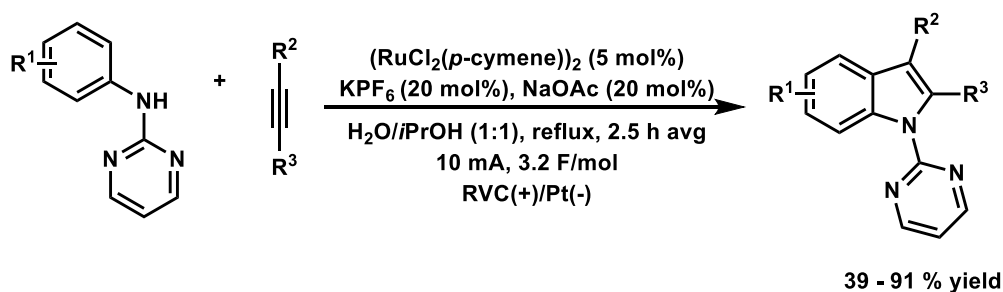
After finding the optimized conditions, they subjected the Xiamycin A (which was prepared in 4 steps) to the electrochemical system to synthesize an atropisomeric indoloterpenoid dixiamycin A (scheme 1.1).

This is a straightforward example that clearly demonstrates electrochemistry's ability to selectivity dial in a required potential needed for the desired transformation.

Transition metal catalyzed C – H functionalization reactions offer a direct route to convert inactive C – H bonds of organic molecules into various other functional groups in a single step. However, many metal catalyzed C – H functionalizations require a stoichiometric amount of chemical oxidant, such as peroxide, hypervalent iodine, hypochlorite etc. for the catalytic turnover.^{50,51} Employing a chemical oxidant could also influence the reductive elimination from the metal centre.⁵²

Electrochemistry can be used advantageously not only to replace chemical oxidants by using traceless electric current but also to selectively oxidize the metal centres by controlling the working potentials.

Xu and co-workers have reported a ruthenium-catalyzed dehydrogenative alkyne annulation in an electrochemical setup (scheme 1.3).⁵³

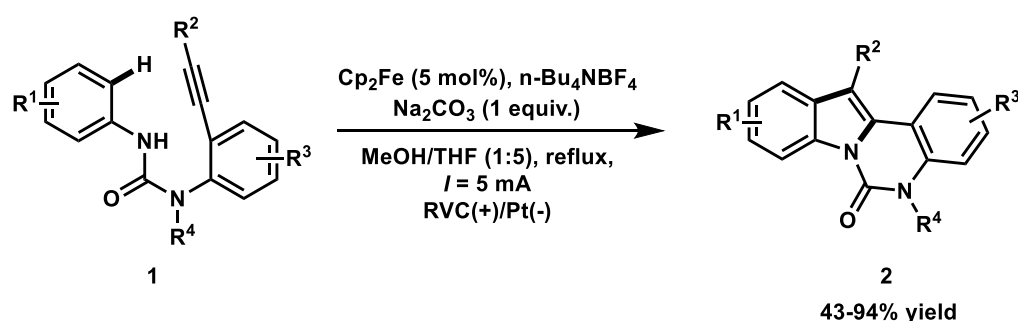


Scheme 1.5 – Electrochemical dehydrogenative alkyne annulation

The authors demonstrated the generation of an active Ru(II) complex electrochemically in a simple undivided electrochemical cell and an aqueous solution. This showcases the ability of an electrochemical transformation to yield complex products under mild conditions.

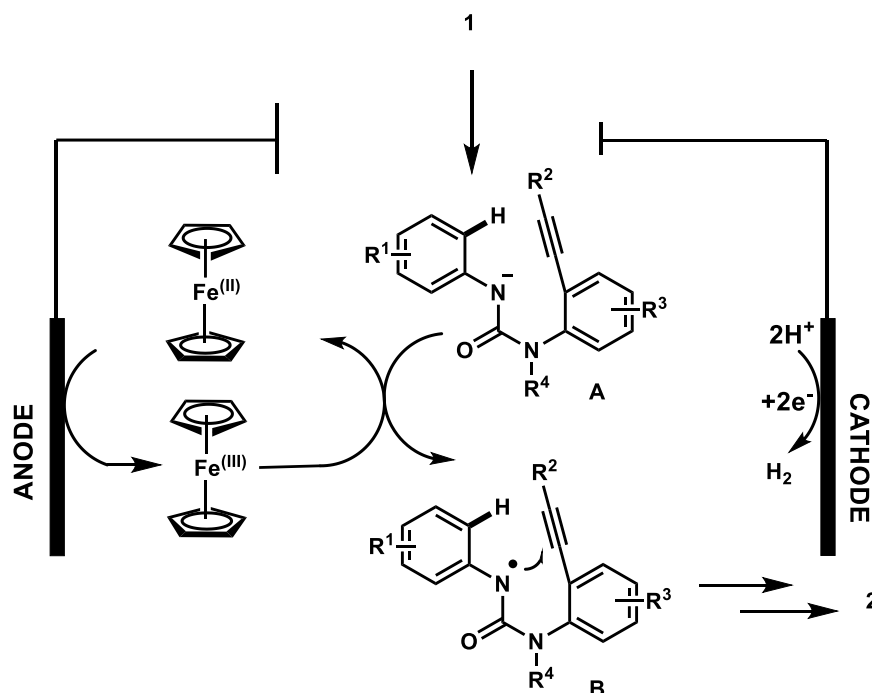
N-centred radicals exhibit diverse reactivity and provide ample opportunities in forging C – N bonds that are challenging to access through alternative methods. Traditionally *N*-centred radicals are generated by the cleavage of relatively weak N – heteroatom bonds by photochemical or thermal decomposition.^{54–56}

Xu and co-workers have utilized an indirect electrolysis approach in the generation and utilization of *N*-aryl-amidyl radicals. They reported an intramolecular addition *N*-aryl-amidyl radicals to a tethered alkyne to obtain indoles and azaindoles chemo- and regioselectivity (scheme 1.4).⁵⁷



Scheme 1.6 – Electrochemical generation of *N*-aryl-amidyl radicals

The authors proposed a plausible mechanism which starts with oxidation of the redox mediator ferrocene (Fc) to Fc^+ and simultaneous reduction of methanol to liberate hydrogen gas and form methoxide (^-OMe). The *in situ* generated base would deprotonate **1** to furnish the anion **A** and a subsequent single-electron transfer (SET) between **A** and Fc^+ would form an electron deficient *N*-centered radical **B** and regenerate the redox mediator. The *N*-centered radical **B** would undergo a cascade of radical additions to form the product **2**.



Scheme 1.7 – Plausible mechanism

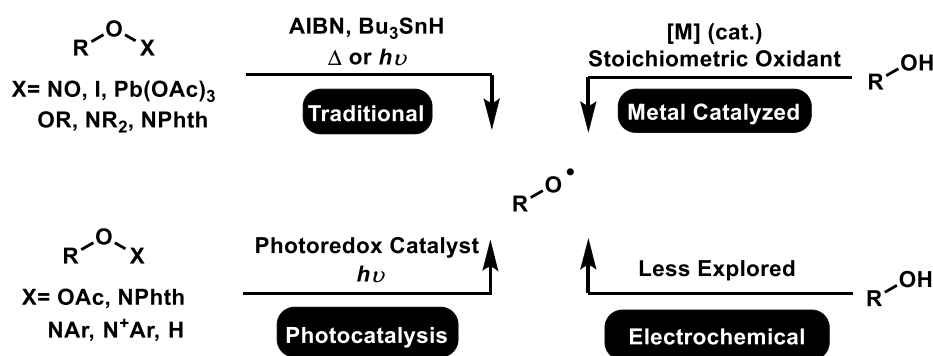
1.6. Aims and Objectives

Electrochemistry can provide a greener, more environmentally friendly alternative to existing classical transformations. In addition, new reactivity modes could also be explored by using electrochemistry and finally, electrochemistry offers reliable cost-effective scaleup of the synthesis of small and desirable organic molecules.

Alkoxy radicals have been historically known for their diverse reactivity and have been used in wide variety of synthetic transformations.^{58,59} Traditionally alkoxy radicals are generated from the chemical, thermal or photolytic homolysis of prefunctionalized *O*-heteroatom bonds. These methods are not very atom economical and requires rather harsh conditions.

The aims of this PhD were as follows: to research and develop new electrochemical methods for the generation and utilization of alkoxy radicals from simple unfunctionalized tertiary alcohols. The known methods in the literature are either dependent on the prefunctionalization of the alcohols and then thermolysis or photolysis

of the weak *O*-heteroatom bond or using stoichiometric amounts of oxidants in combination with catalytic quantities of transition metals.



Scheme 1.8 – Aims and objectives

The objectives were to employ the electrochemically generated alkoxy radical to invoke the different reactivity modes of alkoxy radicals such as, β -scissions, 1,5-HAT, and addition to π systems.

1.7. References

- 1 M. Schmittel and A. Burghart, *ChemInform*, 2010, **29**, 2550–2589.
- 2 K. Uneyama, H. Asai, Y. Dan-Oh and H. Matta, *Electrochim. Acta*, 1997, **42**, 2005–2007.
- 3 S. Torii, K. Uneyama and M. Ono, *Tetrahedron Lett.*, 1980, **21**, 2741–2744.
- 4 Tung Siu, and Christine J. Picard and A. K. Yudin, *J. Org. Chem.*, 2005, **70**, 932–937.
- 5 A. Guirado, A. Zapata, J. L. Gómez, L. Trabalón and J. Gálvez, *Tetrahedron*, 1999, **55**, 9631–9640.
- 6 L.-J. Li, Y.-Y. Jiang, C. M. Lam, C.-C. Zeng, L.-M. Hu and R. D. Little, *J. Org. Chem.*, 2015, **80**, 11021–11030.
- 7 F. Kakiuchi, T. Kochi, H. Mutsutani, N. Kobayashi, S. Urano, M. Sato, S. Nishiyama and T. Tanabe, *J. Am. Chem. Soc.*, 2009, **131**, 11310–11311.
- 8 J. Yoshida, R. Hayashi and A. Shimizu, *Green Oxid. Org. Synth.*, 2019, 409–437.
- 9 T. Sunaga, M. Atobe, S. Inagi and T. Fuchigami, *Chem. Commun.*, 2009, 956–958.
- 10 F. Bu, L. Lu, X. Hu, S. Wang, H. Zhang and A. Lei, *Chem. Sci.*, 2020, **11**, 10000–

- 10004.
- 11 T. Morofuji, A. Shimizu and J. Yoshida, *J. Am. Chem. Soc.*, 2013, **135**, 5000–5003.
 - 12 L. D. Pachón, C. J. Elsevier and G. Rothenberg, *Adv. Synth. Catal.*, 2006, **348**, 1705–1710.
 - 13 Y. Yuan and A. Lei, *Acc. Chem. Res.*, 2019, **52**, 3309–3324.
 - 14 Y. Gao, Y. Wang, J. Zhou, H. Mei and J. Han, *Green Chem.*, 2018, **20**, 583–587.
 - 15 H. Takakura and S. Yamamura, *Tetrahedron Lett.*, 1999, **40**, 299–302.
 - 16 C. Zhu, N. W. J. Ang, T. H. Meyer, Y. Qiu and L. Ackermann, *ACS Cent. Sci.*, 2021, **7**, 415–431.
 - 17 B. A. Frontana-Urbe, R. D. Little, J. G. Ibanez, A. Palma and R. Vasquez-Medrano, *Green Chem.*, 2010, **12**, 2099–2119.
 - 18 M. Yan, Y. Kawamata and P. S. Baran, *Chem. Rev.*, 2017, **117**, 13230–13319.
 - 19 V. Alessandro, *Philos. Trans. R. Soc. London*, 1800, **90**, 403–431.
 - 20 F. Michael, *Philos. Trans. R. Soc. London*, 1834, **124**, 77–122.
 - 21 F. Joschka Holzhäuser, J. B. Mensah and Regina Palkovits, *Green Chem.*, 2020, **22**, 286–301.
 - 22 A. Hickling, *Trans. Faraday Soc.*, 1942, **38**, 27–33.
 - 23 *Nat.* 1959 1844695, 1959, **184**, 1271.
 - 24 J. E. B. Randles, *Trans. Faraday Soc.*, 1948, **44**, 327–338.
 - 25 C. Kingston, M. D. Palkowitz, Y. Takahira, J. C. Vantourout, B. K. Peters, Y. Kawamata and P. S. Baran, *Acc. Chem. Res.*, 2019, **53**, 72–83.
 - 26 H. Kunkely, A. Merz and A. Vogler, *J. Am. Chem. Soc.*, 2002, **105**, 7241–7243.
 - 27 B. Lee, H. Naito, M. Nagao and T. Hibino, *Angew. Chemie Int. Ed.*, 2012, **51**, 6961–6965.
 - 28 L. E. Sattler, C. J. Otten and G. Hilt, *Chem. – A Eur. J.*, 2020, **26**, 3129–3136.
 - 29 S. Rodrigo, C. Um, J. C. Mixdorf, D. Gunasekera, H. M. Nguyen and L. Luo, *Org. Lett.*, 2020, **22**, 2021.
 - 30 L. Schulz and S. R. Waldvogel, *Synlett*, 2019, **30**, 275–286.
 - 31 T. Shono, *Compr. Org. Synth.*, 1991, 789–813.
 - 32 J. M. Friedrich, C. Ponce-de-León, G. W. Reade and F. C. Walsh, *J. Electroanal. Chem.*, 2004, **561**, 203–217.
 - 33 T. X. Huong Le, M. Bechelany and M. Cretin, *Carbon N. Y.*, 2017, **122**, 564–591.
 - 34 D. M. Heard and A. J. J. Lennox, *Angew. Chemie Int. Ed.*, 2020, **59**, 18866–18884.
 - 35 G. Hilt, *ChemElectroChem*, 2020, **7**, 395–405.

- 36 M. Rafiee, M. N. Mayer, B. T. Punchihewa and M. R. Mumau, *J. Org. Chem.*, 2021, **86**, 15866–15874.
- 37 R. Francke and R. D. Little, *Chem. Soc. Rev.*, 2014, **43**, 2492–2521.
- 38 J. Simmonet and J. F. Pilard, *organic electrochemistry*, 2001.
- 38a N. L. Bauld, J. T. Aplin, W. Yueh, and A. Loinaz, *J. Am. Chem. Soc.*, 1997, **119**, 11381–11389
- 39 R. Francke and R. D. Little, *Chem. Soc. Rev.*, 2014, **43**, 2492–2521.
- 40 C. C. Zeng, N. T. Zhang, C. M. Lam and R. D. Little, *Org. Lett.*, 2012, **14**, 1314–1317.
- 41 J. A. Miranda, C. J. Wade and R. D. Little, *J. Org. Chem.* 2005, **70**, 20, 8017–8026.
- 42 R. D. Little, *Chem. Rev.*, 2002, **96**, 93–114.
- 43 N. Elgrishi, K. J. Rountree, B. D. McCarthy, E. S. Rountree, T. T. Eisenhart and J. L. Dempsey, *J. Chem. Educ.*, 2017, **95**, 197–206.
- 44 C. Sandford, M. A. Edwards, K. J. Klunder, D. P. Hickey, M. Li, K. Barman, M. S. Sigman, H. S. White and S. D. Minter, *Chem. Sci.*, 2019, **10**, 6404–6422.
- 45 M. M. Baizer, *Pure Appl. Chem.*, 1986, **58**, 889–894.
- 46 B. R. Rosen, E. W. Werner, A. G. O'Brien and P. S. Baran, *J. Am. Chem. Soc.*, 2014, **136**, 5571–5574.
- 47 P. S. Baran. and J. M. Richter, *J. Am. Chem. Soc.*, 2004, **126**, 7450–7451.
- 48 W. H. Perkin and S. H. Tucker, *J. Chem. Soc. Trans.*, 1921, **119**, 216–225.
- 49 J. F. Ambrose, L. L. Carpenter and R. F. Nelson, *J. Electrochem. Soc.*, 1975, **122**, 876.
- 50 W. E. Geiger, *Organometallics*, 2007, **26**, 5738–5765.
- 51 P. Gandeepan and L. Ackermann, *Chem*, 2018, **4**, 199–222.
- 52 K. M. Engle, T.-S. Mei, X. Wang and J.-Q. Yu, *Angew. Chemie Int. Ed.*, 2011, **50**, 1478–1491.
- 53 F. Xu, Y.-J. Li, C. Huang and H.-C. Xu, *ACS Catal.*, 2018, **8**, 3820–3824.
- 54 N. Chen and H.-C. Xu, *Green Synth. Catal.*, 2021, **2**, 165–178.
- 55 M. D. Kärkäs, *Chem. Soc. Rev.*, 2018, **47**, 5786–5865.
- 56 M. D. Kärkäs, *ACS Catal.*, 2017, **7**, 4999–5022.
- 57 Z.-W. Hou, Z.-Y. Mao, H.-B. Zhao, Y. Y. Melcamu, X. Lu, J. Song and H.-C. Xu, *Angew. Chemie Int. Ed.*, 2016, **55**, 9168–9172.
- 58 A. Hu, J.-J. Guo, H. Pan, H. Tang, Z. Gao and Z. Zuo, *J. Am. Chem. Soc.*, 2018, **140**, 1612–1616.
- 59 J. J. Guo, A. Hu and Z. Zuo, *Tetrahedron Lett.*, 2018, **59**, 2103–2111.
- 60 J.-F. Zhao, B.-H. Tan and T.-P. Loh, *Chem. Sci.*, 2011, **2**, 349–352.

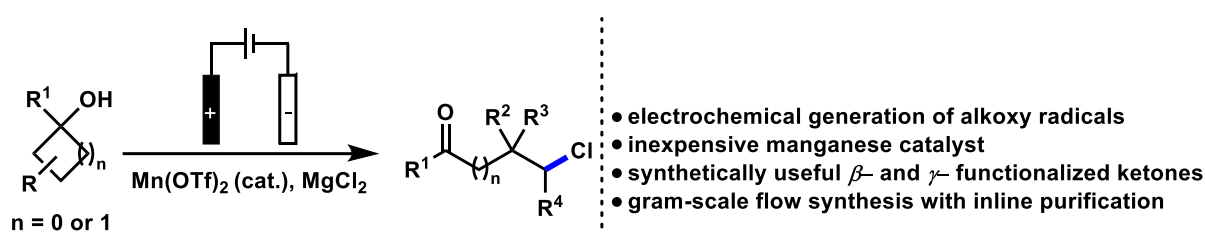
“We shall not cease from exploration
And the end of all our exploring
Will be to arrive where we started
And know the place for the first time.
Through the unknown, remembered gate
When the last of earth left to discover
Is that which was the beginning;
At the source of the longest river
The voice of the hidden waterfall
And the children in the apple-tree
Not known, because not looked for
But heard, half-heard, in the stillness
Between two waves of the sea.

—T.S. Eliot, from “Little Gidding,” *Four Quartets* (Gardners Books; Main edition, April 30, 2001) Originally published 1943.

Chapter 2: Manganese-Catalyzed Electrochemical Deconstructive Chlorination of Cycloalkanols *via* Alkoxy Radicals

2. Preface

This chapter discusses the development of an electrochemical method for the generation and utilization of alkoxy radicals in deconstructive functionalizations of cycloalkanols. In total, 23 examples were reported demonstrating a wide substrate scope. This chapter also highlights some of the limitations of this methodology.



Publication: Benjamin D. W. Allen[†], Mishra Deepak Hareram[†], Alex C. Seastram, Tom McBride, Thomas Wirth, Duncan L. Browne*, and Louis C. Morrill*, *Org. Lett.*, 2019, **21**, 9241-9246.

Acknowledgements

Benjamin D. W. Allen – Responsible for the optimization and substrate scope

Mishra Deepak Hareram – Responsible for part of the optimization and substrate scope

Alex C. Seastram – Responsible for substrate scope and the mechanistic studies

Tom McBride – Responsible for scale-up by flow electrochemistry

Thomas Wirth – Part supervisor of Benjamin D. W. Allen

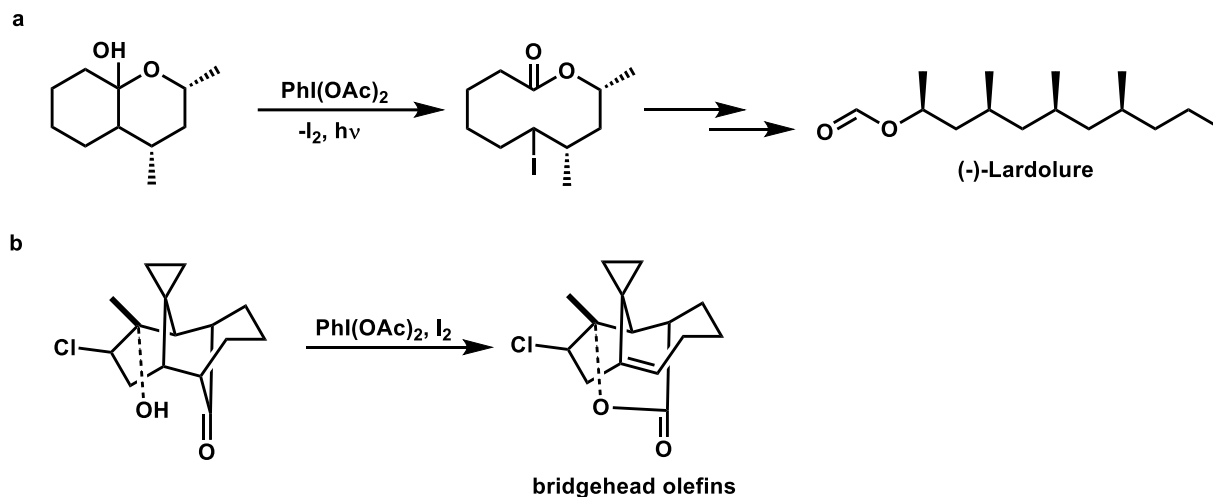
Duncan L. Browne – Supervisor of Tom McBride and part supervisor of Benjamin D. W. Allen

Louis C. Morrill – Supervisor for Benjamin D.W. Allen, Mishra Deepak Hareram and Alex C. Seastram, Cardiff University

2.1. Introduction

A free radical is an atom, molecule, or ion that has unpaired valance electron or an open electron shell; typically, radicals are extremely reactive and short-lived intermediates. The reactive radical intermediates that originate from an oxygen molecule or atom are generally termed as oxygen-centered (*O*-centered) radicals. The *O*-centered radicals can be further classified into hydroxyl radicals ($\cdot\text{OH}$), superoxide radicals ($\text{O}_2\cdot^-$), peroxy radicals ($\text{ROO}\cdot$) and alkoxy radicals ($\text{RO}\cdot$).¹

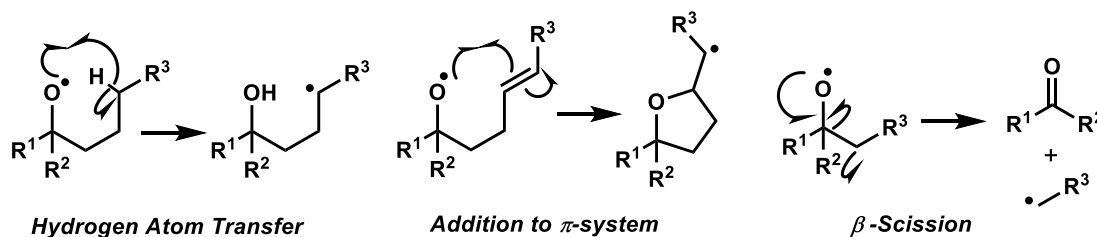
In context with synthetic organic chemistry, alkoxy radicals have been recognized as one of the most versatile reactive intermediates and have been judiciously used in a wide variety of synthetic transformations.²⁻⁵ Yamamoto and co-workers utilized the alkoxy radical intermediated as one of the key steps in the synthesis of (-) – Lardolure, an aggregation pheromone found in acarid mite (scheme 2.1 a).^{5a} Cha and co-workers also used alkoxy radicals to construct bridgehead olefins which allowed them to introduce additional functional groups (scheme 2.2 b).^{5b}



Scheme 2.1 – Alkoxy radicals in the synthesis of natural product derivatives

Alkoxy radicals can be traced back to 1911, when Heinrich Wieland suggested the participation of alkoxy radicals in the formation of tetraphenyldiphenoxyethane from bis(triphenylmethyl)peroxide (trityl peroxide).⁶ Generation of hydroxyl radicals from hydrogen peroxide in the presence of iron (II) salts (Fenton's reagent) is also considered as one of the earliest methods to generate *O*-centered radicals.⁷

The basic structural unit of an alkoxy radical includes a monovalent oxygen atom which is attached to an alkyl group. Theoretical studies suggest that the unpaired electron is mainly located at the oxygen atom in a p-type orbital.⁸ Due to the lack of stabilization provided by mesomeric effects and spin density delocalization found in other oxygen centered radicals (e.g., aryloxy radicals), they are particularly high energy species.



Scheme 2.2 – Elementary reactions of alkoxy radicals

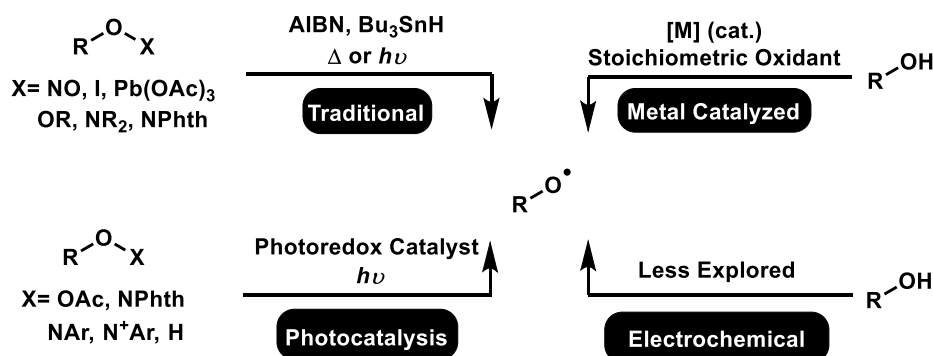
Owing to the highly transient nature of alkoxy radicals, they exhibit a diverse reactivity such as hydrogen atom transfer (HAT),^{9,10} addition to π -systems¹¹ and β -scission processes^{12,13} (scheme 2.2).

Due to their high synthetic importance, efficient methods for the generation of alkoxy radicals is extremely desirable. Direct generation of alkoxy radicals from simple aliphatic alcohols is challenging on account of high bond dissociation free energy (BDFE) of RO–H bonds (~ 105 kcal/mol),² and frequent presence of weaker aliphatic C–H bonds in the same substrate makes the process more challenging.

2.1.1. Methods of Generation of Alkoxy Radicals

Present methods for the generation of alkoxy radicals includes traditional methods which involves the use of radical initiators (chemical, thermal or photochemical) to homolyze the weak oxygen–heteroatom bonds within prefunctionalized radical precursors (scheme 2.3).^{9,10} Alternatively, transition metal catalysts can be employed in combination with stoichiometric oxidants (e.g., $K_2S_2O_8$ or hypervalent iodine reagents) for the generation of alkoxy radicals.¹³ More recently, photoredox approaches have also been utilized to generate alkoxy radicals from various radical precursors including

peroxides,¹⁴ *N*-alkoxyphthalimides,^{15,16} *N*-alkoxypyridiniums,¹⁷ *N*-alkoxybenzimidazoles,¹⁸ *N*-alkoxytriazoliums¹⁹ and from unprotected alcohols.^{20–25}



Scheme 2.3 – Methods of generation of alkoxy radicals

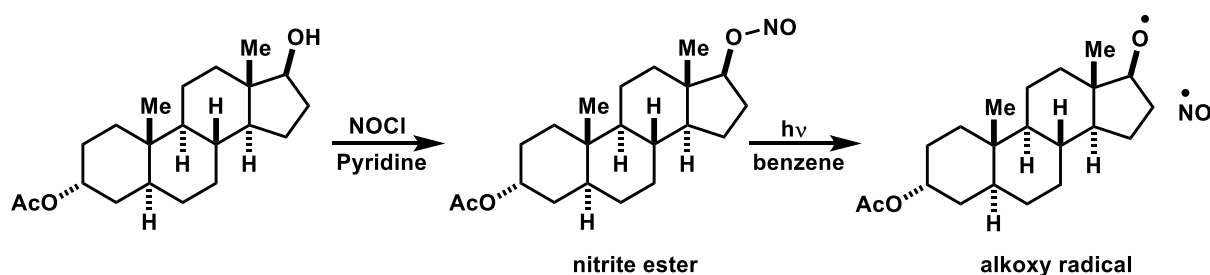
However, reports of electrochemical methods for the generation of alkoxy radicals are scarce in literature in comparison with the other methods mentioned above. Thus, this presents an opportunity to explore the development of electrochemical methods to access alkoxy radicals and to utilize their unique reactivity to generate synthetically useful compounds.

To further understand the different methods for the generation of alkoxy radicals and their synthetic transformation, each method described above will be discussed in the following sections.

2.1.1.1. Traditional Methods for the Generation of Alkoxy Radicals

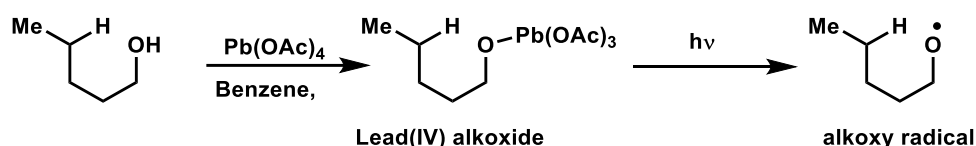
As discussed earlier, direct generation of alkoxy radicals from simple aliphatic alcohols is challenging owing to their high BDFE. To circumvent this limitation, chemists of the past have modified the alcohols into chemically moderately stable but weaker oxygen–heteroatom bond.^{9,10}

The Barton reaction, in which the alcohol is converted into nitrite which upon subsequent photolysis of the RO-NO bond (53 kcal/mol) furnishes an alkoxy radical, is one of the most extensively used method (scheme 2.4).²⁶



Scheme 2.4 – Barton reaction in generation of alkoxy radical

Lead tetraacetate (LTA) is also known to furnish alkoxy radicals in non-polar solvents, such as benzene or cyclohexane, under thermal or photolytic conditions (scheme 2.5).²⁷ The formation of the alkoxy radical involves the homolytic decomposition of lead(IV) alkoxides.



Scheme 2.5 – Lead tetraacetate promoted generation of alkoxy radical

Table 2.1 describes the other traditional methods that have been employed in the generation of alkoxy radicals.⁹

Table 2.1 – Alkoxy radical precursors, reagents, and conditions

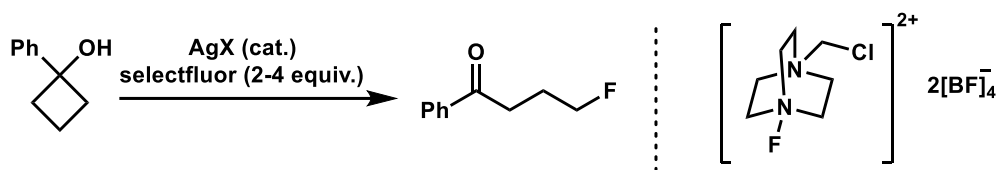
Entry	Precursor of RO [•] X (X=)	Reagents and conditions for O–X homolysis	Name of reaction
1	Pb(OAc) ₃	Heat or hν	LTA oxidation ^{9a-e}
2	NO	hν	Barton reaction ^{9f}
3	Cl	hν or Fe ²⁺	Photolysis of alkyl hypochlorite ^{9g}
4	Br	Ag ⁺ , HgO	Hypobromite ^{9h}
5	I	[LTA, HgO, Ph(OAc) ₂]+ I ₂ , hν	Hypoiodite ⁹ⁱ
6	OH	Fe ²⁺	decomposition of ROOH ^{9j}
7	Ce ⁴⁺	heat	Ce ⁴⁺ oxidation of alcohols ^{9k}
8	SPh(Ar)	Bu ₃ Sn [•] + hν	photolysis of alkyl benzenesulfenates ^{9l}

Traditional methods have been used extensively to utilize the synthetic potential alkoxy radicals in the synthesis of a variety of compounds. However, these methods require the transformation of alcohols into weak but stable *O*-heteroatom species. Also, the use of the harsh conditions (such as, acidic conditions, thermolysis, strong UV irradiations, use of toxic metals etc.) frequently required is not desirable when there are sensitive functional group present. These drawbacks of prefunctionalization have been addressed to some extent using transition metals in the generation of alkoxy radicals.

2.1.1.2. Transition metals for the Generation of Alkoxy Radicals

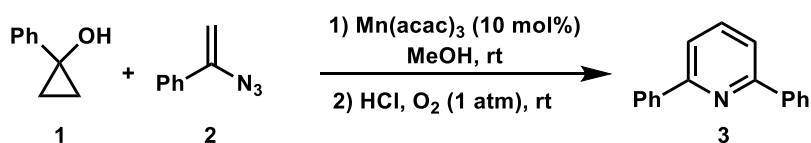
In contrast with the traditional methods, where, in addition to prefunctionalized alcohols, stoichiometric quantities of metal salts have been used, this relatively modern chemistry utilizes transition metals in catalytic amounts along with stoichiometric amounts of oxidant to access alkoxy radicals.²⁸

Among the transition metals, manganese (Mn) and silver (Ag) salts have been used extensively in the generation of alkoxy radicals. The Zhu, Loh and Murakami groups have independently reported a silver-catalyzed ring opening fluorination of cyclic alcohols. This type of ring opening reaction of cyclic alcohols is presumed to go *via* alkoxy radical intermediates (scheme 2.6).²⁹⁻³² Here Selectfluor acts as both fluorinating agent and as an oxidant.



Scheme 2.6 – Silver catalyzed ring opening of cycloalkanols via alkoxy radicals

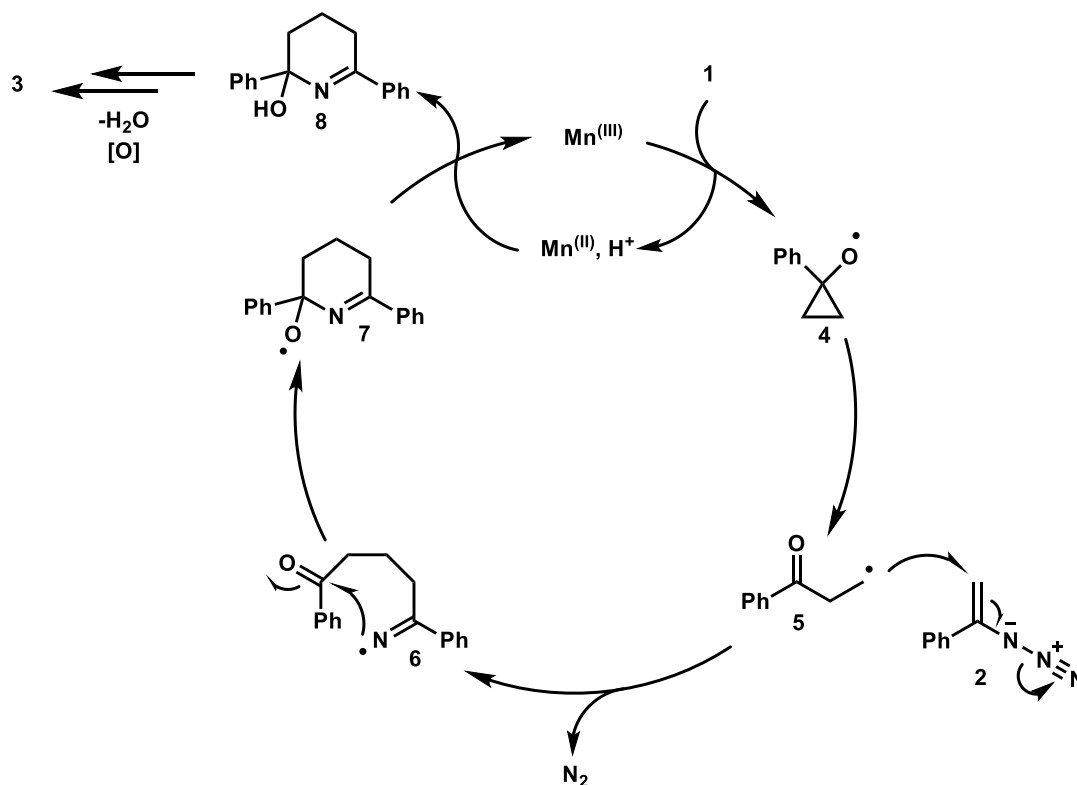
Chiba and co-workers provided a unique synthetic method for the synthesis of pyridines by employing catalytic quantities of Mn(III) salts (scheme 2.7).³³ The method describes a ring opening strategy which goes via the alkoxy radical pathway from cyclopropanol. This highly efficient ring opening can also be attributed to the inherent ring strain of the cyclopropanols.



Scheme 2.7 – Chiba's pyridine synthesis via alkoxy radical

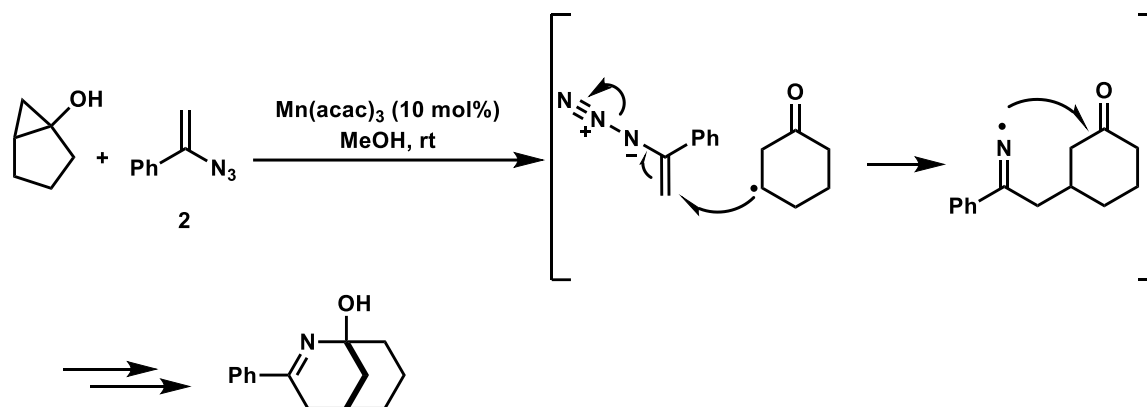
Mechanistically, authors propose a single electron oxidation of **1** in presence of a $\text{Mn}^{\text{(III)}}$ species to furnish either a metal bound alkoxy radical intermediate **4**.

Subsequent β -scission of **4** generates carbon centered radical **5**, which adds to vinyl azide **2** to give an iminyl radical intermediate **6** with the exclusion of dinitrogen. This *N*-centered radical is assumed to add to the carbonyl group in 6-*exo-trig* fashion to again furnish an alkoxy radical intermediate **7**, which is oxidized by the $\text{Mn}^{\text{(II)}}$ species to regenerate the active $\text{Mn}^{\text{(III)}}$ species. Subsequent protonation of and further oxidation furnishes the final product **3** (scheme 2.8).



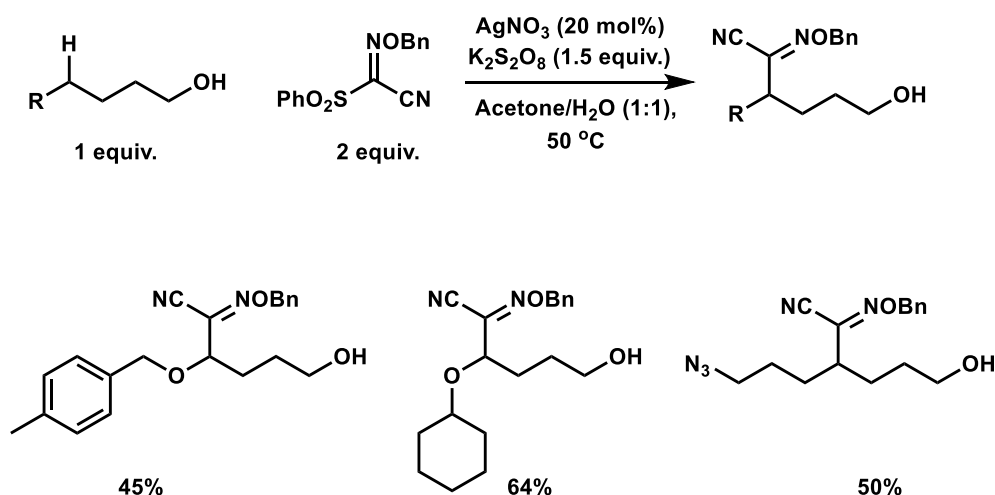
Scheme 2.8 – Proposed pathway for pyridine formation

The authors also reported the formation of 2-azabicyclo[3.3.1]non-2-en-1-ol, when bicyclic cyclopropanols were used (scheme 2.9). More than 30 examples of pyridine products and 6 examples of unusual Aza-bicyclic products were reported with moderate to excellent yields.



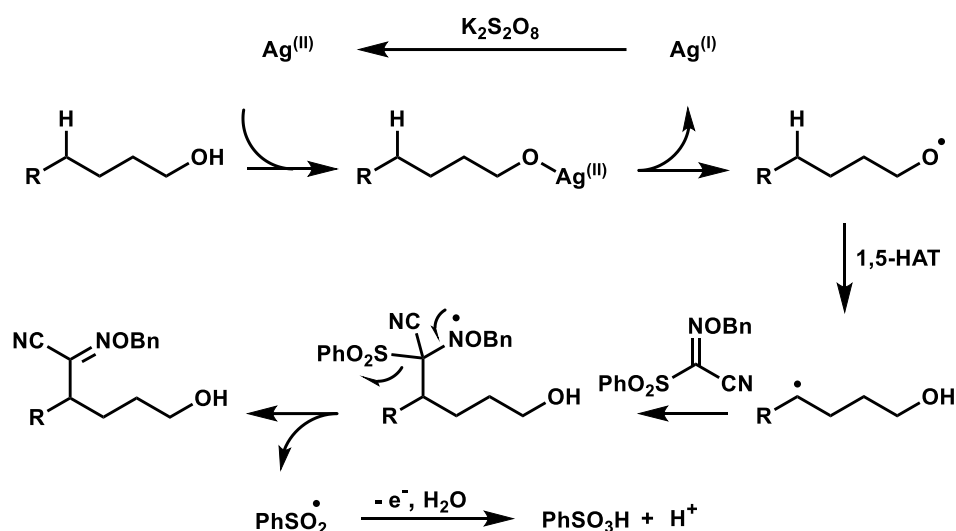
Scheme 2.9 – Formation of 2-Azabicyclo[3.3.1]non-2-en-1-ol

More recently, Jiao and co-workers in 2018 reported a silver catalyzed formation of alkoxy radicals to promote 1,5-HAT and subsequent C(sp³)-H bond functionalization to form oxime ether products (scheme 2.10).³⁴ The authors identify AgNO₃ and K₂S₂O₈ as the optimal metal/oxidant pair to induce 1,5-HAT by generating an alkoxy radical intermediate.



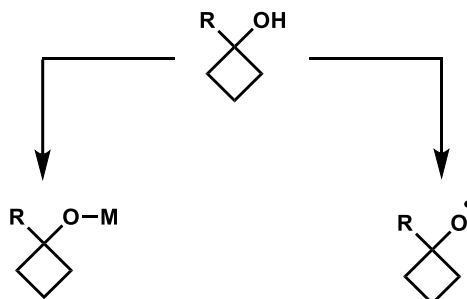
Scheme 2.10 – Silver catalyzed generation of alkoxy radical

The method illustrates an interesting transformation; however, the yields are moderate to high over 25 examples. The reaction is postulated to start with the oxidation of Ag^{I} to Ag^{II} by $\text{K}_2\text{S}_2\text{O}_8$, which then coordinates with the alcohol substrate. The resulting Ag^{II} complex subsequently undergoes homolysis to furnish the alkoxy radical intermediate and Ag^{I} . The alkoxy radical intermediate then undergoes a 1,5 HAT to furnish an alkyl radical, which adds to the SOMOphile where after subsequent rearrangement and extrusion of a sulfonyl radical the final product is furnished (scheme 2.11).



Scheme 2.11 – Mechanism of silver catalyzed generation of alkoxy radical

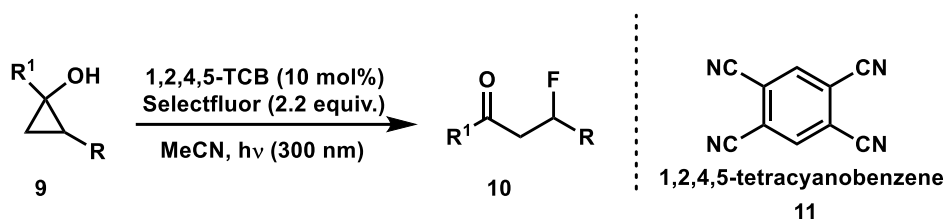
In almost all cases, the transition metal catalyzed generation of alkoxy radicals requires stoichiometric quantities of oxidant to regenerate the catalyst. Thus, making the transformations less green. Also, there is an ambiguity in the transition metal catalyzed reactions as in, if they furnish a free alkoxy radical or a metal bound alkoxide, when the alcohols with inherent ring strain is used (scheme 2.12)?¹³



Scheme 2.12 – Free alkoxy radical of metal bound alkoxide

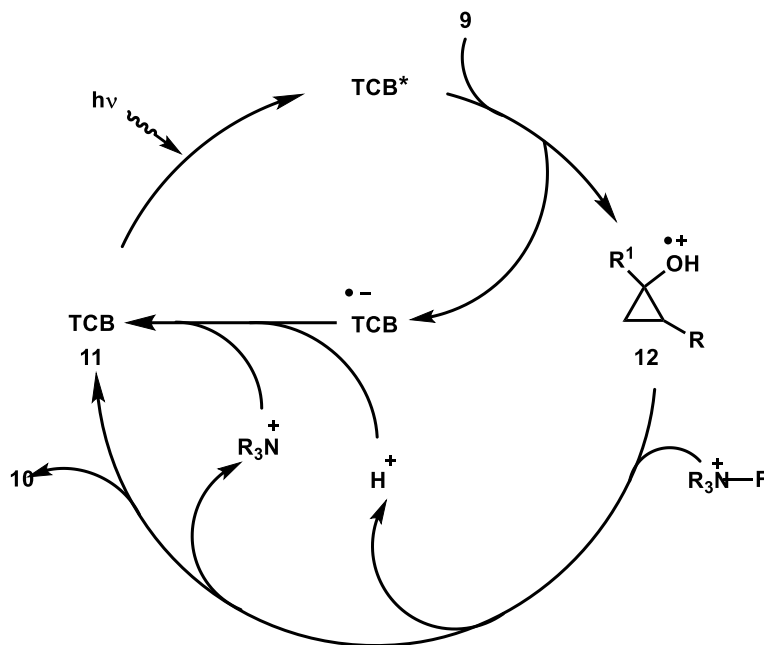
2.1.1.3. Photoredox Methods for the Generation of Alkoxy Radicals

Photoredox mediated approach has recently provided a potent alternative method in the generation and application of alkoxy radicals.³⁵ Lectka and co-workers reported an organic photosensitizer mediated ring-opening fluorination of cyclopropanols (scheme 2.13).³⁶



Scheme 2.13 – 1,2,4,5-TCB mediated photoredox enabled fluorination of cyclopropanols

The authors proposed a mechanism involving an alkoxy radical intermediate. The catalytic cycle could start with the sensitization of the photocatalyst **11**, which would then undergo a SET with the substrate to furnish cyclopropyl radical cation **12**.

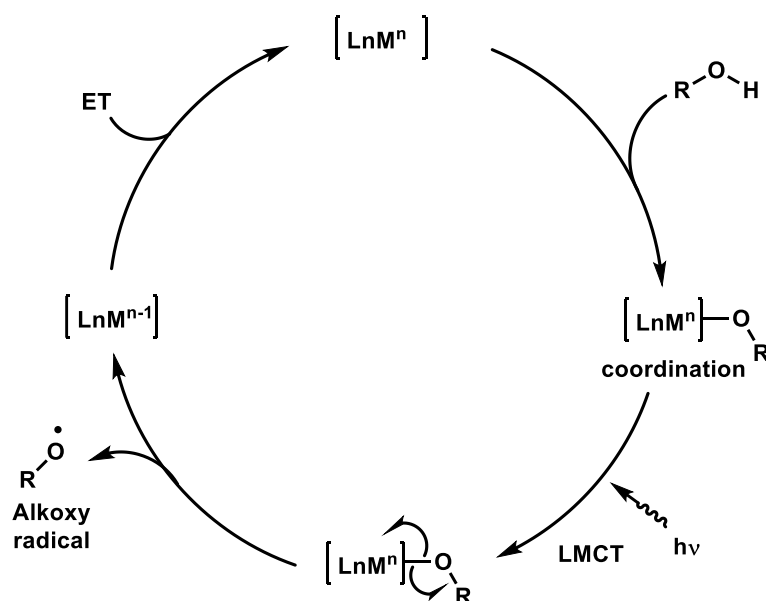


Scheme 2.14 – Mechanistic proposal

The oxidised species **12** then undergoes β-scission to furnish a carbon centered radical, which intercepts a fluorine atom to afford the β-fluorinated product. The radical cation of

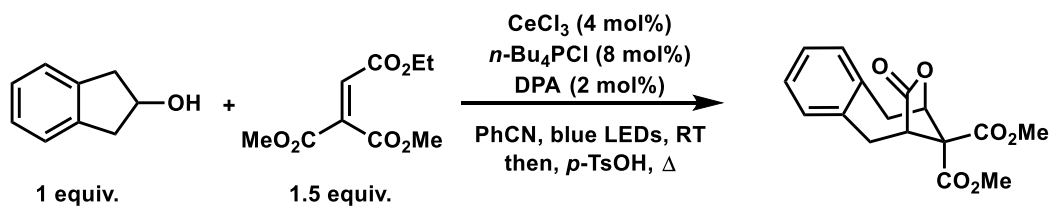
Selectfluor that is generated is then reduced by the TCB radical anion to regenerate the photocatalyst and ammonium salt as by-product (scheme 2.14).

Ligand-to-metal charge transfer (LMCT) involves complexes of transition metals with an empty valance shell, where in an electron from a high-energy ligand orbital is excited to a low laying metal-centered orbital.³⁷ LMCT catalysis proceeds through sequential substrate coordination to the transition metal catalyst, LMCT excitation, and homolysis of the metal-ligand bond (scheme 2.15).³⁸



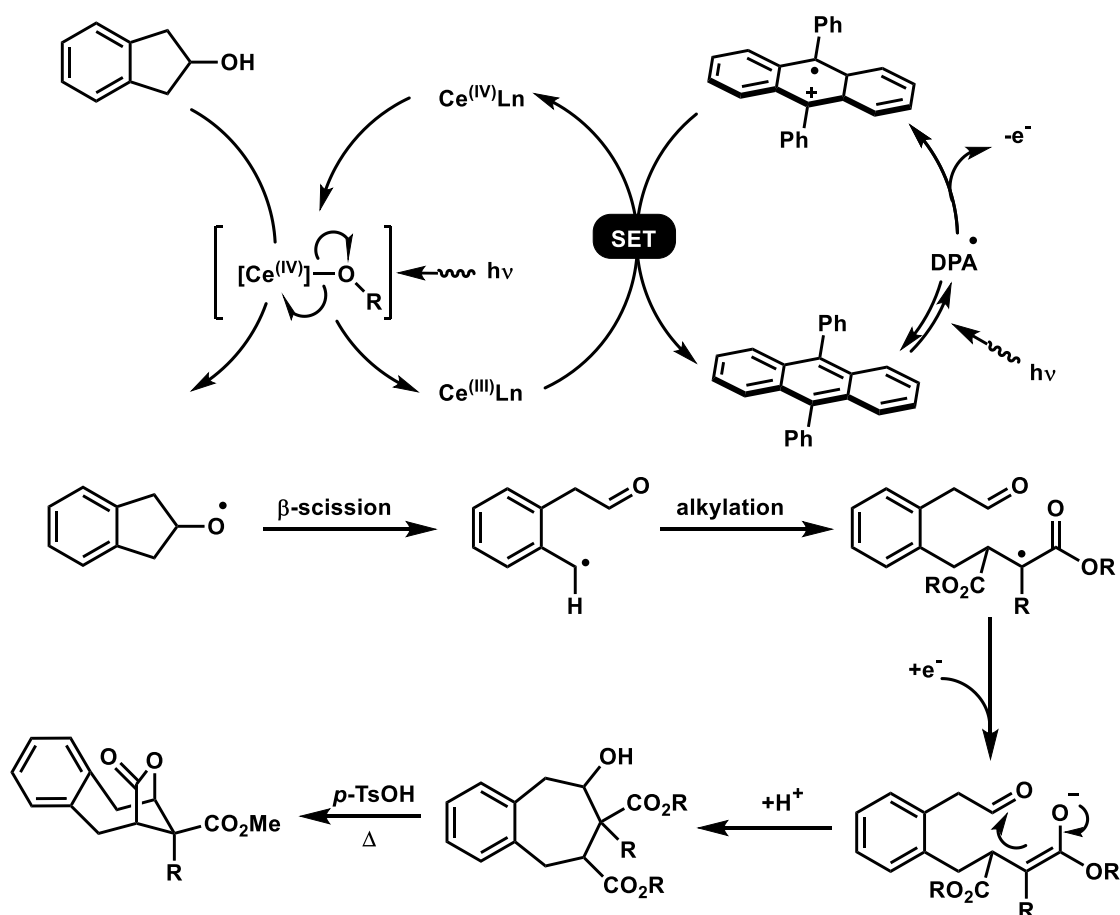
Scheme 2.15 – LMCT strategy for the generation of alkoxy radical

Zuo and co-workers have reported several transformations exploiting LMCT strategy in the generation and application of alkoxy radicals.^{39–43} In one of their works, they disclosed an application of cerium-catalyzed β -scission and ring expansion of cycloalkanols for the synthesis of bridged lactones (scheme 2.16).⁴⁴



Scheme 2.16 – Cerium catalyzed β -scission and ring expansion of cycloalkanols

Mechanistically, the authors indicated that the redox potential of Ce^{III} ($E_{1/2}(\text{Ce}^{\text{IV}}/\text{Ce}^{\text{III}}) = 0.40 \text{ V vs SCE in MeCN}$), and the regeneration of photoactive Ce^{IV} to complete the catalytic cycle would require a sufficiently oxidizing radical intermediate. To fulfil this requirement, 9,10-diphenylanthracene (DPA) was used as an electron transfer catalyst to oxidize Ce^{III} to Ce^{IV} (scheme 2.17).



Scheme 2.17 - Cerium-catalyzed β -scission and ring-expansion of cycloalkanols

The reaction with irradiation first triggers LMCT, promoting $\text{Ce} - \text{OR}$ bond homolysis to form the alkoxy radical intermediate. The subsequent β -scission furnishes an alkyl radical that then adds to an electron-deficient alkene, forming an α -acyl radical. This nascent radical is reduced to form an enolate by the photoexcited DPA ($E_{1/2} = -1.77 \text{ V vs SCE in MeCN}$). This electron transfer oxidizes photoexcited DPA \cdot to DPA $^{+\bullet}$. The enolate formed undergoes an intramolecular aldol reaction to serve annulation to a ring-expanded

intermediate, which upon treatment with *p*-TsOH, furnishes the bridged lactone. while DPA^{•+} ($E_{1/2} = 1.13$ V vs SCE in MeCN) oxidizes Ce^(III) back to catalytically active Ce^(IV).

Substitution on the indanols is well tolerated including those containing functional groups prone to transition-metal-catalyzed insertions, forming [4.2.1]-bridged lactones. Cyclobutanol derivatives are also converted easily to diverse range of [3.2.1] ring systems (figure 2.1).

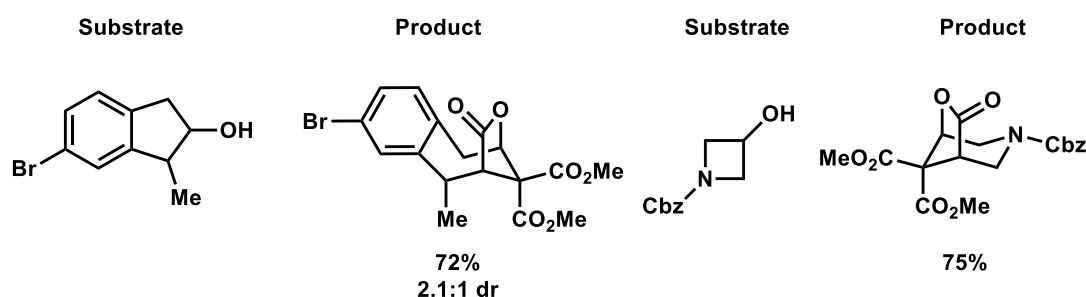


Figure 2.1 – selected examples

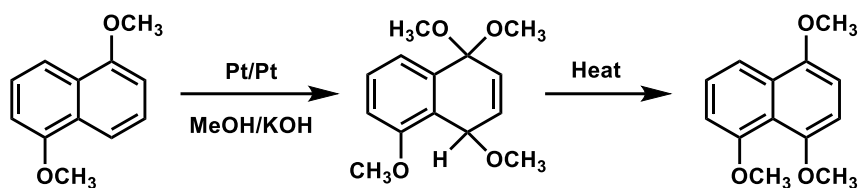
In addition to the photochemical LMCT approach, the Knowles group leveraged proton-coupled electron transfer (PCET) in the generation of alkoxy radicals, which provides an alternative mechanism for direct O–H bond homolysis. PCET strategy is used in this thesis in an electrochemical setting for the generation of alkoxy radical and will be discussed in the next chapter.

Photoredox chemistry presents a mild alternative for the generation of alkoxy radicals, however the use of precious metals, heat dissipated during the irradiation and in most instances, long reaction times are some of the immediate disadvantages.

2.1.1.4. Electrochemical Methods for the Generation of Alkoxy Radicals

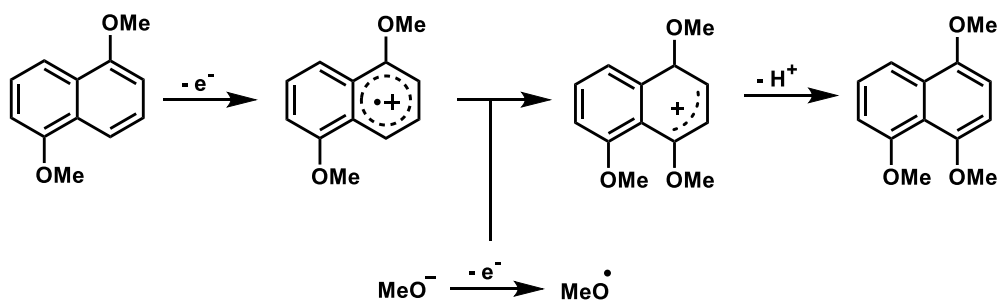
Organic electrochemistry has emerged as an alternative and one of the cleanest possible chemical processing technologies, which has attracted synthetic organic chemists, partly due to increasing availability of standardized batch and flow electrochemical reactors.^{45–48} Despite the many advantages electrochemistry offers, there are few reports on the

electrochemical generation of the alkoxy radicals. In one of the first reports of the electrochemical generation of alkoxy radicals, Swenton and co-workers reported an anodic oxidation of substituted naphthalenes with 1% methanolic potassium hydroxide as solvent (scheme 2.18).⁴⁹



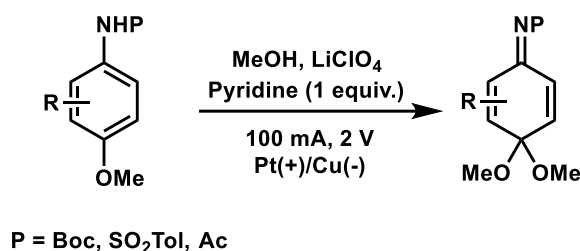
Scheme 2.18 – Anodic oxidations of substituted naphthalenes

The authors proposed an EECrC_p type mechanism for the formation of the observed products. In an EECrC_p mechanism, the first two symbols denote the electrochemical steps required to form a methoxy radical and a radical cation species of the naphthalene and C_r and C_p refers to chemical steps involving radical and polar intermediates, respectively (scheme 2.19).



Scheme 2.19 – Anodic oxidation via EECrC_p mechanism

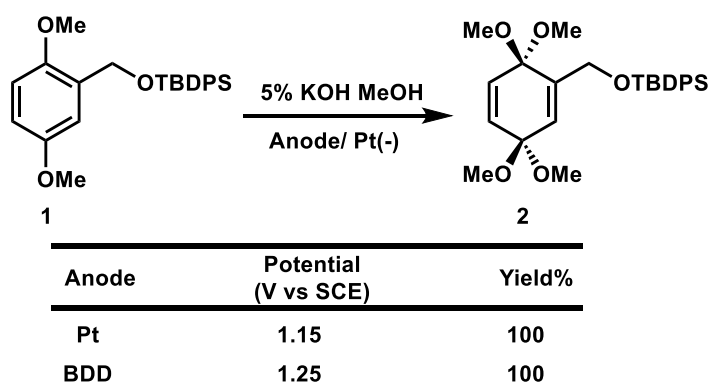
A similar report by Carreño and co-workers illustrated the anodic oxidation of *N*-protected 4-methoxy anilines in the synthesis of *N*-protected quinone imine acetals. The authors predicted the formation of methoxy radicals from methanol (scheme 2.20).⁵⁰



Scheme 2.20 – Synthesis of *N*-protected quinone imine acetals

More recently Nishiyama and co-workers also reported the generation of methoxy radicals by electrochemical oxidation of methanol on the surface of boron-doped diamond (BDD) as anode.⁵¹ In their earlier studies, the authors reported an oxidative dimethoxy-acetalization reaction in a basic MeOH solution at a platinum electrode (Pt) as one of the key steps in the synthesis of (±)-parasitenone, a novel inhibitor of NF-κB.⁵²

In their further studies, it was observed that the dimethoxy-acetalization efficiency when using a BDD anode was similar to when a platinum anode was employed (scheme 2.21).



Scheme 2.21 – Anodic oxidative dimethoxy acetalization

The authors indicated the intermediacy of methoxy radicals as described by Swenton and co-workers. They also proposed the reaction mechanism involving EECrCp.⁴⁹

In their further investigations to ascertain the involvement of the radical species, electron spin resonance (ESR) studies using radical trapping agent 5,5-dimethyl-1-pyrroline-*N*-oxide (DMPO) were conducted. A methanolic solution of DMPO was electrolyzed at constant potential (1.06 V vs SCE) using BDD, Pt and glassy carbon (GC) electrodes as anodes and the product mixtures were analysed by ESR.

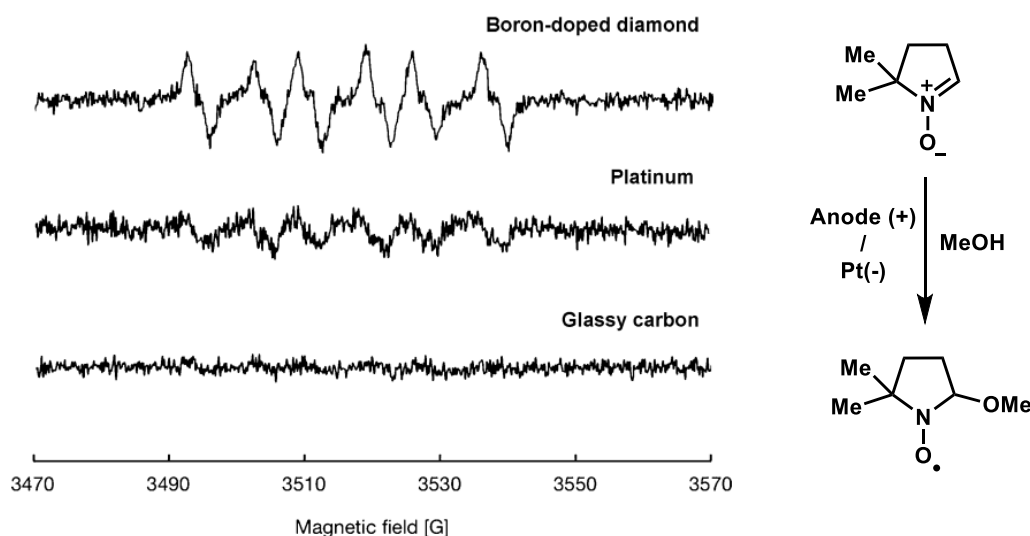


Figure 2.2 – ESR spectra of electrolysis products of MeOH and DMPO (figure produced with permission)

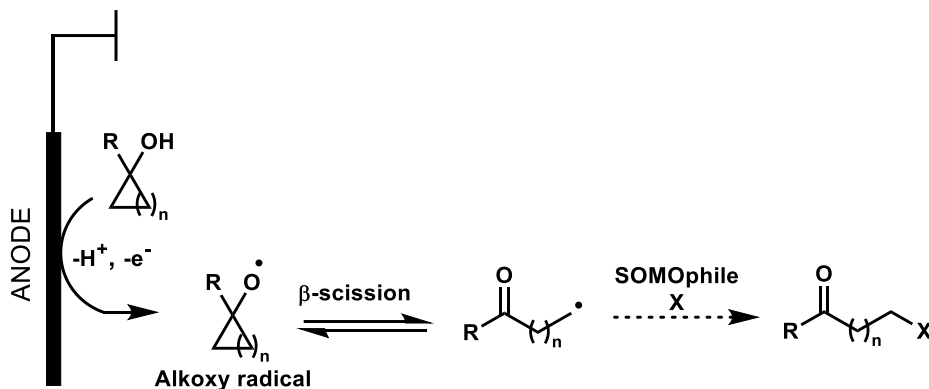
The intensities of the ESR signal for the formed radical varied with the anode used (BDD > Pt > GC). Thus, it can be interpreted that methoxy radicals are generated in electrochemical reactions of MeOH and BDD produces the methoxy radicals with greater efficiency. Recently authors have applied this strategy in the oxidation of C-glycoside as well.⁵³

2.2. Aims and Objectives

The utilization of alkoxy radicals in an electrochemical set up remains relatively underexplored and remains largely limited to the generation of methoxy radicals. This presents an opportunity for the development of electrochemical methods for the generation and utilization of alkoxy radicals through the various reactivity modes that were discussed in section 2.1.

Owing to the tendency of tertiary alcohols to undergo β -fragmentation after the generation of alkoxy radical, cycloalkanol substrates were selected as a logical starting point. Taking inspiration from the literature, especially from the works of Zhu, Loh and Murakami^{29–32} and from exploiting the potential of electrochemistry, an alternate

method for the generation of alkoxy radicals was envisaged. A representative scheme for such postulated method is depicted below (scheme 2.22).



Scheme 2.22 – Proposed electrochemical generation of alkoxy radical

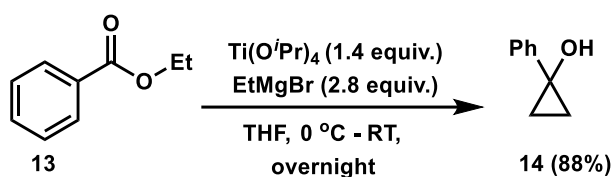
Under the oxidative electrochemical conditions, a loss of a proton followed by an anodic oxidation would allow for generation of the alkoxy radical intermediate. The alkoxy radical thus formed would then undergo a reversible β -fragmentation of the C-C bond generating a distal carbon-centered radical, which can be intercepted by various SOMOphiles. This will furnish the distally functionalized ketones which could be employed further in various synthetic transformations such as Baeyer-Villiger oxidation, Grignard addition, Mannich reaction, Wittig reaction etc.

2.3. Results and Discussion

2.3.1. Electrochemical β -scission of 1-phenylcyclopropan-1-ol

2.3.1.1. Direct electrolysis

As per the works of Narasaka, Murakami and other research groups, it is evident that cyclopropanols with their inherent ring strain tends to undergo β -scission upon the generation of alkoxy radical. Hence, 1-Phenylcyclopropanol was synthesized in one step following a modified Kulinkovich cyclopropanation reaction from ethyl benzoate **13**. The desired 1-phenylcyclopropan-1-ol **14** was isolated in 88% yield (scheme 2.23).⁵⁴

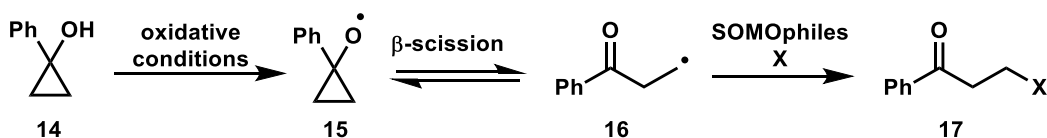


Scheme 2.23 – Synthesis of 1-phenylcyclopropan-1-ol

With the starting material **14** in hand, initial electrochemical attempts began.

Initial aims of the electrochemical experiments were to familiarize with the experimental set-up and various parameters of electrolysis in general.

Based on the various literature precedents,^{55–59} the working hypothesis was as follows: if we subject the tertiary alcohol **14** to oxidative conditions, we should be able to generate an alkoxy radical intermediate **15**. Intermediate **15** can then undergo a reversible β -scission process to generate a distal carbon-centered radical **16**, which can be trapped with various SOMOphiles (scheme 2.24).



Scheme 2.24 – working hypothesis for β -scission of 1-phenylcyclopropan-1-ol

Following up on the initial hypothesis, **14** was subjected to various electrochemical conditions using ElectraSyn 2.0 as a standard electrolysis apparatus in an undivided cell. The reactions were performed at a 0.3 mmol reaction scale and the dilution was kept at 0.05 M in indicated solvents. 1,4-cyclohexadiene (1,4-CHD) was used as a SOMOphile. The results of the initial experiments are shown below (table 2.2, NMR yields determined by ^1H spectroscopy of the crude reaction mixture, relative to 0.1 equivalents of mesitylene as internal standard).

Entry **1** demonstrated that when **14** was subjected to electrochemical conditions comprised of graphite as both anode and cathode, lithium perchlorate (LiClO_4) (2 equiv.) as supporting electrolyte in THF/MeOH (5:1) at constant current $I = 5$ mA for total charge passed $Q = 1$ F/mol, no conversion was observed and 80% of **14** was returned. Entry **2**

showed that by including Cs_2CO_3 (1 equiv.) and keeping all other parameters the same as in entry **1**, the starting material was consumed (40% of **2** was returned) and products **18**, **19**, and **20** were formed in 13, 12 and 13% yields respectively. When MeOH was swapped with HFIP in entry **3**, no appreciable improvement was observed, however ^1H NMR analysis indicated that formation of product **19** was suppressed.

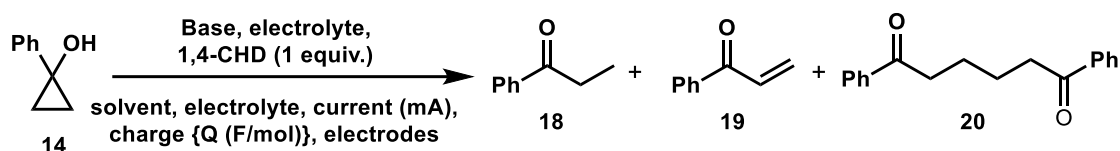


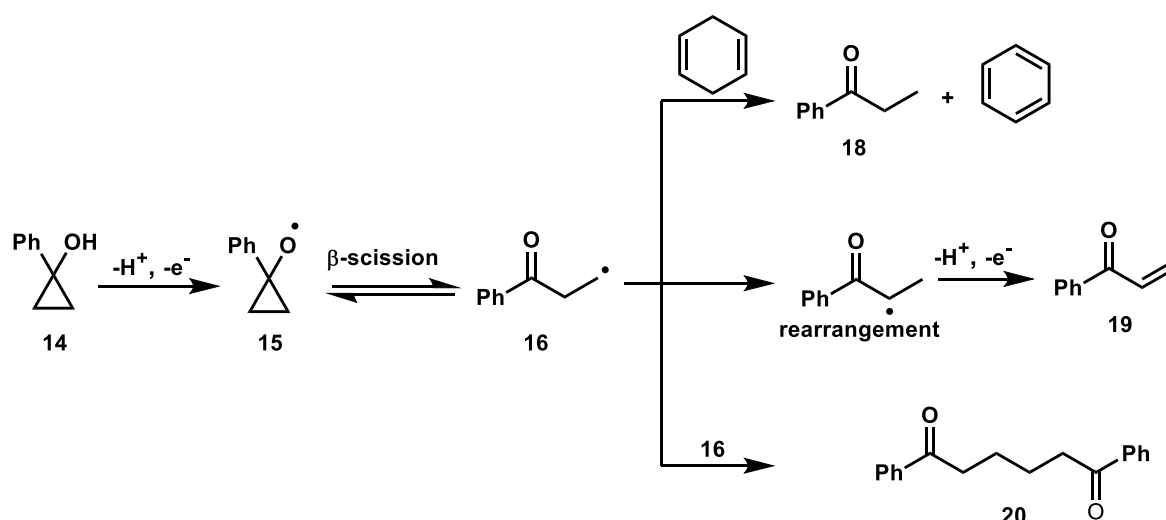
Table 2.2 – Initial electrochemical experiments with 1-phenylcyclopropan-1-ol

Entry	I (mA)	Solvent	Base (equiv.)	Electrolyte (equiv.)	Charge (Q) (F/mol)	18 (%)	19 (%)	20 (%)	14 (%)
1 ^a	5	THF/MeOH (5:1)	0	LiClO_4 (2)	1	<2	<2	0	80
2 ^a	5	THF/MeOH (5:1)	Cs_2CO_3 (1)	LiClO_4 (2)	1	13	12	13	40
3 ^a	5	THF/HFIP (5:1)	Cs_2CO_3 (1)	LiClO_4 (2)	1	12	<2	12	62
4 ^a	5	THF/MeOH (1:1)	Cs_2CO_3 (1)	LiClO_4 (2)	2	25	<2	21	38
5 ^a	5	THF/MeOH (1:1)	K_2CO_3 (1)	LiClO_4 (2)	2	28	<2	25	32
6 ^a	10	THF/MeOH (1:1)	K_2CO_3 (1)	LiClO_4 (2)	2	37	<2	29	<20
7 ^a	10	THF/MeOH (1:1)	K_2CO_3 (1)	Bu_4NClO_4 (2)	2	21	<2	18	62
8 ^a	10	THF/MeOH (1:1)	K_2CO_3 (1)	Bu_4NPF_6 (2)	2	<2	<2	<2	70
9 ^a	10	THF/MeOH (1:1)	K_2CO_3 (1)	Bu_4NBr (2)	2	13	<2	<2	46
10 ^b	10	THF/MeOH (1:1)	K_2CO_3 (1)	LiClO_4 (2)	2	<2	<2	<2	62
11 ^c	10	THF/MeOH (1:1)	K_2CO_3 (1)	LiClO_4 (2)	2	<2	<2	<2	59

a: graphite was used as both anode and cathode; b: platinum as anode, graphite as cathode; c: graphite as anode, platinum as cathode. 1,4-CHD was used as a SOMOphile.

Entry **4** showed that the solvent system of THF/MeOH (1:1) increased the formation of **18** and **20** when 2 F/mol of charge was passed. Changing the base to K₂CO₃ in entry **5**

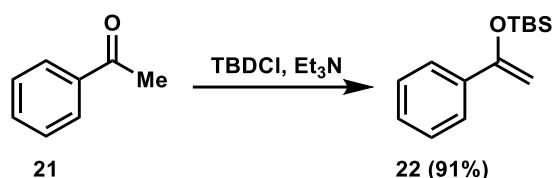
also showed the slight increase in the formation of **18** and **20**. However, similar to entry **4**, the formation of **19** was not observed at all. The best conversion of **14** to products **18** and **20** was observed in entry **6**, 37 and 29% respectively, when the electrolysis was performed at 10 mA of constant current. Change of supporting electrolyte proved detrimental to the formation of products **18** and **20** (entries **7-9**). Alterations to the electrode materials used such as changing the anode to platinum (Pt) as in entry **10** and changing the cathode to Pt as in entry **11**, seemed to shut down the reaction with no appreciable formation of products **18**, **19** or **20**. The observation of the formation of the interesting products **18**, **19** and **20** can be rationalized as follows (scheme 2.25).



Scheme 2.25 – Rationalization for the formation of products **6**, **7** and **8**

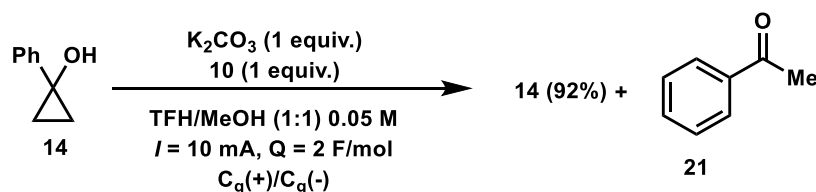
In the presence of base **14** will form an alkoxide, which can be oxidized at the anode to generate the alkoxy radical intermediate **15**. Reversible β -scission of **15** will yield the ketone intermediate **16**. In the presence of 1,4-CHD, **16** can abstract a hydrogen atom to furnish **18** along with oxidized benzene. Formation of **19** could be rationalized as follows, **16** could undergo a 1,2 radical rearrangement to furnish a more stable secondary radical, which upon subsequent oxidation at the anode and loss of proton will give product **19**. On the other hand, **16** can dimerize in a radical cage to form product **20**.

Further attempts to selectively form product **18** were unsuccessful, it was understood that SOMOphile 1,4-CHD is being oxidized quicker than it could be trapped with the intermediate **16**. Based on the works of Narasaka,⁵⁹ silyl enol ether **10** was synthesized from acetophenone **21** and *tert*-butyldimethylsilyl chloride (scheme 2.26).



Scheme 2.26 – Synthesis of silyl enol ether **10**

When the SOMOphile **22** was used in the electrochemical reaction instead of 1,4-CHD, no product formation was observed, and the starting material **14** was recovered in 92% yield by ^1H NMR spectroscopy. It was also found that the silyl enol ether **22** was deprotected in the reaction, reverting back to **21** in a greater than 90% yield (scheme 2.27).



Scheme 2.27 – Electrochemical reaction silyl enol ether **10** as SOMOphile

2.3.1.2. Mediated Electrolysis

Up to this point, direct electrolysis was performed, where the substrate was interacting with the electrodes. The experiments suggests that direct electrolysis was inefficient and causing multiple side reactions, and SOMOphile degradation was also observed.

Again, based on the works of Narasaka,^{59,60} Chiba^{33,57,58} and Zhu,⁶¹ using manganese (II) salts in catalytic amounts was considered. Based on the pervious experiments, the idea of using a more stable SOMOphile was also incorporated in the experiments.

Table 2.3 describes the electrochemical experiments performed with 1-phenylcyclopropan-1-ol **14**, with various manganese (II) salts in catalytic amounts along with benzothiazole **23** as an alternate SOMOphile. The reactions were run at 0.3 mmol of **14**. Dilutions of the reactions were kept at 0.05 M in indicated solvents (NMR yields determined by ^1H spectroscopy of the crude reaction mixture, relative to 0.1 equivalents of mesitylene as internal standard).

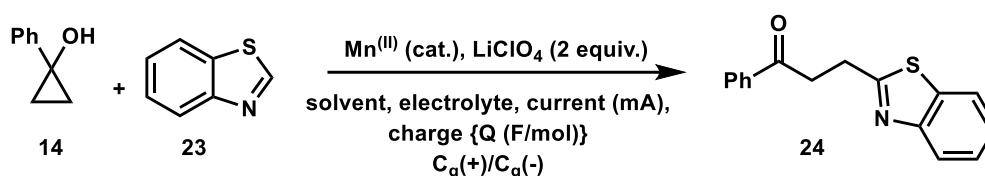


Table 2.3 – Manganese mediated electrochemical reactions of 1-phenylcyclopropan-1-ol

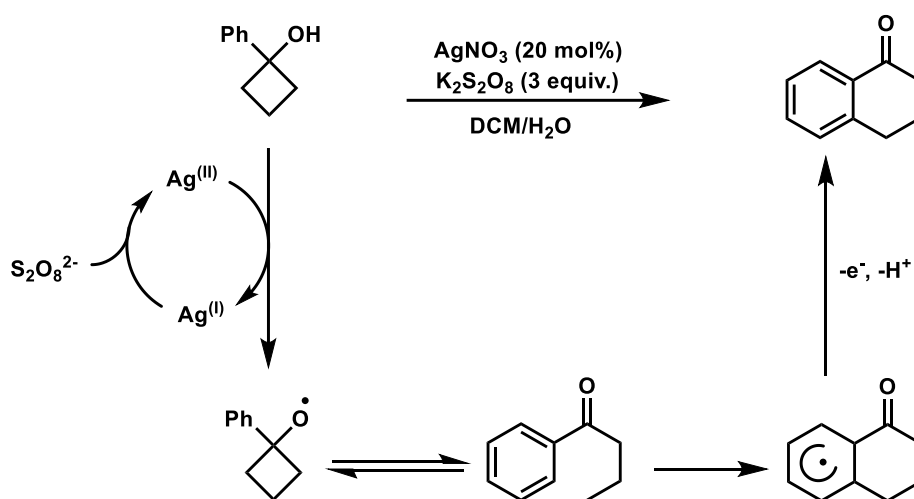
Entry	I (mA)	Solvent	Mn(II) (mol%)	Electrolyte (equiv.)	Charge (Q) (F/mol)	24 (%)	14 (%)
1	5	MeCN/AcOH (7:1)	MnCl ₂ ·4H ₂ O (2.5)	LiClO ₄ (2)	2	<2	50
2	5	MeCN/AcOH (7:1)	MnCl ₂ ·4H ₂ O (5)	LiClO ₄ (2)	2	26	<2
3	5	MeCN/AcOH (7:1)	Mn(OAc) ₂ ·4H ₂ O (5)	LiClO ₄ (2)	2	<2	30
4	5	MeCN/AcOH (7:1)	MnBr ₂ ·4H ₂ O (5)	LiClO ₄ (2)	2	42	40
5	5	MeCN/AcOH (7:1)	Mn(OTf) ₂ (5)	LiClO ₄ (2)	2	16	37

Entry **1** showed that, when the electrolysis was performed with 5 mol% of MnCl₂·4H₂O at a constant current of 5 mA until 2 F/mol of charge was passed in MeCN/AcOH (7:1) and LiClO₄ as supporting electrolyte, the desired product **24** was formed in less than 10% by ^1H NMR analysis. Increasing the catalyst loading to 5 mol% increased the product formation to 26% (entry 2). Several other Mn(II) salts were tried, entries **3** to **5**, which indicated that MnBr₂·4H₂O was the best catalyst with 42% of the desired product **24** formed. However, the yields did not increase further and experimentations with 1-phenylcyclopropan-1-ol were stopped.

The mediated electrolysis with Mn^{II} salts showed some promising results and it was decided to continue the β -scission investigations with 1-phenylcyclobutan-1-ol as a model substrate.

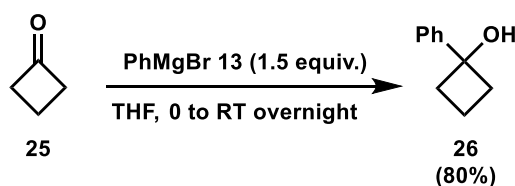
2.3.2. Electrochemical β -scission of 1-phenylcyclobutan-1-ol

1-Phenylcyclopropanol were suspected to be unstable in the electrochemical reactions and to circumvent this cyclobutanols were tested. Zhu and co-workers in 2015 reported a silver-catalyzed ring expansion for cyclobutanols in the formation of 1-tetralones (scheme 2.28).⁶² The active silver^(II) form of the catalyst was accessed using 4 equiv. of $\text{K}_2\text{S}_2\text{O}_8$ as oxidant.



Scheme – 2.28 – Silver catalyzed ring expansion of cyclobutanols

1-Phenylcyclobutan-1-ol **26** was synthesized by reacting 1.5 equiv. of phenylmagnesium bromide with cyclobutanone **25** in dry THF. Product **26** was isolated in 80% yield (scheme 2.29).



Scheme 2.29 – Synthesis of 1-phenylcyclobutan-1-ol

To begin the electrochemical trials, substrate **26** was first subjected to the initial conditions from table 2.2 entry **8**, without any mediator in the presence of 2 equiv. of K_2CO_3 entry **1** (table 2.4).

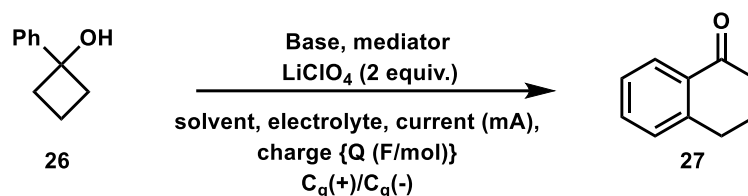


Table 2.4 – Electrochemical reactions of 1-phenylcyclobutan-1-ol

Entry	I (mA)	Solvent	Base (equiv.)	Mediator (mol%)	Electrolyte (equiv.)	Charge (Q) (F/mol)	27 NMR (%)	26 NMR (%)
1	5	THF/MeOH (1:1)	K_2CO_3 (2)	–	$LiClO_4$ (2)	2	<2	90
2	5	MeCN	–	$AgNO_3$ (5)	$LiClO_4$ (2)	2	13	70
3	5	MeCN	–	$Ag(OTf)$ (5)	$LiClO_4$ (2)	2	20	69
4	5	MeCN	–	$MnCl_2 \cdot 4H_2O$ (5)	$LiClO_4$ (2)	2	32	40
5	5	MeCN	–	$Mn(acac)_2$ (5)	$LiClO_4$ (2)	2	48	42

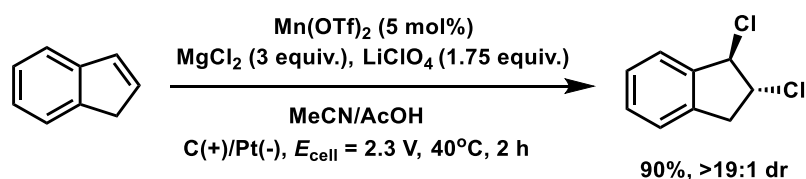
Reactions performed at 0.3 mmol in ElectraSyn 2.0. Crude reaction mixture was analyzed by 1H NMR spectroscopy using 1,3,5-trimethylbenzene as internal standard.

Electrolysis of **26** at 5 mA, for 2 F/mol with $LiClO_4$ as supporting electrolyte, resulted in a return of 90% of the starting material **26**. When performed with 5 mol% of $AgNO_3$ as a mediator, formation of the desired product was observed in 13% yield by 1H NMR, entry **2**. No appreciable change was observed when the mediator was changed to $Ag(OTf)$ in entry **3**, showing 20% conversion to **27** and 69% of **26** returned. Entry **4** shows the use of $Mn^{(II)}$ salt as mediator/catalyst, in which formation of tetralone **27** was observed in 32%. Several other manganese salts were tried, and the best conversion of **26** to **27** was obtained using $Mn(acac)_2$, in 48% yield, entry **5**. By this time, the proof of concept was already established with the results obtained from these electrochemical experiments. Both 1-phenylcyclopropan-1-ol **2** and 1-phenylcyclobutan-1-ol **15** underwent the desired

β -scission transformation, yielding the expected products. With these promising preliminary results, Dr Benjamin Allen, PDRA in the lab also started looking into the electrochemical β -scission reactions of cycloalkanols. Dr Benjamin Allen soon found conditions which yielded a synthetically useful γ -chlorinated ketone, starting from **26**.

2.3.3. Manganese Catalyzed Electrochemical Deconstructive Chlorination of Cycloalkanols

Taking inspirations from Lin and co-workers, where the authors reported a manganese^(III) catalyzed dichlorination of alkenes (scheme 2.30).⁶³ They reported an electrochemical generation of a Mn^(III) species from a Mn^(II) pre-catalyst.



Scheme 2.30 – Electrochemical dichlorination of alkenes

Dr Benjamin Allen, when subjecting the substrate 1-phenylcyclobutan-1-ol to slightly modified conditions of Lin's reported method, observed formation of a γ -chlorinated ketone product 30% yield by ¹H NMR spectroscopy.

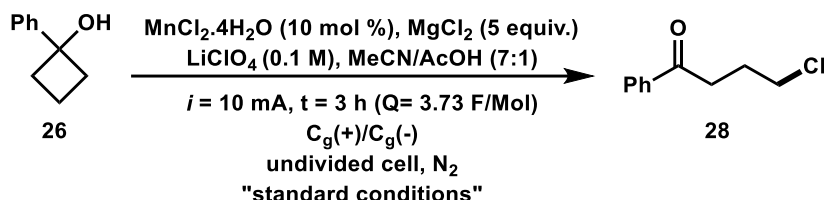


Table 2.5 shows the final optimization table for the deconstructive chlorination of **26**. Dr Benjamin Allen found that an electrochemical system composed of $\text{MnCl}_2 \cdot 4\text{H}_2\text{O}$ (10 mol%) as the catalyst, MgCl_2 (5 equiv.) as the chloride source, and LiClO_4 as the supporting electrolyte in MeCN/AcOH (7:1, [15] = 0.05 M) using galvanostatic conditions ($I = 10 \text{ mA}$, $j_{\text{anode}} = 7.8 \text{ mA/cm}^2$, $Q = 3.73 \text{ F/mol}$) and graphite electrodes at 25°C for 3 h

under N₂, enabled the deconstructive chlorination of **26**, giving γ -chlorinated ketone **28** in an 82% NMR yield (entry **1**). No conversion occurs in the absence of electricity or the manganese catalyst (entries **2** and **3**). Employing a constant cell potential ($E_{\text{cell}} = 2.4$ V) or variation of the current ($I = 12.5$ mA or 7.5 mA) lowered the NMR yield of **17** (entries **4-6**). Employing TBAPF₆ as electrolyte (entry **7**) or substituting the graphite cathode for Pt foil or Ni plate (entries **8** and **9**) each had a negligible impact on conversion. However, upon evaluating alternative Mn(III) salts (entries **10** and **11**), it was found that 97% conversion was obtained using Mn(Otf)₂ as catalyst, which was adopted for further optimization. Employing LiCl or NaCl as the chloride source was detrimental to conversion, presumably due to decreased solubility in MeCN/AcOH (entries **12** and **13**).

Table 2.5 – Optimization table for the electrochemical deconstructive chlorination of cycloalkanols

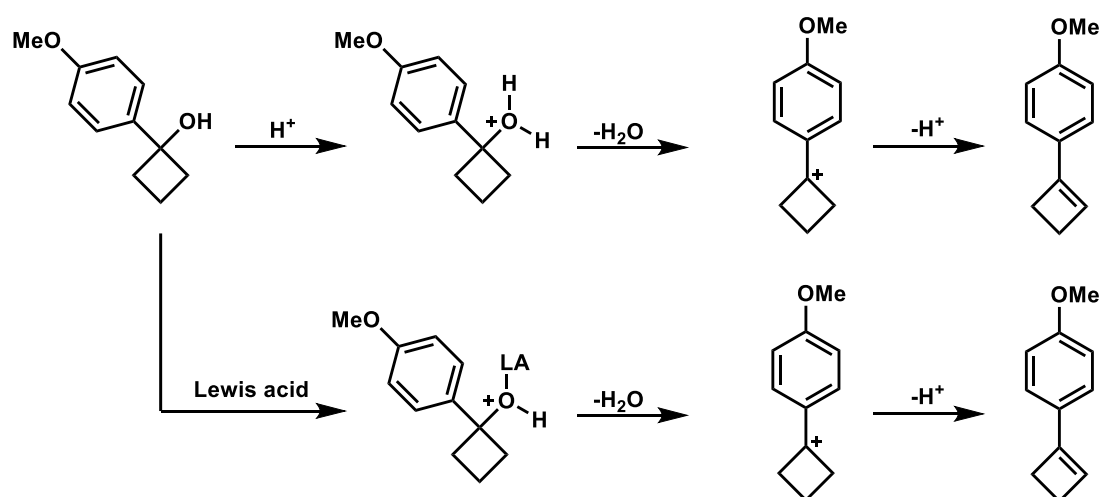
Entry	Variation from “standard” conditions	Yield (%)
1	none	82
2	No electricity	<2
3	no MnCl ₂ ·4H ₂ O	<2
4	$E_{\text{cell}} = 2.4$ V	66
5	$I = 12.5$ mA, $j_{\text{anode}} = 9.8$ mA/cm ²	74
6	$I = 7.5$ mA, $j_{\text{anode}} = 5.9$ mA/cm ²	80
7	TBAPF ₆ instead of LiClO ₄	82
8	Pt foil cathode instead of graphite	82
9	Ni plate cathode instead of graphite	75
10	Mn(Oac) ₂ ·4H ₂ O instead of MnCl ₂ ·4H ₂ O	82
11	Mn(Otf) ₂ instead of MnCl ₂ ·4H ₂ O	97 (78)
12a	LiCl instead of MgCl ₂	64
13 a	NaCl instead of MgCl ₂	<2
14 a	MgCl ₂ (2 equiv)	76
15 a	Mn(Otf) ₂ (5 mol %)	75
16 a,b	$Q = 2$ F/mol	67

Reactions performed with 0.3 mmol of cyclobutanol **15** using the ElectraSyn 2.0 batch electrochemical reactor. [15] = 0.05 M. Yield after 3 h as determined by ¹H NMR analysis of the crude reaction mixture with 1,3,5-trimethylbenzene as the internal standard. Isolated yield given in parentheses. ^aMn(Otf)₂ as catalyst. ^b96 min reaction time.

It was observed that the quantities of MgCl_2 and $\text{Mn}(\text{Otf})_2$ could be lowered to 2 equiv. and 5 mol% respectively, without any significant reduction in conversion (entries **14** and **15**). A Faradaic efficiency of 67% was obtained when 2 F/mol of charge was passed (entry **16**), from which it can be inferred that most of the electricity passing through the electrochemical cell is utilized productively.

From these results obtained from the optimization studies carried out by Dr Benjamin Allen, the conditions of entry **11** was deemed as the “standard conditions”. Comprising of 10 mol% of $\text{Mn}(\text{Otf})_2$ as a pre-catalyst, 5 equiv. of MgCl_2 as the chlorine source, 2 equiv. LiClO_4 as the supporting electrolyte in an MeCN/AcOH (7:1) solvent system at a constant current (i) of 10 mA (current density (j_{anode}) = 7.8 mA/cm^2) employing graphite as both the anode and the cathode for 3 h ($Q = 3.73$ F/mol) under a N_2 atmosphere.

With these optimized conditions in hand, Dr Benjamin Allen, Alex Seastram, and myself began the substrate scope starting with the deconstructive chlorination of cyclobutanols to form γ -functionalized ketones. From the outset, it was found that 1-arylcyclobutan-1-ols containing aromatic systems with electron-releasing groups at the 2- or 4-positions (e.g., 4-*t*Bu, 4-Ome) or extended π -systems (e.g., 4-Ph) underwent decomposition when subjected to the optimized conditions. This instability can be attributed to ionization of the C–OH bond in the presence of Brønsted and/or Lewis acids, forming stabilized carbocations that are unproductive for the desired transformation (scheme 2.31).



Scheme 2.31 – Decomposition of 1-arylcyclobutan-1-ol containing electron-releasing groups at the 4-position in the presence of Brønsted or Lewis acids

To prevent the decomposition of these electron-rich substrates, Dr Benjamin Allen and I again went to optimization. Several parameters were examined to stop or slow down the decomposition such as. These included switching to less Lewis acidic electrolytes, alteration of the proton source and slow addition of substrate to the reaction mixture comprising of $\text{Mn}(\text{OTf})_2$, MgCl_2 , and the electrolyte in the solvent mixture.

2.3.4. Optimization of Substrates with Electron Releasing Substituents

Combined efforts of Dr Benjamin Allen and myself resulted in realisation that employing TBAOAc as a supporting electrolyte increased the yield of the reaction considerably. To further enhance the yield of the product formation, slow addition of the substrate *via* syringe pump was also employed. Addition of the substrate in MeCN (2 mL) to the reaction mixture containing $\text{Mn}(\text{OTf})_2$, MgCl_2 , LiClO_4 in MeCN (3.25 mL) and AcOH (0.75 mL) *via* syringe pump over 2 h yielded in 61% conversion of the product by ^1H NMR spectroscopy. When the supporting electrolyte was changed to TBAOAc, the yield was increased to 80%. Finally, when the substrate was added after 2 minutes of starting the electrolysis 91% conversion by NMR was observed the product was isolated in 80% yield (table 2.6).

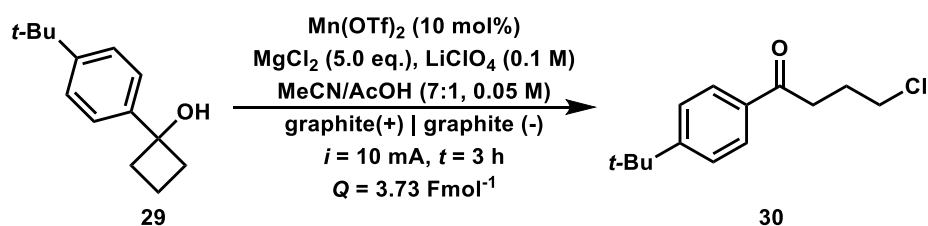
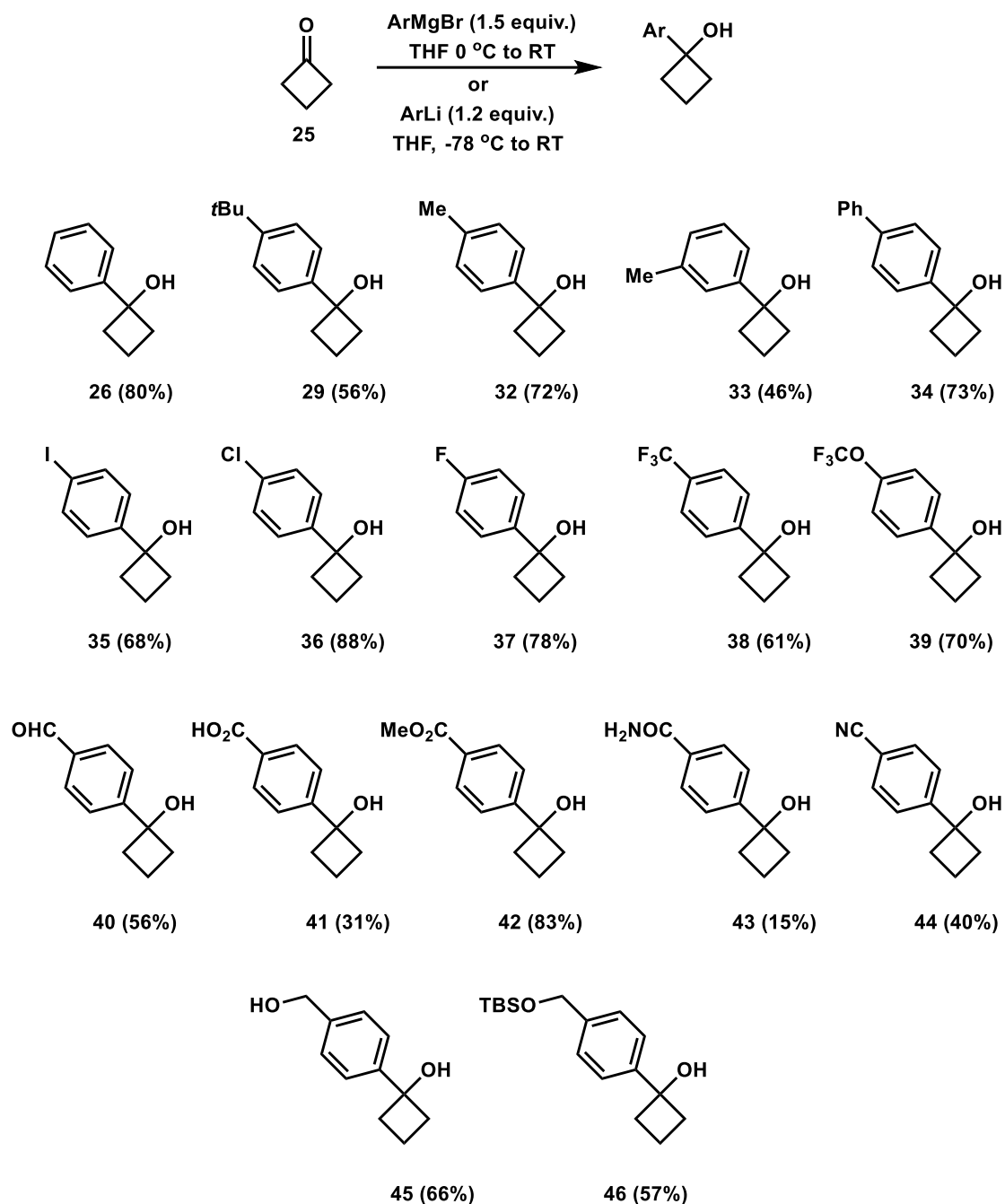


Table 2.6 – Optimization for electron donating aromatic substituent

Entry	Conditions	NMR Yield / %
1	Addition of substrate in MeCN (2 mL) to reaction mixture in MeCN (3.25 mL) and AcOH (0.75 mL) over 2 h	61
2	As in entry 1, but TBAOAc as electrolyte	80
3	As in entry 2, but 2-minute delay between start of electrolysis and addition of substrate	91 (80)

2.3.5. Substrate scope

With a choice of two suitable reaction conditions in hand, the substrate scope was started. A range of 1-arylcyclobutan-1-ols were synthesized by adding either a corresponding Grignard reagent of the desired aryl substituent or halogen-lithium exchange to cyclobutanone **25** (scheme 2.32).

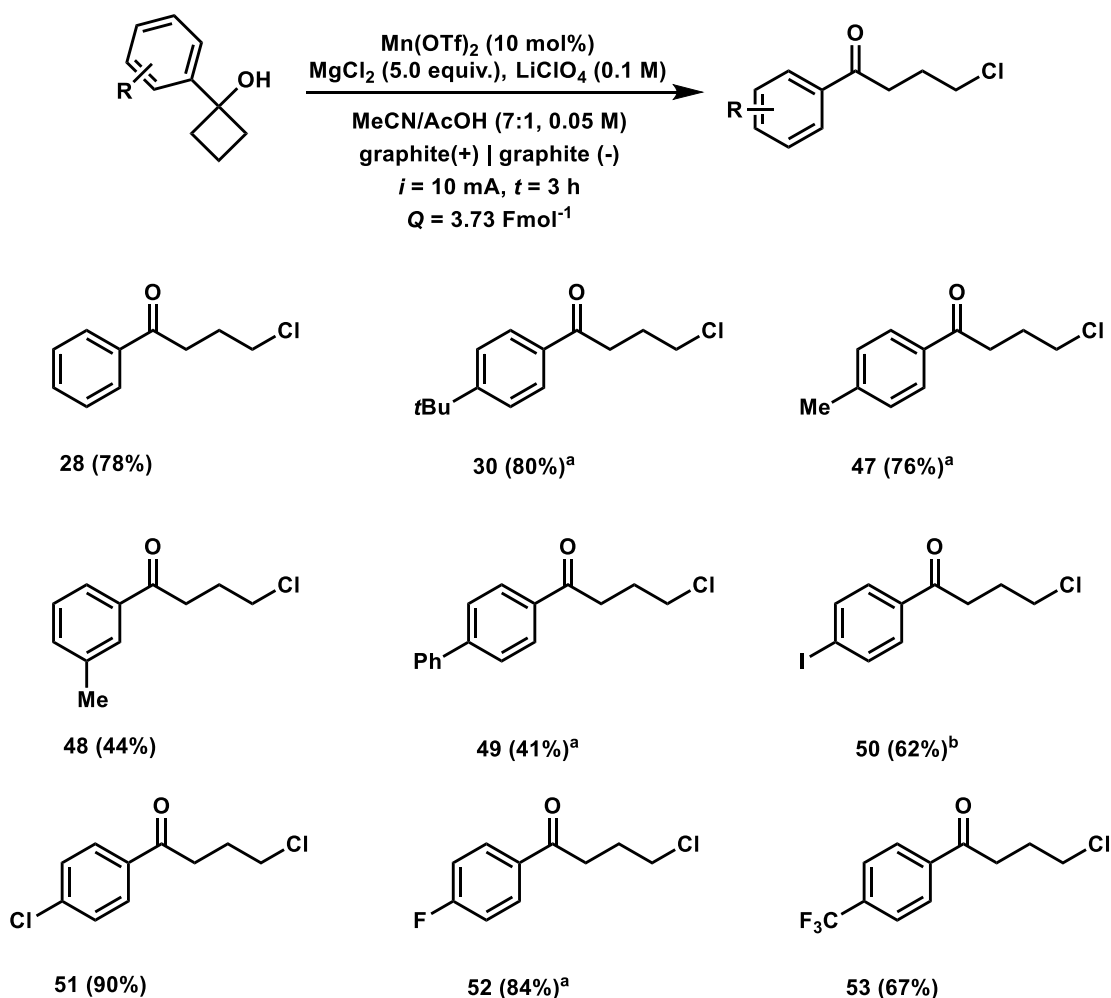


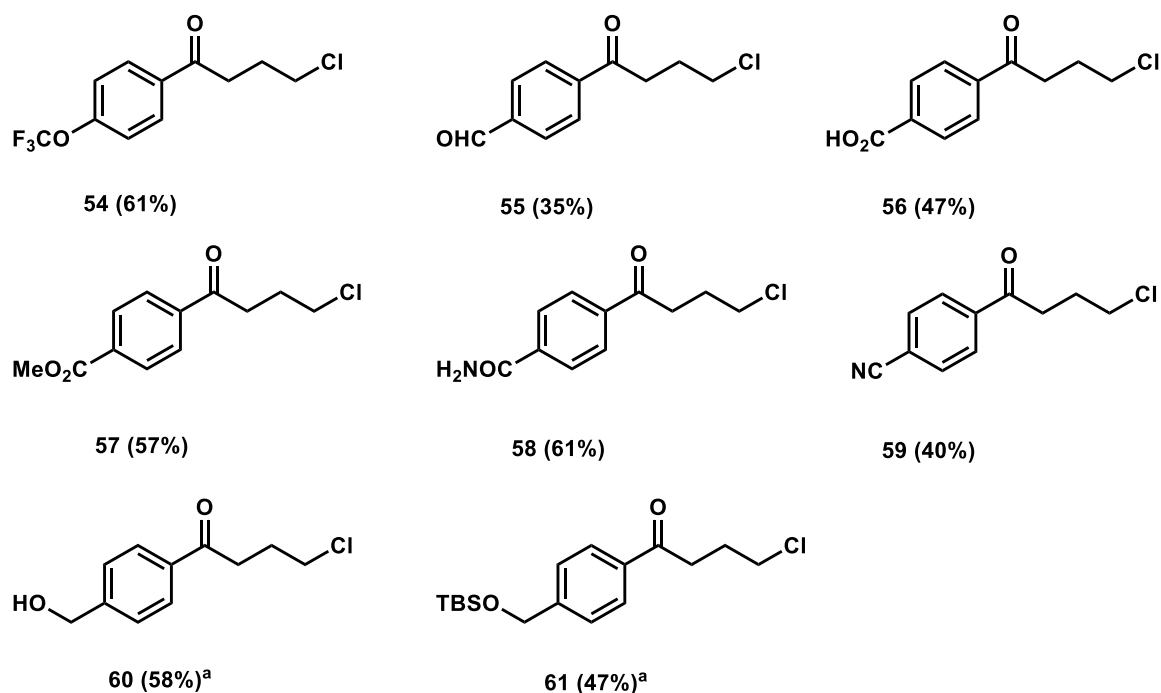
Scheme 2.32 – Synthesized 1-arylcyclobutan-1-ols with variation on aromatic unit

A range 1-arylcyclobutan-1-ols in which electron-releasing substituents at 4-and 2-positions within the aromatic unit were prepared in good to excellent yields (**29**, **32-34**, 80%, 56%, 72%, 46% and 73% respectively). A range of substrates having electron withdrawing group at 4-postion within the aromatic unit were also prepared in good to excellent yields (**35-39**, 68%, 88%, 78%, 61%, and 70% yield respectively).

Aromatic units containing sensitive functional group such as an aldehyde, carboxylic acid, ester, amide, and nitrile were also synthesized in 56%, 31%, 83%, 15%, and 40% respectively. Substrates with a benzyl alcohol and TBS protected benzyl alcohol worked well with yields of 66% and 57% respectively.

With these substrates in hand, they were subjected to the optimized electrochemical conditions indicated in the scheme 2.33.





Reactions performed with 0.3 mmol of cycloalkanol using the ElectraSyn 2.0 batch electrochemical reactor with isolated yields after chromatographic purification quoted. ^aCycloalkanol was added over 2 h via syringe pump, TBAOAc (0.1 M) as electrolyte. ^bTBAOAc (0.1 M) as electrolyte.

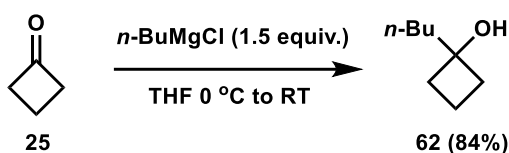
Scheme 2.33 – Substrate scope of 1-arylcyclobutan-1-ol

The substrate scope revealed that, a variety of 1-arylcyclobutan-1-ols containing various substitutions within the aromatic units were well tolerated and yielded γ -chlorinated ketones in moderate to excellent yields. Electron-releasing substituents at the 4-positions within the aromatic unit substrates yielded products **30** and **47** in 80% and 76% yields respectively. Substrate **33**, where the aryl is substituted at the 3-position with a methyl group also yielded product **48** in 44% yield. Substrate **34** is an example of extended π -system and was also tolerated moderately, yielding γ -chlorinated product **49** in 41% yield.

Electron-withdrawing groups at 4-position within the aromatic unit resulted in excellent yields of the products **50-53** in 62%, 90%, 84%, 67% and 61% respectively.

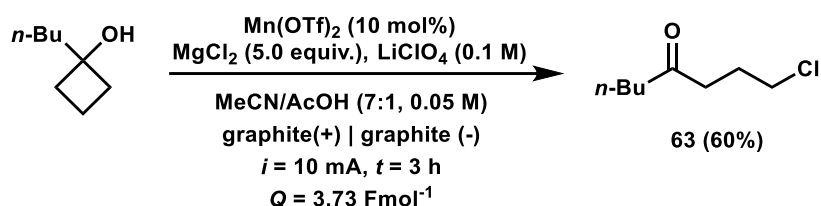
The electrochemical method exhibited good functional group tolerance as demonstrated by the presence of aldehyde **55**, carboxylic acid **56**, methyl ester **57**, primary amide **58**,

nitrile **59**, benzylic primary alcohol **60**, and silyl ether **61** functionalities present in within the products obtained in 35%, 47%, 57%, 61%, 40%, 58% and 47% respectively. No starting material was recovered in the low yielding reactions.



Scheme 2.34 – Synthesis of 1-n-butylcyclobutan-1-ol

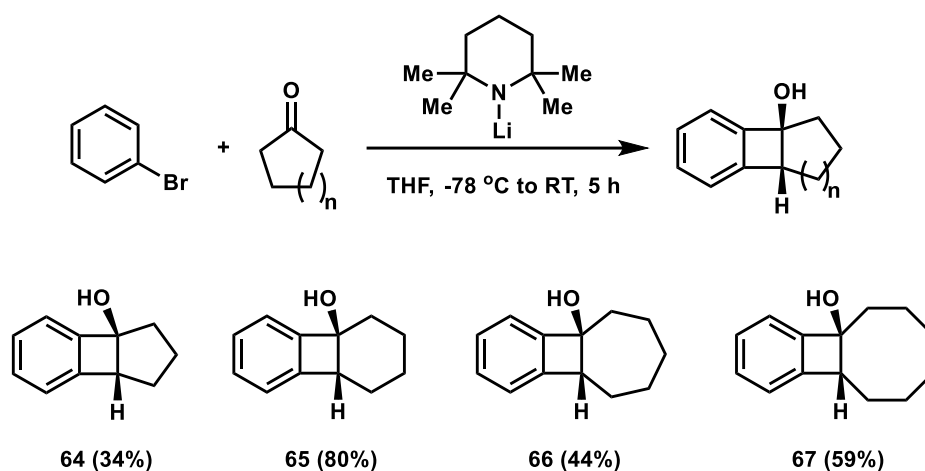
1-n-butylcyclobutan-1-ol **62** was prepared by reacting cyclobutanone with n -butylmagnesium chloride in 84% isolated yield (scheme 2.34).



Scheme 2.35 – Deconstructive chlorination of 1-n-butylcyclobutan-1-ol

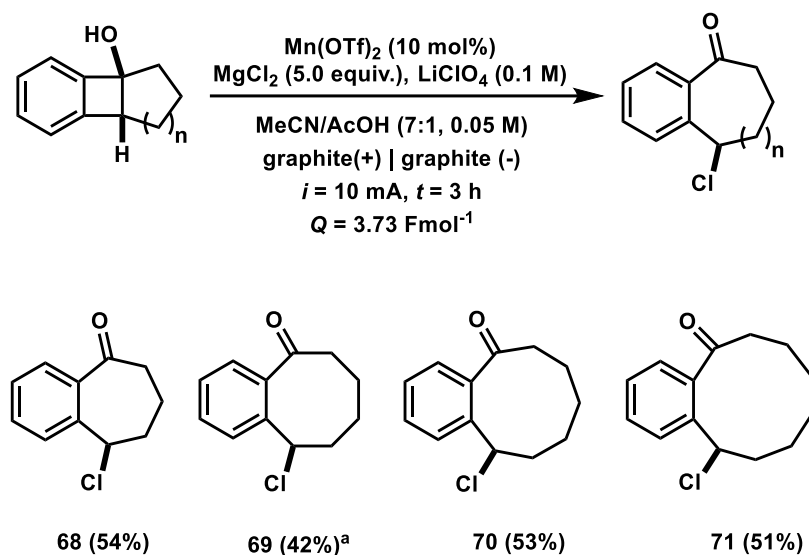
Going from aromatic substitution to alkyl substitution within the cyclobutanols, yielded the γ -chlorinated product **63** in 60% yield (scheme 2.35). This example demonstrated that the electrochemical conditions are tolerant to alkyl substitution as well.

To further demonstrate a wider application of the deconstructive chlorination, benzo-fused cyclobutanols were synthesized by the reaction of benzynes, generated from halobenzenes with lithium tetramethylpiperidide (LTMP) at -78°C , with enolates. Benzo-fused cyclobutanols **64**, **65**, **66**, and **67** containing 5, 6, 7, and 8 membered rings were isolated in 34%, 80%, 44%, and 59% respectively (scheme 2.36).



Scheme 2.36 – Synthesis of benzo-fused cyclobutanols

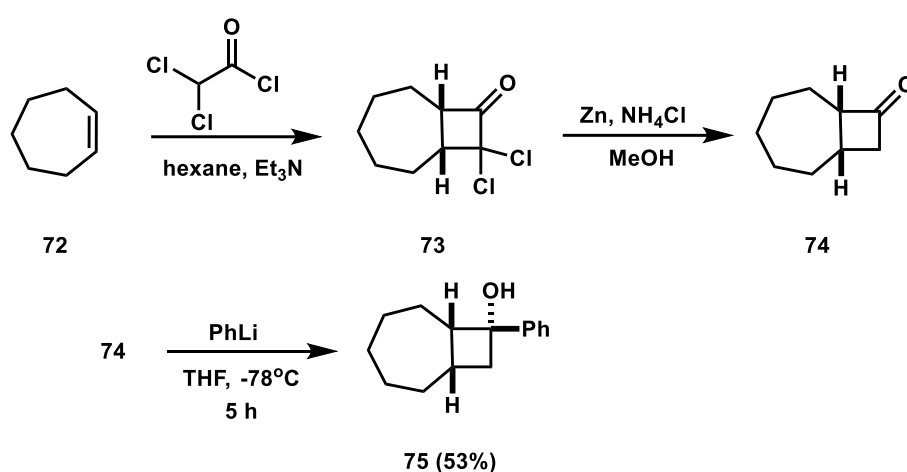
Upon subjecting the benzo-fused cyclobutanols to the optimized electrochemical method, they participated in deconstructive chlorination, affording ring expanded benzyl chloride products **68**, **69**, **70**, and **71** in 54%, 42%, 53%, and 51% respectively (scheme 2.37).



^aCycloalkanol was added over 2 h via syringe pump, TBAOAc (0.1 M) as electrolyte

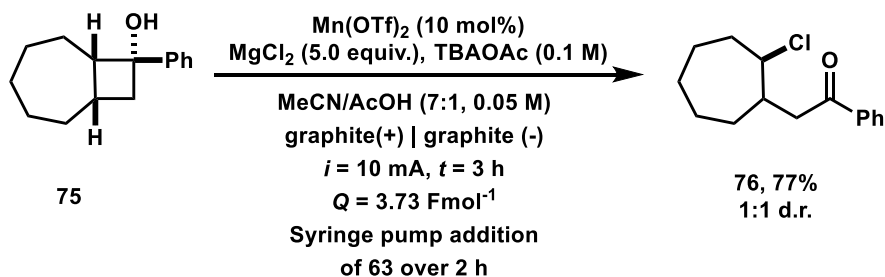
Scheme 2.37 – Deconstructive ring expansion chlorination of benzo-fused cyclobutanols

Furthermore, the ring opening strategy was employed in deconstructive chlorination of bicyclic substrate **75**. This was prepared by a modified three step procedure. Dichloroketone **73** was synthesized by a [2+2] cycloaddition of an in situ generated dichloroketene from dichloroacetyl chloride with cycloheptene **72**. Ketone **74** was obtained after di-dechlorination of **73** with Zn/NH₄Cl. Finally, substrate **75** was obtained by reaction of ketone **74** with phenyllithium in a 53% yield (scheme 2.38).



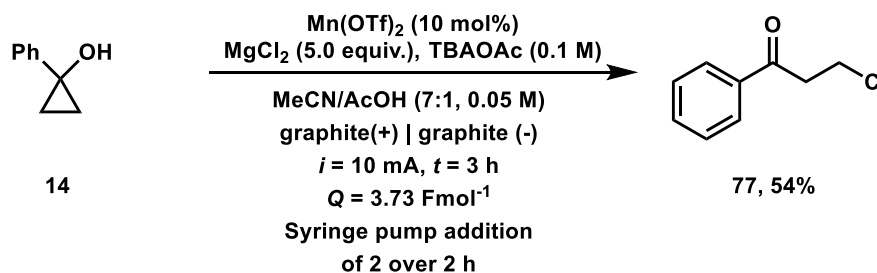
Scheme 2.38 – Synthesis of bicyclic substrate 63

Upon subjecting **75** to the optimized conditions, disubstituted cycloheptane product **76** was obtained in a 77% yield as a mixture of diastereomers (1:1 d.r.) (scheme 2.39).



Scheme 2.39 – Deconstructive chlorination of 8-phenylbicyclo[5.2.0]nonan-8-ol 76

Finally, to complete the substrate scope, deconstructive chlorination of cyclopropanols was demonstrated under the optimized conditions, yielding β -chlorinated product **65** in 54% (scheme 2.40). The syringe pump addition of the substrate helped in overcoming the issue of dehydration of the cycloalkanols as discussed in the section 2.3.4.



Scheme 2.40 – Deconstructive chlorination of cyclopropanol

2.3.6. Flow Electrochemistry – Scale up

To demonstrate the scalability of the reaction, the batch process was translated into a flow electrochemical setup. Tom McBride from Duncan Browne's research group employed the commercially available Ammonite8 flow reactor by Cambridge reactor design (CRD).

Tom McBride evaluated various reaction parameters such as electrolyte loading, temperature, solvent ratio, resident time, charge, and mixing efficiency. However, by using $\text{MnCl}_2 \cdot 4\text{H}_2\text{O}$ (10 mol%) as catalyst, the conversion of **17** could not be increased beyond 20% using single-pass flow electrochemistry (figure 2.3).

Tom McBride then applied the optimized parameters to a recirculating flow electrochemical setup, **17** was isolated in an 84% yield. Due to the decreased distance between the electrodes in flow (0.5 mm) compared to a batch electrochemical setup (1 cm), a supporting electrolyte was not required. A 6-port 2-position switching valve was employed so that the flow system could be redirected from recirculation to the continuous inline purification system that was employed.

This flow setup, designed by Tom McBride, which combines recirculating flow electrochemistry and continuous inline purification for the first time, was able to yield 1.2 g of analytically pure product **17** without the need for purification by chromatography.

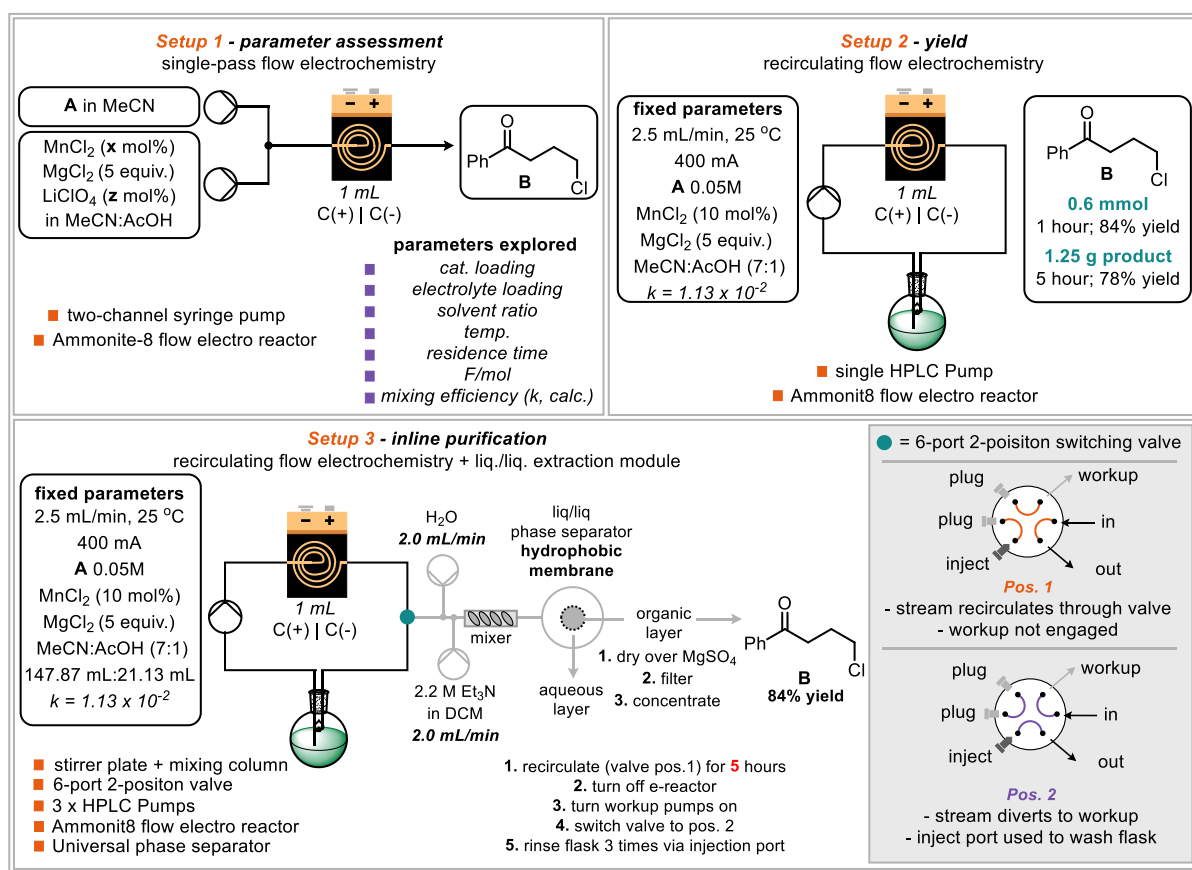
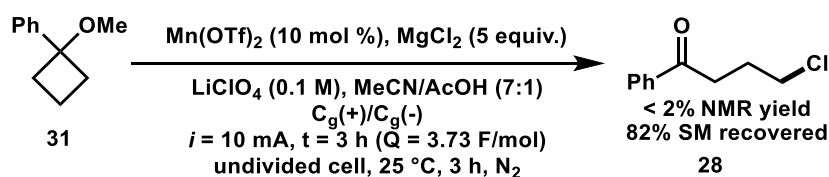


Figure 2.3 – Scale up via Flow Electrochemistry

2.3.7. Mechanistic Studies

To gain the mechanistic insights, Alex Seastram performed cyclic voltametric studies and control experiments.

Alex Seastram subjected the methyl ether of 1-phenylcyclobutan-1-ol **31** in the optimized electrochemical reaction conditions, no γ -chlorinated ketone **28** was observed, and starting material **31** was returned in 82% yield (scheme 2.41).



Scheme 2.41 – Mechanistic probe using methyl ether substrate

This result suggests that a free hydroxyl group is required for the formation of chlorinated product.

Alex Seastram also performed the cyclic voltammetry studies in order to gain mechanistic insight into the electrochemical process. In accordance with literature,⁶³ the combination of $\text{Mn}(\text{OTf})_2$ and MgCl_2 produced a new quasi-reversible redox event at ~ 0.8 V vs Fc/Fc^+ (figure 2.4 left).⁶⁴ This provided evidence for the generation of a $\text{Mn}^{\text{III}}\text{X}_2\text{Cl}$ species from $[\text{Mn}^{\text{II}}\text{X}_2\text{Cl}]^-$. Furthermore, an increase in the oxidation current was observed upon the addition of 15, which suggested that $\text{Mn}^{\text{III}}\text{X}_2\text{Cl}$ is consumed by the substrate (figure 2.5 right)

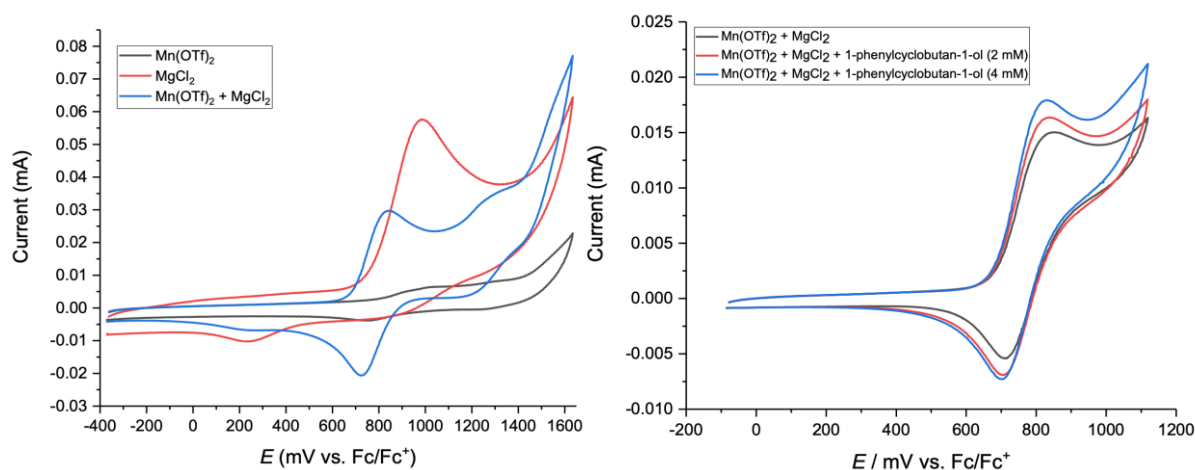


Figure 2.4 left – Cyclic Voltammogram of $\text{Mn}(\text{OTf})_2$, MgCl_2 and their mixture in MeCN/AcOH. (a – black line) $\text{Mn}(\text{OTf})_2$ (2.0 mM); (b – red line) MgCl_2 (8.0 mM); (c – blue line) $\text{Mn}(\text{OTf})_2$ (2.0 mM) and MgCl_2 (8.0 mM) in MeCN with AcOH (60 mM) and LiClO_4 (0.1 M). Scan rate: 100 mV/s. Figure 2.5 right – Cyclic voltammogram of $\text{Mn}(\text{OTf})_2$, MgCl_2 and 1-phenylcyclobutan-1-ol 15 in MeCN/AcOH. (a – black line) $\text{Mn}(\text{OTf})_2$ (2.0 mM) and MgCl_2 (8.0 mM); (b – red line) $\text{Mn}(\text{OTf})_2$ (2.0 mM), MgCl_2 (8.0 mM) and 15 (2.0 mM); (c – blue line) $\text{Mn}(\text{OTf})_2$ (2.0 mM), MgCl_2 (8.0 mM) and 15 (4.0 mM) in MeCN with AcOH (60 mM) and LiClO_4 (0.1 M). Scan rate: 20 mV/s.

2.3.8. Limitations

The deconstructive method worked well for 40 substrates and showed good tolerance of sensitive functional groups to yield β -, γ - and ring expanded chlorinated ketone products from cyclopropanols, cyclobutanols and benzo fused cyclobutanols respectively.

However, the electrochemical method does not tolerate ring sizes greater than 4 with reduced ring strain. For example, when cycloalkanols **78**, **79**, **80**, **81**, and **82** were

subjected to optimized electrochemical conditions found either decomposed (**78**) or were unreactive to yield the desired ring opened ketone products (**79**, **80**, **81**, and **82**) (figure 2.6).

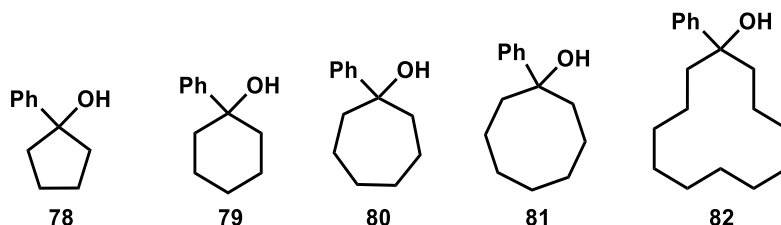


Figure 2.6 – Unreactive substrates

Heterocyclic substituents on the cyclobutanols such as, thiophene (**83**), furan (**84**), pyridine (**85**), and *N*-methyl indole (**86**) gave complex reaction mixtures, when subjected to the electrochemical conditions. It is suspected that the heterocyclic substituted cycloalkanols are unstable in the reaction conditions, as is the case with electron releasing aryl substituents (figure 2.7).

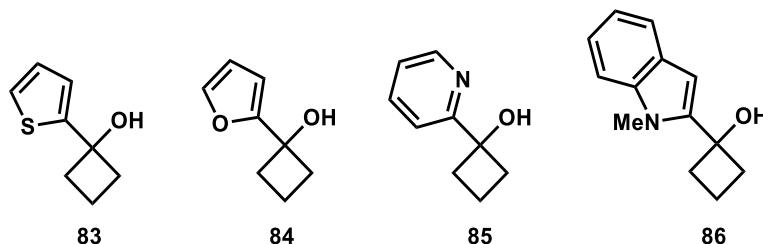
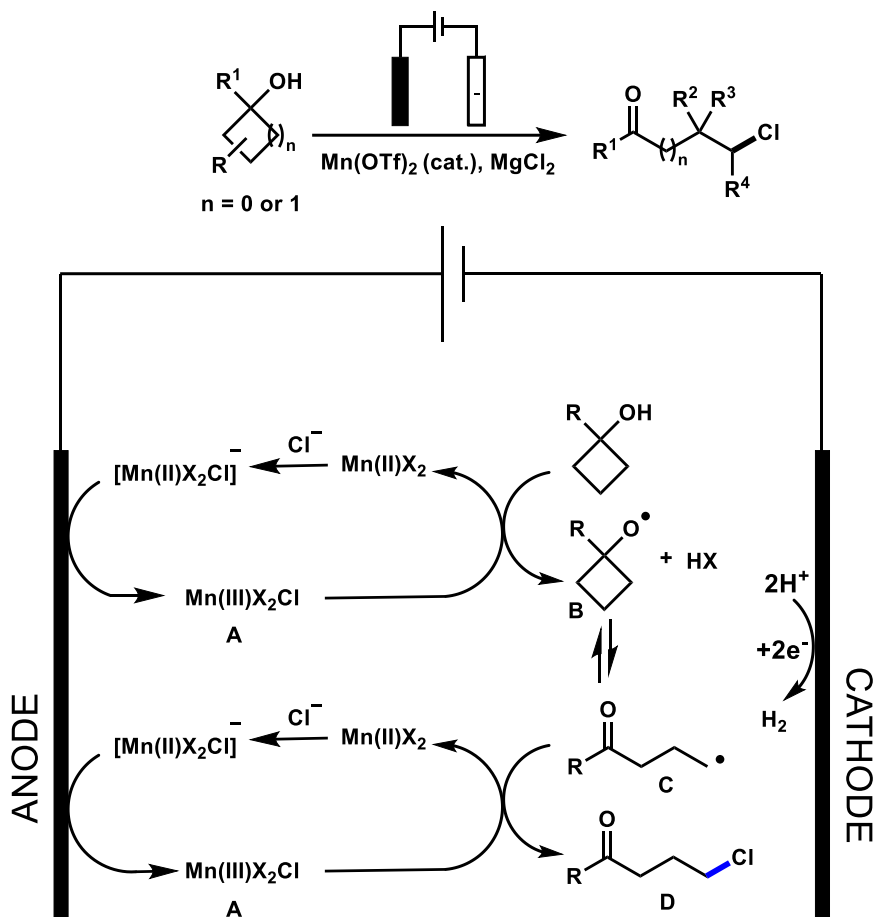


Figure 2.7 – Heterocyclic substituted cyclobutanol

2.3.9. Plausible Mechanism

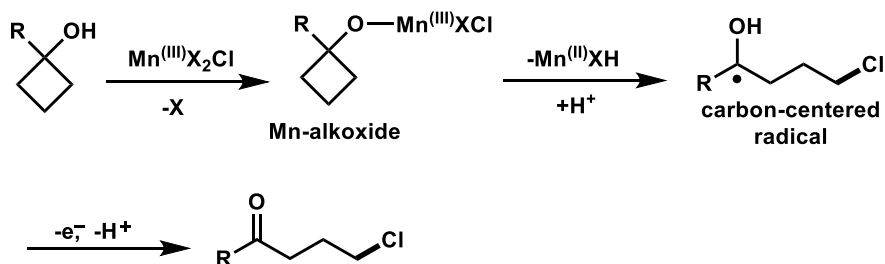
Based on the previous studies,^{63,65} combined with mechanistic studies performed by Alex Seastram, a plausible catalytic turnover of the manganese(III) catalyst can be postulated. The reaction mechanism initiates with the formation of $[\text{Mn}^{\text{II}}\text{X}_2\text{Cl}]^-$ from $\text{Mn}^{\text{II}}\text{X}_2$ and MgCl_2 , which is oxidized at the anode to form $\text{Mn}^{\text{III}}\text{X}_2\text{Cl}$ (scheme 2.41). Intermediate **A** undergoes ligand exchange with the cycloalkanol to form a Mn^{III} alkoxide, with subsequent homolysis generating an alkoxy radical **B**. This can then undergo reversible β -scission to afford a distal *C*-centered radical **C**. Transient radical

intermediate **C** is then trapped with the persistent $\text{Mn}^{\text{III}}\text{X}_2\text{Cl}$ species to form a new C–Cl bond, yielding the product **D**.⁶⁶ Since the larger ring sizes did not yield the distally chlorinated ketone, it is also possible that the Mn^{III} alkoxide is undergoing β -scission due to the inherent ring strain in cyclopropanols and cyclobutanols.



Scheme 2.42 – Plausible mechanism

Scheme 2.42 shows an alternate hypothesis in which the chlorinated ketone could also be formed by Mn^{III} alkoxide promoted β -scission.



Scheme 2.42 – Alternate pathway for the formation of the chlorinated ketones.

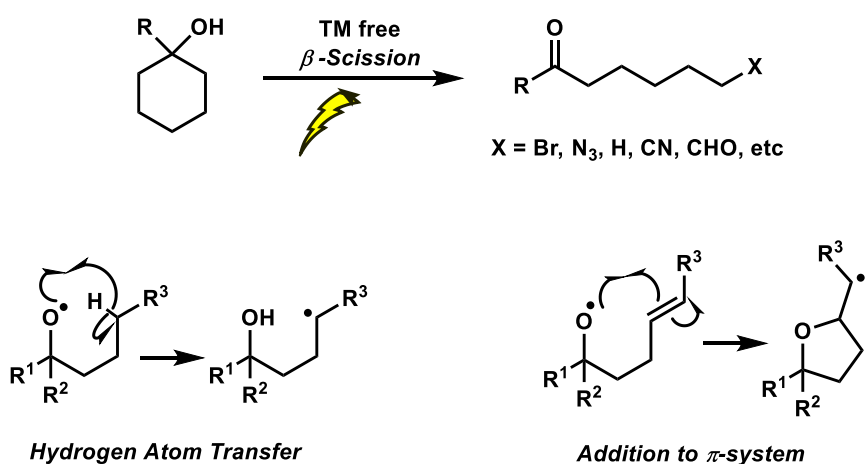
2.4. Future Work

Future work in this area would be to investigate alternate and more generalized methods for the electrochemical generation of alkoxy radicals.

Attempts should be made in the alternate functionalization of the distal C-centered radical formed after β -scission, that could yield synthetically useful products. Dr Benjamin Allen also attempted alternate functionalization such as N₃, CF₃, I, Br, and F. However, these alternate functionalities were not compatible with the Mn catalytic system.

It would also be important to develop an electrochemical method for the generation of alkoxy radicals that excludes the use of transition metals. Employing triaryl amines of suitable redox properties as electron transfer agent would be an interesting approach.⁶⁷

Tapping into different reactivity modes of alkoxy radicals would also be important. This will enhance the prospects of the electrochemical generation and utilization of alkoxy radicals significantly.



Scheme 2.43 – Future Work

It will also be worth to develop single pass flow electrochemical method for scale up, this would make the scale up more efficient which could result into wider acceptance of electrochemical processes in industry.

2.5. Summary

In summary, this chapter demonstrates the efforts made in establishing the proof of concept for the electrochemical generation of alkoxy radicals by exploiting the direct and mediated electrolysis. This includes a “manganese catalyzed electrochemical deconstructive chlorination of cycloalkanols *via* alkoxy radicals” which demonstrates a refined method for the synthesis of β - and γ -chlorinated ketone starting from cyclopropanols and cyclobutanols respectively.⁶⁸ 23 examples of various chlorinated ketones were reported, and range substrates were found to be incompatible.

In context with the aims and objective of this thesis, this work was able to demonstrate a significant improvement over the Nikishin and co-workers previously reported method for the electrochemical methods for the generation of alkoxy radicals. This satisfies the aim to develop methods for the electrochemical generation of alkoxy radicals.

2.6. References

- 1 R. Radi, *PNAS*, 2018, **115**, 5839–5 848.
- 2 J. Hartung, T. Gottwald and K. Špehar, *Synthesis*, **2002**, 11, 1469–1498.
- 3 K. Jia and Y. Chen, *Chem. Commun.*, 2018, **54**, 6105–6112.
- 4 J. J. Guo, A. Hu and Z. Zuo, *Tet. Lett.*, 2018, **59**, 2103–2111.
- 5 P. Gray and A. Williams, *J. Am. Chem. Soc.*, 2018, **140**, 13580–13585.
- 5^a M. Kaino, Y. Naruse, K. Ishihara, and H. Yamamoto, *J. Org. Chem.*, 1990, **55**, 23, 5814–5815.
- 5^b J. Lee, J. Oh, S. Jin, J. Choi, J. L. Atwood, and J. K. Cha, *J. Org. Chem.*, 1994, **59**, 6955-6964
- 6 H. Wieland, *Ber. Dtsch. Chem. Ges.*, 1911, **44**, 2550–2556.
- 7 C. Walling, *Acc. Chem. Res.*, 2002, **8**, 125–131.
- 8 T. M. Ramond, G. E. Davico, R. L. Schwartz and W. C. Lineberger, *J. Chem. Phys.*, 2000, **112**, 1158.
- 9 Ž. Čeković, *Tetrahedron*, 2003, **59**, 8073–8090.

- 9^a K. Heusler, J. Kalvoda, *Angew. Chem., Int. Ed. Engl.*, 1964, **3**, 525-538, 9^b - M.L. Mihailović, Ž. Čeković, *Synthesis*, 1970, 209-224
- 9^c J. Kalvoda, K. Heusler, *Synthesis*, 1971, 501-526
- 9^d M.L. Mihailović, Ž. Čeković, L. Lorenc, W.J. Mijs, C.R.H.I. de Jonge (Eds.), *Oxidations with Lead Tetraacetate in Organic Synthesis by Oxidation with Metal Compounds*, Plenum, New York, 1986, 758-816
- 9^e Rotermund, G.W., *Methoden der Organische Chemie* (Houben-weil), Band 4. Teil 1b, Oxidation II, 204-220, Ed. Muller, E., George Thieme, Stuttgart.
- 9^f Barton, D. H. R.; Beaton, J. M., *J. Am. Chem. Soc.*, 1960, **82**, 2641-2642; Barton, D. H. R.; Beaton, J. M., *J. Am. Chem. Soc.*, 1961, **83**, 4083-4089.
- 9^g C. Walling, A. Padwa, *J. Am. Chem. Soc.*, 1963, **85**, 1597-1601
- 9^h - M.L. Mihailović, Ž. Čeković, J. Stanković, *J. Chem. Soc.*, 1969, 981-982, R.A. Sneen, N.P. Matheny, *J. Am. Chem. Soc.*, 1969, **86**, 3905-3906
- 9ⁱ C. Meystre, K. Heusler, J. Kalvoda, P. Wieland, G. Anner, A. Wettstein, *Helv. Chim. Acta*, 1962, **45**, 1317-1343
- 9^j Close Ž. Čeković, M.M. Green, *J. Am. Chem. Soc.*, 1974, **96**, 3000-3002
- 9^k W.S. Trahanovsky, M.G. Young, P.M. Nave, *Tet. Lett.*, 1969, 2501-2504
- 9^l G. Petrović, Ž. Čeković, *Tet. Lett.*, 1997, **38**, 627-630
- 10 M. Salamone and M. Bietti, *Acc. Chem. Res.*, 2015, **48**, 2895-2903.
- 11 J. Hartung, *Eur. J. Org. Chem.*, 2001, 619-632
- 12 X. Wu and C. Zhu, *Chemical Record*, 2018, **18**, 587-598.
- 13 R. Ren and C. Zhu, *Synlett*, 2016, **27**, 1139-1144.
- 14 D. A. DiRocco, K. Dykstra, S. Krska, P. Vachal, D. v. Conway and M. Tudge, *Angew. Chem.*, 2014, **53**, 4802-4806.
- 15 J. Zhang, Y. Li, F. Zhang, C. Hu and Y. Chen, *Angew. Chem.*, 2016, **55**, 1872-1875.
- 16 C. Wang, K. Harms and E. Meggers, *Angew. Chem.*, 2016, **55**, 13495-13498.
- 17 X. Bao, Q. Wang and J. Zhu, *Angew. Chem.*, 2019, **58**, 2139-2143.
- 18 W. Zheng, C. A. Morales-Rivera, J. W. Lee, P. Liu and M.-Y. Ngai, *Angew. Chem.*, 2018, **57**, 9645-9649.
- 19 J. W. Lee, W. Zheng, C. A. Morales-Rivera, P. Liu and M.-Y. Ngai, *Chem. Sci.*, 2019, **10**, 3217-3222.
- 20 H. G. Yayla, H. Wang, K. T. Tarantino, H. S. Orbe and R. R. Knowles, *J. Am. Chem. Soc.*, 2016, **138**, 10794-10797.
- 21 K. Jia, F. Zhang, H. Huang and Y. Chen, *J. Am. Chem. Soc.*, 2016, **138**, 1514-1517.

- 22 J.-J. Guo, A. Hu, Y. Chen, J. Sun, H. Tang and Z. Zuo, *Angew. Chem.*, 2016, **55**, 15319–15322.
- 23 X. Wu, M. Wang, L. Huan, D. Wang, J. Wang and C. Zhu, *Angew. Chem.*, 2018, **57**, 1640–1644.
- 24 J. Schwarz and B. König, *Chem. Commun.*, 2019, **55**, 486–488.
- 25 G.-X. Li, X. Hu, G. He and G. Chen, *Chem. Sci.*, 2019, **10**, 688–693.
- 26 D. H. R. BARTON, *Pure and Applied Chemistry*, 1968, **16**, 1–16.
- 27 K. Heusler and J. Kalvoda, *Angew. Chem.*, 1964, **3**, 525–538.
- 28 M. Murakami and N. Ishida, *Chem. Lett.*, 2017, **46**, 1692–1700.
- 29 H. Zhao, X. Fan, J. Yu and C. Zhu, *J. Am. Chem. Soc.*, 2015, **137**, 3490–3493.
- 30 N. Ishida, S. Okumura, Y. Nakanishi and M. Murakami, *Chem. Lett.*, 2015, **44**, 821–823.
- 31 S. Ren, C. Feng and T.-P. Loh, *Org. Biomol. Chem.*, 2015, **13**, 5105–5109.
- 32 Q. Tian, B. Chen and G. Zhang, *Green Chem.*, 2016, **18**, 6236–6240.
- 33 Y.-F. Wang and S. Chiba, *J. Am. Chem. Soc.*, 2009, **131**, 12570–12572.
- 34 Y. Zhu, K. Huang, J. Pan, X. Qiu, X. Luo, Q. Qin, J. Wei, X. Wen, L. Zhang and N. Jiao, *Nat. Commun.*, 2018, **9**, 2625.
- 35 X. Wu and C. Zhu, *Chin. J. Chem.*, 2019, **37**, 171–182.
- 36 S. Bloom, D. D. Bume, C. R. Pitts and T. Lectka, *Chem. Eur. J.*, 2015, **21**, 8060–8063.
- 37 V. Balzani, P. Ceroni, A. Juris, *Photochemistry and Photophysics: Concepts, Research, Applications*, Wiley-VCH, 2014.
- 38 E. Tsui, H. Wang and R. R. Knowles, *Chem. Sci.*, 2020, **11**, 11124–11141.
- 39 J.-J. Guo, A. Hu, Y. Chen, J. Sun, H. Tang and Z. Zuo, *Angew. Chem.*, 2016, **55**, 15319–15322.
- 40 A. Hu, J.-J. Guo, H. Pan, H. Tang, Z. Gao and Z. Zuo, *J. Am. Chem. Soc.*, 2018, **140**, 1612–1616.
- 41 A. Hu, Y. Chen, J.-J. Guo, N. Yu, Q. An and Z. Zuo, *J. Am. Chem. Soc.*, 2018, **140**, 13580–13585.
- 42 A. Hu, J. J. Guo, H. Pan and Z. Zuo, *Science*, 2018, **361**, 668–672.
- 43 Q. An, Z. Wang, Y. Chen, X. Wang, K. Zhang, H. Pan, W. Liu and Z. Zuo, *J. Am. Chem. Soc.*, 2020, **142**, 6216–6226.
- 44 A. Hu, Y. Chen, J.-J. Guo, N. Yu, Q. An and Z. Zuo, *J. Am. Chem. Soc.*, 2018, **140**, 5.

- 45 A. Wiebe, T. Gieshoff, S. Möhle, E. Rodrigo, M. Zirbes and S. R. Waldvogel, *Angew. Chem.*, 2018, **57**, 5594–5619.
- 46 K. D. Moeller, *Chem. Rev.*, 2018, **118**, 4817–4833.
- 47 M. D. Kärkäs, *Chem. Soc. Rev.*, 2018, **47**, 5786–5865.
- 48 M. Yan, Y. Kawamata and P. S. Baran, *Chem. Rev.*, 2017, **117**, 13230–13319.
- 49 M. G. Dolson¹ and J. S. Swenton, *J. Am. Chem. Soc.*, 1981, **103**, 1981.
- 50 M. C. Carreño and M. Ribagorda, *J. Org. Chem.*, 2000, **65**, 1231–1234.
- 51 T. Sumi, T. Saitoh, K. Natsui, T. Yamamoto, M. Atobe, Y. Einaga and S. Nishiyama, *Angew. Chem.*, 2012, **51**, 5443–5446.
- 52 T. Saitoh, E. Suzuki, A. Takasugi, R. Obata, Y. Ishikawa, K. Umezawa and S. Nishiyama, *Bioorganic & Medicinal Chem. Lett.*, 2009, **19**, 5383–5386.
- 53 S. Yajima, T. Saitoh, K. Kawa, K. Nakamura, H. Nagase, Y. Einaga and S. Nishiyama, *Tetrahedron*, 2016, **72**, 8428–8435.
- 54 A. Ilangoan, S. Saravanakumar and S. Malayappasamy, *Org. Lett.*, 2013, **15**, 4968–4971.
- 55 R. Ren, Z. Wu and C. Zhu, *Chem. Commun.*, 2016, **52**, 8160–8163.
- 56 D. Wang, R. Ren and C. Zhu, *J. Org. Chem.*, 2016, **81**, 8043–8049.
- 57 Y. Wang, S. Chiba and M. Sciences, 2009, 10–12.
- 58 Y. F. Wang, K. K. Toh, E. P. J. Ng and S. Chiba, *J. Am. Chem. Soc.*, 2011, **133**, 6411–6421.
- 59 S. Chiba, Z. Cao, S. A. A. el Bialy and K. Narasaka, *Chem. Lett.*, 2005, **35**, 18–19.
- 60 Iwasawa N, Funahashi M, Hayakawa S and Narasaka K, *Chem. Lett.*, 1993, 545–548.
- 61 L. Huan and C. Zhu, *Org. Chem. Front.*, 2016, **3**, 1467–1471.
- 62 J. Yu, H. Zhao, S. Liang, X. Bao and C. Zhu, *Org. Biomol. Chem.*, 2015, **13**, 7924–7927.
- 63 N. Fu, G. S. Sauer and S. Lin, *J. Am. Chem. Soc.*, **139**, 15548–15553.
- 64 C. Sandford, M. A. Edwards, K. J. Klunder, D. P. Hickey, M. Li, K. Barman, M. S. Sigman, H. S. White and S. D. Minter, *Chem. Sci.*, 2019, **10**, 6404–6422.
- 65 N. Fu, Y. Shen, A. R. Allen, L. Song, A. Ozaki and S. Lin, *ACS Catal.*, 2019, **9**, 746–754.
- 66 A. Studer, *Chem. Eur. J.*, 2011, **6**, 7.
- 67 R. Francke and R. D. Little, *Chem. Soc. Rev.*, 2014, **43**, 2492–2521.

68 Y. N. Ogibin, M. N. Elinson and G. I. Nikishin, *Russ. Chem. Rev.*, 2009, **78**, 89–140.

“Nothing in the world can take the place of persistence.

Talent will not; nothing is more common than unsuccessful men with talent.

Genius will not; unrewarded genius is almost a proverb.

Education will not; the world is full of educated derelicts.

Persistence and determination alone are omnipotent.”

Calvin Coolidge (1872–1933), U.S. President

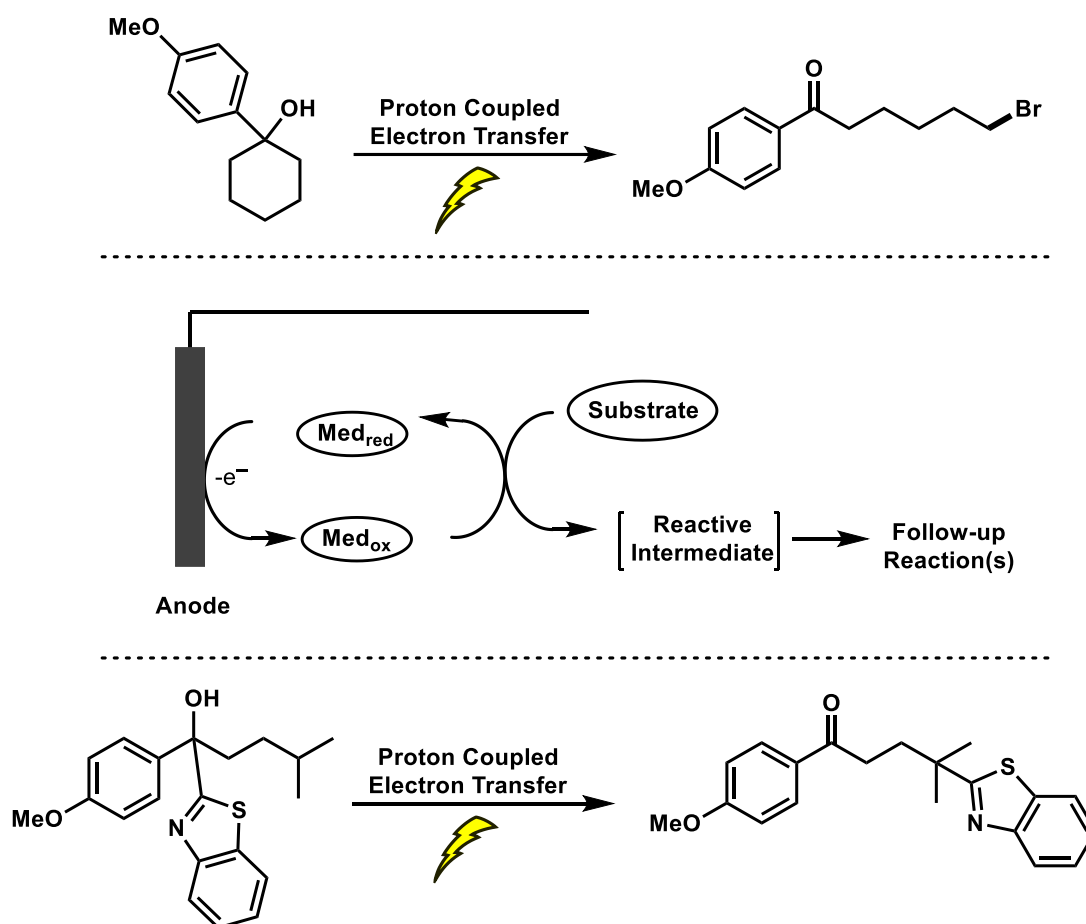
Chapter 3: Application of Proton-Coupled Electron Transfer (PCET) in the Generation and Utilization of Alkoxy Radicals

3. Preface

This chapter describes work that addresses the limitations encountered in chapter 2 in the electrochemical generation of alkoxy radicals, and discusses the advancements made into increasing the overall utility of the electrochemical β -scission of cycloalkanols *via* alkoxy radical intermediates.

A range of triarylamine and imidazole based organic redox mediators were screened as potential electron transfer agents. Electron rich aromatic units installed on the cycloalkanols were oxidized by the redox mediator to induce Proton Coupled-Electron Transfer (PCET) for the successive generation of an alkoxy radical.

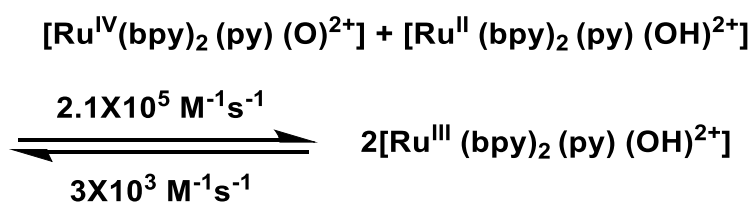
The batch electrochemical method was translated into flow electrochemical setup for scale up. After initial optimization in recirculating flow set up, a single pass flow method has additionally been demonstrated.



3.1. Introduction

Electron transfer (ET) and proton transfer (PT) are the most fundamental and ubiquitous processes in nature as well as in chemistry. Many reactions found in organic, biological, inorganic, environmental, and other areas of chemistry exhibit the transfer of both protons and electrons. Reactions in which a proton and an electron are both transferred in a concerted manner can be classified as a Proton-Coupled Electron Transfer (PCET).¹

The term PCET was coined in 1981 by Meyer and co-workers to describe a concerted transfer of electron and proton that was observed in the comproportionation reaction between $\text{Ru}^{\text{IV}}(\text{bpy})_2(\text{py})(\text{O})^{2+}$ ($\text{Ru}^{\text{IV}}=\text{O}^{2+}$) and $\text{Ru}^{\text{II}}(\text{bpy})_2(\text{py})(\text{OH})^{2+}$ ($\text{Ru}^{\text{II}}=\text{O}^{2+}$) (scheme 3.1).

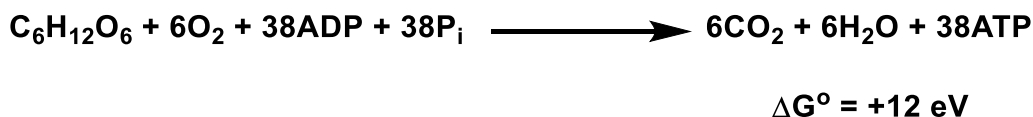


Scheme 3.1 – Comproportionation reaction

In this reaction an electron and proton are transferred simultaneously from ($\text{Ru}^{\text{II}}=\text{O}^{2+}$) to ($\text{Ru}^{\text{IV}}=\text{O}^{2+}$) to give $2 \text{Ru}^{\text{III}}-\text{OH}^{2+}$.²

A plethora of reactions can be found in nature in which multielectron and multiproton PCET half reactions are exploited for energy storage and conversion. Photosynthesis is one of the most important examples in which light-driven reduction of CO_2 by water results in the synthesis of carbohydrates. The reverse of photosynthesis in which the oxidation of glucose by oxygen occurs releasing energy also exploits PCET (scheme 3.2).³

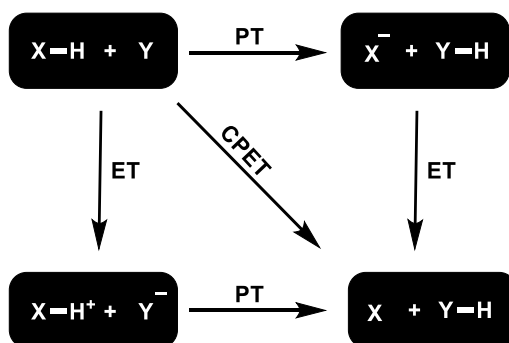
Photosynthesis is a spectacle of PCET at work, where the transfer of 24 electrons and 24 protons driven by 48 photons.



Scheme 3.2 – PCET in photosynthesis

3.1.1. Definition and Thermochemistry of PCET

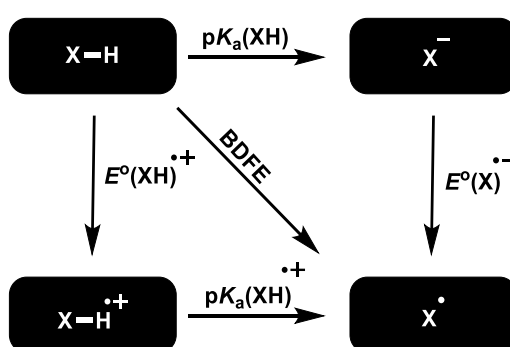
PCET is generally defined as a concerted electron (e^-)/ proton (H^+) transfer which is comprised of electron transfer (ET), proton transfer (PT), electron-proton transfer (EPT), multisite EPT, hydrogen atom transfer (HAT) and hydride transfer ($2e^-/1H^+$) as available elementary steps (scheme 3.3).³



Scheme 3.3 – Elementary steps and PCET

Knowing the thermochemistry of each elementary steps in PCET process is indispensable. It would be impossible to rationalize an electron transfer or proton transfer without knowing the relevant redox potentials (E 's) or acidities (pK_a 's). To a large extent this is also critical for PCET.

Thermochemistry of a PCET reaction is the sum of its constituent ET and PT steps. For a $1\text{ e}^-/\text{H}^+$ PCET reagent XH in a given solvent is described by five parameters as shown in scheme 3.4. These are the acidity/basicity of the oxidized and reduced forms, given by the pK_a s of $\text{XH}^{\bullet+}/\text{X}^\bullet$ and XH/X^- pairs. Also involved is the reduction potentials of the protonated and deprotonated substrate, $E^\circ[\text{XH}^{\bullet+}/\text{XH}]$ and $E^\circ[\text{X}^\bullet/\text{X}^-]$, and finally the homolytic bond dissociation free energy (BDFE) (scheme 3.4).



Scheme 3.4 – Thermochemical square for a PCET reagent

All of these parameters are free energies and can be converted into the same units (scheme 3.5). In the equations 1 and 2 R is the gas constant, T is the temperature, and F is the Faraday constant). E° is the free energy of the chemical reaction and is the sum of the half reaction of interest, such as $\text{X}^\bullet + \text{e}^- \rightarrow \text{X}^-$, and the half reaction for the standard redox couple (NHE for aqueous values). For a reaction such as $\text{HX} + \text{Y} \rightarrow \text{X} + \text{HY}$, the pK_a and E° values for the HX and HY systems determine the free energies of PT, ET, and H^\bullet transfer steps.

$$\Delta G^\circ_{\text{PT}} = -RT \ln(K_a) = 2.303RT(\text{pK}_a) = -(1.37 \text{ kcal mol}^{-1})\text{pK}_a \quad (1)$$

$$\Delta G^\circ_{\text{ET}} = -FE^\circ = -(23.06 \text{ kcal mol}^{-1} \text{ V}^{-1})E^\circ \quad (2)$$

Scheme 3.5 – Free energies of PT and ET steps

The pK_a and E° values can be determined by titration either vs pH (in aqueous media) or vs a standard acid or base (in organic solvents). The redox potentials ($E_{1/2}$) are typically determined electrochemically by taking the average of the anodic and cathodic peaks in a cyclic voltammogram. Redox potentials are a good measure for the thermodynamic potential (E°).

Hence the BDFE of the PCET reagent XH can be calculated by adding the free energies of PT and ET steps (scheme 3.6).

$$\text{BDFE (X-H)} = 1.37pK_a + 23.06 E^\circ + C_g(\text{solvent}) \quad (3)$$

Scheme 3.6 – BDFE equation

C_g is the solvation energy equivalent to the H^+/H^\bullet standard reduction potential in that solvent. The values of C_g for some of the frequently employed solvents are as follows: MeCN (54.9), DMSO (71.1), DMF (69.7), Methanol (65.3), and Water (57.6).

PCET is thermochemically more favorable than the first step in competing consecutive processes involving stepwise ET and PT.

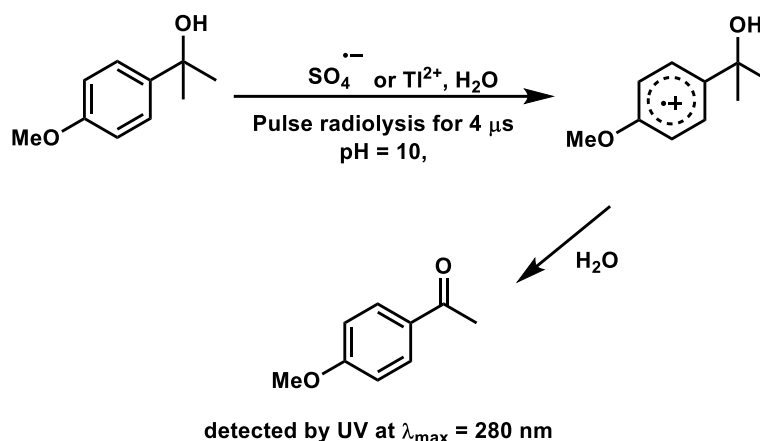
Hence by carefully selecting the pK_a and E° values for any given redox system, it is possible to overcome the thermodynamic bias posed by the series of elementary steps involved in the formation of X^\bullet by the homolytic bond dissociation of X-H.

3.1.2. Exploitation of PCET in the Generation of Alkoxy Radicals

As discussed in the chapter 2, the limiting factor in the generation of alkoxy radicals from alcohols is the high BDFEs ~ 105 kcal/mol. PCET presents an intriguing opportunity in the development of new methodologies involving the homolytic activation of O–H bonds.

In oxidative PCET reactions a one-electron oxidant and a Brønsted base function together to abstract proton and an electron from a substrate in a concerted elementary step.

Steenkeen and co-workers first reported that the O–H bonds of alcohols adjacent to arene radical cations undergo selective deprotonation to furnish alkoxy radical intermediates (scheme 3.7).⁴ The authors speculated that a PCET event could be the mechanistic explanation for this observation.

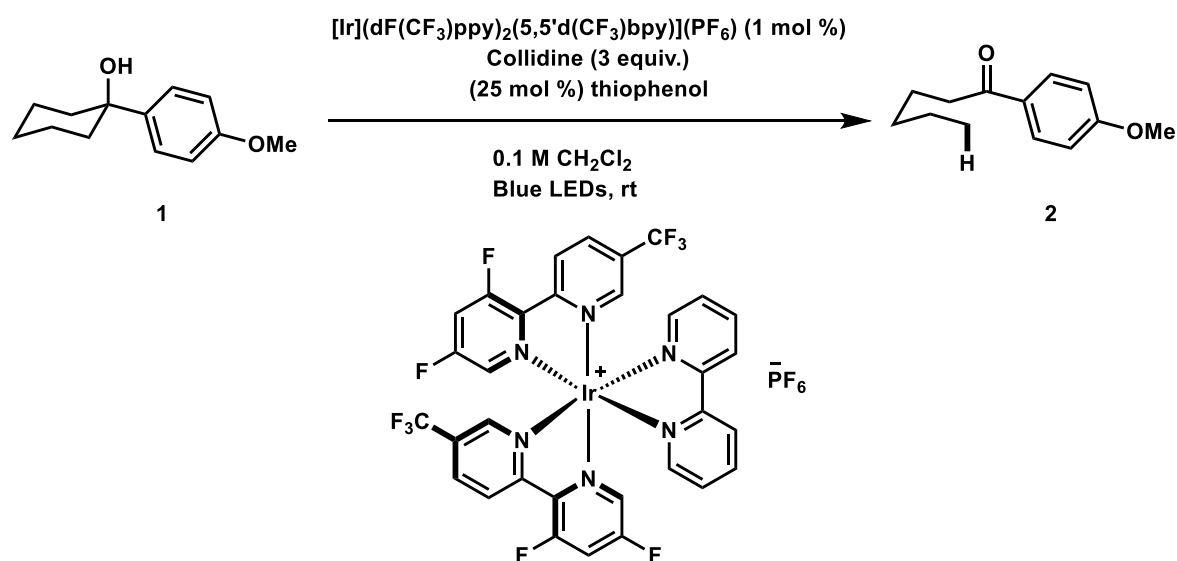


Scheme 3.7 – Pulse radiolysis of 4-methoxycumyl alcohol

When 4-methoxycumyl alcohol was subjected to pulse radiolysis for 4 μs in water using $\text{SO}_4^{\bullet-}$ or TI^{3+} as an oxidant at $\text{pH} = 10$, formation of 4-methoxyacetophenone was observed at $\lambda_{\text{max}} = 280 \text{ nm}$.

The authors rationalized that the formation of 4-methoxyacetophenone occurs *via* the deprotonation of the OH group of the 4-methoxycumyl radical cation by OH^- . This is then followed by an electron transfer which generates the 4-methoxycumyl alkoxy radical. The alkoxy radical thus formed could then undergo a β -scission to yield 4-methoxyacetophenone.

Knowles and co-workers built on these preliminary results and reported an elegant new photocatalytic protocol for the redox neutral isomerization of cycloalkanols to ketones *via* β -scission. In this approach, by varying the oxidant and base independently, the thermochemistry of PCET process can be tuned as per the BDFE of the substrate (scheme 3.8).⁵



Scheme 3.8 – Photocatalytic activation of cycloalkanols via PCET

The authors reported optimized reaction conditions comprised of 1 mol% of iridium catalyst as an oxidant, 3 equiv. of collidine as a Brønsted base, 25 mol% of thiophenol as a hydrogen atom donor in DCM. The irradiation of the reaction mixture with blue LED light at room temperature resulted in the desired ring opened product **2** in 91% by ^1H NMR analysis.

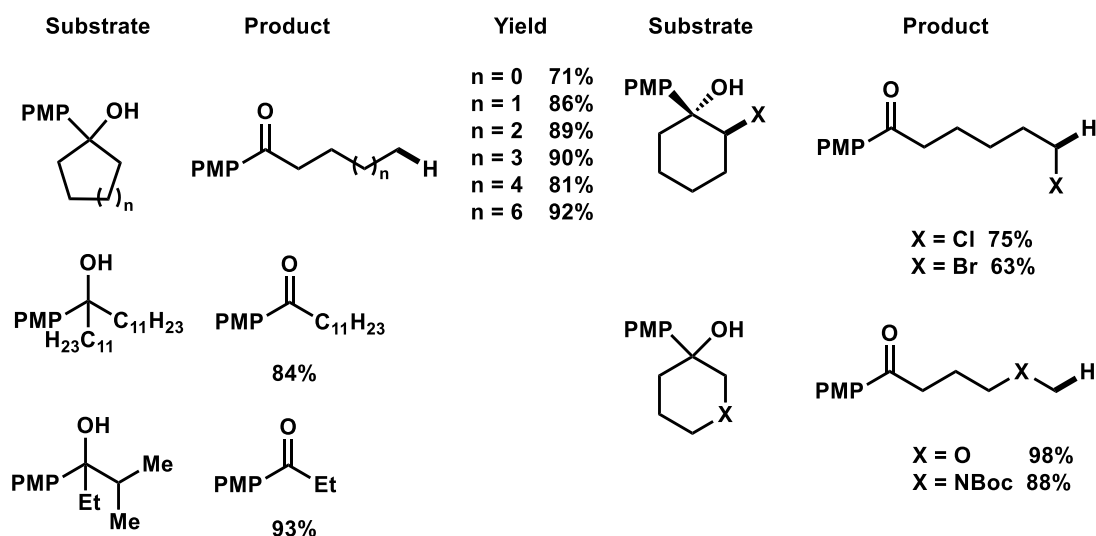
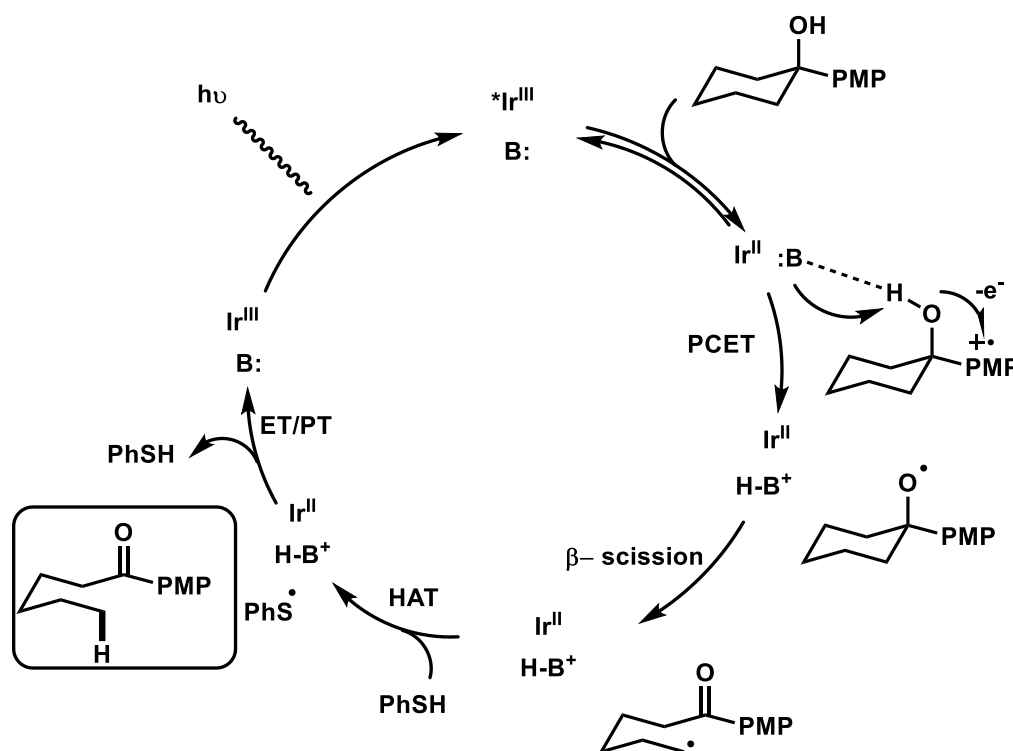


Figure 3.1 – Substrate scope

The authors reported more than 33 examples of various ring sizes with varying substitution on the ring (fig 3.1).

Mechanistically, the authors suggested a photocatalytic cycle starting with the irradiation of the photocatalyst Ir^{III} ($E_{1/2} = 1.30$ V vs Fc/Fc⁺) to its excited state, which then oxidizes the electron rich para methoxyphenyl (PMP) ring of the tertiary cycloalkanol starting material ($E_{p/2} = 1.22$ V vs Fc/Fc⁺). The PMP radical cation thus formed now acts as an internal oxidant and in a single kinetic step the Brønsted base abstracts the O–H proton and the electron is transferred to the PMP radical cation. This results in the generation of an alkoxy radical which undergoes a β -scission process to furnish the distal C-centered radical, which is intercepted by the H atom donor affording the ketone product.



Scheme 3.9 – Proposed catalytic cycle

Finally, reduction of the thiophenol radical by the reduced state of the photocatalyst (Ir^{II}) and protonation by the conjugate acid of the Brønsted base completes the catalytic cycle (scheme 3.9).

The authors also compared the effective BDFE of the oxidant/base combination to that of substrates (cycloalkanols) to rationalize the formation of ring opened ketone products. They observed that when the effective BDFE of the oxidant/base combination approaches or exceeds that of the substrate (O-H BDFE ~ 102 kcal/mol), the reactions yielded the desired ketone products. Little or no ring opened products were observed when the effective BDFEs is less than ~98 kcal/mol (figure 3.2).

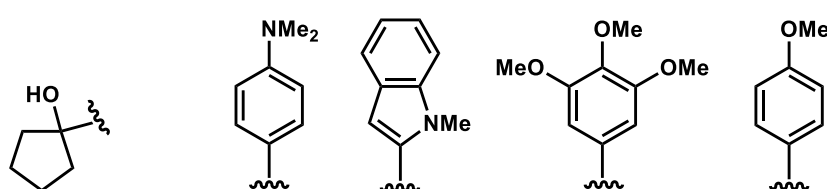
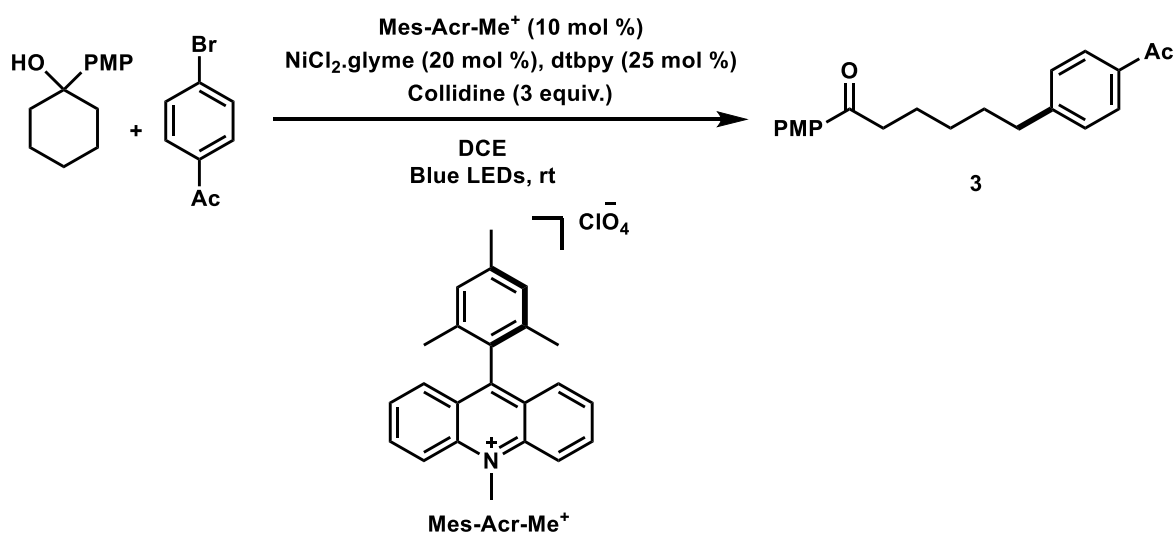
					
Base	$E_{p/2}$ (v)	0.39	0.69	0.92	1.22
2-MeO-pyridine $pK_a = 9.9$	BDFE	77	84	90	97
	Yield (%)	0	0	0	0
pyridine $pK_a = 12.5$	BDFE	81	88	93	100
	Yield (%)	0	0	0	16
CF_3COO^- $pK_a = 12.5$	BDFE	81	88	93	100
	Yield (%)	0	0	0	87
collidine $pK_a = 15$	BDFE	84	91	97	104
	Yield (%)	0	0	<5	86

Figure 3.2 – Effective BDFE correlations with reactivity

The effective BDFE can be calculated by plugging the respective values of pK_a of different bases and $E_{p1/2}$ of substrates using equation from scheme 3.6.

$$\text{BDFE (O-H)} = 1.37pK_a (\text{base}) + 23.06 E_{p/2} (\text{Ar}^{0/.+}) + 54.9 C_g(\text{MeCN})$$

Rueping and co-workers have extended the PCET enabled activation of O–H bonds approach by employing Nickel-catalyzed cross coupling in the functionalization of the C-centered radical formed after the β -scission of the cycloalkanols (scheme 3.10).⁶

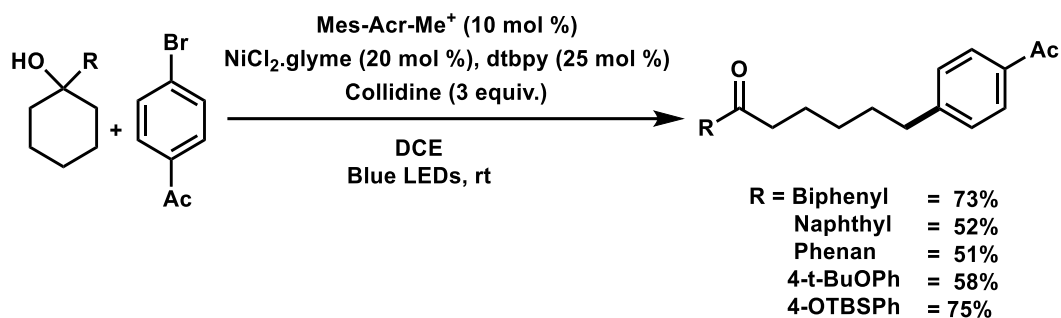


Scheme 3.10 – Nickel catalyzed cross-coupling arylation via PCET

In this publication the site-specific arylation of ketones *via* the combination of photoredox-mediated multisite concerted proton–electron transfer (MS-PCET) and nickel catalysis was reported. The reaction conditions are comprised of 10 mol% of Arc-Mes photocatalyst as an oxidant, 20 mol% NiCl₂.glyme, 25 mol% of dtbpy, 3 equiv. of collidine as base, 3 equiv. of cycloalkanol, 1 equiv. of aryl halide in DCE. When irradiated with blue LEDs the reaction afforded the ketone **3** in 85% isolated yield.

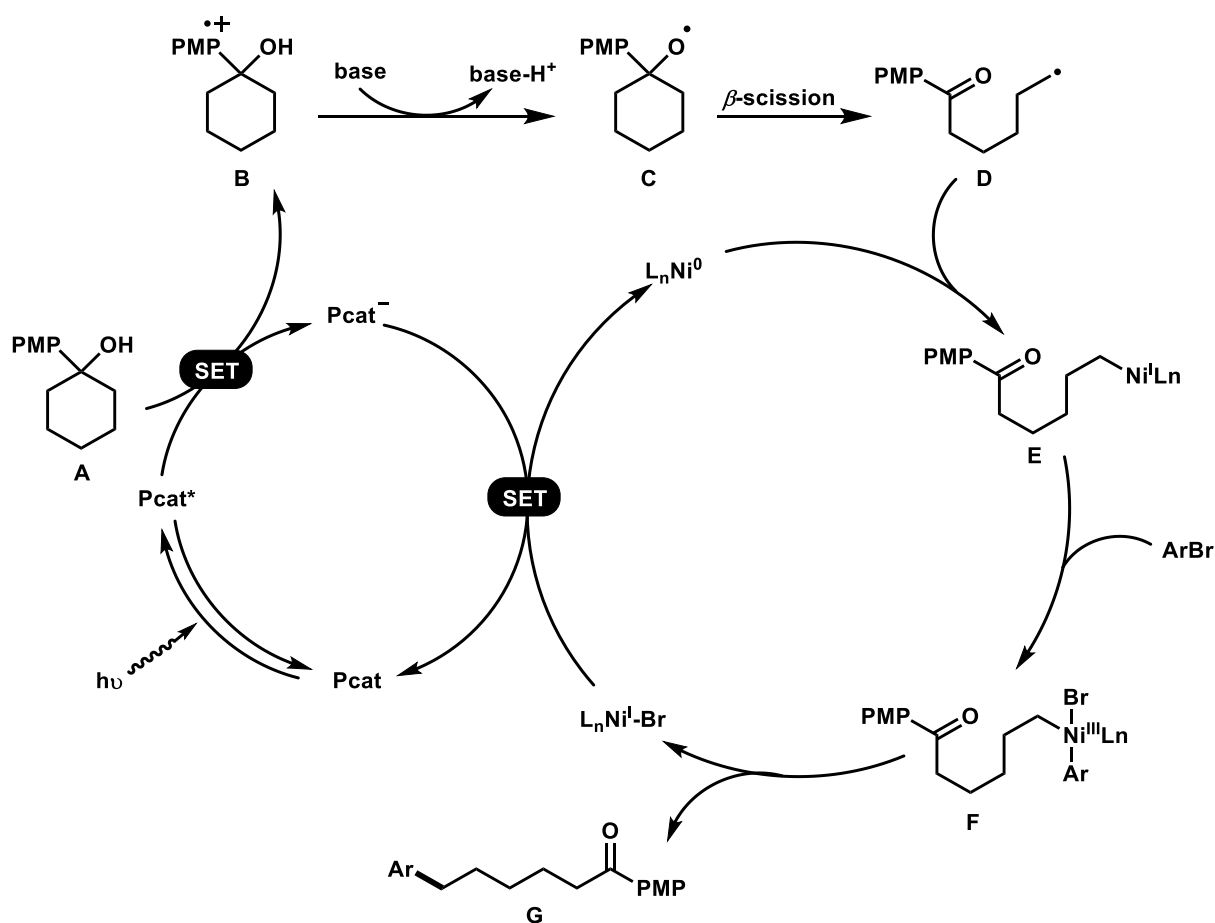
The authors reported a wide substrate scope, varying the aryl halide coupling partner. They also have reported the deconstructive functionalization of cycloalkanols of various ring sizes in moderate to excellent yields.

In comparison with Knowles and co-workers' report, Rueping and co-workers used a photocatalyst of higher oxidation potential (2.06 V vs SCE). This enabled them to oxidize the cycloalkanols with higher oxidation potentials than PMP substitution (scheme 3.11).



Scheme 3.11 – Substrate with higher oxidation potential than PMP substitution

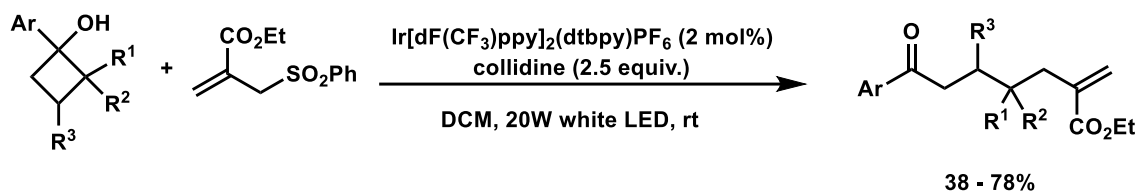
The proposed mechanism of the cross-coupling reaction starts with the electron transfer from the excited state of the photocatalyst to tertiary alcohol **A** (scheme 3.12). The arene radical **B** thus formed undergoes PCET in the presence of suitable base to furnish alkoxy radical **C**. The alkoxy radical **C** undergoes β -scission to furnish alkyl radical **D**. The alkyl radical **D** then reacts with the nickel catalyst to form the nickel species **E**. The nickel species **E** then reacts with the aryl bromide **ArBr** to form the nickel species **F**. The nickel species **F** then undergoes reductive elimination to furnish the alkyl ketone **G**.



Scheme 3.12 – Proposed mechanism Nickel-catalyzed cross-coupling arylation via PCET

radical **C**, which undergoes a β -scission to give distal C-centered radical **D**. The alkyl radical is then captured by the Ni^0 and gives an alkylnickel^I species **E**, which is expected to undergo oxidative addition with an aryl halide, generating a Ni^{III} species **F**. Reductive elimination from **F** would deliver the cross-coupled product **G** and the Ni^{I} intermediate. The reduced form of the photocatalyst then can reduce the Ni^{I} to Ni^0 to regenerate the active form of nickel and the photocatalyst, thus completing the catalytic cycle.

Xia and co-workers have employed PCET strategy in the regiospecific allylation/formylation of cycloalkanols (scheme 3.13).⁷



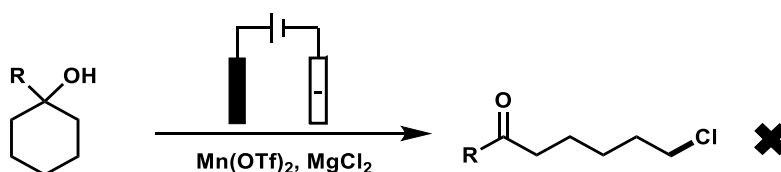
Scheme 3.13 – PCET enabled regiospecific allylation of cycloalkanols

The examples discussed above clearly demonstrate the successful application of PCET strategy in the generation and utilization of alkoxy radicals in overcoming the thermochemical bias associated in the homolytic fission of O–H bonds. By carefully selecting pK_a of the Brønsted base and oxidation potential ($E_{\text{p}/2}$) of the cycloalkanols, it is possible to induce the PCET events that can generate the desired alkoxy radicals.

The photoredox mediated approach in inducing PCET however poses certain limitations. These include the use of precious metals as photocatalysts, fairly long reaction times, requirement of cooling fans to dissipate the heat from UV irradiations, and still evolving scale up capabilities. As such, electrochemistry offers a benign alternative in inducing electron transfer from the surface of the electrodes, directly or with the help of redox mediators to the substrate. An electrochemical approach in the generation of alkoxy radical *via* PCET would certainly be helpful in accessing the various reactivity modes of the alkoxy radicals.

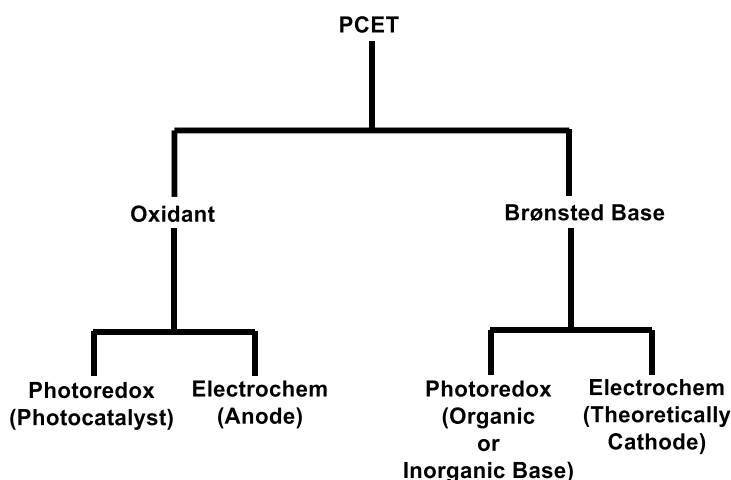
3.2. Aims and Objectives

The primary aims and objectives of this chapter was to overcome the limitations encountered in chapter 2. Manganese catalyzed deconstructive functionalization of cycloalkanols was limited to cyclopropanols and cyclobutanols and only chlorine functionalization could be achieved.



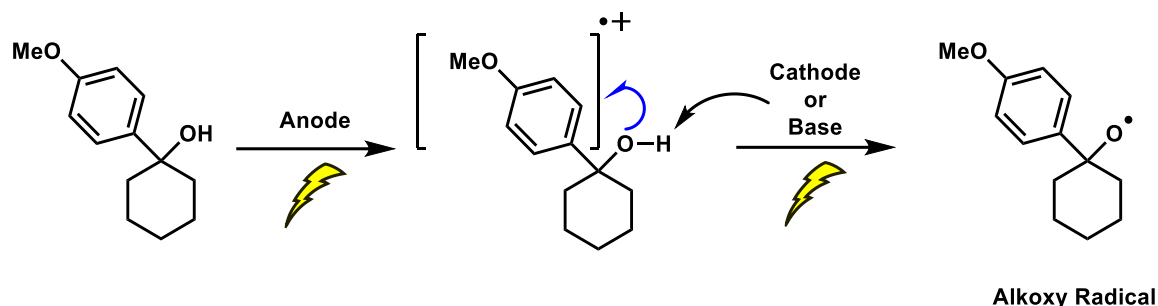
Taking inspiration from Knowles' ⁵ seminal work which was followed by Xia ⁷ and Rueping's⁶, it was envisaged that the photoredox PCET approach could be translated into an electrochemical setting. Various factors associated with oxidative PCET was evaluated.

It was hypothesized that by swapping a photoredox catalyst with an anode as an oxidant along with either using a Brønsted base or cathode for removing proton, it was likely that PCET could be induced which could in turn generate an alkoxy radical intermediate, starting from cycloalkanols (scheme 3.14).



Scheme 3.14 – Requirements for oxidative PCET

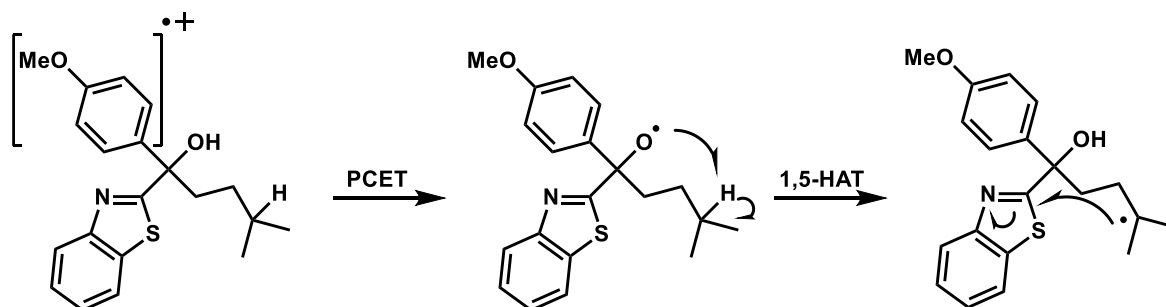
Taking these factors into consideration, a representative scheme for such postulated method is depicted below (scheme 3.15).



Scheme 3.15 – Proposed electrochemical generation of alkoxy radicals via PCET

As previously stated, one drawback of the photochemical approach to such transformations is the challenging nature of photochemical process scale up. As such, demonstration of reaction scale up utilizing an electrochemical flow reactor was an important objective of this work. In contrast with the recirculation flow electrochemical scale up, continuous single pass offers a more efficient method for producing chemicals at scale. Therefore, a secondary objective was to be able to demonstrate the flow electrochemical scale up in a continuous single pass.

Another objective of the work described in this thesis was to access other reactivity modes of the alkoxy radicals in addition to β -scission (e.g., 1,5 HAT). By employing PCET to generate the alkoxy radicals, it was also proposed that it should be possible to engage the alkoxy radical intermediate in 1,5 Hydrogen Atom Transfer (HAT) reactions (scheme 3.16).

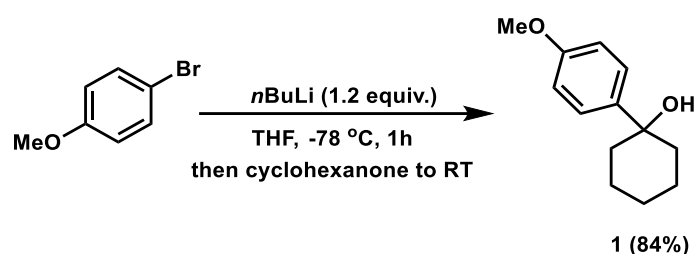


Scheme 3.16 – Proposed HAT reactivity mode of alkoxy radical

3.3. Results and Discussions

3.3.1. Electrochemical Deconstructive Bromination of Cycloalkanols via Alkoxy Radicals Enabled by PCET

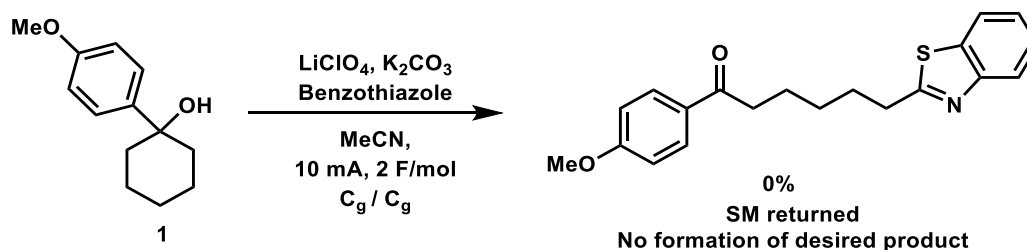
The investigations were started with the synthesis of 1-(4-methoxyphenyl)cyclohexan-1-ol **1** by addition of cyclohexanone to 4-methoxyphenyl lithium in THF in 84% yield (scheme 3.17).



Scheme 3.17 – Synthesis of PMP cyclohexanol

3.3.1.1. Direct Electrolysis

With substrate **1** in hand, attempts were made to generate the alkoxy radical by direct electrolysis. Initially, **1** was subjected to an electrochemical system comprised of LiClO_4 (2 equiv.) as supporting electrolyte, K_2CO_3 (2 equiv.) as base, benzothiazole (1.2 equiv.) as SOMOphile in dry MeCN (0.05 M) under galvanostatic conditions of 10 mA for 2 F/mol using graphite electrodes as anode and cathode (scheme 3.18).



Scheme 3.18 – Initial attempts

The crude reaction mixture was analyzed by ^1H NMR spectroscopy and resulted into 90% return of the starting material and no product formation was observed.

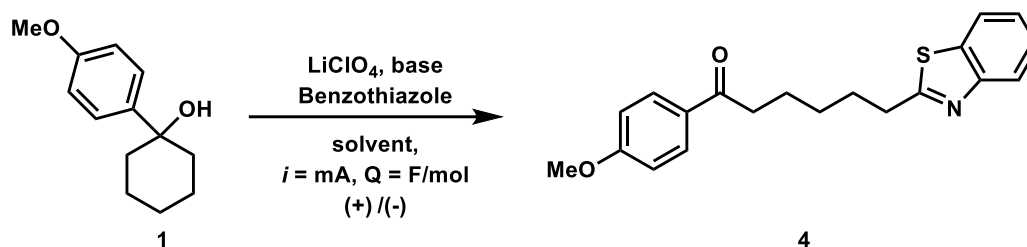


Table 3.1 – Screening of conditions

Entry	Base (equiv.)	Solvent (0.05 M)	(+)/(-)	Current mA	Charge F/mol	1 %	4%
1	K ₂ CO ₃ (2)	MeCN	C _g /C _g	5	2.5	>90	<2
2	K ₂ CO ₃ (2)	MeCN	C _g /C _g	10	2.5	>90	<2
3	Collidine (2)	MeCN	C _g /C _g	5	2.5	>90	<2
4	Collidine (2)	MeCN	C _g /C _g	10	2.5	>90	<2
5	K ₂ CO ₃ (2)	MeCN/HFIP	C _g /C _g	5	2.5	>81	<2
6	K ₂ CO ₃ (2)	MeCN/HFIP	C _g /C _g	10	2.5	>78	<2
7	Collidine (2)	MeCN/HFIP	C _g /C _g	5	2.5	>60	<2
8	Collidine (2)	MeCN/HFIP	C _g /C _g	10	2.5	>51	<2
9	Collidine (2)	MeCN/HFIP	BDD/C _g	10	2.5	>40	<2
10	Collidine (2)	MeCN/HFIP	BDD/Pt	10	2.5	>40	<2

Reactions were performed at 0.30 mmol scale of **1** using Electrasyn 2.0, benzothiazole (1.2 equiv.), crude reaction mixture was analyzed by ^1H NMR using 1, 3, 5-trimethylbenzene

Table 3.1 shows the initial screening of conditions by varying different parameters such as base, solvent, electrode, current and charge. By running the reaction in MeCN at 5 and 10 mA of constant current for 2.5 F/mol of charge employing graphite electrodes as the anode and cathode, no conversion was observed. In such cases **1** was returned in more than 90%, when K₂CO₃ and collidine was used as base (entries **1** – **4**). However, when HFIP was used as a proton source in combination with MeCN as solvent, an apparent

consumption of **1** was observed (entries **5 – 8**). When the anode was changed to BDD electrode, the percentage of starting material was further decreased (entry **9**). In entry **10**, the cathode was changed to platinum keeping the anode as BDD also furnished the similar results as entry **9**. Further attempts to increase current and charge passed were futile, as the formation of the desired product was not observed.

The results from the initial screening suggested that a proton source is required to see any considerable consumption of starting material, possibly a proton source is essential in engaging the cathode, and secondly that direct electron transfer from the anode to the substrate is not efficient.

With these results, employing a redox mediator to facilitate the electron transfer process was then considered.

3.3.1.2. Mediated Electrolysis

In the selection of a suitable redox mediator, it was essential to know the exact oxidation potential of 1-(4-methoxyphenyl)cyclohexan-1-ol, **1**. Cyclic voltametric results indicated the $E_{p/2} = 1.10$ V vs Fc/Fc⁺ which was in accordance with the previously reported values.^{6,8} Triarylamine based redox mediators have been reported to oxidize a variety of functional groups over a wide potentials⁹⁻¹¹, hence were selected as a logical starting point.

Various triarylamines were either purchased or synthesized having redox potential ranging from $E_{1/2} = 0.78$ V to 1.56 V vs Fc/FC⁺ (figure 3.2). RM-1 and RM-3 are commercially available and were purchased and used out of the bottle.

RM-2 was synthesized in a single step from 4-fluoro nitrobenzene and aniline in DMSO in an 82% isolated yield (scheme 3.19).

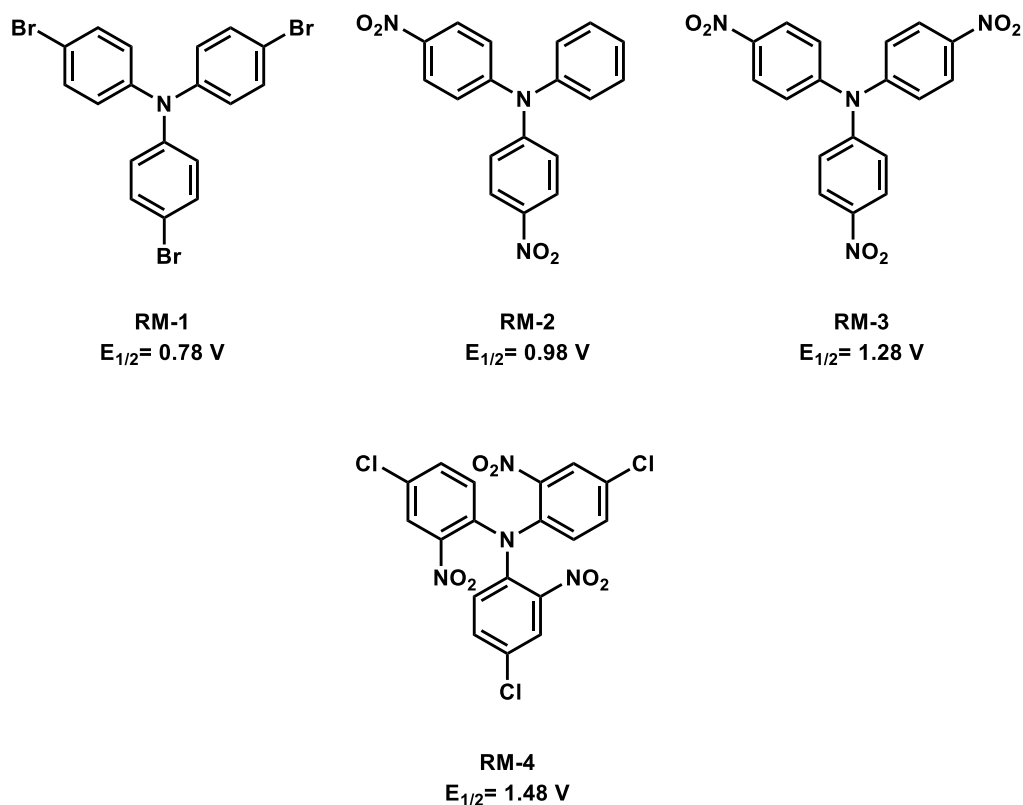
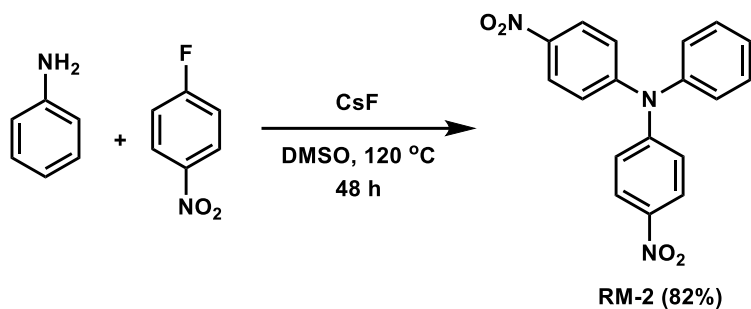
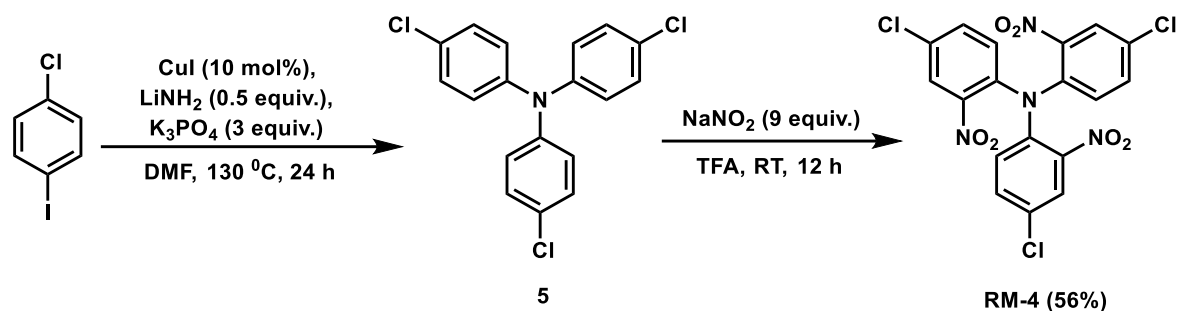


Figure 3.2 – List of triarylamine redox mediators



Scheme 3.19 – Synthesis of RM-2

RM-4 was synthesized in 2 steps starting with the synthesis of tris(4-chlorophenyl)amine **5** by following a reported procedure by Taillefer and co-workers¹² using 10 mol% CuI, 0.5 equiv. LiNH₂ and 3 equiv. of K₃PO₄. Subsequent nitration of **5** yielded RM-4 in 56% isolated yield (scheme 3.20).



Scheme 3.20 – Synthesis of RM-4

With the above redox mediators in hand, the screening for deconstructive functionalization of cycloalkanols began.

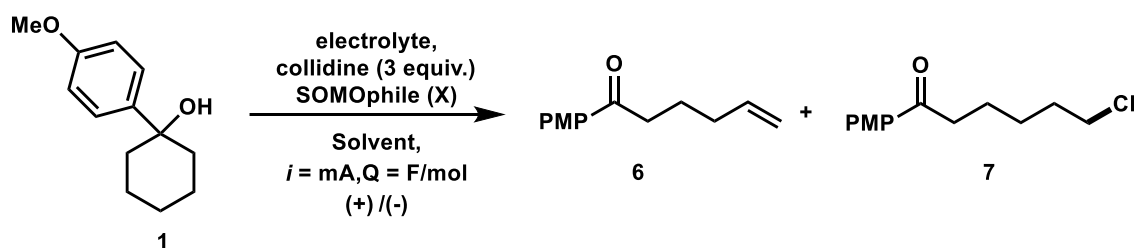


Table 3.2 – Screening of conditions with redox mediators

Entry	RM (mol%)	Electrolyte 0.1 M	X (equiv.)	Solvent 0.05 M	(+)/ (-)	<i>i</i> mA	Q F/mol	1 %	6 %	7 %
1	RM-1 (10)	LiClO ₄	BZT (1.2)	MeCN/ MeOH	C _g /C _g	2	2.5	78	<2	<2
2	RM-1 (10)	LiClO ₄	BZT (1.2)	MeCN/ MeOH	C _g /C _g	5	2.5	75	<2	<2
3	RM-1 (10)	LiClO ₄	BZT (1.2)	MeCN/ MeOH	C _g /C _g	10	2.5	69	<2	<2
4	RM-1 (10)	Bu ₄ NPF ₆	BZT (1.2)	MeCN/ MeOH	C _g /C _g	10	2.5	70	<2	<2
5	RM-2 (10)	Bu ₄ NPF ₆	BZT (1.2)	MeCN/ MeOH	C _g /C _g	2	2.5	90	<2	<2

6	RM-2 (10)	Bu ₄ NPF ₆	BZT (1.2)	MeCN/ MeOH	C _g /C _g	5	2.5	88	<2	<2
7	RM-2 (10)	Bu ₄ NPF ₆	BZT (1.2)	DCM/ MeOH	C _g /C _g	2	2.5	76	5	<2
8	RM-2 (10)	Bu ₄ NPF ₆	BZT (1.2)	DCM/ MeOH	C _g /Pt	3	6.76	72	10	<2
9	RM-2 (10)	Bu ₄ NPF ₆	BZT (1.2)	DCE/ MeOH	C _g /Pt	3	6.76	65	18	<2
10	RM-2 (10)	Bu ₄ NPF ₆	—	DCE/ MeOH	C _g /Pt	3	6.76	<20	50	<2
11	RM-2 (10)	Bu ₄ NCl	—	DCE/ MeOH	C _g /Pt	3	6.76	<20	<2	40
12	RM-2 (10)	Bu ₄ NCl	—	DCE/ MeOH	Fe/Pt	3	6.76	90	<2	<2
13	RM-2 (10)	Bu ₄ NCl	—	DCE/ MeOH	RVC/ Pt	3	6.76	90	<2	<2
14	RM-2 (10)	Bu ₄ NCl	—	DCE/ MeOH	Ni/Pt	3	6.76	80	<2	<2
15	RM-2 (10)	Bu ₄ NCl	—	DCE/ TFE	C _g /Pt	3	6.76	<20	<2	<2
16	RM-2 (10)	Bu ₄ NCl	—	DCE/ HFIP	C _g /Pt	3	6.76	<20	<2	<2
17	RM-2 (10)	Bu ₄ NCl	—	DCE/ H ₂ O	C _g /Pt	3	6.76	60	<2	<2
18	RM-3 (10)	Bu ₄ NCl	—	DCE/ MeOH	C _g /Pt	3	6.76	55	<2	<2

Reactions were performed at 0.30 mmol scale of 1 using Electrasyn 2.0, crude reaction mixture was analyzed by ¹H NMR using 1, 3, 5-trimethylbenzene

Table 3.2 shows the screening of reaction conditions with triarylamines as redox mediators. Experiments started with 10 mol% of redox mediator using the reaction conditions from the non-mediated screening (table 3.1).

Employing RM-1 ($E_{1/2} = 0.78$ vs Fc/Fc⁺), 10 mol%, under galvanostatic conditions ranging from 2 to 10 mA using LiClO₄ as supporting electrolyte (entries **1-3**), Bu₄NPF₆ (entry **4**) in the presence of 1.2 equiv. of benzothiazole until 2.5 F/mol of charge was passed, using graphite as the anode and cathode, did not result in the formation of the desired product and showed the consumption of **1** to some extent.

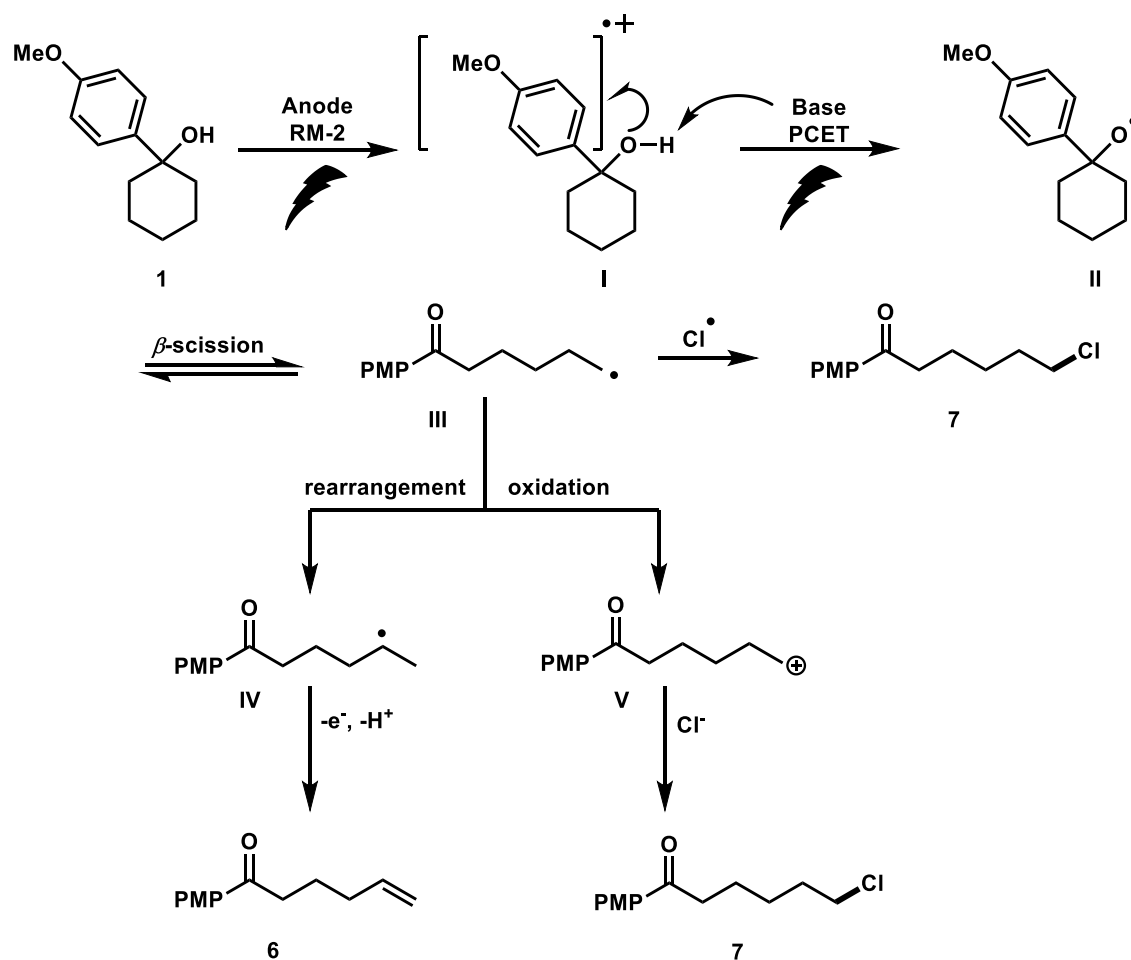
Observing negligible effect of RM-1, RM-2 ($E_{1/2} = 0.98$ V vs Fc/Fc⁺) was employed in the following reactions. Since, Bu₄NPF₆ exhibited stable cell potential in the entry **4**, it was the choice of supporting electrolyte. Entries **5** and **6** shows the reaction with the conditions similar to earlier reactions showed no formation of the desired product.

When MeCN was changed to DCM (entry **7**), formation of an unexpected product **6** was observed in 5%. Changing the cathode to platinum resulted in an increase in the formation of **6** (entry **8**), and a further incremental increase to 18% was observed when DCE was used as solvent (entry **9**). Upon further analysis, product **6** was characterized as a ring-opened product with a terminal alkene. Whilst unexpected, the formation of product **6** was a significant finding as ring opening was observed, which was a proof of concept for the generation of alkoxy radical, probably *via* PCET.

Inspired by the outcome of the reaction, the results suggested that benzothiazole was not a suitable SOMOphile in this case. With these observations, in the following reactions benzothiazole was excluded from the reactions. Entry **10** shows a significant increase in the yield of **6** (50%) in the absence of benzothiazole. This supports the inference that benzothiazole was unable to intercept the C-centered radical formed after β -scission.

To understand the effect of the supporting electrolyte Bu₄NPF₆ was changed to Bu₄NCl and formation of a new distally chlorinated product **7** was observed (entry **11**) in 40%. Presumably the chlorine radical is coming from Bu₄NCl. Changing anode material proved detrimental to the formation of **6** (entries **12 – 14**). A slightly acidic proton source caused decomposition of **1** (entries **15** and **16**). Use of water as a proton source inhibited the reaction (entry **17**). RM-3 ($E_{1/2} = 1.28$ V vs Ag/AgNO₃) was sparingly soluble, and no product formation was observed (entry **18**). The decomposition of the starting material was observed in almost all the cases which could have resulted into the formation of unknown products.

Formation of the chlorinated product **7** indicates either an over oxidation of the C-centered radical to carbocation, followed by a nucleophilic attack by the chlorine anion furnished from Bu₄NCl, or a radical combination of a C-centered radical and a chlorine radical (scheme 3.21).



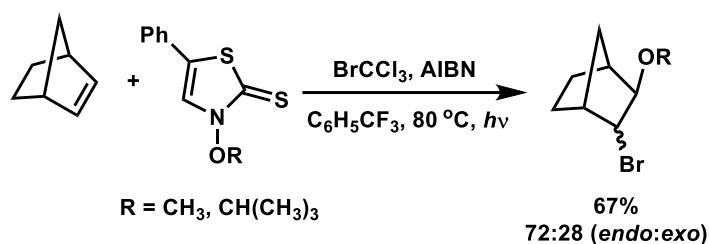
Scheme 3.21 – Rationale for the observed products

Formation of products **6** and **7** can be rationalized as follows; **1** is oxidized by the RM-2 to furnish radical cation intermediate **I** which undergoes a PCET process to generate an alkoxy radical **II**. β -scission pathway of **I** would yield the distal C-centered radical **III**, which could either be trapped by a Cl^\bullet to furnish product **7** or undergo an unlikely oxidation of 1° radical to generate an unstable 1° carbocation **V** which can be intercepted by a Cl^- to yield **7**. Conversely, **III** could undergo a 1,2-rearrangement to furnish intermediate **IV**, which upon subsequent loss of e^- and H^+ would form the alkene **6**.

The evidence of ring-opening was encouraging, however, formation of products **6** and **7** was surprising. Since a SOMOphile has no effect in the formation of these products, it was deduced that employing a suitable SOMOphile would solve this problem.

An ideal SOMOphile should be stable under oxidative conditions as well as form benign by-products after transferring group/atom. Bromotrichloromethane (BrCCl_3) is known to trap the C-centered radicals in the presence of number of radical initiators such as peroxides,^{12a} light,^{12b} AIBN,^{12c} SmI_2 ^{12d} etc.

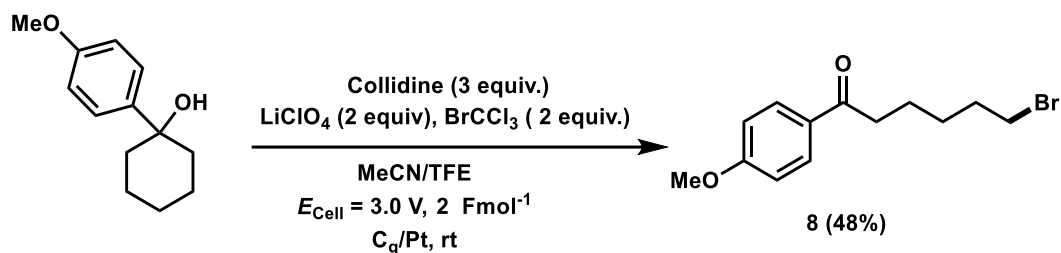
Hartung and co-workers reported the synthesis of β -bromohydrine ethers *via* intermolecular alkoxy radical additions to bicyclo[2.2.1]heptane (scheme 3.21a).^{12e}



Scheme 3.21a – BrCCl_3 as a brominating agent

Knowles and co-workers have also employed BrCCl_3 in the report.⁵

After considering several SOMOphiles, BrCCl_3 was selected as a SOMOphile of choice. As the by-product after the transfer of the bromine atom would either be hexachloroethane after the dimerization or simply chloroform (refer section 3.3.1.6). Gratifyingly, the very first reaction tried with BrCCl_3 resulted in the formation of the brominated product **8** in 48% yield. The reaction was carried out under potentiostatic conditions of $E_{\text{cell}} = 3.0\text{ V}$ using 3 equiv. of collidine, LiClO_4 (0.1M), BrCCl_3 (3 equiv.) in the solvent system comprised of MeCN/TFE (12:1) using graphite as anode and platinum as cathode until 2 F/mol of charge has been passed (scheme 3.22).



Scheme 3.22 – Deconstructive bromination of cycloalkanols enabled by PCET

It is worth noting here that this particular reaction was run without redox mediator and still the reaction showed good conversion. As mentioned in the introduction, effective BDFE plays an integral part in the PCET process. If we plug the respective values of the $E_{p/2}$ of the substrate, pK_a of the base in the equation **1**, we get the value of an effective BDFE of the system.⁵ The effective BDFE is closer to the BDFE of the homolysis of O–H bond, hence it is logical to say the reaction is driven by PCET.

$$\text{BDFE (O-H)} = 1.37pK_a (\text{base}) + 23.06 E_{p/2} (\text{Ar}^{0/+}) + 54.9 C_g(\text{MeCN}) \quad \text{1 eqn}$$

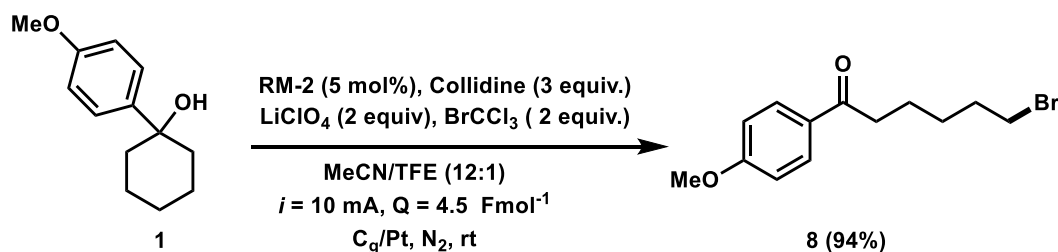
$$pK_a \text{ collidine} = 15 \quad E_{p/2} \text{ of PMP cyclohexanol} = 1.23 \text{ V}$$

$$1.37 \times 15 + 23.06 \times 1.23 + 54.9 C_g(\text{MeCN}) = 103.8 \text{ Kcal/mol}$$

Encouraged by these results, extensive optimization studies were performed. In these optimization studies various parameters were studied after which optimized conditions were fixed.

3.3.1.3. Optimized Conditions

After methodical and extensive optimization studies, optimized conditions were found. A reaction system comprised of 5 mol% of RM-2 as redox mediator, 3 equiv. of collidine as Brønsted base, LiClO₄ (0.1 M) as supporting electrolyte, BrCCl₃ (2 equiv.) in a solvent system of MeCN/TFE (12:1) under the constant current of 10 mA using graphite as the anode and platinum as cathode, until 4.5 F/mol of charge has been passed at ambient temperature, quantitative conversion by ¹H NMR was observed and the brominated product **8** was isolated in 94% yield (scheme 3.23).



Scheme 3.23 – Optimized condition

Table 3.3 – Variations from the optimized conditions

Entry	Variation	1 (%)	8 (%)
1	none	<2	98 (94) ^a
2	No electricity	95	<2
3	1 equiv. of Collidine	30	65
4	2 equiv. of Collidine	16	81
5	7.5 mA instead of 10 mA	14	74
6	12.5 mA instead of 10 mA	<2	98
7	20 mA instead of 10mA	<2	92
8	2.5 F mol ⁻¹ instead of 4.5	26	56
9	No redox mediator	68	32
10	1 mol% redox mediator	23	50
11	Nickel as cathode	32	63
12	Graphite as Cathode	49	34
13	1.1 equiv of BrCCl ₃	<2	49
14	HFIP as proton source	51	49
15	No proton Source	<2	53
16	TBAPF ₆ as supporting electrolyte	20	80
17	DCE as solvent	40	51
18	DCM as solvent	<2	74

Reactions were performed at 0.30 mmol scale, yields calculated by analyzing crude reaction mixture by ¹H NMR spectroscopy using 1,3,5 trimethoxybenzene, ^a isolated yield

Table 3.3 shows the variations from the optimized conditions. All the reactions were performed at 0.30 mmol of **1** using an Electrasyn 2.0. The crude reaction mixture was analyzed by ^1H NMR spectroscopy using 0.1 equiv. of 1,3,5-trimethoxybenzene as an internal standard. In the absence of electricity, no conversion was observed (entry **2**). Decreasing the amount of collidine had a detrimental effect on the formation of **8** (entries **3** and **4**). These results are consistent with the PCET theory, in which pre-association of the Brønsted base with the substrate is a requirement and is consistent with the previous reports.⁶⁻⁸

Decreasing the current to 7.5 mA also resulted in lower yield of **8** (entry **5**). However, an increase in current to 12.5 mA and 20 mA showed a little effect on the conversion (entries **6** and **7**). On the other hand, when 2.5 F/mol of charge was passed only 26% formation of **8** and 56% of starting material was returned (entry **8**).

In the absence of redox mediator, formation of **8** was observed in 32% and 68% of starting material was returned (entry **9**). This signifies that the direct electron transfer from the surface of the electrode is inefficient. 1 mol% of the redox mediator showed an increase in the formation of **8** (entry **10**).

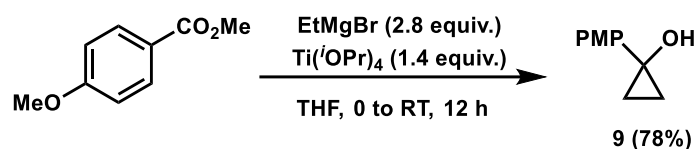
Changing the cathode and anode material separately proved detrimental to the formation of **8** (entries **11** and **12**). Reaction with 1.1 equiv. of BrCCl_3 showed 49% formation of **8** and no starting material (entry **13**). The inadequate mass balance suggests the decomposition of **1** in the absence of adequate amount of BrCCl_3 .

Changing the proton source to HFIP resulted in 49% formation of the product, however the mass balance was 100% (entry **14**). This observation could be explained by comparing the pK_a 's of HFIP (9.3 in H_2O) to that of TFE (12.46 in H_2O). The lowering of the pK_a could possibly lower the effective BDFE of the system which in turn could be detrimental to the PCET process. The reaction was lower yielding in the absence of a proton source (entry **15**).

TBAPF₆ as an electrolyte had little effect on the conversion and gave good mass balance (entry **16**). And finally changing MeCN to DCE and DCM proved detrimental to the formation of **8** (entries **17** and **18**).

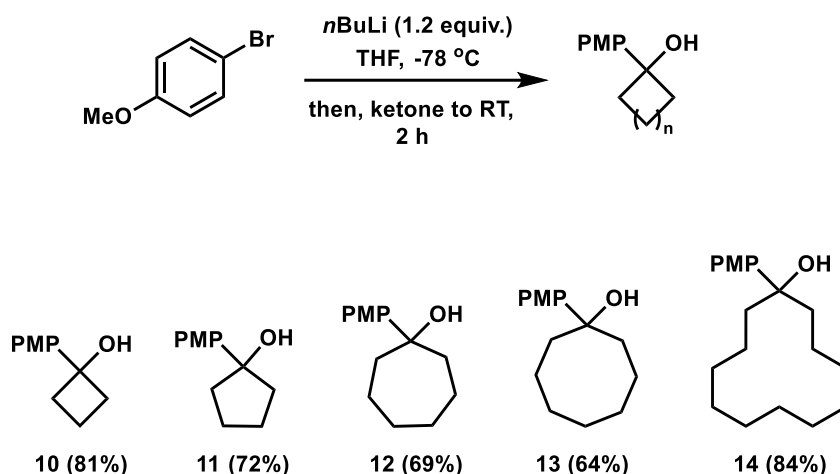
3.3.1.4. Substrate Scope

With the optimized conditions in hand, the full scope of the electrochemical process was explored starting with the deconstructive bromination of the cycloalkanols with varied ring sizes. 4-PMP cyclopropan-1-ol **9** was prepared by the Kulinkovich reaction of methyl 4-methoxybenzoate with ethyl magnesium bromide in the presence of $\text{Ti}(\text{iOPr})_4$ in dry THF, and was isolated in a 78% yield (scheme 3.24).



Scheme 3.24

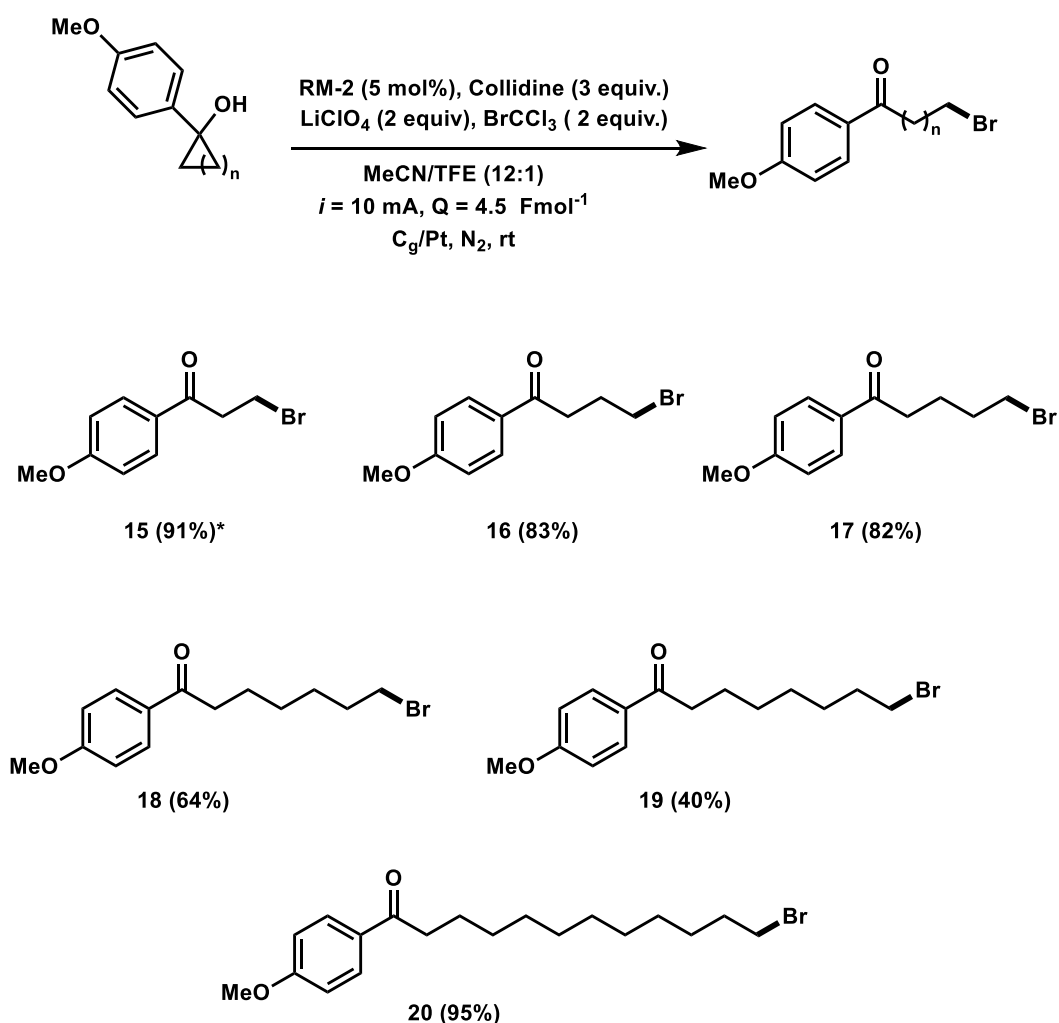
Substrates with larger ring sizes were prepared by a lithium-halogen exchange reaction using $n\text{BuLi}$ and 4-bromoanisole, followed by the addition of the corresponding ketone. (scheme 3.25).



Scheme 3.25 – Synthesis of substrates

PMP cycloalkanols bearing various ring sizes were obtained in good to excellent yields. 4-PMP-cyclobutanol **10** in 81%, 4-PMP-cyclopentanol **11** in 72%, 4-PMP-cycloheptanol **12** in 69%, 4-PMP-cyclooctanol **13** in 64%, and 4-PMP-cyclododecanol **14** in 84% yield.

With the various cycloalkanols in hand, they were subjected to the optimized electrochemical conditions (scheme 3.26).



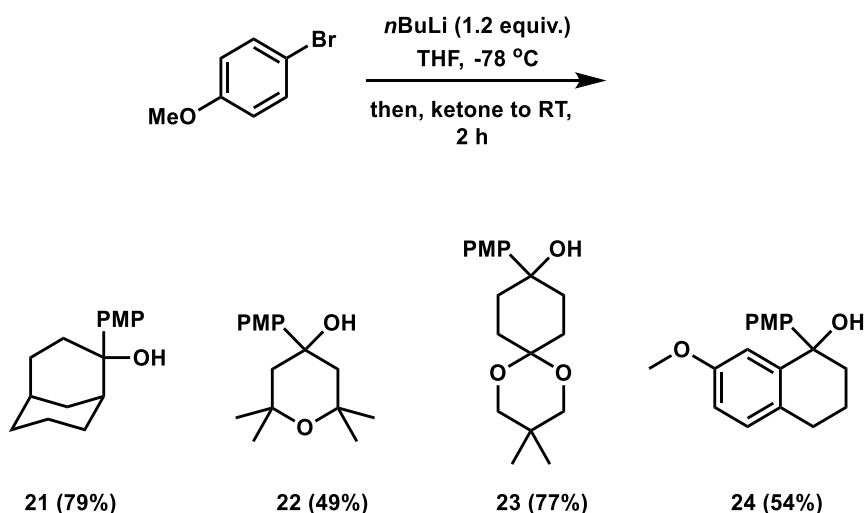
Reactions were performed at 0.30 mmol scale using Electrasyn 2.0. isolated yield in parentheses, * NMR yield.

Scheme 3.26 – Substrate scope of cycloalkanols bearing various rings sizes

4-PMP-cyclopropanol **9** under the optimized electrochemical conditions performed well and gave the ring opened β -brominated ketone **15** in 91% NMR yield. 4-PMP-cyclobutanol **10** and cyclopentanol **11** also formed the ring opened ketones **16** and **17** in 83% and 82% yields respectively. 4-PMP-cycloheptanol **12** proceeded smoothly to yield **18** in 64% yield. However, the yield when using of 4-PMP-cyclooctanol **13** was comparatively low with 40% of ketone **19**. 4-PMP-cyclododecanol **14** furnished the ring opened ketone **20** in quantitative ^1H NMR yield and was isolated in 95% yield.

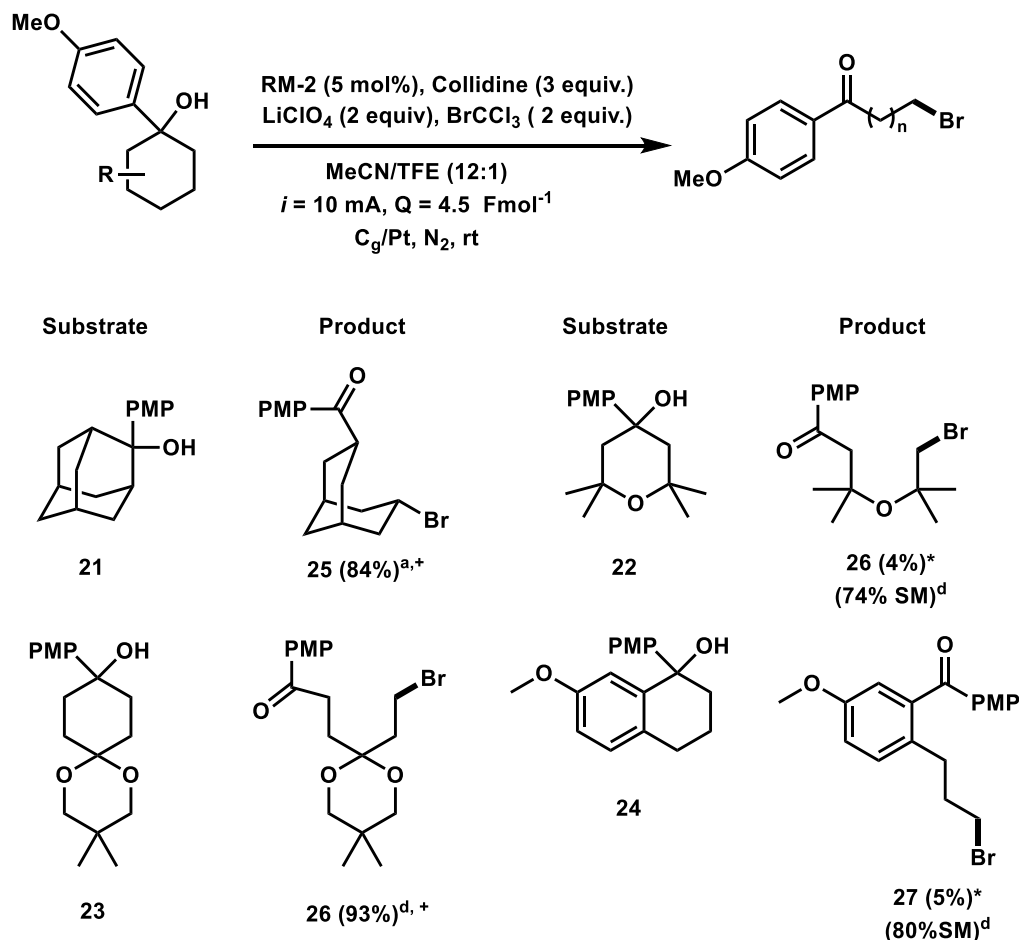
After an excellent performance of the various ring sizes in the optimized electrochemical conditions, variations on the six-membered ring were tried. Substrates **21**, **22**, **23** and **24** were synthesized by following the synthetic procedure from scheme 3.25.

4-PMP-adamantanone **21** was isolated in 79%, 4-(4-PMP)-2,2,6,6-tetramethyltetrahydro-2H-pyran-4-ol **22** was isolated in 49%, spiro alcohol **23** in 77%, and 7-methoxy tetralone derivative **24** was isolated in 54% yield (scheme 3.27).



Scheme 3.27 – substrates with varied six-membered ring

The substrates then were subjected to the electrochemical conditions (scheme 3.28).

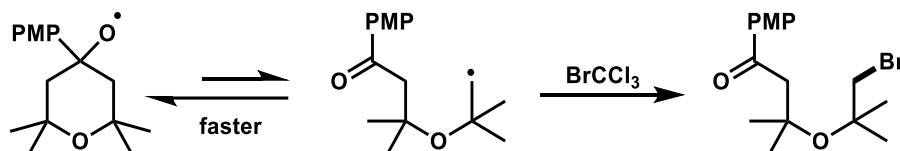


Reactions were performed at 0.30 mmol scale using Electrasyn. a: standard conditions, d: 6 F/mol of charge was passed, + = isolated yields, * = ¹H NMR yield

Scheme 3.28 – Electrochemical reaction

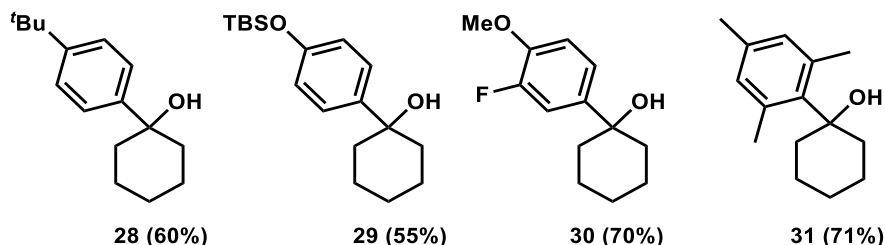
Under standard conditions 4-PMP adamantanol **21** underwent deconstructive bromination in 84% yield. However, 4-(4-PMP)-2,2,6,6-tetramethyltetrahydro-2H-pyran-4-ol **22**, under standard reaction conditions was unreactive and only 4% conversion of **26** was observed by ¹H NMR spectroscopy when 6 F/mol of charge was passed. Spiro substrate **23** yielded 93% of brominated product **26** on passing 6 F/mol of charge. Substrate **24** was again found unreactive and only 5% of **27** could be observed by ¹H NMR spectroscopy ($Q = 6 \text{ F/mol}$).

The rationale for unreactive substrates could be given as: substrate **22** would form a relatively stable alkyl radical intermediate and the reversible reaction to re-form the substrate would be more favourable (scheme 3.29); for substrate **24**, the presence of two different electron rich units could impede the PCET process.



Scheme 3.29 – Rationale for low yield

Substrates bearing electron rich aromatic unit other than PMP were also explored. Substrates **28**, **29**, **30** and, **31** were synthesized by following the synthetic procedures from scheme 3.27 and were obtained in 60%, 55%, 70% and 71% respectively (scheme 3.30)



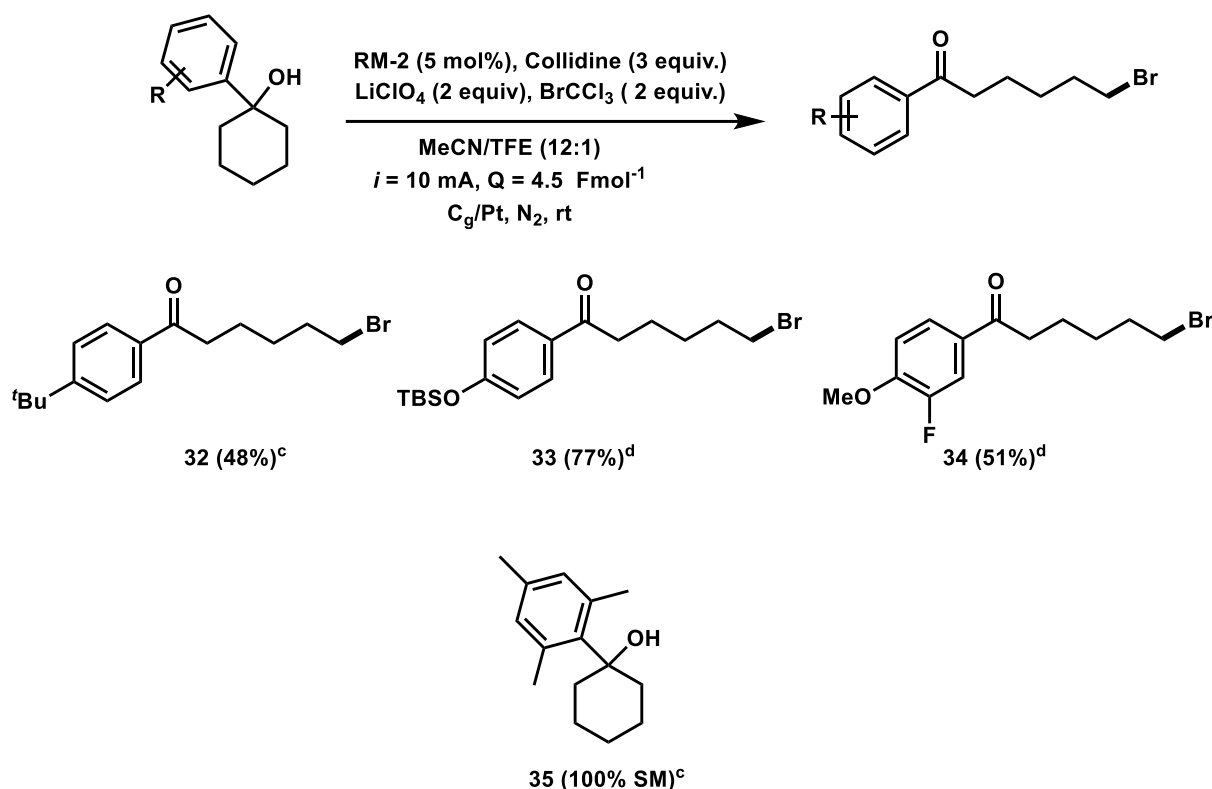
Scheme 3.30 – Variation of electron rich aromatic unit on cyclohexanols

On subjecting these substrates to the standard electrochemical conditions, all the substrates were either unreactive or gave less conversion by ^1H NMR spectroscopy.

As expected, cyclic voltammetry revealed that the oxidation potential of these substrates was higher than the parent substrate. Hence, RM-2 was unable to oxidize the electron rich aromatic unit of the substrates, which is the first step in the generation of alkoxy radical *via* PCET process. To circumvent this problem, RM-4 ($E_{1/2} = 1.48$ V vs Fc/Fc $^{+}$) was employed.

Gratifyingly, substrate **28** ($E_{p/2} = 1.53$ V vs Fc/Fc⁺) when subjected under electrochemical conditions with 10 mol% of RM-4 at 20 mA of constant current for 9 F/mol of charge, yielded the brominated product **32** in 48% isolated yield.

Substrate **29** ($E_{p/2} = 1.20$ V vs Fc/Fc⁺) and **30** ($E_{p/2} = 1.19$ V vs Fc/Fc⁺) when subjected under standard conditions but passing 6 F/mol of charge furnished the brominated ketones **33** and **34** in 77% and 51% isolated yields respectively. Substrate **31** ($E_{p/2} = 1.47$ V vs Fc/Fc⁺) remained unreactive under RM-4 conditions (scheme 3.31).



Reactions were performed at 0.30 mmol scale, crude reaction mixture was analyzed by ¹H NMR spectroscopy using 1,3,5-trimethoxybenzene as an internal standard. c: 10 mol% RM-4, 20 mA, 9 F/mol, d: 6 F/mol

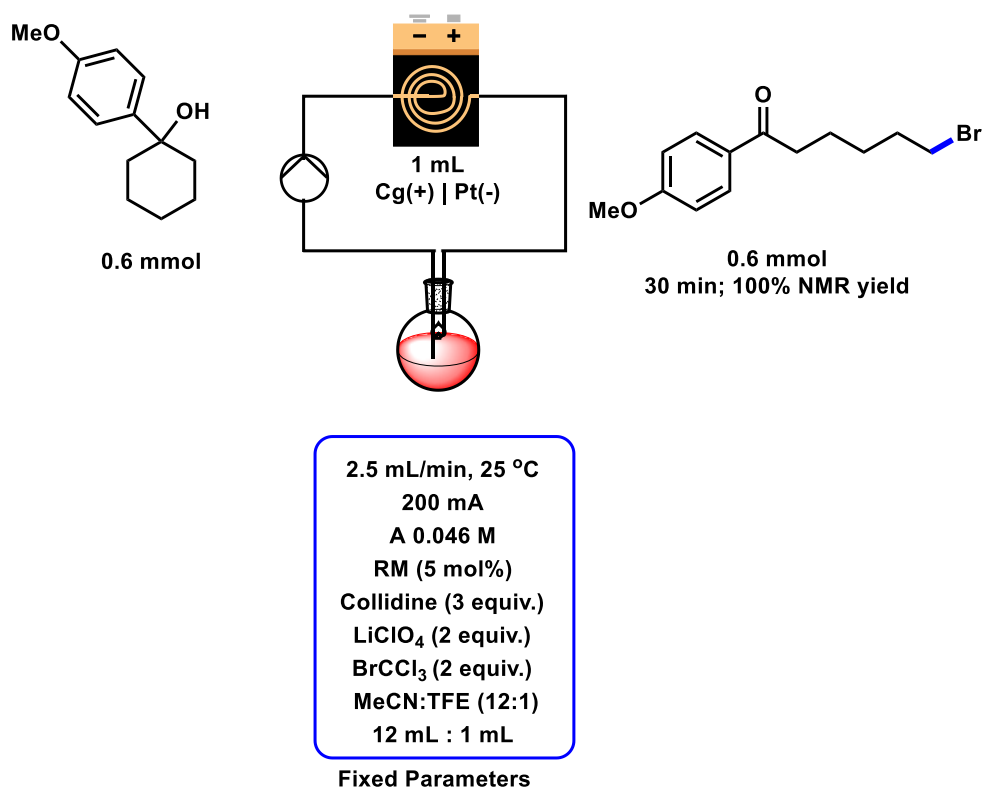
Scheme 3.31 – Electrochemical reactions of substrates with varied electron rich aromatic unit

Currently, to expand the scope of the reaction, a wide variety of substrates and redox mediators are being tried by the other members of the group.

3.3.1.5. Flow Electrochemical Scale Up

To demonstrate the scalability, the batch electrochemical process was translated to a flow electrochemical setup. By employing the commercially available Ammonite 8 flow electroreactor, the conversion of 0.6 mmol of the parent substrate **1** was attempted in recirculating flow electrochemical setup.

Gratifyingly, keeping the stoichiometry of the optimized conditions unchanged, under recirculating flow electrolysis utilising a 2.5 mL/ min flow rate and a constant current of 200 mA, 100% conversion was obtained in 30 minutes (scheme 3.32).



Scheme 3.32 – Recirculation flow electrochemical scale up

Excluding electrolyte (LiClO₄) from the reaction proved detrimental to the yield of the reaction, and no further attempts were made to alter the recirculating flow conditions.

Motivated by the results obtained from the recirculating flow electrolysis experiments, to further make the scale up more efficient it was decided that development of a continuous single pass flow electrochemical set up should be undertaken to improve the utility and desirability of the electrochemical flow system. By evaluating the various parameters such as current, charge and flow rate, translation of recirculation into continuous pass was studied. The stoichiometric parameters and the electrode materials from the batch optimized conditions were kept unchanged.

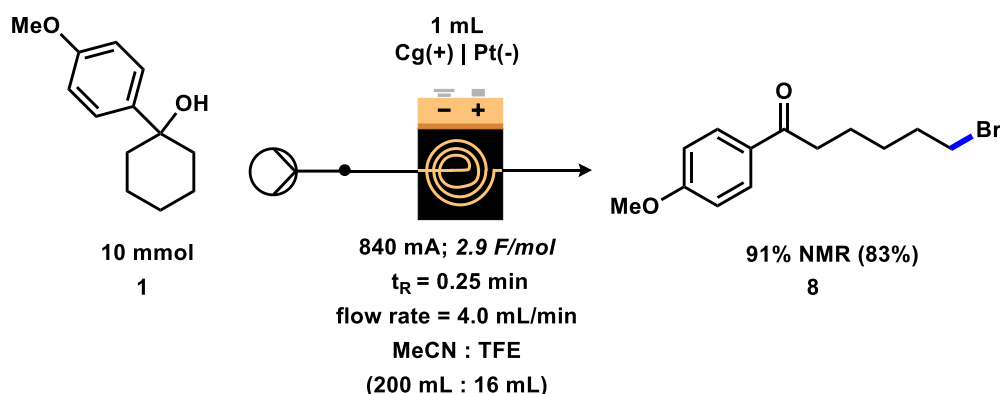


Table 3.4 – Continuous flow optimization

Entry	SM mmol	Current mA	Charge F/mol	Flow rate mL/min	8 %	1 %
1	0.6	200	2.2	1.25	65	32
2	0.6	200	4.6	0.6	55	43
3	0.6	300	3.3	1.25	30	67
4	0.6	400	4.4	1.25	30	5
5	0.6	500	1.7	4.00	80	17
7	10	840	2.9	4.00	91(83)	0

Reactions were performed at 0.30 mmol scale, yields calculated by analyzing crude reaction mixture by ^1H NMR spectroscopy using 1,3,5 trimethoxybenzene

Table 3.4 shows the optimization results of the continuous single pass electrochemical scale up. In just few trials, the optimized conditions were obtained. A flow rate of 4.0 mL/min at the constant current of 840 mA and 2.9 F/mol of total charge passed yielded the product **8** in 83% isolated yield at 10 mmol scale. Entry **4** showed a deviation, which was corrected by just cleaning the flow reactor with IPA and MeCN.

3.3.1.6. Mechanistic Studies

To gain the mechanistic insight of the reaction, cyclic voltammetry was employed. The parent substrate showed the $E_{p/2} = 1.10$ V vs Fc/Fc⁺. Redox potential of RM-2 was found to be $E_{1/2} = 0.98$ V vs Fc/Fc⁺.

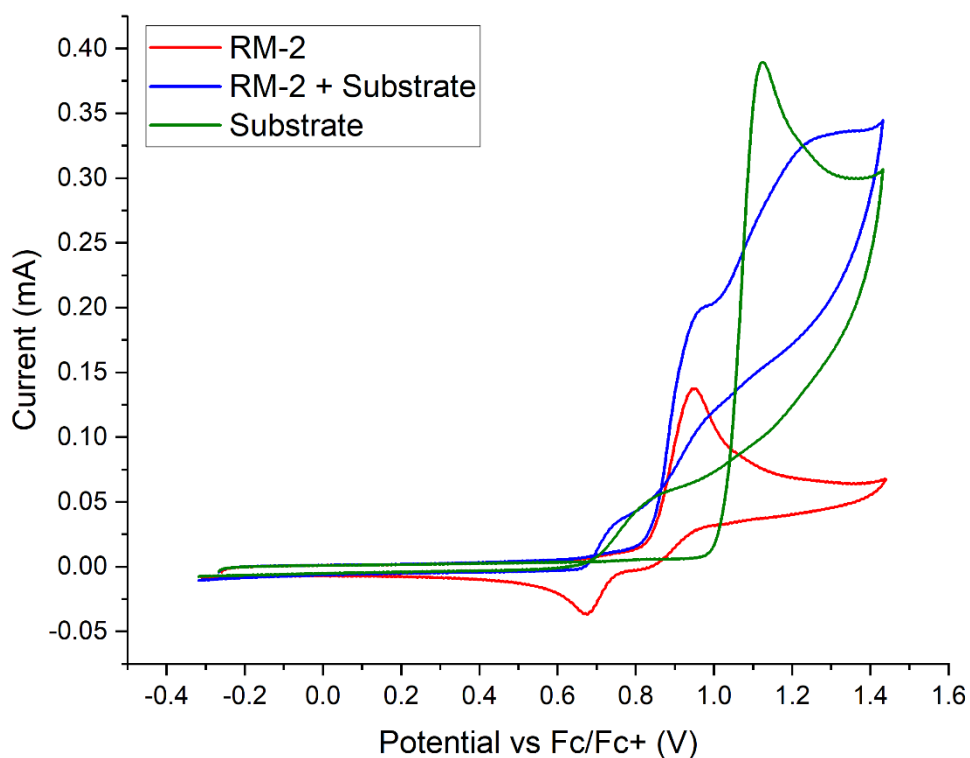


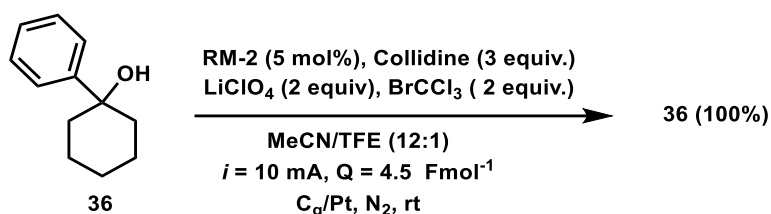
Figure 3.3 – Cyclic voltammogram of (red line) RM-2 (4.0 mM), (green line) parent substrate (4.0 mM) and RM-2 + parent substrate (blue line), in MeCN/TFE (12:1), LiClO₄ (0.1 M). Scan rate: 100 mV/s

Figure 3.3 shows the cyclic voltammogram of RM-2 (red line), the parent substrate (green line) and RM-2 + substrate (blue line). CV signifies that, when the parent substrate was scanned in the presence of RM-2, an increase in anodic current (c.a. 0.98 V) is observed. Also, the disappearance of the parent substrate oxidation peak was seen. An increase in

the anodic current at 0.98 V can be attributed to the interaction between RM-2 and the parent substrate.

From the CV data, it could be inferred that in the presence of RM-2, the parent substrate gets oxidized at lower potential.

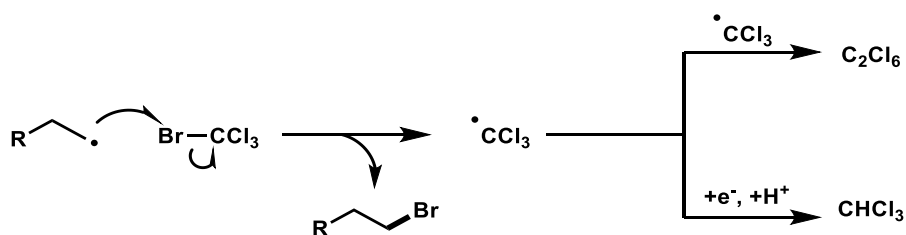
Triarylaminines have been reported to mediate the electron transfer processes for up to 500 mV range.¹³ In a control experiment, 1-phenylcyclohexan-1-ol **36** was subjected to the optimized reaction conditions. As expected, under the standard reaction conditions, **36** was returned in 100% yield by ¹H NMR spectroscopy (scheme 3.33).



Scheme 3.33 – Control experiment

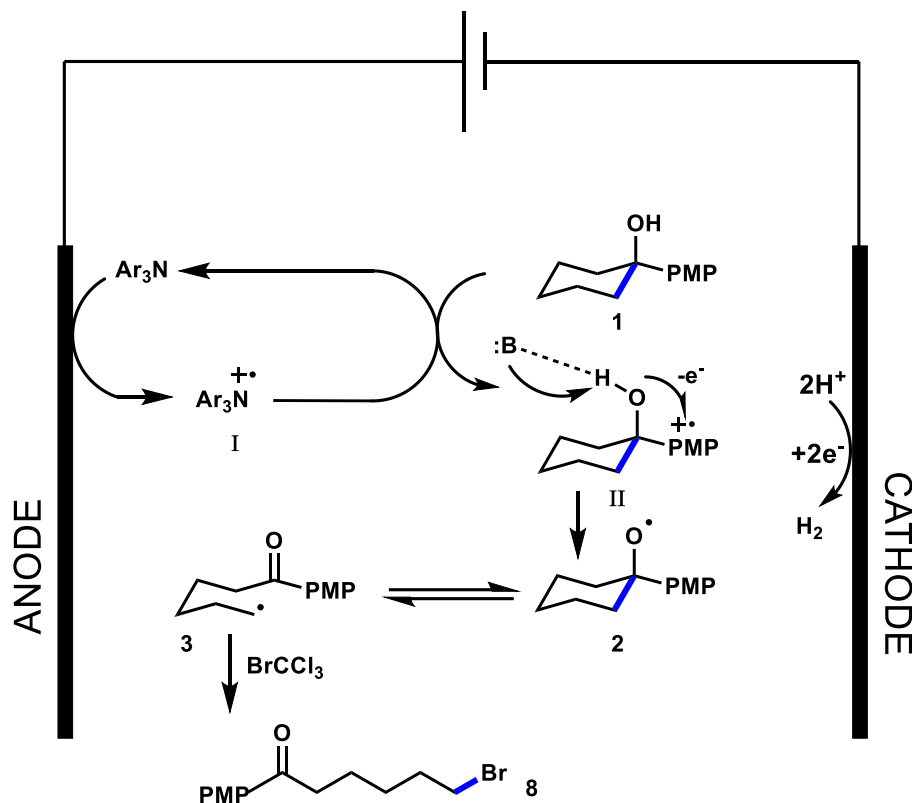
Cyclic voltammetry showed the $E_{p/2} = 1.61 \text{ V}$ vs FC/FC⁺, which is indeed higher than the electron transfer range of the RM-2. Hence, no reaction of **36** was observed.

The fate of the brominating agent BrCCl₃ was also rationalized. It is believed that BrCCl₃, after trapping the alkyl radical, furnishes the [•]CCl₃. This could either dimerize to form hexachloroethane (C₂Cl₆)^{14,15} or get reduced at cathode to form ⁻CCl₃ which can abstract a proton to form chloroform (CHCl₃) (scheme 3.34). The crude NMR of the reaction mixture confirmed the formation of chloroform in CD₃CN.



Scheme – 3.34 – Fate of [•]CCl₃

Based on the cyclic voltammetric data and previous reports⁸, a plausible catalytic cycle can be proposed for the formation of the product (scheme 3.35).



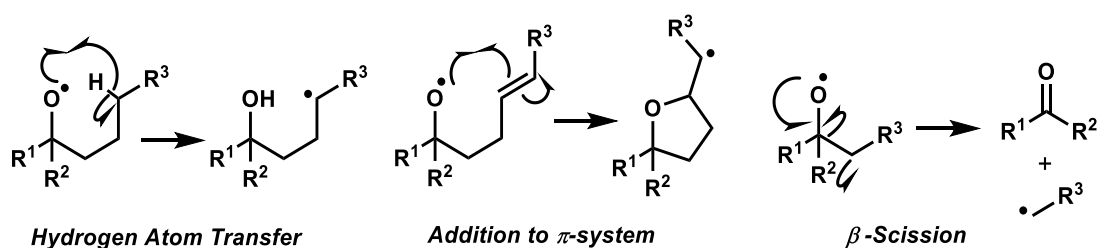
Scheme 3.35 – Plausible mechanism

The reaction would start with the oxidation of triarylamine (RM-2) on the surface of the anode to furnish the radical cation **I**. The substrate **1** then undergoes an electron transfer with **I** to furnish radical cation intermediate **II**. In the presence of collidine as base (**B**), the intermediate would undergo a PCET process in which the base abstracts the proton and subsequent electron transfer to the oxidized aromatic ring would facilitate the formation of an alkoxy radical intermediate **2**. A reversible β -scission of the alkoxy radical intermediate would generate the distal C-centered radical intermediate **3**, which can intercept BrCCl_3 to form the brominated product **8**. Electron transfer from **I** to **1** would reduce the triarylamine redox mediator and the catalytic cycle will continue.

3.3.2. Electrochemical Remote Functionalization of C(sp³)-H Bond via Alkoxy Radical Induced 1,5 - Hydrogen Atom Transfer (HAT) and Functional Group Migration enabled by Proton Coupled Electron Transfer (PCET)

3.3.2.1. Introduction

In addition to β -scission, alkoxy radicals also exhibit 1,5 - Hydrogen Atom Transfer (HAT)¹⁶ reactivity and inter or intramolecular addition to π -systems¹⁷ (scheme 3.36).



Scheme 3.36 – Alkoxy radicals reactivity modes

1,5-HAT involves the formation of a chair like six-membered cyclic state in the transposition of the radical centre from alkoxy to the γ -carbon (figure 3.4). The six-membered transition state resembles like a flattened chair in which oxygen and α , β , and γ carbons are coplanar and the migrating hydrogen is slightly out of plane.^{18–20}

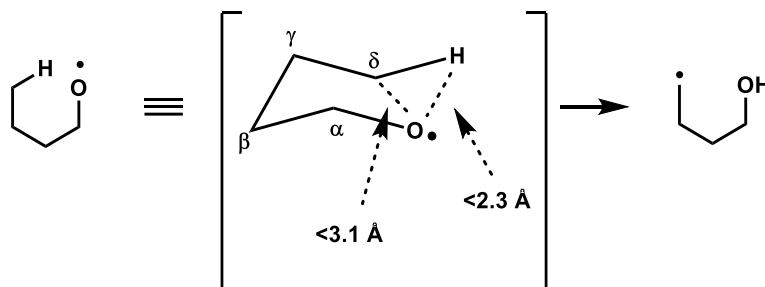
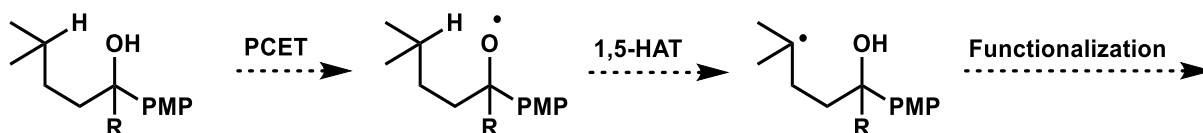


Figure 3.4 – transition state of 1,5-HAT

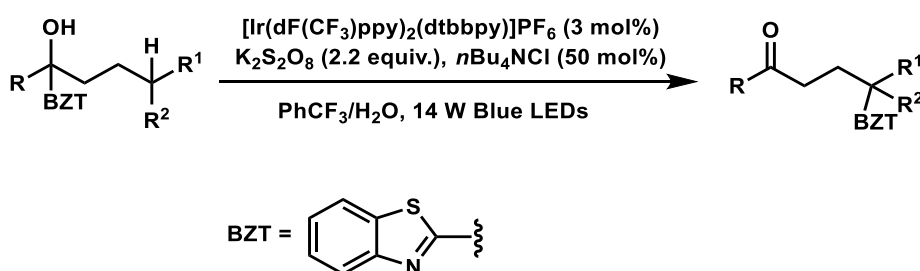
After establishing the proof-of-concept for the electrochemical generation of alkoxy radical from tertiary alcohols *via* PCET and accessing the β -scission reactivity mode, accessing 1,5-HAT and addition to π -systems were also envisaged. It was also one of the objectives of this thesis (scheme 3.37).



Scheme 3.37 – Proposal for the electrochemical 1,5-HAT

In an initial proposal it was conceived that the existing substrate for the bromination can be engineered for the 1,5-HAT reactivity mode. This could potentially provide a new method for the C(sp³)-H bond functionalization.

Zhu and co-workers have reported a photoredox method for the functionalization of remote C(sp³)-H bond by 1,5-HAT and functional group migrations (scheme 3.38).²¹



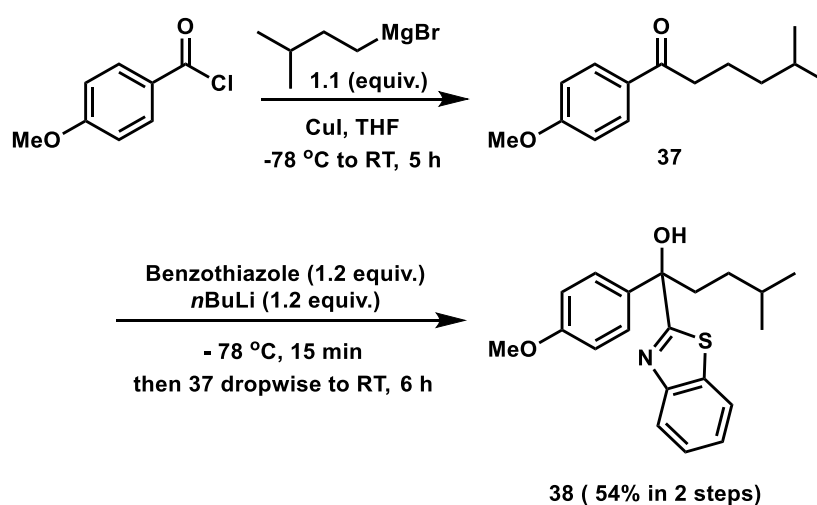
Scheme 3.38 – Photoredox 1,5 HAT and FG migrations

The authors reported a wide substrate scope demonstrating tolerance of various functional groups on (R, R¹, and R²). The mechanism of the transformation was presumed *via* PCET which involved the Ir(III) and Ir(IV) catalytic cycle in the presence of K₂S₂O₈ as an oxidant. However, the formation and homolysis of iridium-oxygen bond (Ir(IV) – O-R) can also not be ruled out.

3.3.2.2. Results and Discussions

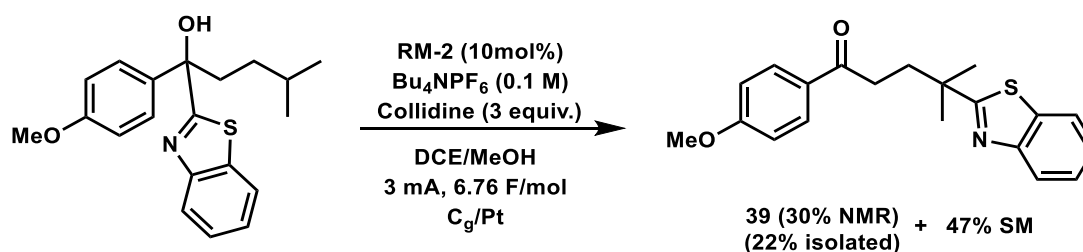
Inspired by Zhu and co-workers' report, the investigations into the electrochemical 1,5-HAT began by the synthesis of the substrate **38**.

Substrate **38** was synthesized in 2 steps from anisoyl chloride and isolated in 54% yield over 2 steps (scheme 3.39).



Scheme 3.39 – Synthesis of substrate

With substrate **38** in hand, electrochemical reaction trials were carried out following the initial reaction conditions developed for the deconstructive bromination (scheme 3.40).



Scheme 3.40 – Electrochemical reaction

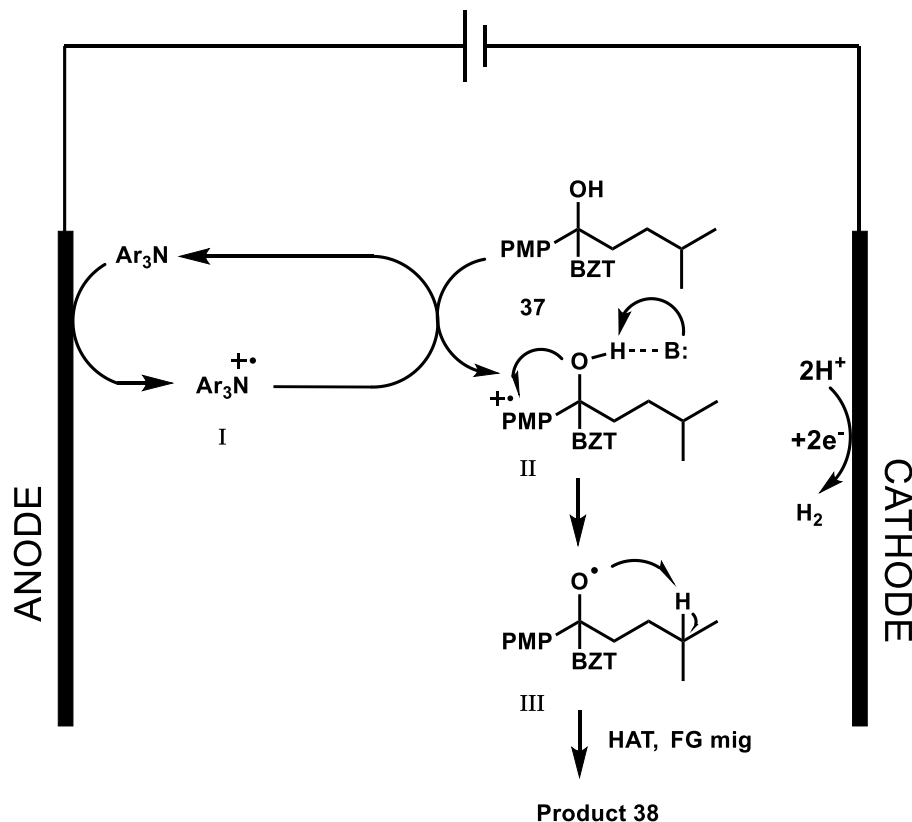
Delightfully, when **38** was subjected to the electrochemical system comprised of 10 mol% of RM-2, 0.1 M Bu₄NPF₆ as supporting electrolyte, 3 equiv. collidine as Brønsted base under the galvanostatic conditions of 3 mA for 6.76 F/mol in DCE/MeOH employing graphite as the anode and platinum as the cathode yielded the product **39** in 30% yield by ¹H NMR and 22% isolated yield.

This result was very satisfying and was one of the proudest moments in the lab.

The rest of the optimizations and mechanistic studies will be done by the other members of the lab.

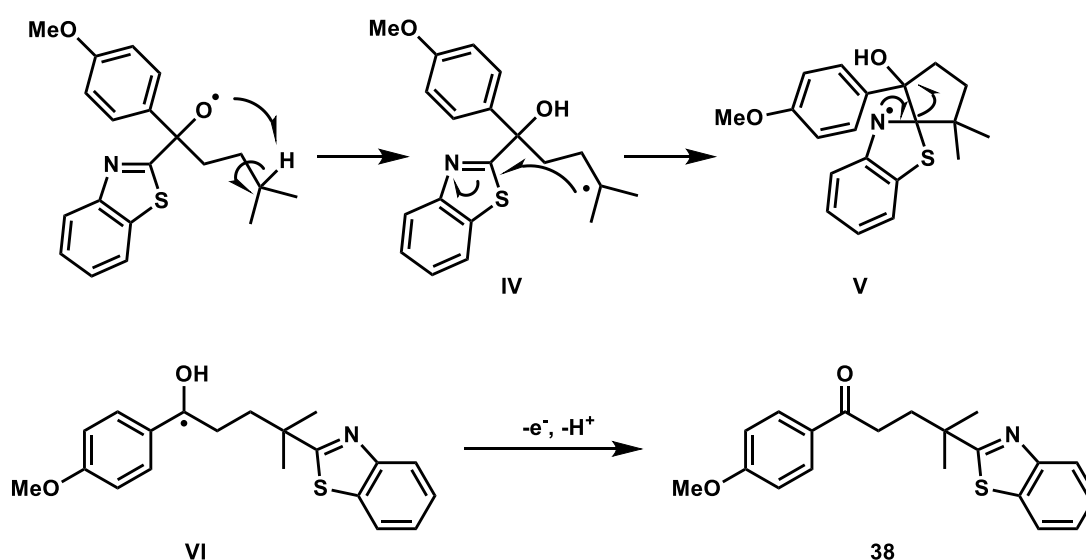
3.3.2.3. Plausible Mechanism

Not enough mechanistic studies have been done to elucidate the mechanism of this transformation. However, based on the formation of the product **38** and developed understanding from the β -scission project, a plausible mechanism can be proposed (scheme 3.41).



Scheme 3.41 – Plausible mechanism

The reaction likely starts with the oxidation of the triarylamine redox mediator on the surface of the anode to furnish the radical cation of triarylamine **I**. Upon electron transfer with the substrate **37**, the triarylamine radical cation would reduce to regenerate the redox mediator and result in the formation of an arene radical cation **II** on the substrate. The subsequent PCET process would then lead to the formation of alkoxy radical intermediate **III**. The alkoxy radical intermediate can then undergo a 1,5-HAT to generate a distal alkyl radical **IV** (scheme 3.42).



Scheme 3.42 – Plausible mechanism

The alkyl radical then would attack on the benzothiazole in a 5-*exo-dig* fashion to generate a five membered transition state **V**, which upon rearrangement would form the benzothiazole migrated intermediate **VI**. This intermediate would likely undergo oxidation at the anode to furnish the product **38**.

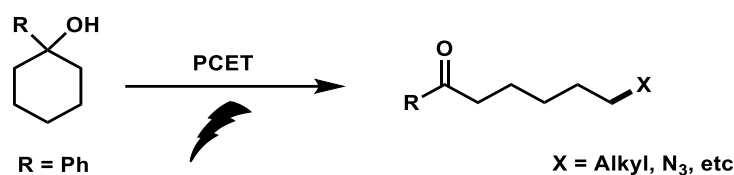
After the formation of intermediate **III**, it could either undergo 1,5-HAT or a β -scission. However, since the tendency of O-centered radicals is to form strong bonds to hydrogen atoms (O–H BDFE \sim 105 kcal/mol) by hydrogen abstraction from weaker C–H (aliphatic) bonds (BDFE \sim 98 -102 kcal/mol), 1,5-HAT should be preferred over the β -scission of the acyclic C–C bonds.^{22,23}

3.4. Future Work

3.4.1. Electrochemical Deconstructive Functionalization via PCET

The immediate/ongoing work in electrochemical generation of alkoxy radicals by PCET would be to complete the substrate scope for the deconstructive bromination project and communicate the result in a peer reviewed journal.

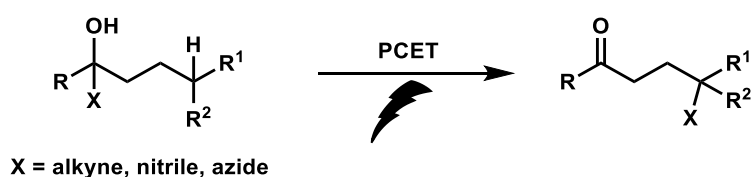
The follow up work for this methodology would be to look for a generalized method for the deconstructive functionalization of cycloalkanols by removing the requirement of a particular electron rich aromatic unit. Also, an alternate functionalization of distal C-centered radical would also be something which would make the method more synthetically useful and diverse (scheme 3.43).



Scheme 3.43 – Future work in electrochemical deconstructive functionalization of cycloalkanols

3.4.2. Electrochemical Remote Functionalization of C(sp³)-H Bond via Alkoxy Radical Induced 1,5 – Hydrogen Atom Transfer (HAT)

For 1,5-HAT and functional group migration, complete optimization studies should be done, where understanding the various factors affecting the yield of the reaction must be carried out before attempting the substrate scope



Scheme 3.44 – Future work in electrochemical 1,5-HAT and FG migrations.

It would also be important to study the possibilities of migration of various other functional groups (scheme 3.44). Along with that, thorough mechanistic studies would also be advantageous to understand the mechanism of the reaction which will also be helpful to discover new projects.

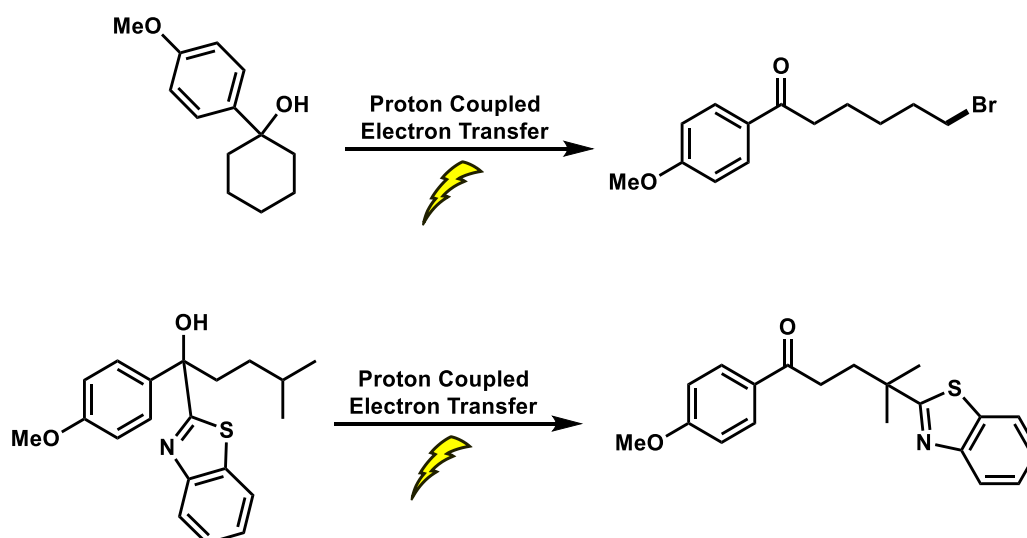
3.5. Summary

In summary, this chapter describes the efforts made in the discovery of a new electrochemical method for the generation of alkoxy radicals enabled by a Proton Coupled Electron Transfer (PCET) process and exploiting the triarylamine redox mediators as electron transfer agents.

This includes an “electrochemical deconstructive bromination of cycloalkanols *via* alkoxy radicals enabled by PCET” in which full optimization studies were carried out, 15 examples are reported, translation into a continuous single pass electrochemical flow has been demonstrated at 10 mmol scale and mechanistic studies were performed.

In addition, another reactivity mode of the alkoxy radicals was exploited which could result in a high impact publication.

The work undertaken in this chapter satisfies the aims and objectives of this thesis.



3.6. References

- 1 J. M. Mayer, *Annual Review of Physical Chemistry*, 2004, **55**, 363–390.
- 2 R. A. Binstead, B. A. Moyer, G. J. Samules and T. J. Meyer, *J. Am. Chem. Soc.*, 1981, **103**, 2897.
- 3 D. R. Weinberg, C. J. Gagliardi, J. F. Hull, C. F. Murphy, C. A. Kent, B. C. Westlake, A. Paul, D. H. Ess, D. G. McCafferty and T. J. Meyer, *Chem. Rev.*, 2012, **112**, 4016–4093.
- 4 Enrico Baciocchi, Massimo Bietti, Osvaldo Lanzalunga and Steen Steenken*, *J. Am. Chem. Soc.*, 1998, **120**, 11516–11517.
- 5 H. G. Yayla, H. Wang, K. T. Tarantino, H. S. Orbe and R. R. Knowles, *J. Am. Chem. Soc.*, 2016, **138**, 10794–10797.
- 6 L. Huang, T. Ji and M. Rueping, *J. Am. Chem. Soc.*, 2020, **0**, 3–10.
- 7 J. Wang, B. Huang, C. Shi, C. Yang and W. Xia, *J. Org. Chem.*, 2018, **83**, 9696–9706.
- 8 H. G. Yayla, H. Wang, K. T. Tarantino, H. S. Orbe and R. R. Knowles, *J. Am. Chem. Soc.*, 2016, **138**, 10794–10797.
- 9 C. Y. Cai, X. M. Shu and H. C. Xu, *Nat. Comm*, 2019, **10**, 4953.
- 10 T. Fuchigami, M. Tetsu, T. Tajima and H. Ishii, *Synlett*, 2001, **8**, 1269–1271.
- 11 S. Dapperheld, E. Steckhan, K.-H. Grosse Brinkhaus, T. Esch, S. Dapperheld, E. Steckhan, K.-H. G. Brinkhaus and T. Esch, *Substituted Triarylamine Cation-Radical Redox Systems-Synthesis, Electrochemical and Spectroscopic Properties, Hammet Behavior, and Suitability as Redox Catalysts*, .
- 12 A. Tlili, F. Monnier and M. Taillefer, *Chem. Commun.*, 2012, **48**, 6408–6410.
- 12a M. S. Kharasch, E. V. Jensen, W. H. Urry, *J. Am. Chem. Soc.* 1947, **69**, 1100.
- 12b M. S. Kharasch, O. Reinmuth, W. H. Urry, *Am. Chem. Soc.*, 1947, **69**, 1105.
- 12c K. Matsui, A. Negishi, Y. Takahatake, K. Sugimoto, T. Fujimoto, T. Takashima, K. Kondo, *Bull. Chem. Soc. Jpn.*, 1986, **59**, 221
- 12d S. Ma, X.J. Lu, *Chem. Soc., Perkin Trans.*, 11990, 2031.
- 12e J. Hartung, N. Schneiders, T. Gottwald, *Tetrahedron Lett.*, 2007, **48**, 6027–6030
- 13 R. Francke and R. D. Little, *Chem. Soc. Rev.*, 2014, **43**, 2492–2521.
- 14 W. Shu, A. Genoux, Z. Li and C. Nevado, *Angew. Chem.*, 2017, **129**, 10657–10660.
- 15 D. A. Leas, Y. Dong, J. L. Vennerstrom and D. E. Stack, *Org. Lett.*, 2017, **19**, 2518–2521.

- 16 Ž. Čeković, *Tetrahedron*, 2003, **59**, 8073–8090.
- 17 J. Hartung, *Stereoselective Construction of the Tetrahydrofuran Nucleus by Alkoxy Radical Cyclizations*, .
- 18 V. D. Parker and Mats. Tilset, *J. Am. Chem. Soc.*, 2002, **110**, 1649–1650.
- 19 J. Robertson, J. Pillai and R. K. Lush, *Chem. Soc. Rev.*, 2001, **30**, 94–103.
- 20 R. T. Weavers, *J. Org. Chem.*, 2001, **66**, 6453–6461.

- 21 X. Wu, M. Wang, L. Huan, D. Wang, J. Wang and C. Zhu, *Angew. Chem.*, 2018, **130**, 1656–1660.
- 22 J. J. Warren, T. A. Tronic and J. M. Mayer, *Chem. Rev.*, 2010, **110**, 6961–7001.
- 23 S. J. Blanksby and G. B. Ellison, *Acc. Chem. Res.*, 2003, **36**, 4, 255–263

“Radicals are ever so quizzical,
Some gentle, some wild, some hysterical,
But the ones I’ve seen,
So seldom are clean,
And the clean ones are so seldom radicals”

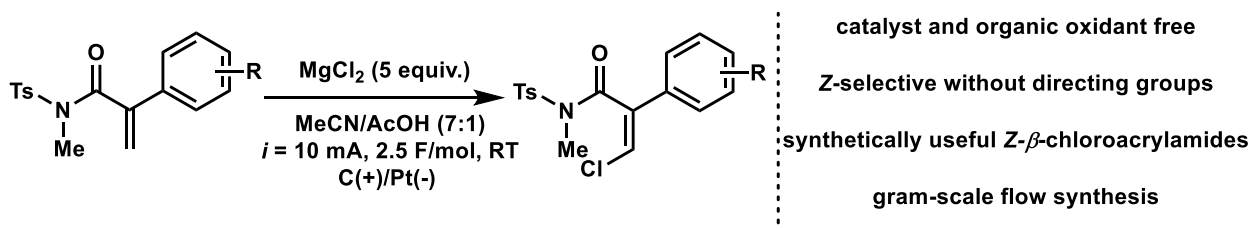
(Parrott –1983)

Chapter 4: Electrochemical Functionalization of Alkenes

4. Preface

This chapter discusses investigations of electrochemical methods for the functionalization of alkenes. An attempt was made to induce an interesting 1,4-desulfonylative migration of aryl functional group by electrochemical trifluoromethylation of acrylamides employing Langlois reagent.

In addition, a serendipitous discovery led to the development of a new electrochemical method for the oxidative C(sp²)-H chlorination of acrylamides. Further work shed light into the reaction mechanism by performing radical clock experiment backed by cyclic voltammetry data.



Publication: James Harnedy, ‡ Mishra Deepak Hareram, ‡ Graham J. Tizzard, Simon J. Coles and Louis C. Morrill* (*manuscript in review*)

Acknowledgements

James Harnedy – Responsible for the optimization, substrate scope and scale up of the electrochemical chlorination. James Harnedy reported 20 examples for this transformation along with post derivatization of the chlorinated acrylamides as well as flow electrochemistry scale up at 4.5 mmol scale.

Mishra Deepak Hareram – Responsible for the discovery of this reaction along with identifying the stereochemistry of the product. Additionally, Mishra Deepak Hareram investigated the reaction mechanism and took part in substrate scope.

Graham J. Tizzard and Simon J. Coles – Responsible for x-ray crystallography. NCS, Southampton.

Louis C. Morrill – Supervisor, Cardiff University

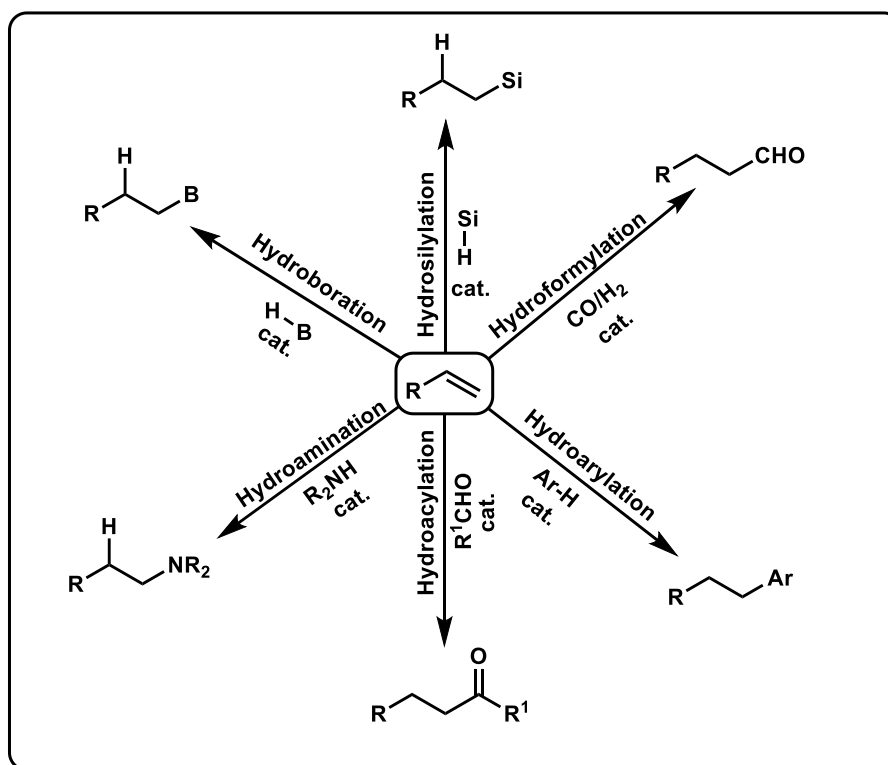
4.1. Introduction

Alkenes are one of the most versatile functional groups in organic chemistry, owing to their ready conversion to many different functional groups (such as Shenvi, Chirik, Norton, Baran etc.) Alkenes exhibit a wide range of reactivity and are considered as a privileged building blocks in organic synthesis.¹ Hence, there is a constant desire for functionalization of alkenes through innovative, efficient, robust, and sustainable methods.^{2,3} Modern practices in alkene functionalization include transition metal catalyzed alkene functionalization⁴ and more recently, radical functionalization of alkenes induced by photoredox catalysis. Electrochemical approaches to alkene functionalization have seen a renaissance pertaining to its reactivity, chemoselectivity and functional group tolerance.^{5,6}

4.1.1. Transition metal catalyzed alkene functionalization

Transition metal catalyzed functionalization of alkenes are one of the attractive and most pursued reactions by which we can access a variety of organic compounds with complex architectures.⁷ There is a plethora of different alkene functionalization reactions in the literature which allow rapid construction of C-H, C-C, C-N, and C-X bonds.^{1,4} These reactions include but are not limited to hydrofunctionalization reactions such as hydroformylation⁸, hydroboration⁹, hydrosilylation⁹, hydroamination¹⁰, hydroarylation¹¹, hydroacylation^{7,12} (scheme 4.1) and carbofunctionalization⁴ reactions such as carboamination^{13,14}, carboetherification^{3,15}, carboacylation,² acylborylation¹⁶ and Heck type reactions¹⁷.

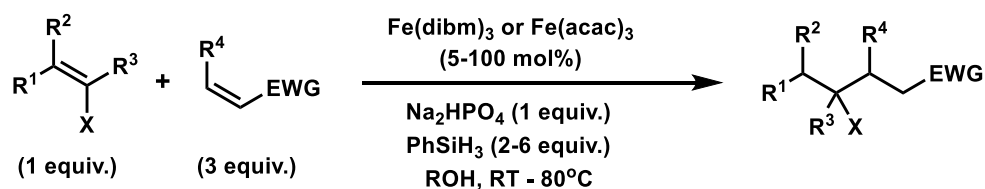
In recent years, interest in iron (Fe), cobalt (Co) and copper (Cu) catalyzed alkene functionalization reactions has increased, with reports from various research groups across the globe because of their high abundance, low cost, and relatively lower toxicity.¹⁸



Scheme 4.1 – Transition metal catalyzed hydrofunctionalization of alkene

4.1.1.1. Iron catalyzed alkene functionalization

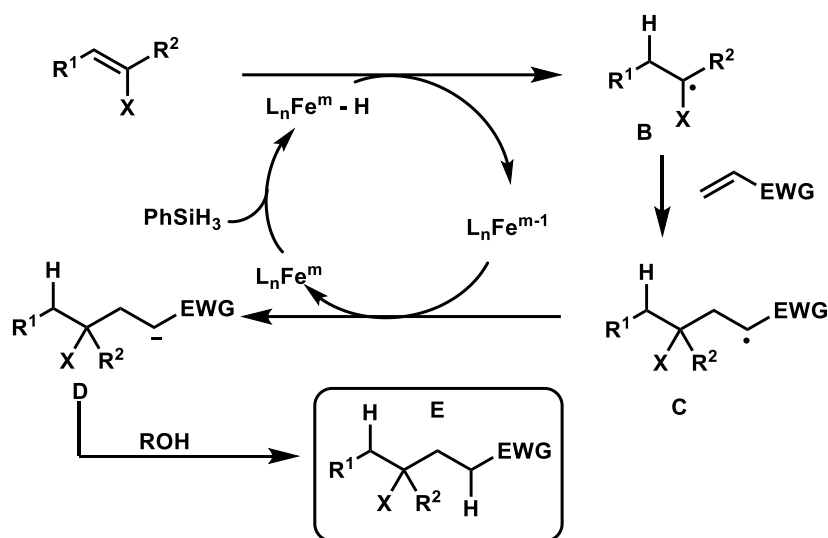
Forging a C-C bond is one of the most sort after reactions in organic synthesis¹⁹. Baran and co-workers developed an iron catalyzed functionalized alkene cross coupling reaction (Scheme 4.2).²⁰ The method elegantly describes a C-C bond formation between a silyl enol ether serving as a donor and cyclohexenone as the acceptor using a $\text{Fe}(\text{dibm})_3$ or $\text{Fe}(\text{acac})_3$ as a catalyst and PhSiH_3 as a stoichiometric reductant.



Scheme 4.2 - Fe catalyzed alkene functionalization

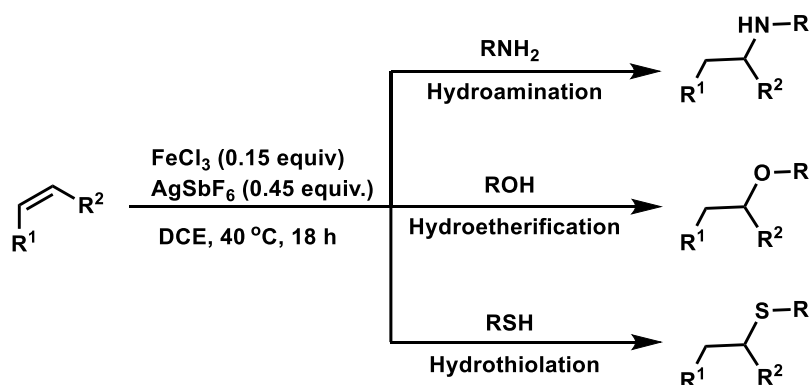
The method demonstrates a wide substrate scope and a relatively good tolerance of different heteroatoms ($\text{X} = \text{O}, \text{N}, \text{S}, \text{B}, \text{Si}, \text{F}, \text{Cl}, \text{Br}, \text{I}$), shorter reactions times and air and moisture compatibility. However, insufficient mechanistic studies were performed, Michael acceptors are not compatible and a few of the reactions resulted in unexpected

regioselectivity. A postulated mechanism (scheme 4.3) suggests that in the initial step, a carbon centered radical is formed **B** from the donor alkene by an *in situ* – generated Fe hydride, which then adds to the acceptor alkene in conjugate fashion and further reduction of **C** would generate a basic site **D**, which can abstract a proton.



Scheme 4.3 – Plausible mechanism of the Fe catalyzed alkene functionalization

Hydrofunctionalization of alkenes offers a direct method to forge carbon–heteroatom bonds in a single step, which is also beneficial in organic synthesis.¹⁸

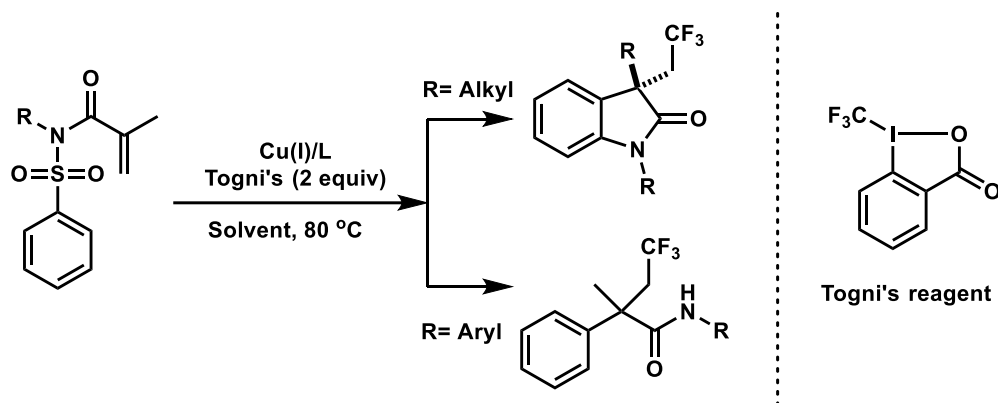


Scheme 4.4 – Iron catalyzed hydrofunctionalization of alkenes

Within the context of hydrofunctionalization, hydroamination²¹ is one of the most pursued transformations, with less attention given to hydroetherification and hydrothiolation. Cook and co-workers reported a versatile method for the construction of C – N, C – O and C – S bonds under mild conditions using a “ligandless” iron catalyst with non-coordinating silver salts to yield hydrofunctionalized products with Markovnikov selectivity, which is a mild alternative to strong Brønsted acid catalysis (scheme 4.4).²²

4.1.1.2. Copper catalyzed alkene functionalization

Another important subclass of alkene functionalization is tandem alkene functionalization and functional group migration.^{23–25} One of the major inspirations that fuelled our interest in electrochemical alkene functionalization reactions was a novel copper – catalyzed one – pot trifluoromethylation/aryl migration/ desulfonylation of acrylamides, reported by Nevado and co-workers.²⁶ The method describes a useful strategy for one – pot trifluoromethylation and arylation of acrylamides (scheme 4.5).

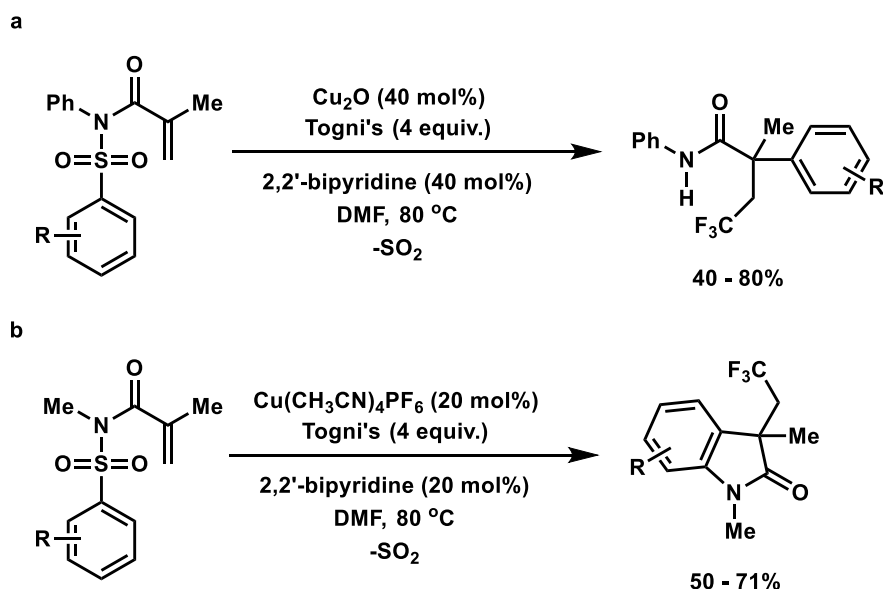


Scheme 4.5 – One-pot trifluoromethylation/ arylation of acrylamides

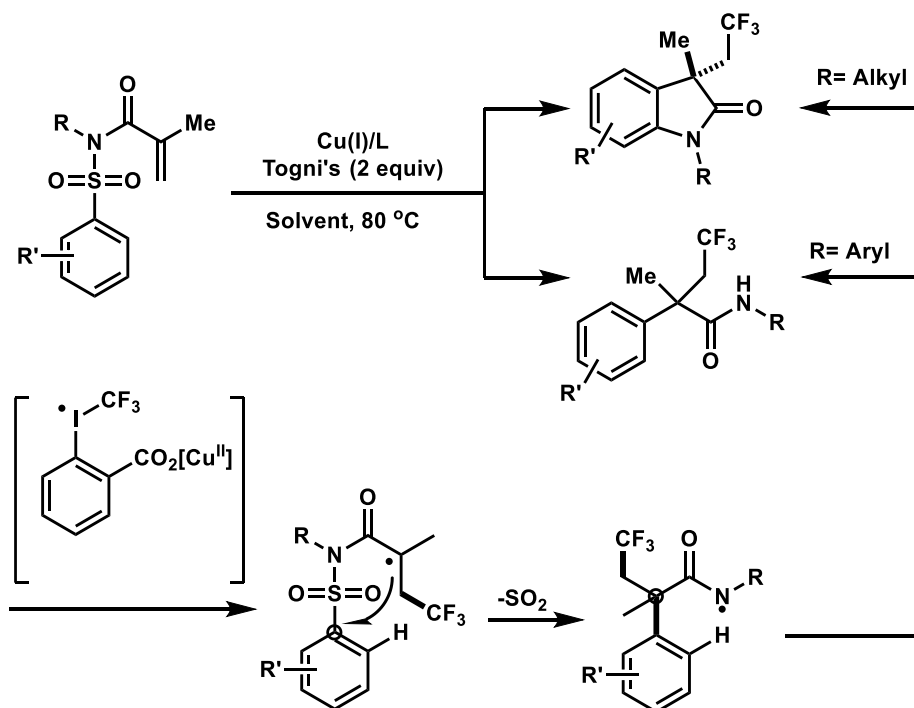
It is worth noting here that depending upon the R group at the nitrogen of the acrylamide, the reaction yielded two different products i.e., trifluoromethylation/aryl migration/ desulfonylation (scheme 4.6 a) or trifluoromethylation/desulfonylation/aryl migration/ cyclization (scheme 4.6 b) with Cu₂O and Cu(MeCN)₄PF₆ respectively.

Reaction (scheme 4.6 b) is completely regioselective, as the 1,4 migration of the aryl group takes place exclusively through the carbon attached to the SO₂ group in the starting material. The product thus formed in a formal 1,3-N migration process is the first example

of such a 1,3 migration. Both the transformations are tolerant to different substitution patterns on the aromatic unit. The mechanism (scheme 4.7) proposed by the authors is based upon several control experiments, including reactions in the presence of radical scavengers (TEMPO or BHT), which resulted in decreased yields pointing towards a radical mechanism.



Scheme 4.6 – trifluoromethylation/aryl migration/ desulfonylation 4.6 a) and trifluoromethylation/ desulfonylation/ aryl migration/ cyclization (4.6 b)



Scheme 4.7 – Mechanism of one pot trifluoromethylation/ arylation

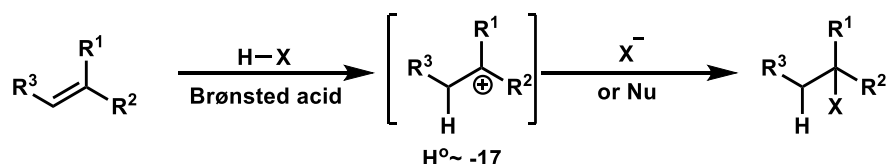
4.1.1.3. Transition metal catalyzed Hydrogen Atom Transfer (HAT)

The last example for the transition metal catalyzed alkene functionalization is the hydrofunctionalization of alkenes by Hydrogen Atom Transfer (HAT) processes, mainly by earth abundant metals such as manganese (Mn), iron (Fe) and cobalt (Co).¹⁸

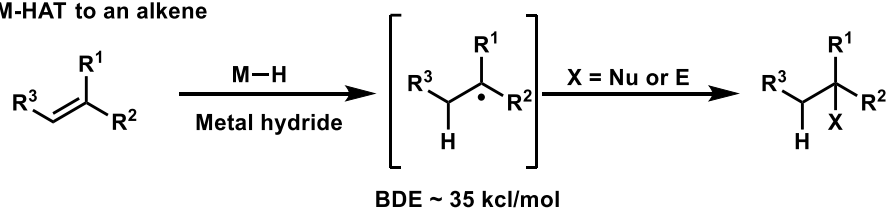
Transition metal catalyzed hydrogen atom transfer (TM-HAT) of alkenes has gained significant attention in synthetic organic chemistry in recent times.^{27,28} Since Halpern discovered the transfer of a hydrogen atom from a cobalt hydride species for the hydrogenation of anthracene,²⁹ and Mukaiyama³⁰ and Drago³¹ reported the catalytic hydration of alkenes under aerobic condition, (TM-HAT) of alkenes has expanded significantly.

One may question the need for (TM-HAT) reactions for the hydrofunctionalization of alkenes, when the same Markovnikov selectivity can be achieved with Brønsted acid reactions. The explanation lies in the formation of the reactive intermediate after the initial C – H bond formation (scheme 4.8).

a. Brønsted acid proton transfer to an alkene



b. TM-HAT to an alkene

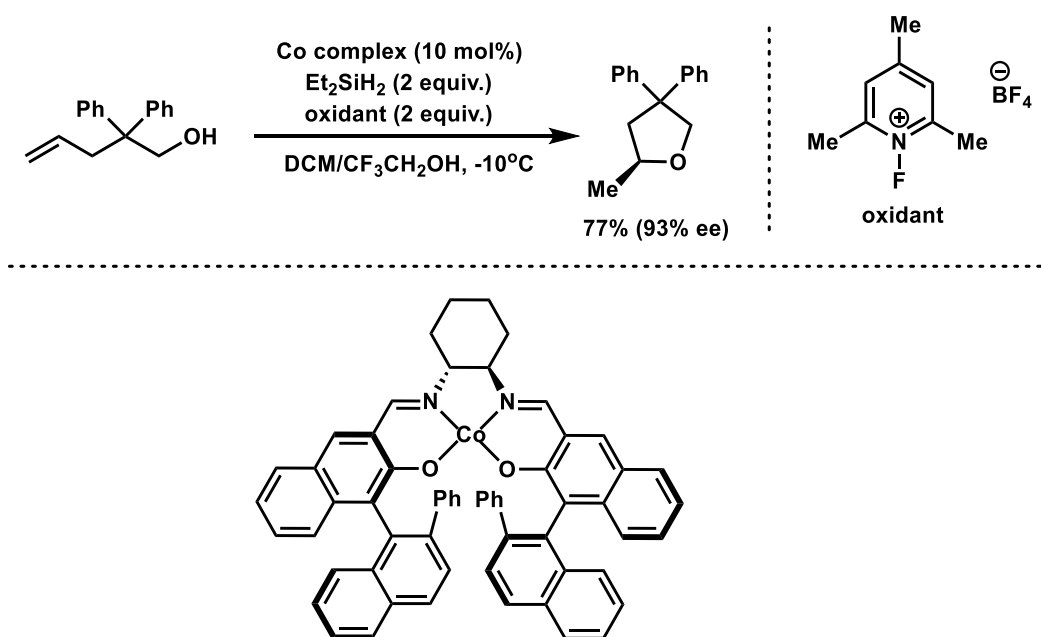


Scheme 4.8 – Proton transfer vs TM-HAT Markovnikov hydrofunctionalization of alkenes

The carbocation formed after the protonation of an alkene by a Brønsted acid is a high energy species. The half-life of a relatively stable *tert*-butyl cation is close to that of a single bond vibration in a water/ trifluoroethanol (TFE) mixture.³² Therefore, alkene protonation in the presence of multiple functional groups can be disfavoured while competing with other low energy barrier reactions. Contrary to the protonation reactions, (TM-HAT) can occur at ambient temperature or lower, at standard pressure

and in the presence of functional groups that are sensitive to acid, base, heat, reductant and or oxidant. Hence, (TM-HAT) is preferred for the hydrofunctionalization of alkenes because it offers milder reaction conditions than protonation and is more chemoselective.³³

One recent example of hydrofunctionalization of alkenes by (TM-HAT) which bestows the advancement of this genre is enantioselective hydrofunctionalization of alkenes by cobalt-catalyzed hydrogen atom transfer and radical-polar crossover developed by Shigehisa and co-workers (scheme 4.9).³⁴

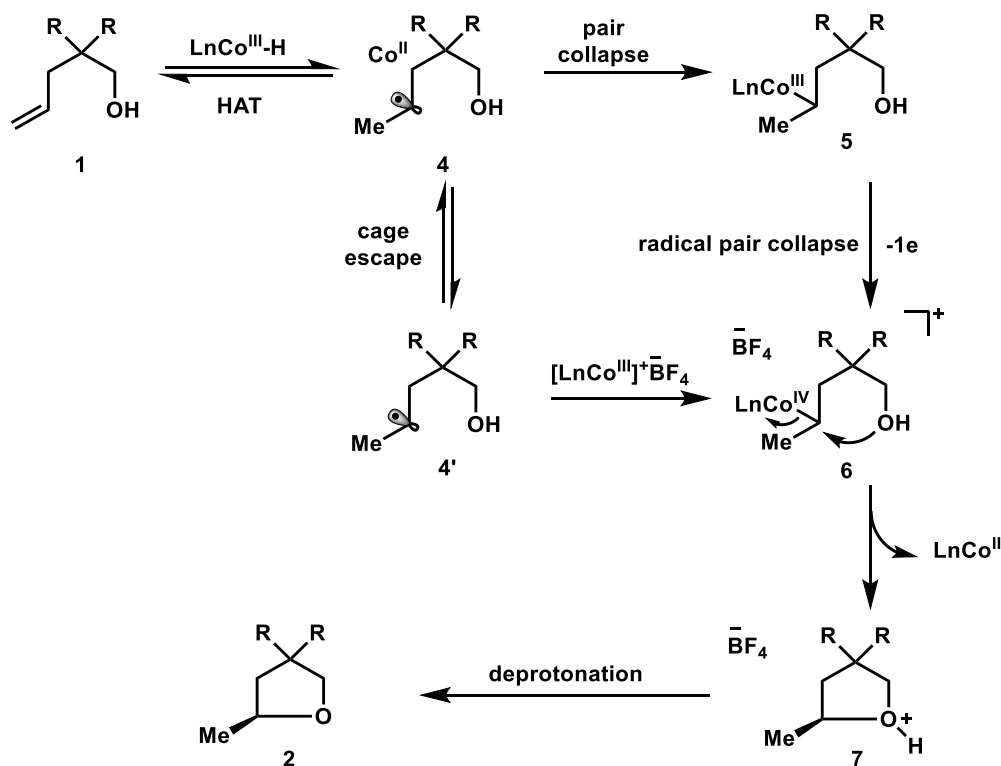


Scheme 4.9 – Cobalt-catalyzed enantioselective hydrofunctionalization of alkenes by cobalt-catalyzed hydrogen atom transfer and radical-polar crossover

The method describes a hydroalkoxylation of nonconjugated alkenes with excellent enantioselectivity using a suitable chiral cobalt catalyst, N-fluoro-2,4,6-collidine tetrafluoroborate as oxidant and diethyl silane as a hydrogen source. Although the substrate scope is moderate, the method showed good tolerance of the functional groups with excellent yields and enantioselectivity.

A thorough investigation into the reaction mechanism and enantioselectivity has been done. The authors proposed the initial formation of a caged radical catalyst pair **4** after the cobalt (III) hydride HAT to the alkene (scheme 4.10). It is suggested that the subsequent bifurcation of the reaction would be: (1) the cage-collapsed alkylcobalt (III)

complex **5** is formed, followed by a single-electron oxidation to generate scalemic alkylcobalt (IV) intermediate **6**, or (2) the pair collapse is bypassed and the escaped diffused radical **4'** is captured by a cationic cobalt (III), thereafter the pathways converge to the key alkylcobalt (IV) intermediate **6**. The C – O bond would be formed by nucleophilic displacement with stereo-inversion to afford **7** and finally, deprotonation of **7** by 2,4,6-collidine would afford product **2**. The enantio-determining nucleophilic displacement of the alkylcobalt (IV) complex **6** can be rationalized by the difference between the two transition states derived from each diastereomeric alkylcobalt (IV) complex. Pronin proposed such an enantioselective kinetic resolution of alkylcobalt (IV) complex with the prior epimerization via a radical chain mechanism.^{34a}

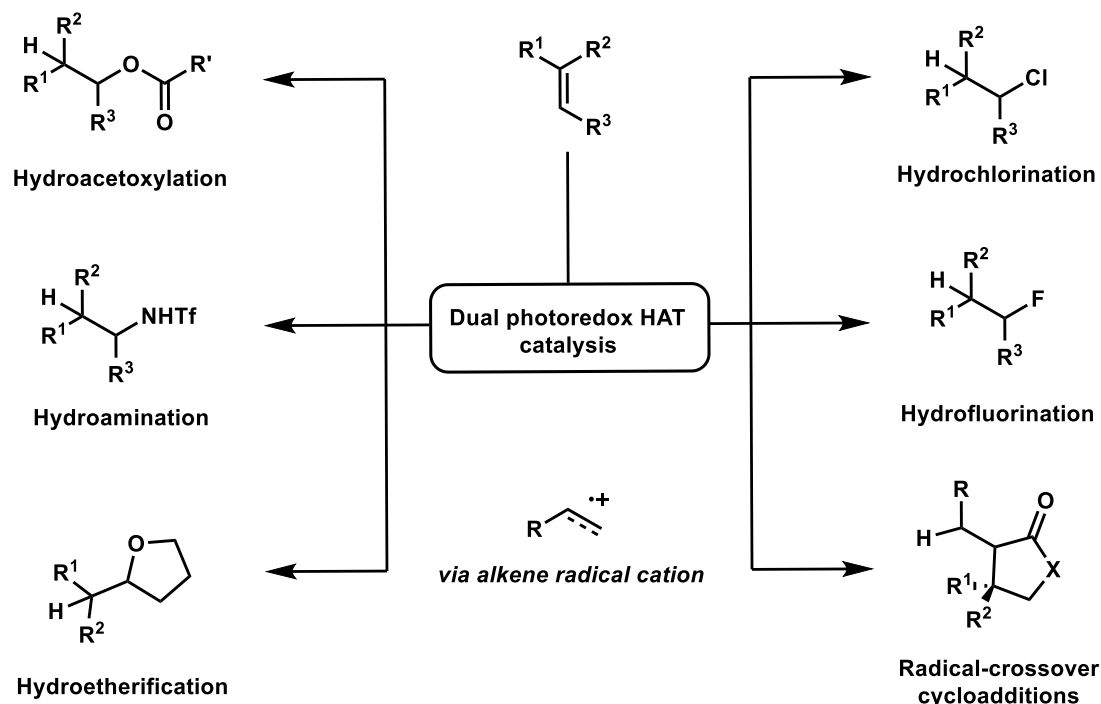


Scheme 4.10 – Proposed mechanism of Cobalt-catalyzed HAT and radical polar cross over

Transition metal catalyzed functionalization of alkenes is a vast research topic and the examples and classes discussed in this thesis are specific to the research areas that we aimed to explore.

4.1.2. Photochemical Methods of Alkene Functionalization

Transition metal catalyzed hydrofunctionalization of alkenes, in almost all cases, results in product formation which takes place in accordance with the Markovnikov rule.¹⁸ In contrast with this, the Nicewicz group reported a series of novel dual photoredox HAT catalysis enabled transformations such as intermolecular hydroacetoxylation³⁵, intra- and intermolecular hydroamination^{36,37}, hydroetherification³⁸, polar radical crossover cycloadditions^{39,40} and methods of direct addition of mineral acids⁴¹ in an anti-Markovnikov fashion (scheme 4.11).

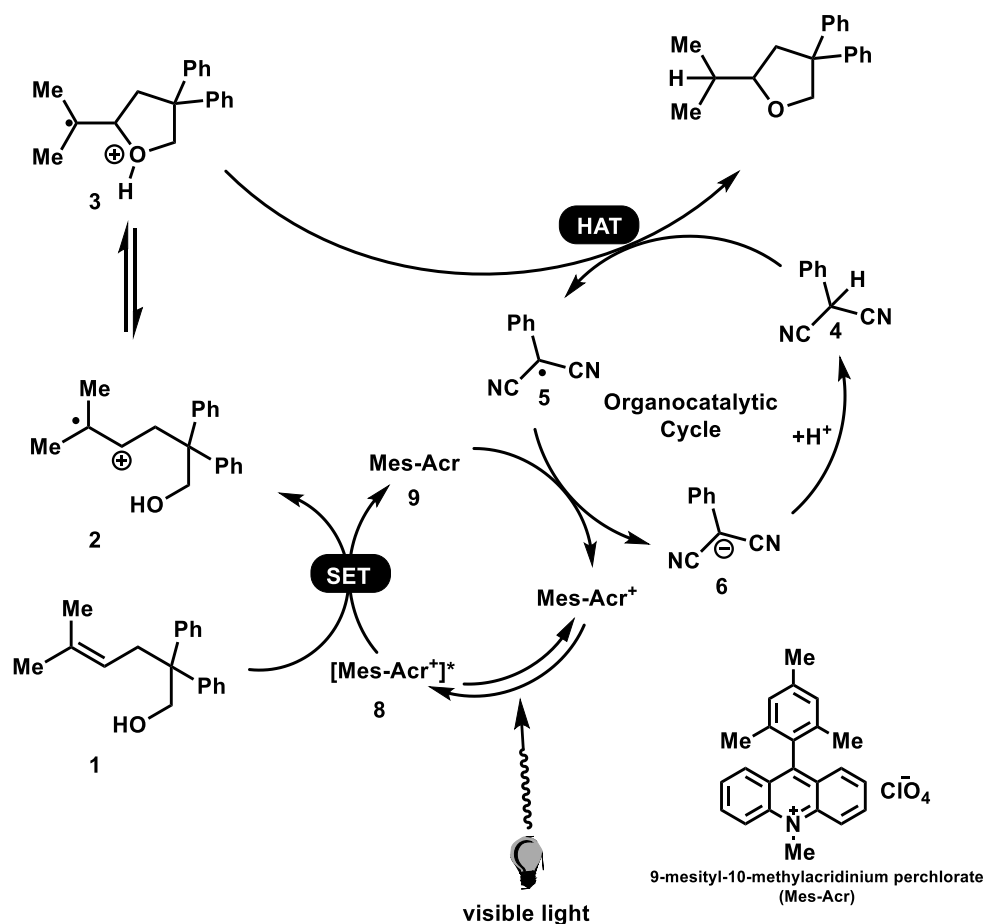


Scheme 4.11 – Anti Markovnikov hydrofunctionalization of alkenes via dual photoredox HAT catalysis

4.1.2.1. Dual Photoredox Strategy

This alternate reactivity mode is achieved by employing a dual photoredox strategy for the hydroetherification of alkenols,³⁸ in which the excited state of the photocatalyst **8** undergoes a single electron transfer with alkene **1** to deliver the corresponding radical

cation **2**. This highly electrophilic species is now primed to intercept a wide range of nucleophiles. However, reduction of the carbon-centered radical **3** with the photocatalyst proceeds with less efficiency. To circumvent this limitation a redox active catalyst **4** is used, wherein, **3** can undergo a HAT event to deliver the tetrahydrofuran product. In the subsequent event, the 2- phenylmalonitrile radical **5** can be readily reduced by the photocatalyst **9**, thereby closing the photoredox cycle and generating anion **6**. Finally, protonation of **6** regenerates the HAT catalyst closes the organocatalytic cycle (scheme 4.12).



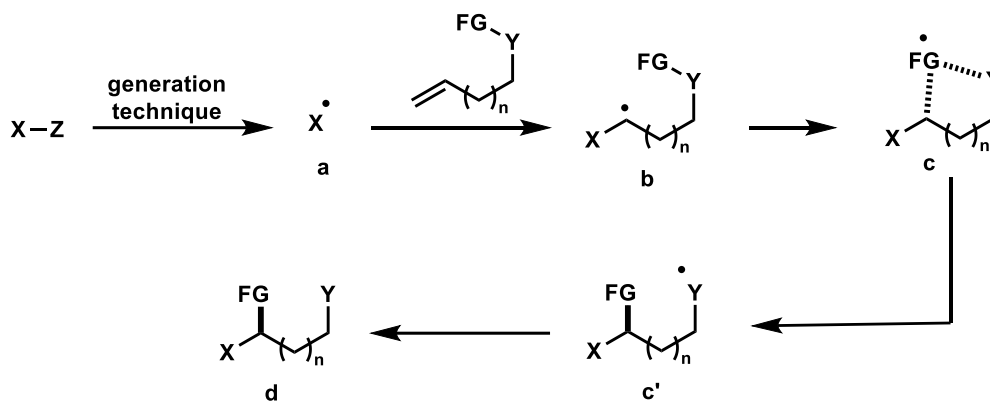
Scheme 4.12 – Proposed mechanism of dual photoredox HAT catalysis for the generation and trapping for alkene radical cations

The above examples describe the advantage of the photoredox chemistry over the transition metal catalyzed alkene functionalization to achieve anti-Markovnikov selectivity.

4.1.2.2. Photochemical “Docking-Migration” Strategy

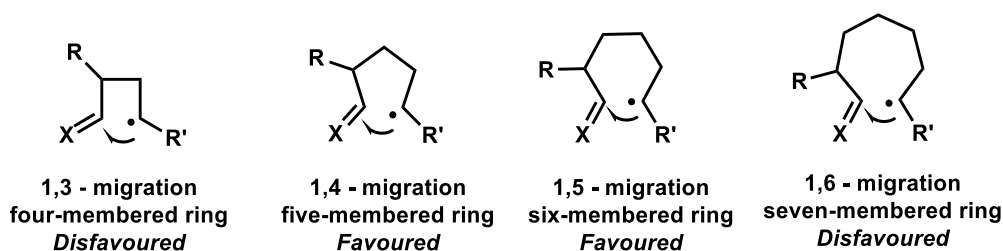
Radical mediated difunctionalization presents a unique strategy to functionalize alkenes^{42,43}. Despite the considerable progress made in the past several decades, state-of-the-art methods are highly dependent upon activated alkenes in which the proximal group with a π -electron system such as aryl, carbonyl, and heteroatom is a prerequisite to accept the incoming alkyl radical intermediate via p- π conjugation or p orbital of the heteroatom. This prerequisite of the activated alkenes can be addressed by installing an intramolecular SOMOphile at the distal end of the alkene, to induce an intramolecular distal functional group migration. ⁴⁴

Mechanistically, a radical-mediated remote functional group migration (FGM) process can be broken down into following steps (scheme 4.13); (a) generation of initial radical (X^\bullet) which can be practically achieved by either transition metals, photoredox process or electrochemically; (b) generation of the proximal radical intermediate X; (c-c') FGM via consecutive cyclic transition state formation/ cleavage to generate the radical intermediate Y; (d) quenching/ termination of the radical intermediate Y (scheme 4.13).



Scheme 4.13 – Schematic representation of radical mediated FGM strategy

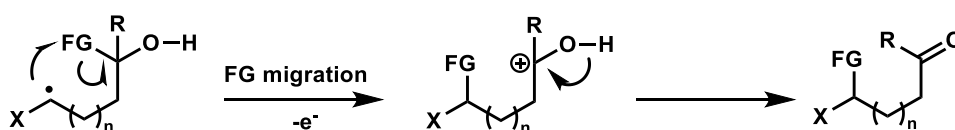
If we consider the range of migrations; 1,4 and 1,5 – functional group migrations are kinetically favoured as it goes *via* a five or six- membered transition state, while 1,3- or 1,6-functional group migrations are disfavoured because of the four or seven – membered transition states respectively (scheme 4.14).^{45,46}



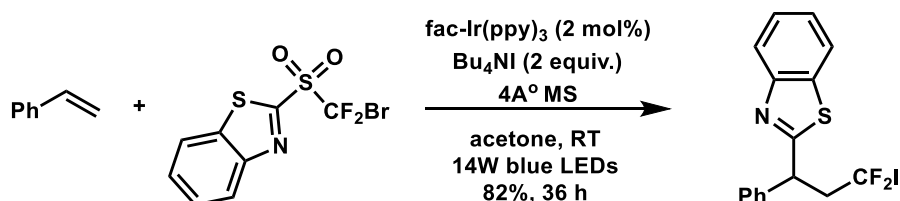
Scheme 4.14 – Transition states for functional group migration

Chen Zhu's research group is at the forefront of this functional group migration strategy. Despite the many advantages of alkene difunctionalization *via* a functional group migration strategy, the major limitation arises from the fact that a strategically designed tertiary alcohol is required. This limitation was overcome by Zhu and co-workers by a new “docking-migration” strategy (scheme 4.15).⁴⁷

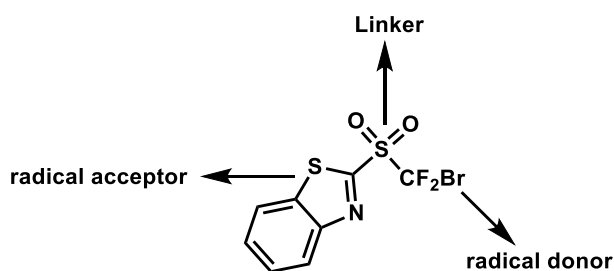
Limitation of the FGM strategy



"Docking - migration" strategy



Use of dual - function reagent

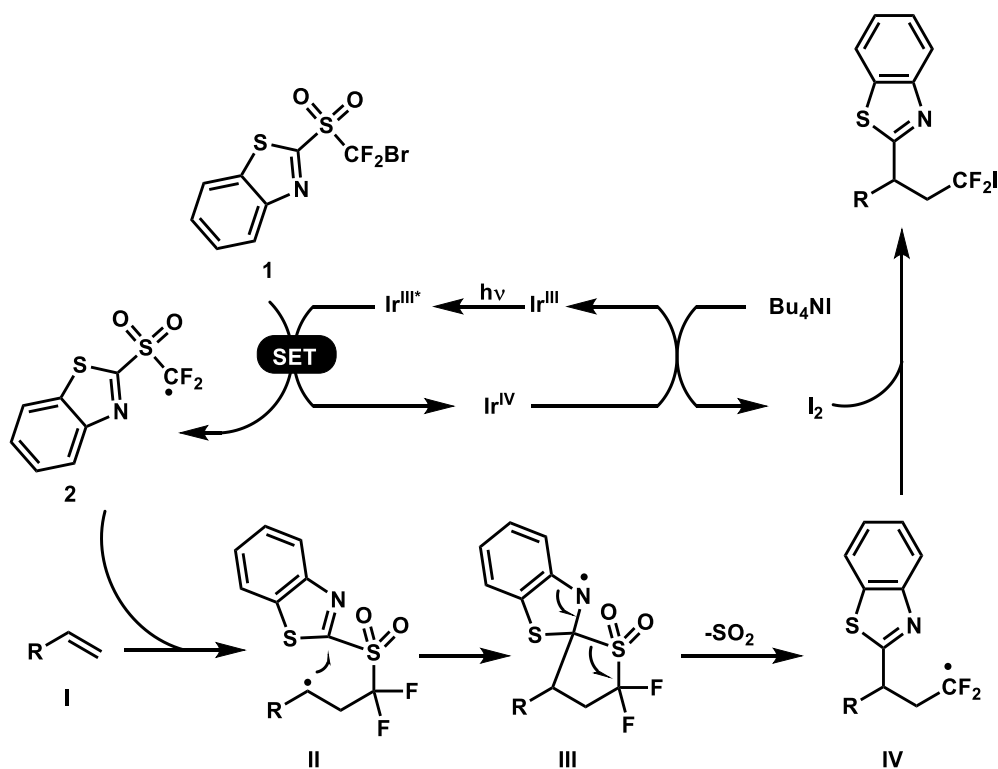


Scheme 4.15 – Limitation of FGM strategy and “Docking – migration” strategy

In this strategy, a dual function reagent is used, for example a sulfone-based reagent (scheme 4.15), which consists of a radical donor and radical acceptor tethered to a traceless linker.

The method demonstrates a wide substrate scope and functional group tolerance. The heteroaryl and difluoromethyl functionalities are simultaneously incorporated into alkenes to afford variety of valuable fluorine-containing compounds. Late-stage functionalization of natural products has also been achieved.

Mechanistically, the authors proposed that the excited state of the photocatalyst (fac-Ir(ppy)₃) is oxidatively quenched by **1** to form difluoromethyl radical **2** and Ir^{IV} species.⁴⁸ Addition of **2** to alkene **I** affords the active alkyl radical intermediate **II**. The simultaneous intramolecular interception of the alkyl radical by benzothiazole via a five-membered transition state generates the spiro-N-radical **III**. Extrusion of SO₂ results in difluoroalkyl radical **IV** and in a concomitant fashion, single-electron transfer (SET) from tetrabutylammonium iodide to Ir^{IV} generates molecular iodine and reduced the Ir^{IV} to Ir^{III} and closes the photoredox cycle. Iodine thus generated reacts with **IV** to furnish final difunctionalized product (scheme 4.16).



Scheme 4.16 – Mechanism of "Docking-Migration"

Photoredox chemistry serves a good alternative for the transition metal catalyzed alkene functionalization. The most important aspect of photoredox approach is that anti-Markovnikov selectivity can be achieved, which is somewhat difficult with the transition metal catalysed processes. However, there are few drawbacks to consider when assessing the photoredox approach such as (a) in some cases, a stoichiometric internal oxidant/reductant is required for turning over the photocatalyst, (b) requires a cooling fan to regulate temperature of the reaction because of the heat emitted by the light/ UV source, (c) long reaction times, (d) often it requires precious metals as photocatalyst, and (e) the scale-up of the photoredox processes is still under development.

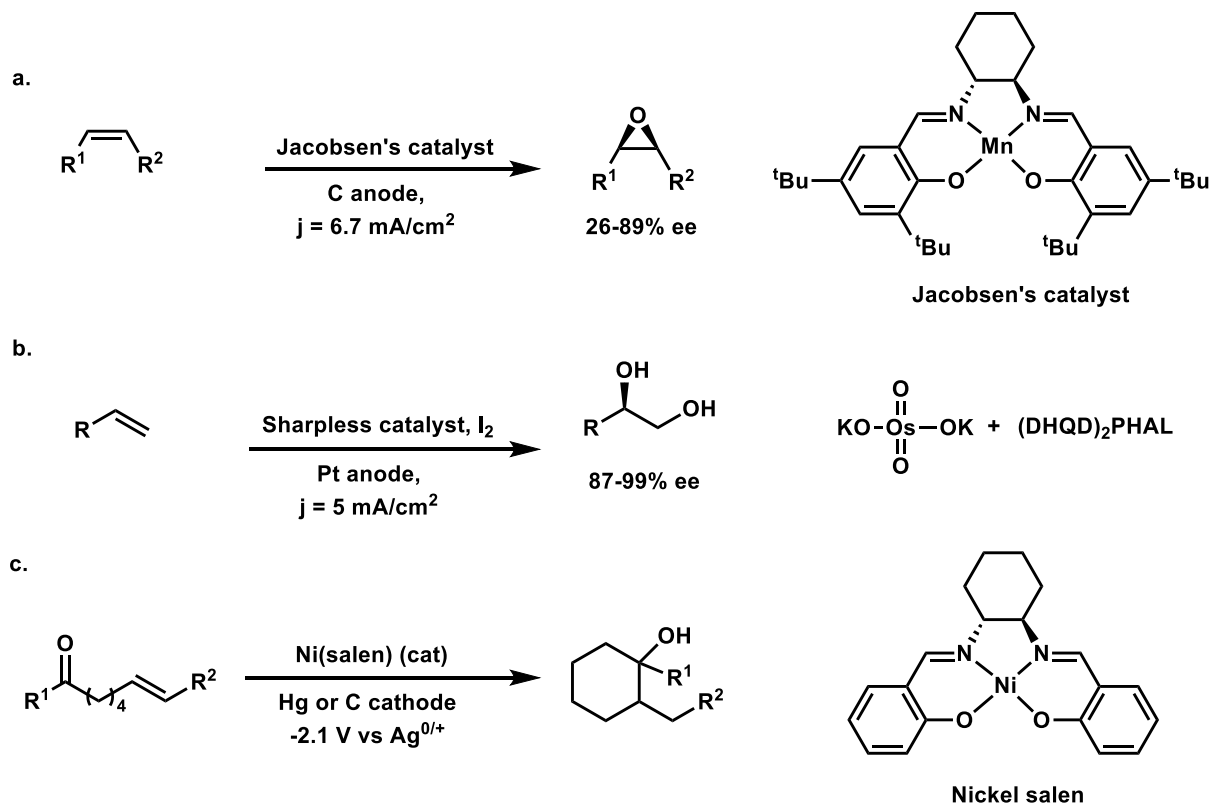
4.1.3. Electrochemical Methods of Alkene Functionalization

Both photoredox and electrochemical methodology use electrons as reagents to generate open-shell radical intermediates. Due to the similar modes of action, it is often possible to translate one method to another by careful selection of conditions.⁴⁹ Electrochemistry can provide a good alternative to photoredox methodology. The transformations can be carried out without precious metals and in much shorter reaction times at the surface of the electrodes, by simply tuning the potential and the rate of addition of electrons thus making the reaction conditions more selective.⁵⁰

Electrochemistry offers an alternative approach to many of the classical alkene functionalizations which are catalyzed by organometallic complexes. For instance, manganese salen complexes have been used in an elegant protocol for the electrochemical olefin epoxidation that mechanistically mimics the Jacobsen – Katsuki epoxidation, which excludes the requirement for hypochlorite.⁵¹ Other such examples include the osmium tetroxide catalyzed alkene dihydroxylation⁵² and nickel catalyzed reductive cyclization⁵³ (scheme 4.17).

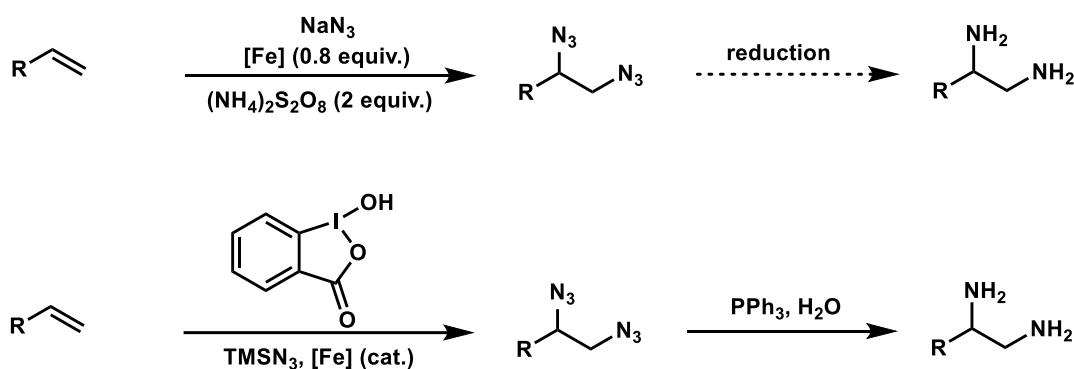
Song Lin and co-workers have reported various electrochemical methods of alkene difunctionalization.⁵⁴ In one of their seminal works they demonstrated a mild and efficient approach to synthesize vicinal diamines via alkene diazidation.⁵⁵ This work is a significant improvement over the existing methods for the synthesis of vicinal diamines. Existing protocols uniformly require stoichiometric quantities of reagents such as

peroxydisulfates⁵⁶, high valent metal salts⁵⁷ or hypervalent iodine reagents⁵⁸ (scheme 4.18).

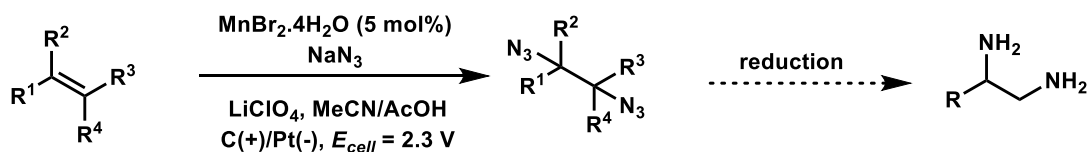


Scheme 4.17 – Organometallic complexes catalyzed alkene functionalization

Existing protocols for alkene diazidation

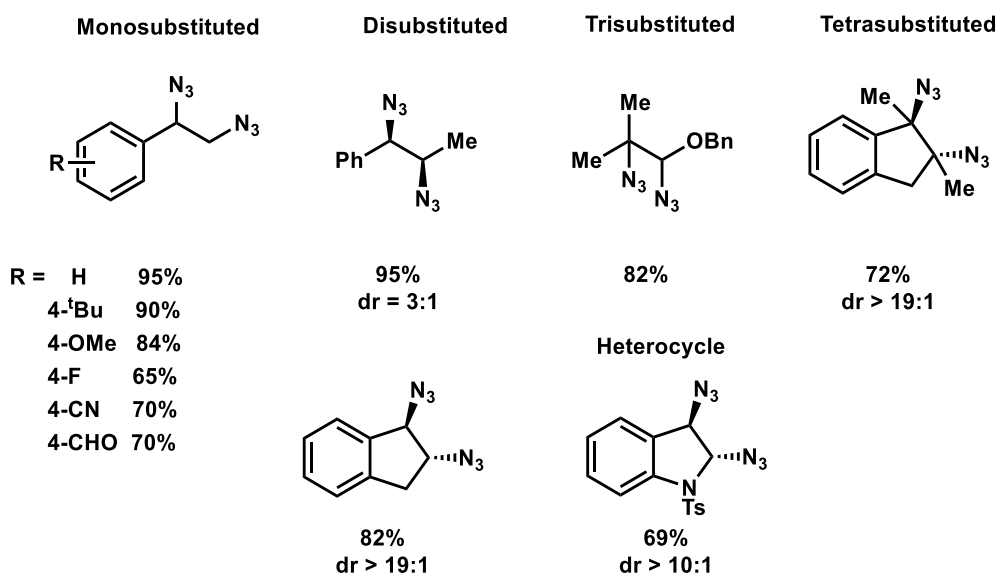


Song Lin's Electrochemical alkene diazidation



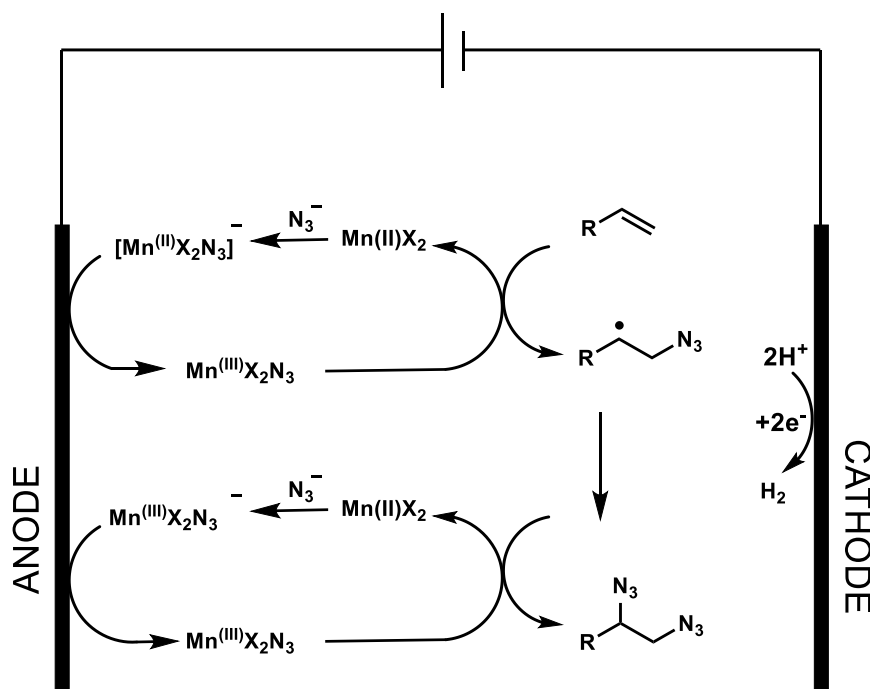
Scheme 4.18 – Methods of diazidation of alkenes

The authors reported a wide substrate scope, with the method tolerating a variety of functional groups such as nitrile, aldehyde, amine, heterocycles etc. The diazidation is not only limited to unsubstituted alkenes, but di, tri and tetrasubstituted alkenes were also tolerated, yielding diazidation products in good to excellent yields (scheme 4.19).



Scheme 4.19 – Substrate scope of electrochemical diazidation

The mechanistic investigations led them to postulate the reaction mechanism in which manganese assisted delivery of two equivalents of azide occurs, first by forming the key group transfer agent, $\text{Mn}^{\text{III}}\text{-N}_3$. This intermediate forms through ligand exchange from $\text{Mn}^{\text{II}}\text{-X}$ ($\text{X} = \text{Br}$ or OAc) to $(\text{Mn}^{\text{II}}\text{-N}_3)^+$ and subsequent oxidation at the anode. This $\text{Mn}^{\text{III}}\text{-N}_3$ species resembles metal – oxo radical chemistry.⁵⁹ The interception of the azidyl radical equivalent by the manganese catalyst is presumably the origin of the observed selectivity seen in the reaction (scheme 4.20).

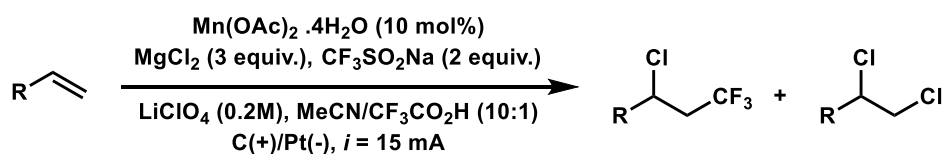


Scheme 4.20 – Proposed mechanism of electrochemical diazidation of alkenes

Organofluorine compounds are of great importance in pharmaceutical, agrochemical and in material science.^{60,61} As such the trifluoromethyl (CF₃) group is highly valuable for application in drug discovery, as the incorporation of CF₃ group significantly improves the lipophilicity, bioavailability, and protein binding affinity of a molecule.⁶² Fluorine has also been used as functional quasi-isostere of oxygen because of its similar electronic properties (Pauling scale : F: 4.0, O: 3.5, H: 2.1).⁶³

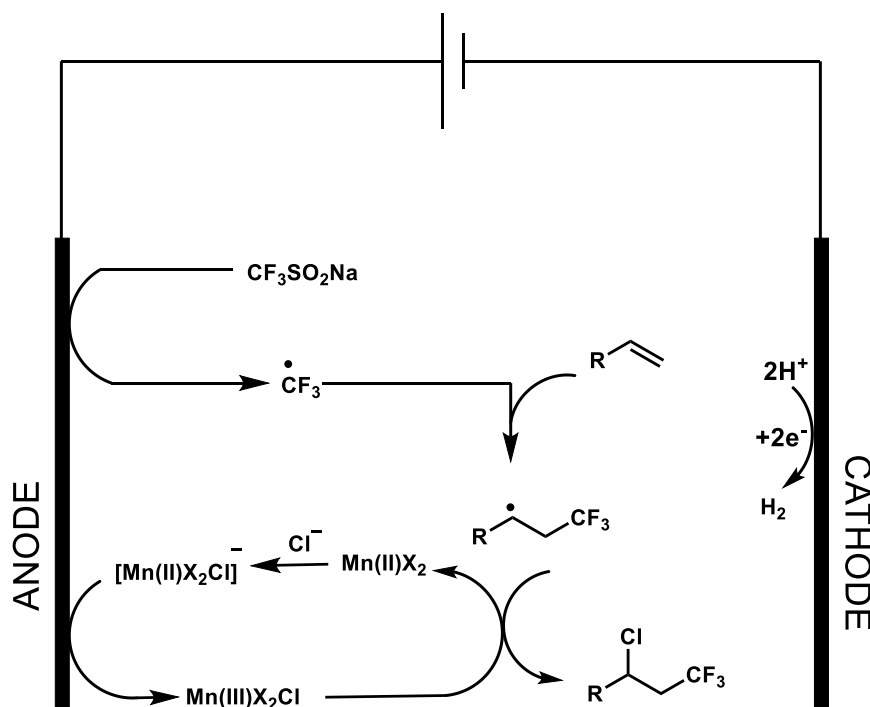
The demand for trifluoromethylation has seen a great development in recent decades, which has resulted in development of a plethora of trifluoromethyl sources and trifluoromethylation methods.⁶⁴ Trifluoromethylation of alkenes in particular is of great interest to organic chemists, as it opens the possibilities of concomitant introduction of other functional groups.⁶³

Electrochemistry has played an important role in the development of greener, efficient, and robust methods of trifluoromethylation. Song Lin and co-workers developed an electrochemical method of heterodifunctionalization of alkenes in which they converted a range of different alkenes to the chlorotrifluoromethylated products, in good to excellent yields (scheme 4.21).⁶⁵



Scheme 4.21 – Electrochemical chlorotrifluoromethylation of alkenes

Mechanistically this transformation is very interesting, as there are two different open-shell reactive intermediates being formed in the reaction. Langlois reagent ($\text{CF}_3\text{SO}_2\text{Na}$) is employed as a trifluoromethyl source and magnesium chloride (MgCl_2) as the chlorine source. Under electrochemical conditions, the same group have reported the generation of $[\text{Mn}^{\text{III}}-\text{Cl}]$ species⁶⁶ which is assumed to act as a radical chlorinating agent. The redox potential of $\text{CF}_3\text{SO}_2\cdot / \text{CF}_3\text{SO}_2^-$ ($E_{p/2} = 800 \text{ mV}$) matches that of $[\text{Mn}^{\text{III}}-\text{Cl}]$ ($E = 780 \text{ mV}$), which can be generated under a sufficient potential, simultaneously. Out of the several outcomes, the formation of the major product can be reasoned by the $\text{CF}_3\cdot$ (a transient free radical) adding to alkene more rapidly than $[\text{Mn}^{\text{III}}-\text{Cl}]$ (a persistent radical) and then the interception of the carbon centred radical formed by $[\text{Mn}^{\text{III}}-\text{Cl}]$ to yield the product (scheme 4.22).



Scheme 4.22 – Plausible mechanism of electrochemical chlorotrifluoromethylation

4.2. Aims and Objectives

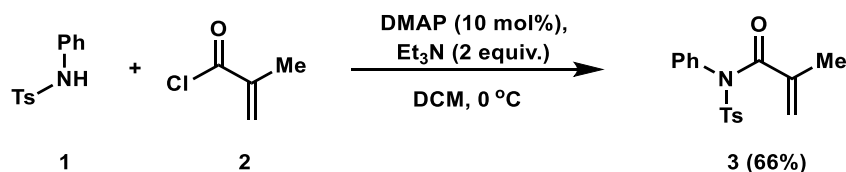
The examples discussed above clearly demonstrate the significance and advantages of electrochemical methods toward alkene functionalization, and indeed were a source of inspiration for our work.

As discussed in the photochemical methods, functional group migration that accompanies alkene functionalization is an attractive method to access highly functionalized compounds. There are a number of reports exhibiting different migrations induced under electrochemical conditions, such as, 1,2-migrations⁶⁷⁻⁷¹ which represent rearrangements (semi-pinacol and Dowd – Beckwith type ring expansions). There are also examples of 1,4-migrations that have been reported which achieve heteroaryl⁷² and alkenyl migrations.⁷³ However, alkene difunctionalization with desulfonylative 1,4 aryl migrations²⁶ have not been explored in an electrochemical system, to the best of our knowledge. Nevado and co-workers reported a copper catalysed trifluoromethylation/desulfonylative aryl migration which employed Togni's reagent was used as the trifluoromethyl source.²⁶ Hence, we selected the acrylamides as our model system to initiate our research by using Langlois reagent⁷⁴ as the trifluoromethyl source. The results will be discussed in detail in the next section.

4.3. Results and discussion

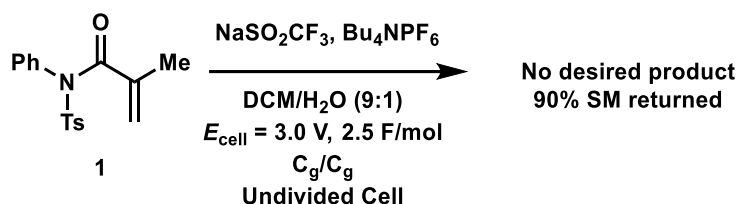
4.3.1. Electrochemical trifluoromethylation of alkenes

Drawing from the works of Lin⁶⁵, Nevado²⁶ and Pan,^{73,75} experiments with acrylamide **3** as a model substrate (as it provides the necessary architecture required for the desulfonylative 1,4-aryl migration) began. The substrate was prepared by following the procedure reported by Pan⁷⁶ by using N-phenyl tosylamine **1** and methacryloyl chloride **2** in one step in a 66% isolated yield (scheme 4.23).



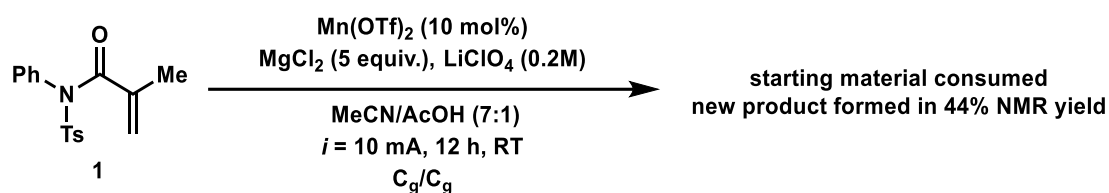
Scheme 4.23 – Synthesis of acrylamide substrate

With substrate **3** in hand, electrochemical trifluoromethylation was attempted using Langlois reagent (NaSO_2CF_3) (2 equiv.) as the trifluoromethyl source under potentiostatic conditions of $E_{\text{cell}} = 3.0$ V with Bu_4NPF_6 (2.5 equiv.) as supporting electrolyte and graphite as the cathode and anode in $\text{DCM}/\text{H}_2\text{O}$ (9:1) (scheme 4.24). The reaction was electrolysed until 3 F/mol of charge had been passed.

Scheme 4.24 – Electrochemical trifluoromethylation of acrylamides. Reaction was analysed by ^1H NMR analysis of the crude reaction mixture, using 1, 3, 5 trimethylbenzene.

^1H NMR analysis of the crude reaction mixture showed no product formation, and 90% of the starting material was returned. It was inferred that the generation of a trifluoromethyl radical is the issue with reaction. The electrolysis was then carried out under galvanostatic conditions at 10, 15 and 20 mA current. This did not result either in the consumption of the starting material or formation of product. Several other parameters were changed in our initial exploration such as solvent, proton source, electrode material, electrolyte and amount of charge passed. Unfortunately, nothing improved the outcome of the reaction.

It was reasoned that either the generation of CF_3^\bullet radical in the electrochemical set-up, or addition of the moderately nucleophilic CF_3^\bullet to the electron deficient acrylamide could be the limiting factors in this reaction. **1** was then subjected to a reaction under our previous reaction conditions⁷⁷, which was originally reported by Lin and co-workers for the dichlorination of alkenes (scheme 4.25).⁶⁶



Scheme 4.25 – Electrochemical chlorination of acrylamides

The acrylamide substrate **1** was subjected to the constant current condition of 10 mA in the presence of Mn(OTf)_2 (10 mol%), MgCl_2 (5 equiv.), LiClO_4 (2 equiv.) in MeCN/AcOH (7:1) for 12 h. ^1H NMR analysis of the crude reaction mixture showed the consumption of the starting material and formation of a new product. Thorough characterization of the product formed revealed an interesting transformation. The project will be discussed in **section 4.2.2** of this thesis in detail.

While the product of the reaction (scheme 4.25) was being characterized, pursuit for trifluoromethylation and 1,4-functional group migrations continued.

After exhausting all the logical attempts to get the reaction (scheme 4.24) working, it was decided to make the alkene more electron neutral in comparison to the electron poor acrylamide. The logic behind engineering the alkene was based upon the fact that if a CF_3^\bullet radical is nucleophilic enough to add on to an electron deficient alkene, then it should add on to an electron neutral alkene (figure 4.1)

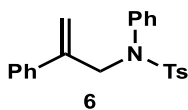
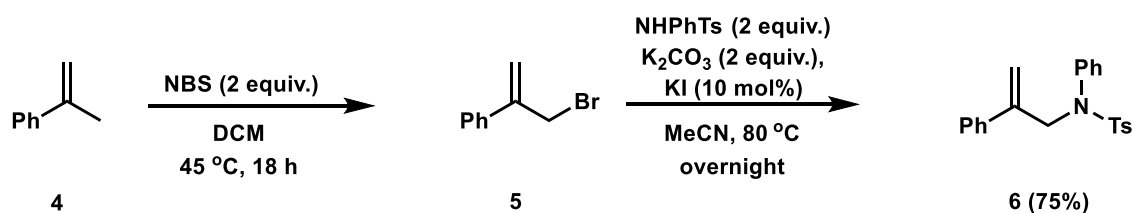


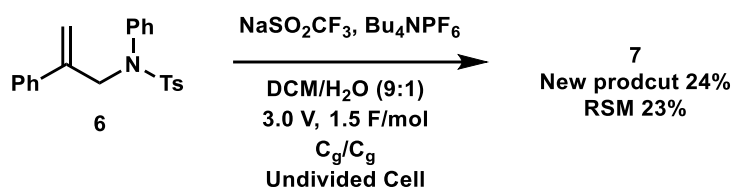
Figure 4.2 – An electron rich alkene

The compound **6** was synthesized in two steps starting with the bromination of α -methyl styrene **4** and then reacting it with N-phenyl tosylamine **1** to yield alkene **6** in 75% yield (scheme 4.26).



Scheme 4.26 – Synthesis of alkene 6

With the desired alkene in hand, trifluoromethylation was attempted again by subjecting the alkene **6** to the exact conditions as described in scheme 4.24. Interestingly, formation of new product **7** was observed in 24% by ^1H NMR analysis and the reaction mixture also contained 23% of starting material (scheme 4.27).



Scheme 4.27 – Screening of electron neutral alkene

The reaction mixture was isolated, and the newly formed product was characterized. The initial characterization by ^1H NMR, ^{13}C NMR, ^{19}F NMR, HMBC, HSQC, HRMS, and IR indicated that an unusual product had formed by aryl migration without the desulfonylation (figure 4.2).

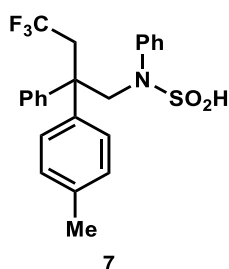


Figure 4.2 – Initially characterized product formed in the electrochemical reaction

^1H NMR analysis showed two sets of diastereotopic protons (figure 4.3) which were assumed to be the four methylene protons, in addition to 15 aromatic protons likely

corresponding to three aromatic rings, one of which being 1,4 disubstituted. We assumed that the singlet at 3.9 ppm is from the SO₂H group.

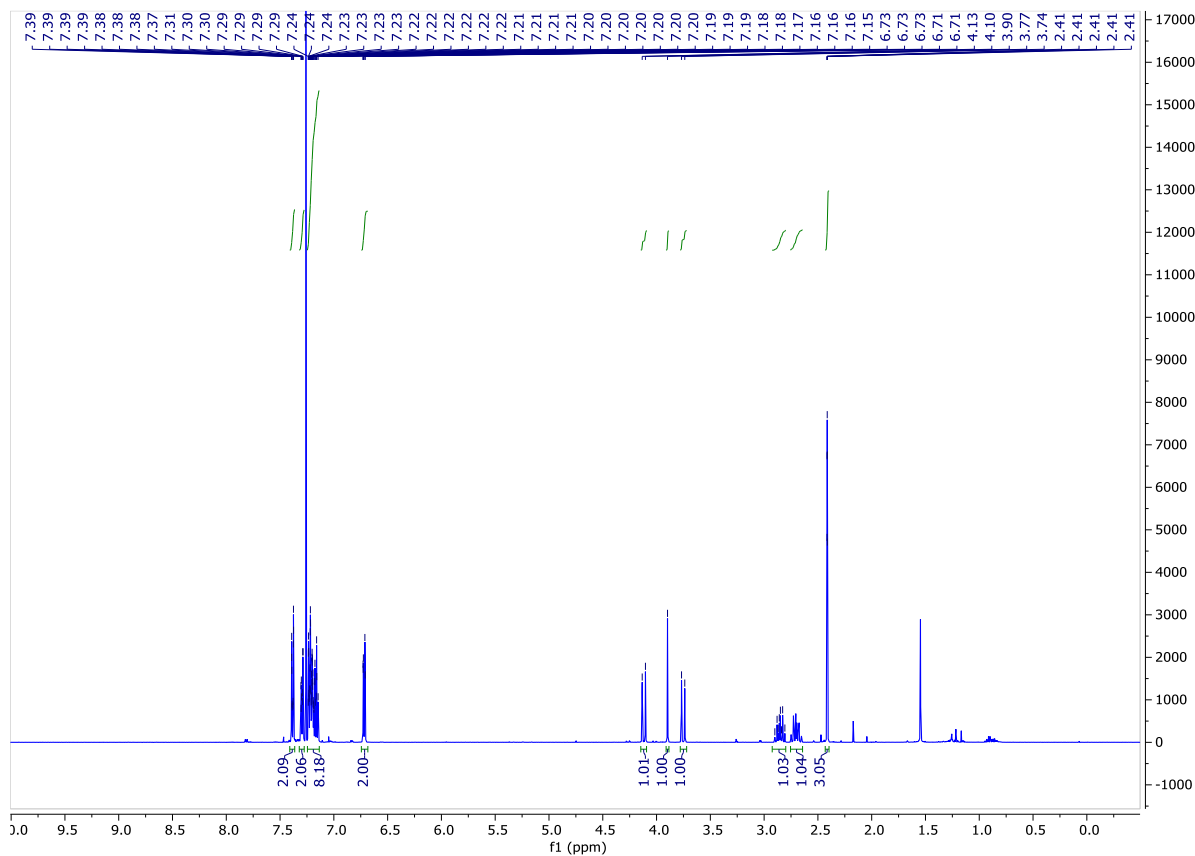


Figure 4.3 – ¹H spectrum of the isolated product

¹⁹F NMR confirmed the presence of CF₃ group. Mass spectrometry also confirmed the molecular ion peak.

At the time, it was assumed the product formed in the reaction was interesting enough to continue the investigation. Thorough optimization studies were carried out (table 4.1 shows the results of optimization).

Table 4.1 – Optimization table for trifluoromethylation.

Entry	CF ₃ Source eq.	Solvent	Proton Source (mL)	(+)	(-)	<i>E</i> _{cell} V	<i>I</i> = mA	Q/F mol ⁻¹	7 %	6 %
1	NaSO ₂ CF ₃ (2)	DCM	H ₂ O (0.6)	C _g	C _g	3.0	—	1.49	24	23
2	NaSO ₂ CF ₃ (2)	DCM	H ₂ O (0.6)	C _g	C _g	—	10	3.73	38	12
3	NaSO ₂ CF ₃ (2)	DCM	H ₂ O (0.6)	C _g	C _g	—	15	5.59	32	12
4	NaSO ₂ CF ₃ (2)	DCM	H ₂ O (0.6)	C _g	C _g	—	20	7.45	23	14
5	NaSO ₂ CF ₃ (2)	DCM	H ₂ O (0.6)	C _g	SS	—	10	3.73	<10	<2
6	NaSO ₂ CF ₃ (2)	DCM	H ₂ O (0.6)	C _g	C _g	—	10	7.40	54	<5
7	NaSO ₂ CF ₃ (2)	DCM	H ₂ O (0.6)	C _g	C _g	—	10	9.94	50	<5
8	NaSO ₂ CF ₃ (3)	DCM	H ₂ O (1.0)	C _g	C _g	—	10	7.40	54	<5
9	NaSO ₂ CF ₃ (4)	DCM	H ₂ O (1.0)	C _g	C _g	—	10	3.73	59	<5
10	NaSO ₂ CF ₃ (2)	DCM	H ₂ O (1.0)	C _g	C _g	—	10	3.5	73	<5
11	NaSO ₂ CF ₃ (2)	DCM	AcOH (1.0)	C _g	C _g	—	10	3.73	29	<5
12	NaSO ₂ CF ₃ (2)	DCM	MeOH (1.0)	C _g	C _g	—	10	3.73	57	14
13	NaSO ₂ CF ₃ (2)	MeCN	AcOH (1.0)	C _g	C _g	—	10	3.73	<2	<2
15	NaSO ₂ CF ₃ (2)	DCM	H ₂ O (1.0)	C _g	Pt	—	10	3.5	66	8
16	NaSO ₂ CF ₃ (2)	DCM	H ₂ O (1.0)	C _g	C _g	—	10	3.5	44	20
17	NaSO ₂ CF ₃ (2)	DCE	H ₂ O (1.0)	C _g	C _g	—	10	3.5	14	23

Reactions were performed at 0.3 mmol scale, yields determined by ¹HNMR spectroscopy

Switching the electrolysis to galvanostatic conditions of 10 mA of constant current passed for 3 hours (3.73 F/mol) immediately resulted into the increased yield of the product to 38% (entry 2). However, further increase in the current had negative effect on the product yield (entries 3 and 4). It was observed that passing a higher charge of 7.4 F/mol at 10 mA of constant current resulted in higher yields (entry 6). The yield of the product didn't increase further at 10 mA when charge higher than 7.4 F/mol was passed (entry

7). When the quantity of water was increased to 1 mL and 4 equivalents of NaSO_2CF_3 , the yield was again increased to 59%. An optimum condition was soon found where 10 mA of constant current was passed for 3 h (3.73 F/mol) using graphite as the anode and cathode in DCM/ H_2O (5:1), giving a conversion of 73% (entry **10**). Keeping the current and the amount of charge constant, varying the proton source proved detrimental to the product formation.

With the optimised conditions in hand, substrate scope was planned. However, efforts were made to elucidate the structure of the product unambiguously. Crystals of the product **7** were grown using slow diffusion technique and sent for x-ray crystallography to National Crystallography Centre (NCS) Southampton.

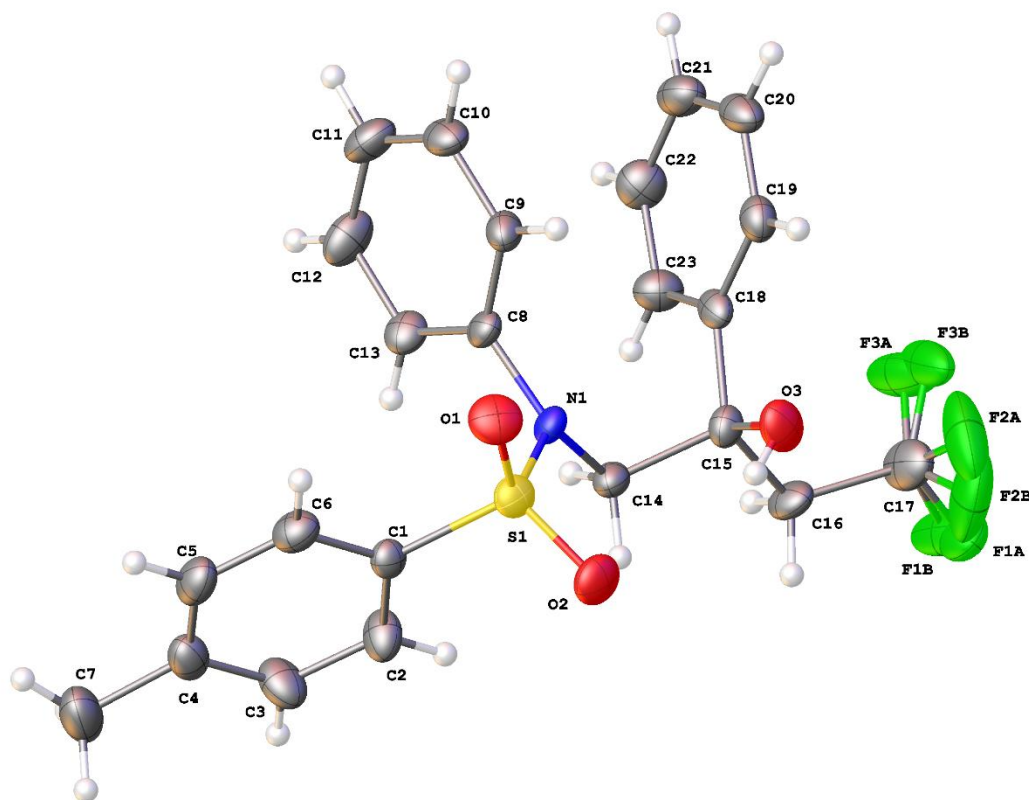
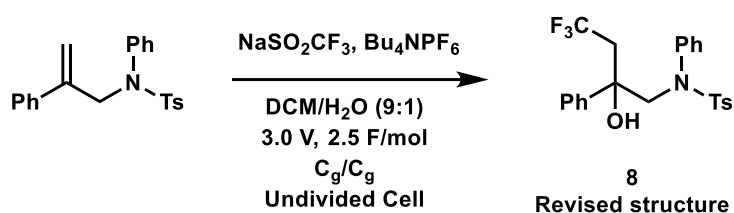


Figure 4.4 – X-ray of the product

Disappointingly, the x-ray analysis (fig 4.4) showed that the functional group migration did not take place. The product contained an OH group at benzylic position (scheme 4.28).

The revised structure of the product was then proposed, where after the addition of $\text{CF}_3\cdot$ to the alkene, the resulting tertiary carbon centred radical was further oxidised to a stable carbocation, which was then trapped by water as a nucleophile. This type of oxytrifluoromethylation has already been reported by Cantillo and co-workers in 2018.⁷⁸



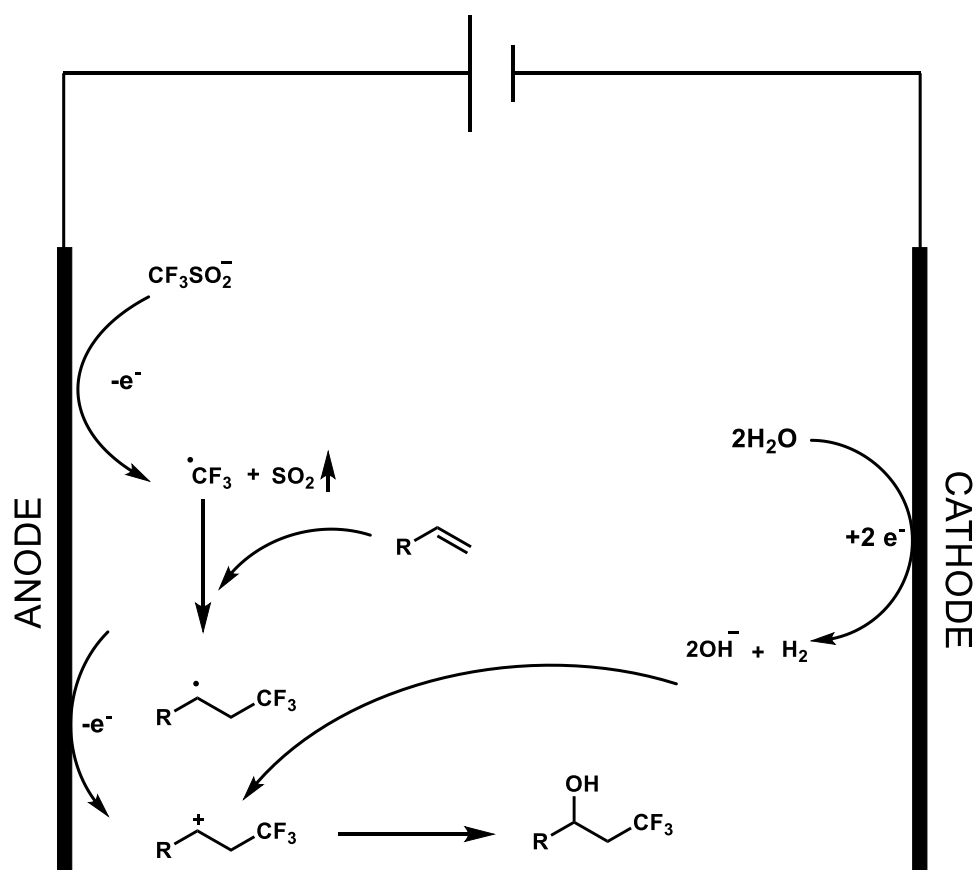
Scheme 4.28 – Revised structure of the product

After this realisation, the project was deemed not interesting enough to pursue and substrate scope and further investigations were stopped.

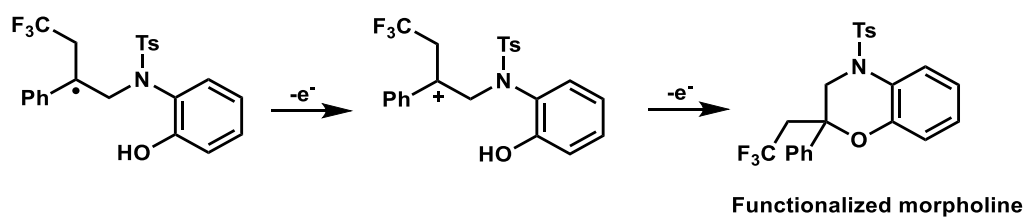
It was however interesting enough to rationalize the formation of the product and consider why the desulfonylative 1,4 – migration was not observed. After careful consideration of the reaction mechanism proposed by Cantillo and co-workers⁷⁸, a plausible mechanism can be proposed to understand the oxytrifluoromethylation of the alkene (scheme 4.29).

As expected, $\text{CF}_3\cdot$ was oxidatively generated at the anode which adds to the alkene, thus generating a benzylic carbon centred radical, which is stable enough to undergo one more oxidation at the surface of the anode to furnish a benzylic carbocation. The carbocation can be trapped by hydroxide ion $[\text{OH}^-]$ to form the oxytrifluoromethylated product.

This established that instead of functional group migration, nucleophilic attack of $[\text{OH}^-]$ is preferred. We envisaged using this information to make subtle changes to the substrate to induce an intramolecular cyclization, so that synthetically useful functionalized morpholines could be prepared (scheme 4.30).

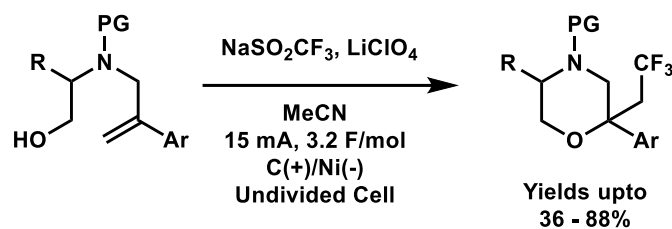


Scheme 4.29 – Plausible mechanism for the oxytrifluoromethylation.



Scheme 4.30 – Proposal for an intramolecular cyclization

Unfortunately, Masson and co-workers reported the same strategy of an electrochemical intramolecular oxytrifluoromethylation of alkenols to access functionalized morpholines (scheme 4.31).⁷⁹ This report was published on the same day as the synthesis of the substrate in the scheme 4.30 was completed.



Scheme 4.31 – Intramolecular oxytrifluoromethylation of alkenols to access functionalized morpholines

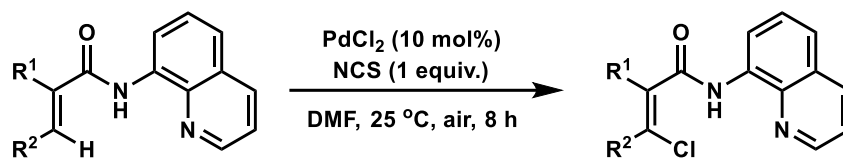
In light of the report from Masson and co-workers it was decided to halt any further investigations into the trifluoromethylation of alkenes (scheme 4.31).

4.3.2. Electrochemical oxidative Z-selective C(sp²)-H chlorination of acrylamides

4.3.2.1. Introduction

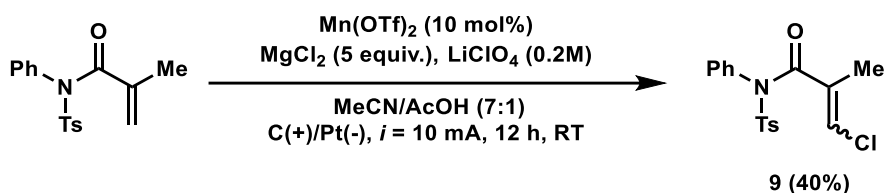
Chlorine containing compounds are abundant in natural products, agrochemicals, pharmaceuticals, and polymers.^{80,81} Furthermore, Z-chloroacrylic acid derivatives are also important building blocks to selectively arrive at ubiquitous Z-configured alkenes.⁸²⁻⁸⁴ In addition to hydrochlorination⁸⁵ and carbochlorination of alkynes^{86,87}, the other synthetic methods to access Z-β-chloroacrylic acid derivatives include Vilsmeier-Haack⁸⁸, Wittig⁸⁹, and chloropalladation /Heck methods⁹⁰. These methods exhibit either poor E/Z selectivity or need prerequisite alkyne architecture. Hence, new synthetic methods that can provide direct access to Z-chloroacrylic acids are highly desirable.

During the course of our studies on acrylamides, Besset and co-workers reported a palladium catalyzed Z-selective chlorination of secondary acrylamides (scheme 4.32). The method used an 8-aminoquinoline as a directing group along with N-chlorosuccinimide as the chlorinating agent.⁹¹

Scheme 4.32 – Pd-catalysed *Z*-selective chlorination

This of course is one of the very few methods in the literature which directly gives access to *Z*- β -chloroacrylamides. However, modern synthetic organic chemistry demands for greener, more sustainable and atom economical methods for the synthesis of valuable targets.

Referring to the scheme 4.25 of previous section, when the acrylamide **1** was subject to the electrochemical method which is comprised of $\text{Mn}(\text{OTf})_2$ (10 mol%), MgCl_2 (5 equiv.), LiClO_4 (2 equiv.) in MeCN/AcOH (7:1) for 12 h, ^1H NMR analysis showed the consumption of starting material and also indicated the formation of a new product **9**. Subsequent analysis of the newly formed product revealed that a chlorine atom has been oxidatively added to the acrylamide to yield a *tri*-substituted alkene (scheme 4.33).



Scheme 4.33 – Oxidative chlorination of acrylamide

To ascertain the stereochemistry of the chlorination unambiguously, crystals were grown by slow diffusion process from DCM and pentane.

Gratifyingly, x-ray crystallography revealed that the chlorine is *trans* to the methyl group, hence the alkene was in *Z*-configuration (figure 4.5).

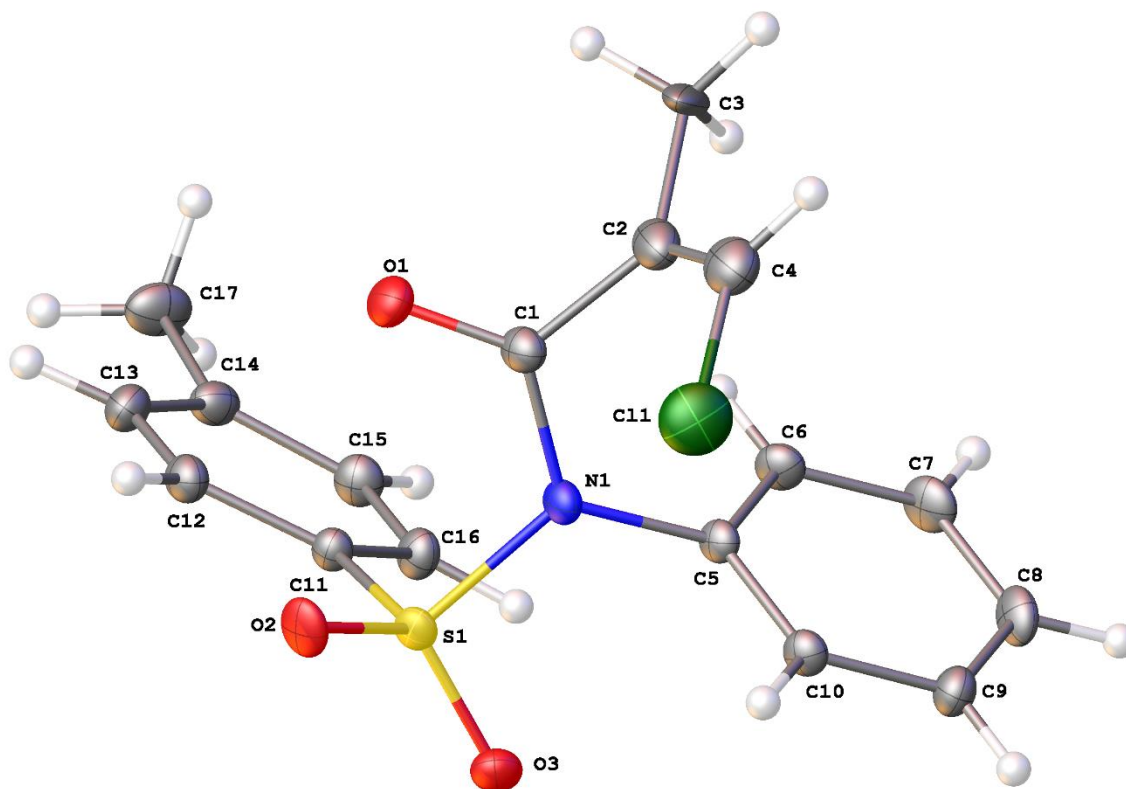
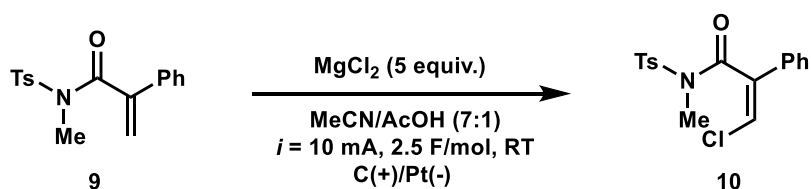


Figure 4.5 – X-ray of the chlorinated acrylamide indication Z-selectivity

With the selectivity of the reaction confirmed, the project was taken over by James Harnedy, a fellow PhD student in the Morrill group. After an extensive and methodical optimisation, James Harnedy discovered that, when the methyl substituent was changed to phenyl at α -position of the acrylamide, the reaction yielded the β -chloroacrylamide in 97% yield, notably excluding the manganese catalyst and supporting electrolyte (scheme 4.34).



Scheme 4.34 – Optimized conditions for Z-selective oxidative chlorination of acrylamides

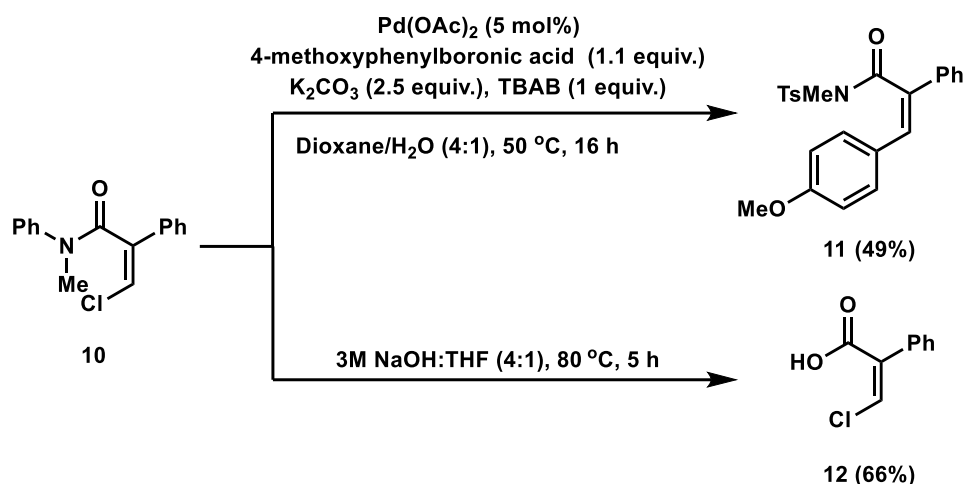
After subsequent screening of various other parameters, James Harnedy arrived at the optimized condition which is MgCl_2 (5 equiv.) in MeCN/AcOH (7:1) under galvanostatic condition of 10 mA for 2 hours ($Q = 2.5 \text{ F/mol}$) in an undivided cell at ambient temperature (table 4.2).

Table 4.2 – Variation from the standard conditions.

Entry	Variation from standard conditions	Yield (%)
1	none	97 (92)
2	No electricity	< 2
3	$E_{\text{cell}} = 3.75 \text{ V}$	91
4	$i = 15 \text{ mA}$, $j_{\text{anode}} = 11.7 \text{ mA/cm}^2$	91
5	$i = 5 \text{ mA}$, $j_{\text{anode}} = 3.9 \text{ mA/cm}^2$	85
6	Graphite cathode instead of Pt foil	83
7	LiCl instead of MgCl_2	83
8	NaCl instead of MgCl_2	25
9	$\text{MeCN}:\text{MeOH}$ (3.5:1)	67
10	MgCl_2 (3 equiv.)	68
11	MgCl_2 (3 equiv.) + LiClO_4 (2 equiv.)	78
12	$Q = 2 \text{ F/mol}$	85

Reactions were performed on 0.3 mmol scale using electrasyn 2.0. Yields were determined by using ^1H NMR using 1, 3, 5 trimethylbenzene.

With optimized conditions in hand, substrate scope of various acrylamide substrates was investigated by James Harnedy. James also demonstrated the synthetic utility by orthogonal functionalization of β -chloroacrylamide (scheme 4.35), where it was found that the $\text{C}(\text{sp}^2)\text{-Cl}$ functionality could serve as a coupling partner in a palladium-catalyzed Suzuki cross-coupling reaction with 4-methoxyphenylboronic acid to afford arylated alkene **11** in 49% yield. Also, hydrolysis of the twisted amide functionality was reported to yield the corresponding carboxylic acid in derivative **12** in 66%.

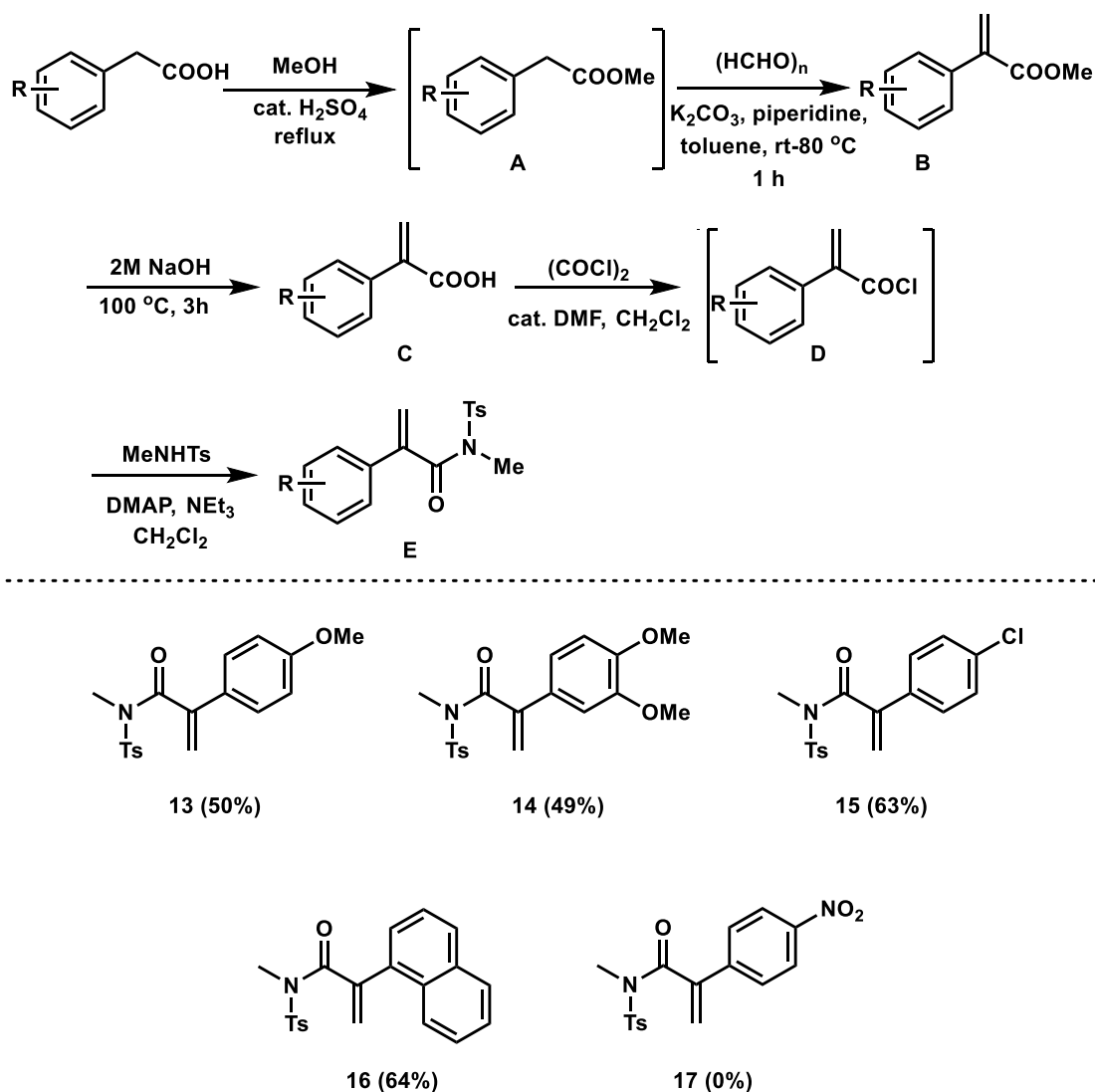


Scheme 4.35 – Synthetic utility of the product

James Harnedy reported 20 examples for this transformation in greater than 60% average yield. The method exhibited good tolerance for electron donating groups and neutral substitution on the aromatic ring at the α -position of the acrylamide and worked with moderately electron withdrawing substituents. Substitution at the amide nitrogen also worked well such as *N*-alkyl, *N*-phenyl and *N*-Benzyl substituents could be incorporated. Finally, James Harnedy also translated the batch electrochemical reaction into a flow electrochemical process at 4.4 mmol scale which demonstrated the scalability of the method.

4.3.2.2. Substrate Scope

The remaining work in this chapter is solely my own. To extend the substrate scope further, a range of acrylamides were synthesized by a modified pathway (scheme 4.36). Substrates with varied substitution in the aromatic unit at the α -position of the acrylamide were prepared by modifying a 5-step preparation.



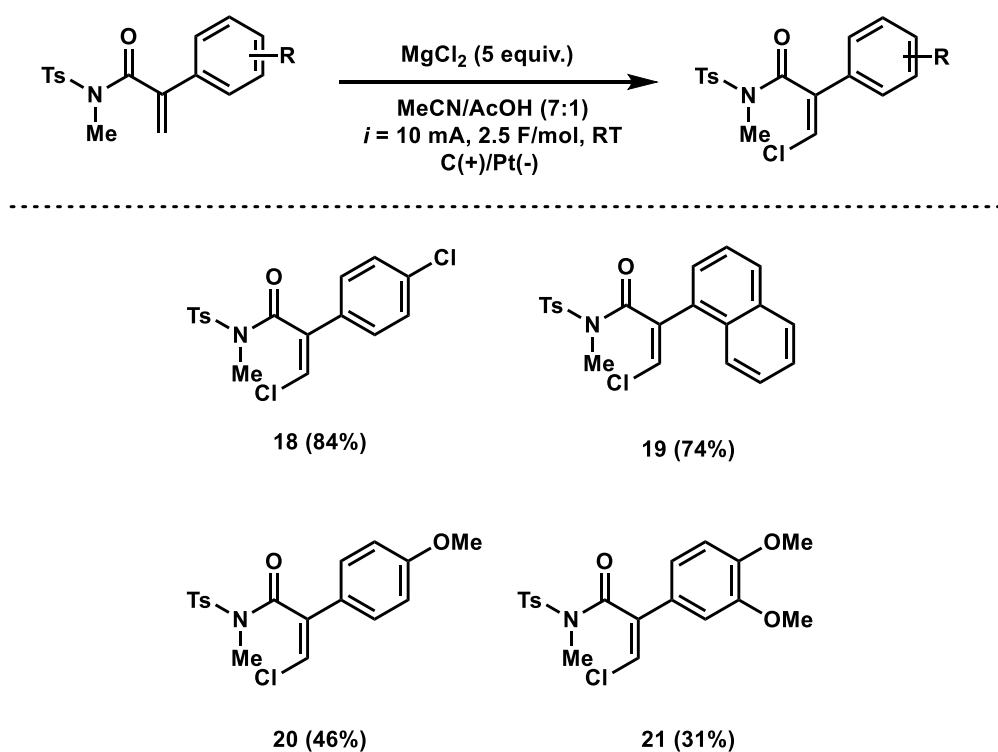
Scheme 4.36 – Synthesis of acrylamide substrates

Substituted phenyl acetic acid was first converted to ester **(A)** followed by a modified Mannich reaction in which the alkene was installed **(B)**. After a base promoted ester hydrolysis, acid **(C)** was then converted into corresponding acid chlorides **(D)**. Finally, a DMAP catalyzed acid chloride **(D)** amine coupling was performed yielding the final substituted acrylamides **(E)**.

This 5-steps preparation yielded the desired acrylamides in acceptable yields. Substrates having electron donating groups performed quite well in the modified Mannich reaction, however the yields of final acid chloride and amine coupling step obtained were average. Whereas, when electron withdrawing substrates especially nitro (NO_2) group, the yield was very poor for all the steps after (A).

4-methoxy and 3,4-dimethoxy substrates **13** and **14** were obtained in yields 50% and 49% respectively, with electron withdrawing substrates **15** and **16**, 4-chloro and 4-naphthyl acrylamide the yield was a little higher than that of electron donating ones; 63% and 64% respectively. It is worth mentioning here that 4-nitro benzoyl chloride failed to deliver coupled acrylamide **17**.

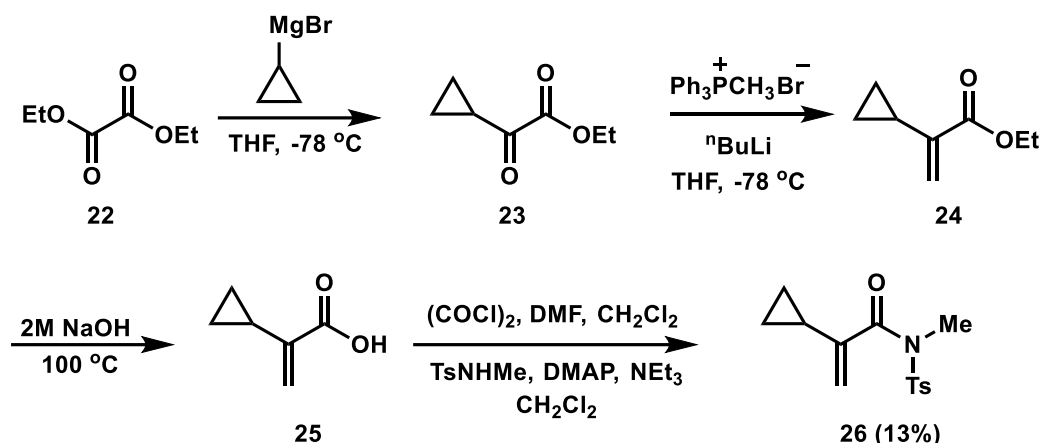
With these substrates in hand, they were subjected to the optimized electrochemical conditions (scheme 4.37). The electrochemical conditions were tolerant to the different substitutions in the aromatic unit at α -position of the acrylamides, yielding the Z- β -chloroacrylamide in good to excellent yields. 4-Chlorophenyl and 4-naphthyl Z- β -chloroacrylamide (**18** and **19**) were obtained in 84% and 74%. Electron donating groups also furnished the desired products **20** and **21** in moderate yields of 46% and 31% respectively.



Scheme 4.37 – Substrate scope

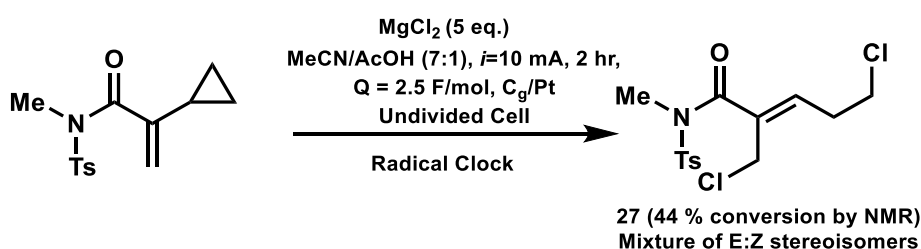
4.3.2.3. Mechanistic Studies

To obtain mechanistic insight of the reaction, a radical clock experiment was designed. Acrylamide **26** containing a cyclopropyl substituent at the α -position of the acrylamide was synthesized as a radical probe (scheme 4.38).



Scheme 4.38 – Synthesis of substrate for radical clock experiment

The radical probe substrate was synthesized by an alternative route. Diethyl oxalate **22** was converted into an α -keto ester **23** by addition of cyclopropylmagnesium bromide. Then the α -keto ester **23** was subjected to Wittig olefination conditions to yield the acrylate **24**. Which upon subsequent hydrolysis furnished the acid **25**. Conversion of **25** to acid chloride and coupling with sulfonamide delivered the substrate **26** in modest 13% yield.



Scheme 4.39 – Radical clock experiment

The radical clock substrate was then subjected to the optimized electrochemical conditions. It was found that ring-opened dichlorinated acrylamide **27** was formed as 1:1 mixture of *Z*:*E* alkene isomers in 44% NMR yield (scheme 4.39). This signifies the likelihood of radical intermediates within the operative reaction mechanism.

Cyclic voltammetry studies indicated that the chloride ion ($E_{\text{ox}} = 1.10 \text{ V vs. Fc/Fc}^+$) should undergo preferential oxidation in the presence of the electron deficient acrylamide **9** ($E_{\text{ox}} = 1.31 \text{ V vs. Fc/Fc}^+$) (figure 4.6 A and 4.6 B).

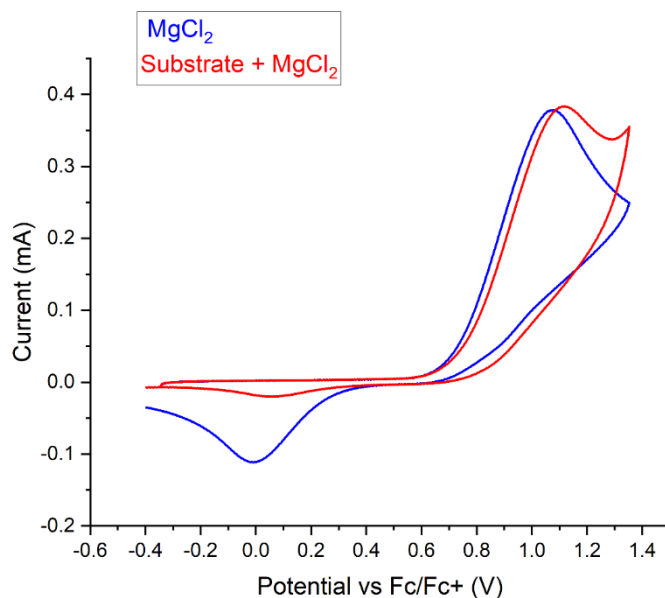


Figure 4.6 A – Cyclic Voltammogram of MgCl_2 and the parent substrate mixture in MeCN/AcOH. (a – blue line) MgCl_2 (8.0 mM); (b – red line) parent substrate (4.0 mM) in MeCN with AcOH and LiClO_4 (0.1 M). Scan rate: 100 mV/s.

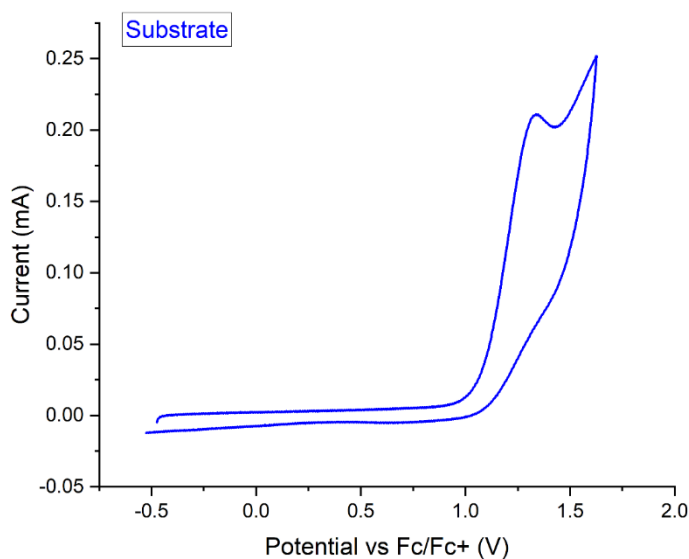


Figure 4.6 B – Cyclic voltammogram of parent substrate (a – blue line) (4.0 mM); (b – red line) **1** in MeCN with AcOH and LiClO_4 (0.1 M). Scan rate: 100 mV/s.

It is also worth mentioning here that, in the cyclic voltammogram of the parent substrate **9** with MgCl_2 (figure 4.6 A) shows a cathodic current of magnitude -0.1 mA diminishes when substrate was added. This could be interpreted as, Cl^\bullet generated in the oxidative sweep of the voltammogram, is not available to reduce further in the reductive sweep, hence it is being consumed by the substrate.

Based on the experimental data obtained from the radical clock experiment, a working mechanism can be proposed for the formation of the dichlorinated product **27** (figure 4.7).

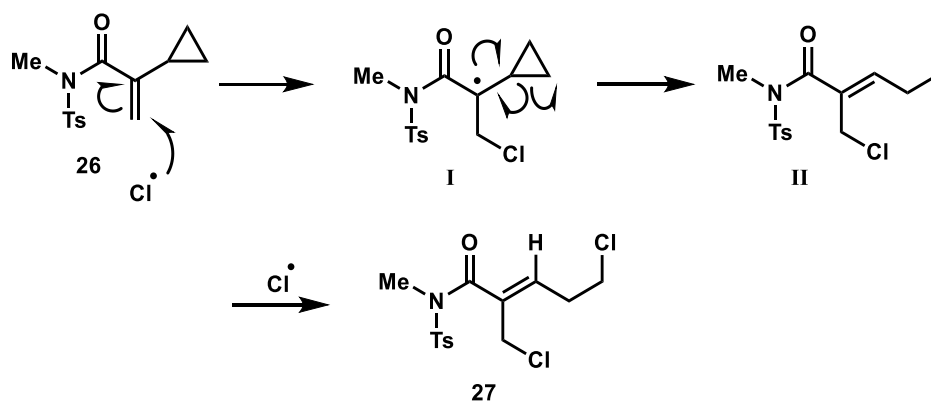


Figure 4.7 – Mechanism for the radical clock experiment

Cl^\bullet generated on the surface of anode adds to the alkene to give intermediate **I**. Thereafter concomitant rearrangement of the carbon centred radical due to ring strain release, should furnish the intermediate **II**. The radical propagation is terminated by radical-radical coupling of another Cl^\bullet with the terminal carbon centred radical to form dichlorinated product **27**.

Further high-resolution mass spectrometry (HRMS) of the dichlorinated product confirmed the fragmentation pattern and thus the product **27** (fig 4.8).

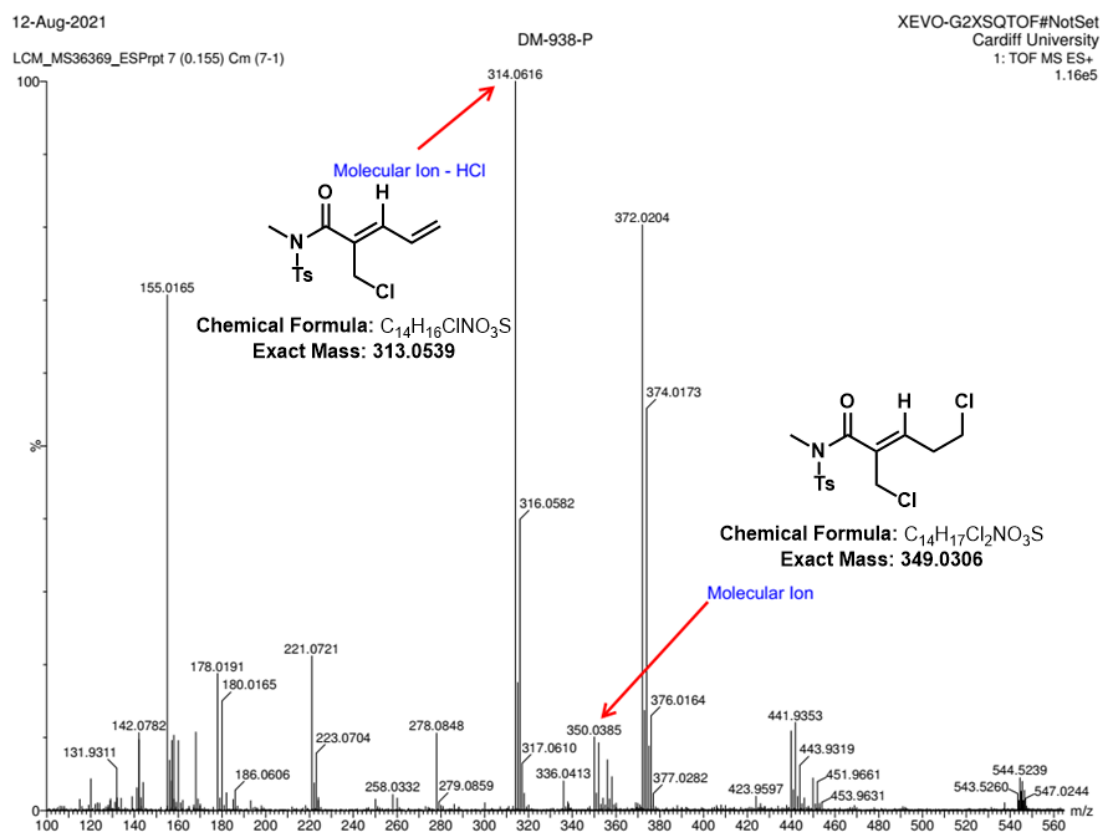


Figure 4.8 – HRMS of the dichlorinated product.

Based on these observations and previous related investigations⁹², a plausible reaction mechanism can be proposed for formation of the *Z*- β -chloroacrylamides. The reaction would initiate with anodic chloride oxidation to form a Cl^\bullet ^{93, 94,95} which undergoes anti-Markovnikov addition to the electron-deficient acrylamide **9** to furnish tertiary C-centered radical **I**. Further anodic oxidation would form carbocation **II**, with subsequent deprotonation providing access to the observed *Z*- β -chloroacrylamide **10** (path a). Presence of a radical stabilizing group at α -position is crucial for the observed reactivity as it will stabilize intermediates **I** and **II**. Deprotonation of carbocation **II** proceeds *via* a conformation that minimizes steric repulsion between the chlorine atom and the phenyl ring to afford the *Z*-isomer as the major product stereoisomer. Alternatively, carbocation **II** or radical **I** could be intercepted by a chlorine anion (path b) or a chlorine radical (path c), respectively, to form dichlorinated compound **III**, which could subsequently generate **10** via loss of HCl. Hydrogen gas is generated *via* proton reduction at the cathode (figure 4.9).

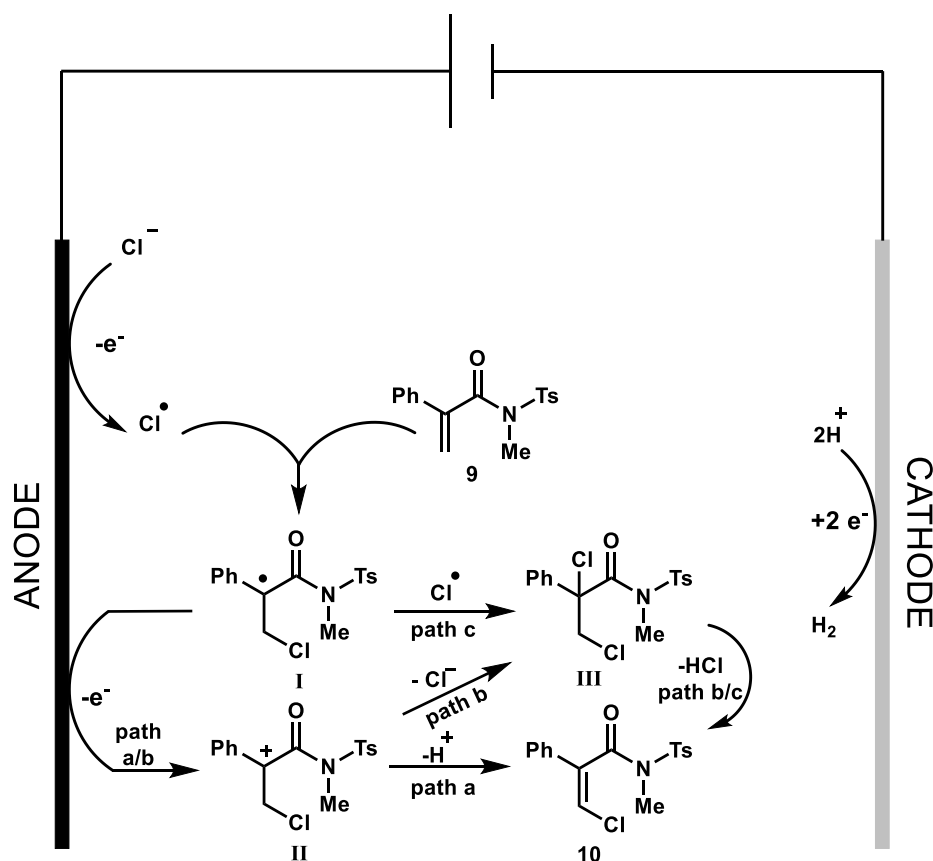


Figure 4.9 – Plausible reaction mechanism

4.3.2.4. Future Work

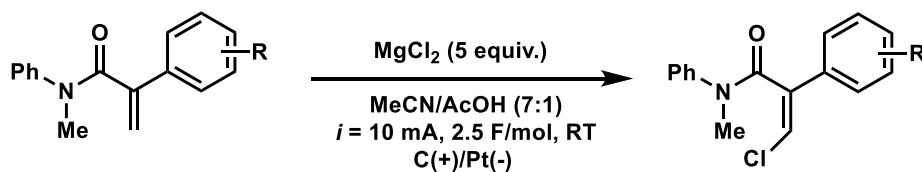
Electrochemical alkene functionalization is a promising and vast field. The immediate future work would be to attempt for the alkene difunctionalization with 1,4-desulfonylative aryl migrations. Efforts in utilizing a compatible donor radical that could be generated anodically could possibly solve the issue of over-oxidation of the C-centered radical formed. It would also be worth exploring the docking-migration strategy⁴⁷ by employing a bifunctional reagent. This could provide methodology to efficiently functionalize alkenes without extensive substrate engineering.

Z- selective oxidative C(sp²) – H functionalization could also be extended further by employing other functionalities such as trifluoromethyl, azide, aromatics etc. Efforts could also be made in employing this strategy in the synthesis of biologically important scaffolds.

4.4. Summary

In summary, this chapter demonstrates the efforts made in the development of electrochemical methods of alkene functionalization. This includes an “Electrochemical oxidative Z-selective C(sp²)-H chlorination of acrylamides”, by establishing the stereochemistry of the product by x-ray crystallography along with 4 different examples were reported. A thorough mechanistic investigation led us to propose a plausible mechanism by conducting radical clock experiment and cyclic voltammetry studies.

In the context of the aims and objectives of this thesis, this work was able to demonstrate a new synthetic methodology for the synthesis of Z- β - chloroacrylamides. This satisfies the aim to develop a new electrochemical methodology for electrochemical alkene functionalization.



Scheme 4.40 - Electrochemical oxidative Z-selective C(sp²)-H chlorination of acrylamides

4.5. References

- 1 K. S. Yang, J. A. Gurak, Z. Liu and K. M. Engle, *J. Am. Chem. Soc.*, 2016, **138**, 14705–14712.
- 2 L. Deng, T. Xu, H. Li and G. Dong, *J. Am. Chem. Soc.*, 2016, **138**, 369–374.
- 3 G. M. Borrajo-Calleja, V. Bizet and C. Mazet, *J. Am. Chem. Soc.*, 2016, **138**, 4014–4017.
- 4 R. K. Dhungana, K. C. Shekhar, P. Basnet and R. Giri, *Chemical Record*, 2018, **18**, 1314–1340.
- 5 H. Yao, W. Hu and W. Zhang, *Molecules (Basel, Switzerland)*, 2020, 26.
- 6 M. Yan, J. C. Lo, J. T. Edwards and P. S. Baran, *J. Am. Chem. Soc.*, 2016, **138**, 12692–12714.
- 7 M. C. Willis, *Chem. Rev.*, 2010, **110**, 725–748.

- 8 R. Franke, D. Selent and A. Börner, *Chem. Rev.*, 2012, **112**, 5675–5732.
- 9 J. v. Obligacion and P. J. Chirik, *Nature Reviews Chemistry*, 2018, **2**, 15–34.
- 10 T. E. Müller, K. C. Hultzs, M. Yus, F. Foubelo and M. Tada, *Chem. Rev.*, 2008, **108**, 3795–3892.
- 11 T. de Haro and C. Nevado, in *Comprehensive Organic Synthesis: Second Edition*, Elsevier Ltd., 2014, vol. 5, pp. 1621–1659.
- 12 A. Ghosh, K. F. Johnson, K. L. Vickerman, J. A. Walker and L. M. Stanley, *Org. Chem. Front.*, 2016, **3**, 639–644.
- 13 W. Zeng and S. R. Chemler, *J. Am. Chem. Soc.*, 2007, **129**, 12948–12949.
- 14 S. N. Gockel, T. L. Buchanan and K. L. Hull, *J. Am. Chem. Soc.*, 2018, **140**, 58–61.
- 15 M. T. Bovino, T. W. Liwosz, N. E. Kendel, Y. Miller, N. Tyminska, E. Zurek and S. R. Chemler, *Angew. Chem.*, 2014, **53**, 6383–6387.
- 16 A. M. Dreis and C. J. Douglas, *J. Am. Chem. Soc.*, 2009, **131**, 412–413.
- 17 I. P. Beletskaya and A. v. Cheprakov, *Chem. Rev.*, 2000, **100**, 3009–3066.
- 18 S. W. M. Crossley, C. Obradors, R. M. Martinez and R. A. Shenvi, *Chem. Rev.*, 2016, **116**, 8912–9000.
- 19 *Springer Netherlands*, 2001, pp. 209–236.
- 20 J. C. Lo, J. Gui, Y. Yabe, C. M. Pan and P. S. Baran, *Nature*, 2014, **516**, 343–348.
- 21 T. E. Müller, K. C. Hultzs, M. Yus, F. Foubelo and M. Tada, *Chem. Rev.*, 2008, **108**, 3795–3892.
- 22 P. T. Marcyk and S. P. Cook, *Org. Lett.*, 2019, **21**, 1547–1550.
- 23 X. Wu and C. Zhu, *Chinese Journal of Chemistry*, 2019, **37**, 171–182.
- 24 X. Wu, S. Wu and C. Zhu, *Tet. Lett.*, 2018, **59**, 1328–1336.
- 25 Z. M. Chen, X. M. Zhang and Y. Q. Tu, *Chem. Soc. Rev.*, 2015, **44**, 5220–5245.
- 26 W. Kong, M. Casimiro, E. Merino and C. Nevado, *J. Am. Chem. Soc.*, 2013, **135**, 14480–14483.
- 27 R. W. Hoffmann, *Chem. Soc. Rev.*, 2016, **45**, 577–583.
- 28 A. Simonneau and M. Oestreich, *Angew. Chem.*, 2015, **54**, 3556–3558.
- 29 S. L. and H. Jack, *J. Am. Chem. Soc.*, 1975, **99**, 8335–8337.
- 30 T. Mukaiyama, S. Isayama, S. Inoki, K. Kato, T. Yamada and T. Takai, *Chem. Lett.*, 1989, 449–452.
- 31 A. Zombeck, D. E. Hamilton and R. S. Drago, *J. Am. Chem. Soc.*, 1982, **104**, 6782–6784.

- 32 M. M. Toteva and J. P. Richard, *Mechanism for Nucleophilic Substitution and Elimination Reactions at Tertiary Carbon in Largely Aqueous Solutions: Lifetime of a Simple Tertiary Carbocation*, 1996.
- 33 B. M. Trost, *Science*, 1983, **219**, 4582.
- 34 K. Ebisawa, K. Izumi, Y. Ooka, H. Kato, S. Kanazawa, S. Komatsu, E. Nishi and H. Shigehisa, *J. Am. Chem. Soc.*, 2020, **142**, 13481–13490.
- 34^b C. A. Discolo, E. E. Touney, and S. V. Pronin *J. Am. Chem. Soc.* 2019, **141**, 17527–17532
- 35 A. J. Perkowski and D. A. Nicewicz, *J. Am. Chem. Soc.*, 2013, **135**, 10334–10337.
- 36 T. M. Nguyen, N. Manohar and D. A. Nicewicz, *Angew. Chem.*, 2014, **53**, 6198–6201.
- 37 T. M. Nguyen and D. A. Nicewicz, *J. Am. Chem. Soc.*, 2013, **135**, 9588–9591.
- 38 D. S. Hamilton and D. A. Nicewicz, *J. Am. Chem. Soc.*, 2012, **134**, 18577–18580.
- 39 M. A. Zeller, M. Riener and D. A. Nicewicz, *Org. Lett.*, 2014, **16**, 4810–4813.
- 40 J. M. M. Grandjean and D. A. Nicewicz, *Angew. Chem.*, 2013, **52**, 3967–3971.
- 41 D. J. Wilger, J. M. M. Grandjean, T. R. Lammert and D. A. Nicewicz, *Nat. Chem.*, 2014, **6**, 720–726.
- 42 Z. M. Chen, X. M. Zhang and Y. Q. Tu, *Chem. Soc. Rev.*, 2015, **44**, 5220–5245.
- 43 P. Sivaguru, Z. Wang, G. Zanoni and X. Bi, *Chem. Soc. Rev.*, 2019, **48**, 2615–2656.
- 44 X. Wu and C. Zhu, *Acc. Chem. Res.*, 2020, **53**, 1620–1636.
- 45 Z. Wu, R. Ren and C. Zhu, *Angew. Chem.*, 2016, **128**, 10979–10982.
- 46 Z. Wu, D. Wang, Y. Liu, L. Huan and C. Zhu, *J. Am. Chem. Soc.*, 2017, **139**, 1388–1391.
- 47 J. Yu, Z. Wu and C. Zhu, *Angew. Chem.*, 2018, **130**, 17402–17406.
- 48 T. P. Yoon, M. A. Ischay and J. Du, *Nat. Chem.* 2010 2:7, 2010, **2**, 527–532.
- 49 R. H. Verschueren and W. M. de Borggraeve, *Molecules*, 2019, **24**.
- 50 J. Liu, L. Lu, D. Wood and S. Lin, *ACS Cent. Sci.*, 2020, **6**, 1317–1340.
- 51 H. Tanaka, M. Kuroboshi, H. Takeda, H. Kanda and S. Torii, *Electrochemical asymmetric epoxidation of olefins by using an optically active Mn-salen complex*, 2001, vol. 507.
- 52 S. Torii, P. Liu and H. Tanaka, *Chem. Lett.*, 1995, **24**, 319.
- 53 J. A. Miranda, C. J. Wade and R. D Little, *J. Org. Chem.*, 2005, **70**, 20, 8017–8026 .
- 54 G. S. Sauer and S. Lin, *ACS Catal.*, 2018, **8**, 5175–5187.
- 55 N. Fu, G. S. Sauer, A. Saha, A. Loo and S. Lin, .

- 56 F. Minisci, M. S. Kharasch, H. Engelmann, F. R. Mayo and C. Walling, *Free Radical Reactions in Preparation Organic Chemistry*, Huyser, 1975, vol. 8.
- 57 W. E. Fristad, T. A. Brandvold, J. R. Peterson and S. R. Thompson, *J. Org. Chem.*, 2002, **50**, 3647–3649.
- 58 Y.-A. Yuan, D.-F. Lu, Y.-R. Chen and H. Xu, *Angew. Chem.*, 2016, **128**, 544–548.
- 59 J. M. Mayer, *Acc. Chem. Res.*, 1998, **31**, 441–450.
- 60 S. Purser, P. R. Moore, S. Swallow and V. Gouverneur, *Chem. Soc. Rev.*, 2008, **37**, 320–330.
- 61 K. Müller, C. Faeh and F. Diederich, *Fluorine in Pharmaceuticals: Looking Beyond Intuition*, .
- 62 J. Sun, X. Zhen, H. Ge, G. Zhang, X. An and Y. Du, *Beilstein J. Org. Chem.*, 2018, **14**, 1452–1458.
- 63 H. Egami and M. Sodeoka, *Angew. Chem.*, 2014, **53**, 8294–8308.
- 64 C. Alonso, E. Martínez De Marigorta, G. Rubiales and F. Palacios, *Chem. Rev.*, 2015, **115**, 1847–1935.
- 65 K. Y. Ye, G. Pombar, N. Fu, G. S. Sauer, I. Keresztes and S. Lin, *J. Am. Chem. Soc.*, 2018, **140**, 2438–2441.
- 66 N. Fu, G. S. Sauer and S. Lin, *Journal of the J. Am. Chem. Soc.*, 2017, **139**, 15548–15553.
- 67 C. Chen, J. C. Kang, C. Mao, J. W. Dong, Y. Y. Xie, T. M. Ding, Y. Q. Tu, Z. M. Chen and S. Y. Zhang, *Green Chem.*, 2019, **21**, 4014–4019.
- 68 H. I. Jung, Y. Kim and D. Y. Kim, *Org. Biomol. Chem.*, 2019, **17**, 3319–3323.
- 69 Z. Guan, H. Wang, Y. Huang, Y. Wang, S. Wang and A. Lei, *Org. Lett.*, 2019, **21**, 4619–4622.
- 70 Y. J. Kim and D. Y. Kim, *Org. Lett.*, 2019, **21**, 1021–1025.
- 71 J. C. Kang, Y. Q. Tu, J. W. Dong, C. Chen, J. Zhou, T. M. Ding, J. T. Zai, Z. M. Chen and S. Y. Zhang, *Org. Lett.*, 2019, **21**, 2536–2540.
- 72 M. W. Zheng, X. Yuan, Y. S. Cui, J. K. Qiu, G. Li and K. Guo, *Org. Lett.*, 2018, **20**, 7784–7789.
- 73 Y. Gao, H. Mei, J. Han and Y. Pan, *Chem. Eur. J.*, 2018, **24**, 17205–17209.
- 74 C. Zhang, *Adv. Synth. Catal.*, 2014, **356**, 2895–2906.
- 75 Z. Zou, W. Zhang, Y. Wang, L. Kong, G. Karotsis, Y. Wang and Y. Pan, *Org. Lett.*, 2019, **21**, 1857–1862.
- 76 Z. Ni, X. Huang and Y. Pan, *Org. Lett.*, 2016, **18**, 2612–2615.

- 77 B. D. W. Allen, M. D. Hareram, A. C. Seastram, T. McBride, T. Wirth, D. L. Browne and L. C. Morrill, *Org. Lett.*, 2019, **21**, 9241–9246.
- 78 W. Jud, C. O. Kappe and D. Cantillo, *Chem. Eur. J.*, 2018, **24**, 17234–17238.
- 79 A. Claraz, T. Courant and G. Masson, *Org. Lett.*, 2020, **22**, 1580–1584.
- 80 B. R. Smith, C. M. Eastman and J. T. Njardarson, *J. Med. Chem.*, 2014, **57**, 9764–9773.
- 81 G. W. Gribble, *J. Nat. Prod.*, 2004, **55**, 1353–1395.
- 82 A. B. D. and and L. E. Overman*, *Chem. Rev.*, 2003, **103**, 2945–2963.
- 83 S. Tang and K. L. Erickson, *J. Nat. Prod.*, 2008, **71**, 898–901.
- 84 A. Français, A. Leyva-Pérez, G. Etxebarria-Jardi, J. Peña and S. v. Ley, *Chem. Eur. J.*, 2011, **17**, 329–343.
- 85 S. Ma, X. Lu and Z. Li, *J. Org. Chem.*, 2002, **57**, 709–713.
- 86 C. M. Le, T. Sperger, R. Fu, X. Hou, Y. H. Lim, F. Schoenebeck and M. Lautens, *J. Am. Chem. Soc.*, 2016, **138**, 14441–14448.
- 87 H. Koo, H. Y. Kim and K. Oh, *Org. Chem. Front.*, 2019, **6**, 1868–1872.
- 88 K. U. Krishnaraj and K. S. Devaky, *Tetrahedron*, 2014, **70**, 6450–6456.
- 89 C. J. Moody, M. Pass, C. W. Rees and G. Tojo, *J. Chem. Soc., Chem. commun.*, 1986, 1062–1063.
- 90 J.-M. Huang, Y. Dong, X.-X. Wang and H.-C. Luo, *Chem. Commun.*, 2010, **46**, 1035–1037.
- 91 M. Y. Chen, X. Pannecoucke, P. Jubault and T. Besset, *Org. Lett.*, 2020, **22**, 7556–7561.
- 92 H.-H. Xu, J. Song and H.-C. Xu, *ChemSusChem*, 2019, **12**, 3060–3063.
- 93 X. Sun, H. X. Ma, T. S. Mei, P. Fang and Y. Hu, *Org. Lett.*, 2019, **21**, 3167–3171.
- 94 X. Meng, Y. Zhang, J. Luo, F. Wang, X. Cao and S. Huang, *Org. Lett.*, 2020, **22**, 1169–1174.
- 95 Q. Liu, B. Sun, Z. Liu, Y. Kao, B.-W. Dong, S.-D. Jiang, F. Li, G. Liu, Y. Yang and F. Mo, *Chem. Sci.*, 2018, **9**, 8731–8737.

“It is not the critic who counts; not the man who points out how the strong man stumbles, or where the doer of deeds could have done them better. The credit belongs to the man who is actually in the arena, whose face is marred by dust and sweat and blood; who strives valiantly; who errs, who comes short again and again, because there is no effort without error and shortcoming; but who does actually strive to do the deeds; who knows great enthusiasms, the great devotions; who spends himself in a worthy cause; who at the best knows in the end the triumph of high achievement, and who at the worst, if he fails, at least fails while daring greatly, so that his place shall never be with those cold and timid souls who neither know victory nor defeat.”

Theodore Roosevelt (1858–1919), U.S. President

Experimental – General Information

Unless otherwise stated, all non-electrochemical reactions were conducted in flame-dried glassware under an atmosphere of dry nitrogen or argon, sealed with septum seals and were stirred with Teflon-coated magnetic stirrer bars. Unless stated otherwise, all electrochemical reactions were performed using oven-dried 10 mL ElectraSyn vials under an atmosphere of dry nitrogen, sealed with an ElectraSyn Teflon cap fitted with a graphite anode and graphite cathode and were stirred with Teflon-coated magnetic stirrer bars. Dry tetrahydrofuran (THF), diethyl ether (Et₂O) and acetonitrile (MeCN) were obtained after passing these previously degassed solvents through activated alumina columns (Mbraun, SPS-800). Tetra-*n*-butylammonium hexafluorophosphate (TBAPF₆) and tetra-*n*-butylammonium tetrafluoroborate (TBABF₄) were recrystallised from ethanol or water, respectively, and dried in the oven before use. All other solvents and commercial reagents were used as supplied without further purification unless stated otherwise.

All electrochemical reactions were conducted using an ElectraSyn 2.0 apparatus, purchased from IKA. Graphite (C_g), reticulated vitreous carbon (RVC), glassy carbon (GC) and Pt electrodes were purchased from IKA and are of uniform dimensions. Graphite electrodes were used as supplied from IKA or were cut from a sheet of carbon foil (2 mm thickness) purchased from Goodfellow from the workshop. Graphite electrodes could be used several times by renewing the top surface of the graphite. This was achieved by scraping away the top layer with a razor blade, sonicating in MeCN for 5 minutes, followed by oven-drying for 30 mins.

Cyclic voltammetry (CV) experiments were conducted using an Autolab PGSTAT204, controlled using Nova 2.1 software. The working electrode was a GC disc (3 mm dia., BASi part number MF-2012), the counter electrode was a Pt-wire (BASi part number MW-4130) and Ag/AgNO₃ reference electrode was used (BASi part number – MF-2052).

Room temperature (rt) refers to 20-25 °C. Ice/water and CO₂(s)/acetone baths were used to obtain temperatures of 0 °C and -78 °C respectively. All reactions involving heating

were conducted using DrySyn blocks and a contact thermometer. *In vacuo* refers to reduced pressure through the use of a rotary evaporator.

Analytical thin layer chromatography was carried out using aluminium plates coated with silica (Kieselgel 60 F₂₅₄ silica) and visualisation was achieved using ultraviolet light (254 nm), followed by staining with a 1% aqueous KMnO₄ solution, or a 10% w/v solution of phosphomolybdic acid in ethanol. Flash column chromatography was performed according to the method of Still^[1] using Kieselgel 60 silica in the solvent system stated using head-pressure by means of a compressed air line.

Melting points were recorded on an a Gallenkamp melting point apparatus and are reported corrected by linear calibration to benzophenone (47 - 49 °C) and benzoic acid (121 - 123 °C).

Infrared spectra were recorded on a Shimadzu IRAffinity-1 Fourier Transform ATR spectrometer as thin films using a Pike MIRacle ATR accessory. The most intense peaks and structurally important peaks are quoted. Absorption maxima (ν_{max}) are recorded in wavenumbers (cm⁻¹).

¹H, ¹³C and ¹⁹F NMR spectra were obtained on a Bruker Avance 300 (300 MHz ¹H, 75 MHz ¹³C), Bruker Avance 400 (400 MHz ¹H, 101 MHz ¹³C, 376 MHz ¹⁹F) or a Bruker Avance 500 (500 MHz ¹H, 126 MHz ¹³C, 471 MHz ¹⁹F) spectrometer at rt in the solvent stated. Chemical shifts are reported in parts per million (ppm) relative to the residual solvent signal. All coupling constants, *J*, are quoted in Hz. Multiplicities are reported with the following symbols: br = broad, s = singlet, d = doublet, t = triplet, q = quartet, m = multiplet and combinations of these were used to denote higher order multiplicities.

High resolution mass spectrometry (HRMS, *m/z*) data was acquired at Cardiff University on a Micromass LCT Spectrometer.

“Petrol” refers to the fraction boiling in the range of 40-60 °C unless otherwise stated.

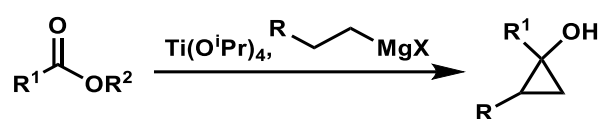
Current density values for the anode, *j_{anode}*, were calculated by dividing the current, *i*, passed during electrolysis by the exposed active surface area of the electrode.

**Chapter 5: Experimental – Manganese-Catalyzed
Electrochemical Deconstructive Chlorination of
Cycloalkanols *via* Alkoxy Radicals**

5. Experimental and Characterization Data

5.1. General Procedures – Substrate Synthesis

5.1.1. General Procedure A – Synthesis of Cyclopropanols via Kulinkovich Reaction



To a flame-dried RBF fitted with a septum seal was added the ester (1.0 eq.), $\text{Ti}(\text{O}^i\text{Pr})_4$ (1.4 eq.), and THF (0.16 M with respect to the ester). The mixture was cooled to 0 °C and a solution of Grignard reagent (2.8 eq.) was added dropwise. After complete addition, the resulting mixture was left to warm to rt and stirred overnight. After completion water was added and the resulting precipitate was filtered under vacuum through celite and washed with EtOAc. The layers of the filtrate were separated, and the aqueous layer was further extracted with EtOAc ($\times 2$). The combined organics were dried (MgSO_4), filtered, and concentrated under reduced pressure. The resultant crude material was purified by flash column chromatography to afford the desired compound.

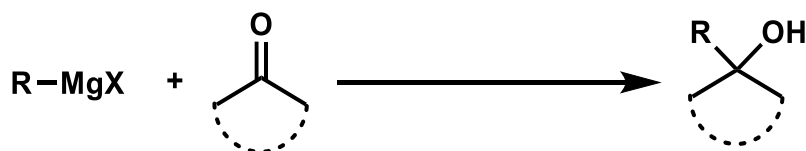
5.1.2. General Procedure B – Generation and Addition of Grignard Reagents to Cycloalkanones



To a three-necked RBF fitted with a condenser, a glass stopper, and a septum seal was added magnesium turnings (1.65 eq.) and the system was flame-dried under a high

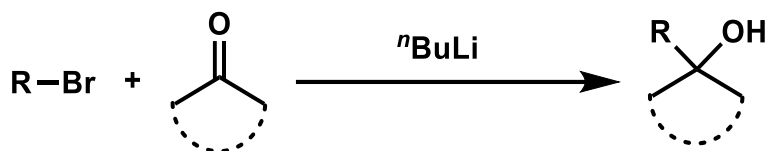
vacuum. After cooling under a N₂ atmosphere, a crystal of iodine was added followed by THF (1 M with respect to RBr). RBr (1.5 eq.) was added dropwise, and the mixture was stirred at rt for 5 min, or until the exotherm had finished. The reaction mixture was then heated at reflux for 1-3 h. Upon cooling to 0 °C, THF was added (0.2 M with respect to cycloalkanone), followed by drop-wise addition of the cycloalkanone (1.0 eq.). The resulting mixture was left to warm to rt and stirred overnight. A saturated solution of NH₄Cl (aq.) was added and the mixture was diluted with EtOAc. The layers were separated, and the aqueous layer was further extracted with EtOAc (× 2). The combined organics were dried (MgSO₄), filtered, and concentrated under reduced pressure. The resultant crude material was purified by flash column chromatography to afford the desired compound.

5.1.3. General Procedure C – Addition of Commercially-Available Grignard Reagents to Cycloalkanones



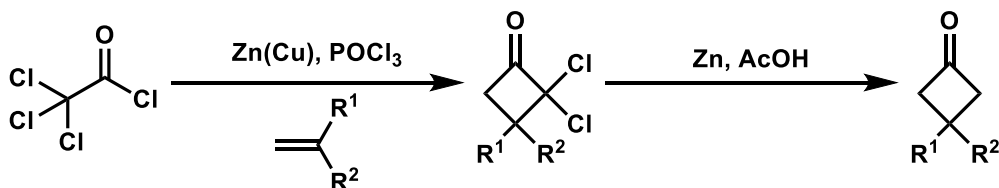
To a flame-dried RBF fitted with a septum seal was added a pre-made Grignard reagent (1.5 eq.) under a N₂ atmosphere. After cooling to 0 °C, the cycloalkanone (1.0 eq.) was added dropwise. After complete addition, the resulting mixture was left to warm to rt and stirred overnight. A saturated solution of NH₄Cl (aq.) was added, followed by a few drops of 1 M HCl (aq.), and the mixture was diluted with Et₂O. The layers were separated, and the aqueous layer was further extracted with Et₂O (× 2). The combined organics were dried (MgSO₄), filtered, and concentrated under reduced pressure. The resultant crude material was purified by flash column chromatography to afford the desired compound.

5.1.4. General Procedure D - Generation and Addition of Organolithium Reagents to Cycloalkanones



To a flame-dried RBF fitted with a septum seal was added a solution of alkyl or aryl halide (1.3 eq.) in THF (0.3 M). The mixture was cooled to $-78\text{ }^{\circ}\text{C}$, and a solution of *n*-butyllithium (solution in hexanes, 1.3 eq.) was added dropwise. The solution was left to stir for 1-3 h before adding a solution of the cycloalkanone (1.0 eq.) in THF (1.0 M) dropwise. The reaction mixture was left to stir for 1-3 h, whilst warming to rt. Water was added dropwise, followed by extraction with EtOAc ($\times 3$). The combined organics were dried (MgSO_4), filtered, and concentrated under reduced pressure. The resultant crude material was purified by flash column chromatography to afford the desired compound.

5.1.5. General Procedure E - Synthesis of Substituted Cyclobutanones

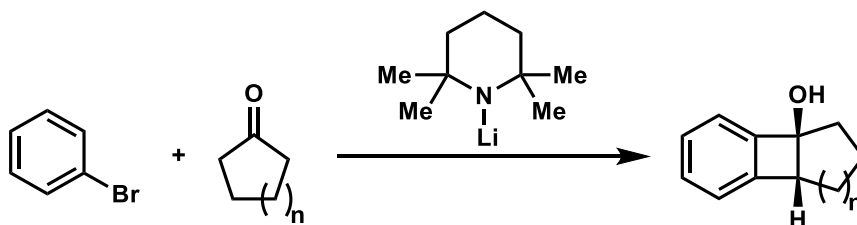


To a flame-dried three-necked RBF fitted with an addition funnel, a reflux condenser and a septum seal was added Zn(Cu) couple^[2] (2.5 eq.), alkene (1.0 eq.) and Et_2O (0.5 M). The dropping funnel was charged with trichloroacetyl chloride (2.0 eq.), phosphoryl chloride (2.0 eq.) and Et_2O (1.0 M). The contents of the dropping funnel were added slowly over

~2 h. The reaction mixture was stirred at 70 °C for 16 h. Upon cooling, the suspension was filtered through a pad of celite, washing with Et₂O and the filtrate was concentrated to ~25% of its original volume. To the resultant mixture was cautiously added water and the organic layer was further washed with a saturated solution of NaHCO₃ (aq.). The aqueous layer was extracted with Et₂O (× 3) and the combined organic layers were dried (MgSO₄), filtered and concentrated. The resultant oil was submitted to the next step without further purification.

The crude residue from the previous step was dissolved in AcOH (0.5 M) and Zn dust (4.0 eq.) was added. The reaction mixture was stirred at 70 °C for 2 h. Acetic acid was removed under reduced pressure and the resultant mixture was filtered through a pad of celite, washing with Et₂O. The filtrate was concentrated, and the crude residue was purified by flash column chromatography to afford the desired compound.

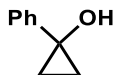
5.1.6. General Procedure F – Synthesis of Benzo-fused Cyclobutanols via Benzyne



To a solution of 2,2,6,6-tetramethylpiperidine (2.5 eq.) in THF (0.83 M) at -78 °C was added *n*-butyllithium (2.5 eq.) dropwise and the resulting mixture was stirred for 20 min. A solution of ketone (1.0 eq.) in THF (0.67 M) was added dropwise followed by aryl halide (1.0 eq.) and the reaction mixture was stirred for 5 h at -78 °C. The reaction was quenched by the addition of a saturated solution of NH₄Cl (aq.) and extracted with EtOAc (× 2). The combined organic layers were dried (MgSO₄), filtered and concentrated under reduced pressure. The crude residue was purified by flash column chromatography to afford the desired compound.

5.2. Characterization of Substrates

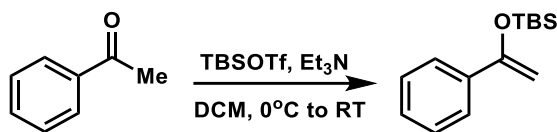
1-Phenylcyclopropan-1-ol (**14**)



Prepared following General Procedure A using ethyl benzoate (3.16 mL, 25.0 mmol), $\text{Ti}(\text{O}^i\text{Pr})_4$ (0.74 mL, 2.5 mmol) and ethylmagnesium bromide (17.7 mL, 3 M in diethyl ether, 53 mmol). Purification by flash column chromatography (10% EtOAc/Petrol, silica gel) to afford **14** (2.93 g, 88%) as a yellow oil.

R_f = 0.15 (15% EtOAc/Petrol); **FTIR** (ν_{max} cm^{-1} , thin film) = 3315 (br), 3090, 3028, 1494, 1546, 1230, 1097, 754, 694; **^1H NMR (500 MHz, CDCl_3)** δ = 7.36 – 7.27 (m, 4H, ArH), 7.24 – 7.21 (m, 1H, ArH), 2.37 (s, 1H, OH), 1.30 – 1.24 (m, 2H, CH_2), 1.09 – 1.02 (m, 2H, CH_2); **^{13}C NMR (126 MHz, CDCl_3)** δ = 144.2 (ArCO), 128.3 (ArC(3,5)H), 126.4 (ArC(5)H), 124.4 (ArC(2,6)H), 56.6 ($\text{PhC}(\text{CH}_2)_2\text{O}$), 17.8 (CH_2)₂; **HRMS** (EI^+) [$\text{C}_9\text{H}_9\text{O}$] requires [M] 133.0657, found 133.0653.

tert-butyldimethyl((1-phenylvinyl)oxy)silane (**10**)



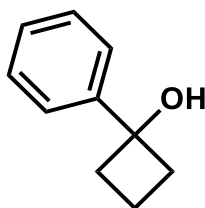
To in a 50 mL round-bottom flask equipped with a stirring bar and filled with DCM (20 mL), acetophenone (5.0 mmol) and triethylamine (1.3 mL, 9.0 mmol) were added. The solution was stirred at room temperature for 15 mins before cooling down to 0 °C. Triisopropylsilyl trifluoromethanesulfonate (1.7 mL, 6.0 mmol) was added by a syringe slowly over 2 min at 0 °C. The resulting mixture was stirred under N_2 atmosphere at 0 °C

for 30 min. The reaction was quenched by saturated NaHCO_3 solution (20 mL) and diluted by cooled DCM (10 mL). The organic layer was washed with cooled saturated NaHCO_3 solution twice, dried over MgSO_4 , filtered, and concentrated under reduced pressure. The crude product was purified by flash column chromatography on Et_3N -treated silica gel eluting with hexane to afford silyl enol ether **10** (1.04 g, 91%) as colourless oil.

R_f = 0.45 (15% EtOAc /Petrol); $^1\text{H NMR}$ (300 MHz, CDCl_3): δ 7.60–7.56 (m, 2H, ArH), 7.31 – 7.23 (m, 3H, ArH), 4.85 (d, J = 1.5 Hz, 1H), 4.39 (d, J = 1.6 Hz, 1H), 0.98 (s, 9H), 0.18 (s, 6H); $^{13}\text{C NMR}$ (75 MHz, CDCl_3): δ 156.0, 137.9, 128.2, 128.1, 125.3, 90.9, 25.9, 18.4, -4.6

These data are consistent with those previously reported in the literature.⁶⁰

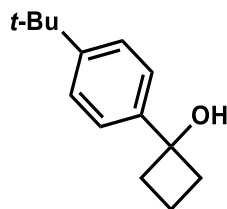
1-Phenylcyclobutan-1-ol (**26**)



Prepared according to General Procedure B using magnesium turnings (2.01 g, 82.5 mmol), bromobenzene (7.90 mL, 75.0 mmol), and cyclobutanone (3.75 mL, 50.0 mmol). The crude residue was purified by flash column chromatography (5→10% EtOAc /Petrol, silica gel) to afford **26** (5.92 g, 80%) as a colourless solid.

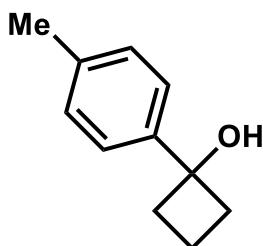
R_f = 0.13 (10% EtOAc /Petrol); **M.p.**: 43–46 °C; $^1\text{H NMR}$ (500 MHz, $\text{DMSO}-d_6$) δ = 7.50 – 7.46 (m, 2H ($\text{ArH}(2,6)$)), 7.35 – 7.30 (m, 2H, ($\text{ArH}(3,5)$)), 7.24 – 7.19 (m, 1H, ($\text{ArH}(4)$)), 5.44 (s, 1H, (OH)), 2.42 – 2.33 (m, 2H, (CH_2)), 2.31 – 2.20 (m, 2H, (CH_2)), 1.98 – 1.85 (m, 1H), 1.70 – 1.55 (m, 1H); $^{13}\text{C NMR}$ (126 MHz, $\text{DMSO}-d_6$) δ = 147.7 (ArCO), 127.9 ($\text{ArC}(3,5)\text{H}$), 126.3 ($\text{ArC}(4)\text{H}$), 124.9 ($\text{ArC}(2,6)\text{H}$), 75.1 ($\text{PhC}(\text{CH}_2)_2\text{O}$), 37.2 (CH_2), 12.7 (CH_2).

These data are consistent with those previously reported in the literature.⁶¹

1-(4-(*Tert*-butyl)phenyl)cyclobutan-1-ol (29)

Prepared according to General Procedure B using magnesium turnings (201 mg, 8.25 mmol), 1-bromo-4-(*tert*-butyl)benzene (1.30 mL, 7.50 mmol), and cyclobutanone (374 μ L, 5.00 mmol). The crude residue was purified by flash column chromatography (5 \rightarrow 10% EtOAc/Petrol, silica gel) to afford **29** (571 mg, 56%) as a colourless solid.

R_f = 0.17 (10% EtOAc/Petrol); **M.p.**: 74-77 °C; **FTIR** (ν_{max} cm⁻¹, thin film) 3329 (br), 2961, 2866, 2361, 2342, 1508, 1464, 1395, 1364, 1275, 1261, 1233, 1138, 1111, 961, 845, 839, 764, 750, 567; **¹H NMR (400 MHz, CDCl₃)** δ = 7.47 – 7.43 (m, 2H), 7.43 – 7.39 (m, 2H), 2.64 – 2.51 (m, 2H), 2.44 – 2.29 (m, 2H), 2.08 – 1.93 (m, 2H), 1.75 – 1.60 (m, 1H), 1.33 (s, 9H); **¹³C NMR (101 MHz, CDCl₃)** δ = 150.3, 143.4, 125.5, 124.9, 77.0, 36.9, 34.6, 31.5, 13.1; **HRMS** (EI⁺) [C₁₄H₂₀O] requires [M-H₂O] 186.1409, found 186.1404.

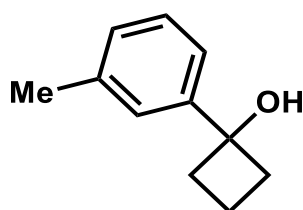
1-(*p*-Tolyl)cyclobutan-1-ol (32)

Prepared according to General Procedure B using magnesium turnings (201 mg, 8.25 mmol), 4-bromotoluene (923 μ L, 7.50 mmol), and cyclobutanone (374 μ L, 5.00 mmol). The crude residue was purified by flash column chromatography (5 \rightarrow 10% EtOAc/Petrol, silica gel) to afford **32** (582 mg, 72%) as a yellow oil.

R_f = 0.17 (10% EtOAc/Petrol); ^1H NMR (500 MHz, CDCl_3) δ = 7.42 – 7.38 (m, 2H), 7.21 – 7.18 (m, 2H), 2.59 – 2.52 (m, 2H), 2.40 – 2.33 (m, 5H), 2.04 – 1.96 (m, 2H), 1.72 – 1.62 (m, 1H); ^{13}C NMR (126 MHz, CDCl_3) δ = 143.5, 137.1, 129.3, 125.1, 77.0, 37.0, 21.2, 13.1.

These data are consistent with those previously reported in the literature ⁶¹

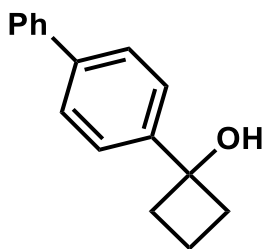
1-(*m*-Tolyl)cyclobutan-1-ol (**33**)



Prepared according to General Procedure B using magnesium turnings (201 mg, 8.25 mmol), 3-bromotoluene (910 μL , 7.50 mmol), and cyclobutanone (374 μL , 5.00 mmol). The crude residue was purified by flash column chromatography (5 \rightarrow 10% EtOAc/Petrol, silica gel) to afford **33** (375 mg, 46%) as a yellow oil.

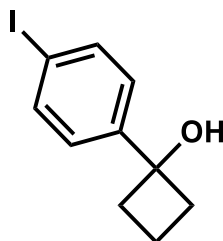
R_f = 0.36 (10% EtOAc/Petrol); ^1H NMR (500 MHz, $\text{DMSO}-d_6$) δ = 7.29 (s, 1H), 7.26 (d, J = 8.0 Hz, 1H), 7.21 (app. t, J = 7.5 Hz, 1H), 7.03 (d, J = 7.5 Hz, 1H), 5.39 (s, 1H), 2.40 – 2.33 (m, 2H), 2.31 (s, 3H), 2.29 – 2.19 (m, 2H), 1.96 – 1.83 (m, 1H), 1.68 – 1.55 (m, 1H); ^{13}C NMR (126 MHz, $\text{DMSO}-d_6$) δ = 147.7, 136.8, 127.8, 126.9, 125.6, 121.9, 75.1, 37.2, 21.2, 12.8.

These data are consistent with those previously reported in the literature.²

1-([1,1'-Biphenyl]-4-yl)cyclobutan-1-ol (34)

Prepared according to General Procedure D using 4-bromo-1,1'-biphenyl (1.40 g, 6.00 mmol, 1.2 eq.), *n*-butyllithium (3.18 mL, 2.36 M in hexanes, 7.50 mmol, 1.5 eq.) and cyclobutanone (374 μ L, 5.0 mmol, 1.0 eq.). The crude residue was purified by flash column chromatography (5 \rightarrow 10% EtOAc/Petrol, silica gel) to afford **34** (0.97 g, 73%) as a white solid.

R_f = 0.29 (10% EtOAc/Petrol); **M.p.**: 84-86 °C; **FTIR** (ν_{max} cm⁻¹, thin film) 3233 (br), 2984, 2938, 1483, 1242, 1140, 1111, 841, 766, 729, 694; **¹H NMR (500 MHz, CDCl₃)** δ = 7.64 – 7.56 (m, 6H), 7.45 (t, *J* = 7.5 Hz, 2H), 7.35 (t, *J* = 7.0 Hz, 1H), 2.66 – 2.58 (m, 2H), 2.46 – 2.37 (m, 2H), 2.10 – 1.98 (m, 2H), 1.79 – 1.68 (m, 1H), **¹³C NMR (126 MHz, CDCl₃)** δ = 145.4, 141.0, 140.4, 128.9, 127.5, 127.4, 127.3, 125.6, 77.1, 37.1, 13.2; **HRMS (EI⁺)** [C₁₆H₁₆O] requires [M] 224.1201, found 224.1203.

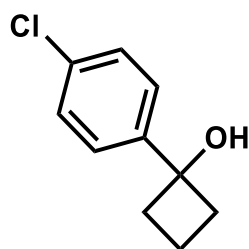
1-(4-Iodophenyl)cyclobutan-1-ol (35)

Prepared according to General Procedure D using 1,4-diiodobenzene (2.14 g, 6.50 mmol) *n*-butyllithium (2.83 mL, 2.3 M in hexanes, 6.50 mmol), and cyclobutanone

(374 μ L, 5.00 mmol). The crude residue was purified by flash column chromatography (5% EtOAc/Hexanes, silica gel) to afford **35** (929 mg, 68%) as an off white solid.

R_f = 0.16 (10% EtOAc/Hexanes); **M.p.**: 66 – 69 °C; **FTIR** (ν_{max} cm^{-1} , thin film) 3335 (br), 2980, 2940, 1489, 1389, 1223, 1128, 1103, 1078, 1005, 961, 839, 812, 642, 523; **¹H NMR (500 MHz, CDCl₃)** δ = 7.71 – 7.67 (m, 2H), 7.27 – 7.23 (m, 2H), 2.55 – 2.48 (m, 2H), 2.40 – 2.31 (m, 2H), 2.08 – 1.95 (m, 2H), 1.75 – 1.64 (m, 1H); **¹³C NMR (126 MHz, CDCl₃)** δ = 146.1, 137.6, 127.2, 92.9, 76.9, 37.1, 13.1; **HRMS** (EI⁺) [C₁₀H₁₁IO] requires [M-H₂O] 255.9749, found 255.9760.

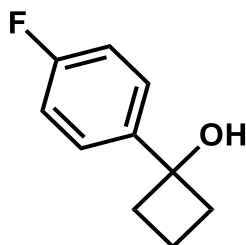
1-(4-Chlorophenyl)cyclobutan-1-ol (**36**)



Prepared according to General Procedure D using 1-chloro-4-iodobenzene (1.14 g, 4.76 mmol, 1.00 eq.), *n*-butyllithium (2.25 mL, 2.13 M in hexanes, 4.76 mmol, 1.00 eq.), and cyclobutanone (374 μ L, 5.00 mmol, 1.05 eq.). The crude residue was purified by flash column chromatography (5→10% EtOAc/Petrol, silica gel) to afford **36** (766 mg, 88%) as a colourless oil.

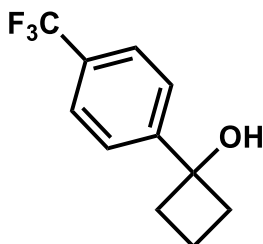
R_f = 0.37 (10 % EtOAc/Petrol); **¹H NMR (500 MHz, CDCl₃)** δ = 7.45 – 7.40 (m, 2H), 7.36 – 7.31 (m, 2H), 2.56 – 2.47 (m, 2H), 2.40 – 2.31 (m, 2H), 2.12 (s, 1H), 2.07 – 1.97 (m, 1H), 1.75 – 1.63 (m, 1H); **¹³C NMR (101 MHz, CDCl₃)** δ = 144.9, 133.1, 128.6, 126.6, 76.7, 37.2, 13.1.

These data are consistent with those previously reported in the literature.²

1-(4-Fluorophenyl)cyclobutan-1-ol (37)

Prepared according to General Procedure B using magnesium turnings (201 mg, 8.25 mmol), 1-bromo-4-fluorobenzene (824 μ L, 7.50 mmol), and cyclobutanone (374 μ L, 5.00 mmol). The crude residue was purified by flash column chromatography (5 \rightarrow 10% EtOAc/Petrol, silica gel) to afford **37** (652 mg, 78%) as a colourless oil.

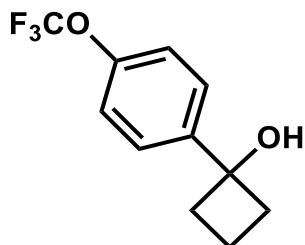
R_f = 0.20 (10% EtOAc/Petrol); **FTIR** (ν_{max} cm^{-1} , thin film) 3327 (br), 2940, 2361, 1601, 1508, 1277, 1225, 1159, 1130, 1098, 957, 889, 835, 750, 542; **¹H NMR (500 MHz, CDCl₃)** δ = 7.50 – 7.42 (m, 2H), 7.08 – 7.00 (m, 2H), 2.58 – 2.48 (m, 2H), 2.41 – 2.31 (m, 2H), 2.14 (s, 1H), 2.07 – 1.96 (m, 1H), 1.74 – 1.61 (m, 1H); **¹³C NMR (126 MHz, CDCl₃)** δ = 162.1 (d, J = 245.5 Hz), 142.2 (d, J = 3.0 Hz), 126.9 (d, J = 8.0 Hz), 115.3 (d, J = 21.0 Hz), 76.8, 37.1, 13.0; **¹⁹F NMR (471 MHz, CDCl₃)** δ = -115.65; **HRMS** (EI⁺) [C₁₀H₁₁OF] requires [M] 166.0794, found 166.0790.

1-(4-(Trifluoromethyl)phenyl)cyclobutan-1-ol (38)

Prepared according to general procedure B using magnesium turnings (438 mg, 18.0 mmol, 1.8 eq.), 1-bromo-4-(trifluoromethyl)benzene (2.10 mL, 15.0 mmol, 1.5 eq.) and cyclobutanone (747 μ L, 10.0 mmol, 1.0 eq.). The crude residue was purified by flash column chromatography (5 \rightarrow 10% EtOAc/Petrol, silica gel) to afford **38** (1.32 g, 61%) as a white solid.

R_f = 0.36 (20% EtOAc/Petrol); **M.p.**: 54-56 °C; **FTIR** (ν_{max} cm⁻¹, thin film) 3240 (br), 2997, 2949, 1620, 1408, 1325, 1155, 1107, 1072, 1012, 835; **¹H NMR (500 MHz, CDCl₃)** δ = 7.63 – 7.63 (m, 4H), 2.64 – 2.50 (m, 2H), 2.47 – 2.32 (m, 2H), 2.19 – 1.99 (m, 2H), 1.85 – 1.68 (m, 1H); **¹³C NMR (126 MHz, CDCl₃)** δ = 150.3, 129.6 (q, J = 32.5 Hz), 125.6 (q, J = 4.0 Hz), 125.4, 124.3 (q, J = 272.0 Hz), 76.9, 37.3, 13.1; **¹⁹F NMR (471 MHz, CDCl₃)** δ = -62.47; **HRMS** (EI⁺) [C₁₁H₉F₃] requires [M-H₂O] 198.0656, found 198.0661.

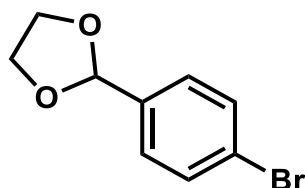
1-(4-(Trifluoromethoxy)phenyl)cyclobutan-1-ol (**39**)



Prepared according to General Procedure D, using 1-bromo-4-(trifluoromethoxy)benzene (1.75 mL, 12.0 mmol, 1.20 eq.), *n*-butyllithium (6.25 mL, 2.3 M in hexanes, 14.3 mmol, 1.43 eq.) and cyclobutanone (747 μ L, 10.0 mmol, 1.00 eq.). The crude residue was purified by flash column chromatography (5 \rightarrow 10% EtOAc/Petrol, silica gel) to afford **39** (1.58 g, 70%) as a white solid.

R_f = 0.20 (10% EtOAc/Petrol); **M.p.**: 29-31 °C; **¹H NMR (500 MHz, CDCl₃)** δ = 7.57 – 7.48 (m, 2H), 7.25 – 7.16 (m, 2H), 2.60 – 2.49 (m, 2H), 2.44 – 2.32 (m, 2H), 2.11 – 1.99 (m, 2H), 1.77 – 1.65 (m, 1H); **¹³C NMR (126 MHz, CDCl₃)** δ = 148.4 (q, J = 2.0 Hz), 145.1, 126.7, 121.0, 120.6 (q, J = 257.0 Hz), 76.7, 37.2, 13.1; **¹⁹F NMR (471 MHz, CDCl₃)** δ = -57.9.

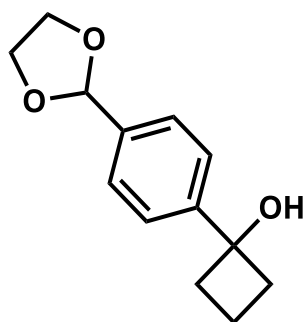
These data are consistent with those previously reported in the literature.⁶²

2-(4-Bromophenyl)-1,3-dioxolane (2-A)

To a 250 mL RBF was added 4-bromobenzaldehyde (4.00 g, 21.6 mmol), *p*-toluenesulfonic acid (100 mg, 0.52 mmol), ethylene glycol (2.40 mL, 34.7 mmol) and toluene (60 mL). The RBF was then fitted with a Dean-Stark condenser and the reaction mixture was refluxed for 10 h and monitored by TLC. Upon completion, the mixture was washed with sat. NaHCO₃ (2 × 20 mL) and extracted with EtOAc (3 × 30 mL). The combined organic layers were dried (MgSO₄), filtered and concentrated under reduced pressure. The crude residue was purified by flash column chromatography (2% EtOAc/Petrol) to afford **2-A** (4.90 g, 97%) as a yellow oil.

R_f = 0.40 (15% EtOAc/Petrol); ¹H NMR (300 MHz, CDCl₃) δ = 7.51 (d, *J* = 8.5 Hz, 2H), 7.36 (d, *J* = 8.5 Hz, 2H), 5.77 (s, 1H), 4.19 – 3.96 (m, 4H); ¹³C NMR (75 MHz, CDCl₃) δ = 137.1, 131.6, 128.3, 123.4, 103.2, 65.5.

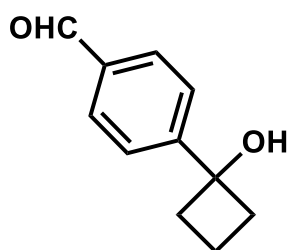
These data are consistent with those previously reported in the literature.⁶³

1-(4-(1,3-Dioxolan-2-yl)phenyl)cyclobutan-1-ol (2-B)

Prepared according to General Procedure D using **2-A** (2.74 g, 12 mmol, 1.2 eq.), *n*-butyllithium (6.25 mL, 2.3 M in hexanes, 14.3 mmol, 1.2 eq.) and cyclobutanone (747 μL, 10 mmol, 1.0 eq.). The crude residue was purified by flash column chromatography (5→15% EtOAc/Petrol, silica gel) to afford **2-B** (2.04 g, 78%) as a colourless viscous oil.

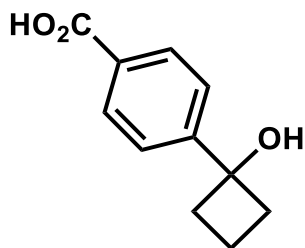
R_f = 0.48 (30% EtOAc/Petrol); **FTIR** (ν_{max} cm⁻¹, thin film) 3425, 2980, 2889, 1377, 1242, 1078, 939, 827; **¹H NMR (500 MHz, CDCl₃)** δ = 7.56 – 7.44 (m, 4H), 5.83 (s, 1H), 4.19 – 3.98 (m, 4H), 2.61 – 2.50 (m, 2H), 2.43 – 2.31 (m, 2H), 2.06 – 1.95 (m, 2H), 1.76 – 1.61 (m, 1H); **¹³C NMR (126 MHz, CDCl₃)** δ = 147.4, 137.0, 126.7, 125.1, 103.6, 77.0, 65.4, 37.0, 13.1; **HRMS** (EI⁺) [C₁₃H₁₃O₃] requires [M-H₂O] 201.0916, found 201.0911.

4-(1-Hydroxycyclobutyl)benzaldehyde (**40**)



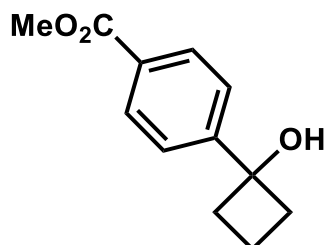
To a solution of **2-B** (1.00 g, 4.5 mmol, 1.0 eq.) in THF (5 mL) was added 1 M HCl (2.0 mL) at 0 °C and stirred for 2 h. The reaction was quenched with the addition of sat. NaHCO₃ (5 mL) and extracted with EtOAc (3 × 5 mL). The combined organic layers were dried (MgSO₄), filtered and concentrated under reduced pressure. The crude residue was purified by flash column chromatography (5 → 15% EtOAc/Petrol, silica gel) to afford **40** (450 mg, 56%) as a colourless viscous oil.

R_f = 0.48 (30% EtOAc/Petrol); **FTIR** (ν_{max} cm⁻¹, thin film) 3385 (br), 2988, 2945, 1695, 1603, 1572, 1215, 1136, 1103, 839, 700, 540; **¹H NMR (500 MHz, CDCl₃)** δ = 9.99 (s, 1H), 7.90 – 7.86 (m, 2H), 6.69 – 7.65 (m, 2H), 2.62 – 2.52 (m, 2H), 2.46 – 2.36 (m, 2H), 2.14 – 2.04 (m, 1H), 1.84 – 1.71 (m, 1H); **¹³C NMR (126 MHz, CDCl₃)** δ = 192.1, 153.2, 135.4, 130.1, 125.6, 76.9, 37.3, 13.1; **HRMS** (EI⁺) [C₁₁H₁₂O₃] requires [M-H] 175.0759, found 175.0751.

4-(1-Hydroxycyclobutyl)benzoic acid (41)

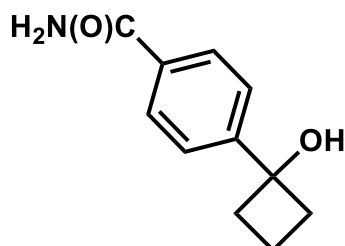
To a solution of 4-bromobenzoic acid (4.0 g, 20 mmol, 1 eq.) in THF (100 mL) at -78 °C was added *n*-butyllithium (17.4 mL, 2.3 M in hexanes, 40.0 mmol, 2.0 eq.) and the resulting mixture was stirred for 30 min. Cyclobutanone (3.3 mL, 44 mmol, 2.2 eq.) was added dropwise to the reaction mixture followed by immediate addition of sat. NH₄Cl (30 mL) and the resulting mixture was warmed to rt. The reaction mixture was then acidified with 1 M HCl and extracted with EtOAc (3 × 50 mL). The combined organics were dried (MgSO₄), filtered and concentrated under reduced pressure. The crude residue was suspended in hexanes and stirred vigorously, which resulted in formation of a white solid. The precipitate was filtered and resuspended in CH₂Cl₂. Slow addition of hexanes followed resulted in precipitation of the white solid which was filtered and dried under a high vacuum to afford **41** (1.23 g, 31%) as white solid.

R_f = 0.56 (80% EtOAc/Petrol); **M.p.:** 149-151 °C; **FTIR** (ν_{max} cm⁻¹, thin film) 3264 (br), 2980, 2671, 2561, 1677, 1612, 1420, 1272, 1130, 856, 702, 542; **¹H NMR (500 MHz, CDCl₃)** δ = 8.15 – 8.08 (m, 2H), 7.47 – 7.41 (m, 2H), 7.66 – 7.59 (m, 1H), 2.64 – 2.53 (m, 2H), 2.47-2.37 (m, 2H), 2.18 – 1.99 (m, 1H), 1.84 – 1.72 (m, 1H); **¹³C NMR (126 MHz, CDCl₃)** δ = 171.3, 152.4, 130.6, 128.1, 125.1, 77.0, 37.3, 13.1; **HRMS** (EI⁺) [C₁₁H₁₁O₃] requires [M-H] 191.0708, found 191.0701.

Methyl 4-(1-hydroxycyclobutyl)benzoate (42)

To a solution of **28** (400 mg, 2.08 mmol, 1.0 eq.) in DMF (5.0 mL, 0.4 M) was added K_2CO_3 (340 mg, 2.50 mmol, 1.2 eq.) and the reaction mixture was stirred for 10 min at rt. Methyl iodide (142 μ L, 2.28 mmol, 1.1 eq.) was added and the reaction mixture was stirred for 4 h. Brine (10 mL) was added and the aqueous layer was extracted with EtOAc (3×10 mL). The combined organic layers were dried ($MgSO_4$), filtered and concentrated under reduced pressure. The crude residue was purified by flash column chromatography (5 \rightarrow 15% EtOAc/Petrol, silica gel) to afford **42** (350 mg, 83%) as a yellow oil.

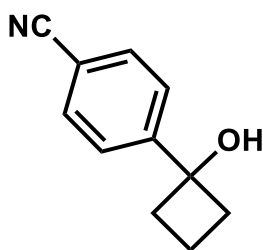
R_f = 0.48 (30% EtOAc/Petrol); **FTIR** (ν_{max} cm^{-1} , thin film) 3439 (br), 2992, 2945, 1721, 1701, 1607, 1437, 1281, 1105, 1018, 856, 772, 706; **1H NMR (500 MHz, $CDCl_3$)** δ = 8.07 – 8.00 (m, 2H), 7.60 – 7.54 (m, 2H), 3.92 (s, 3H), 2.61 – 2.52 (m, 2H), 2.46 – 2.34 (m, 2H), 2.13 – 2.02 (m, 2H), 1.82 – 1.69 (m, 1H); **^{13}C NMR (126 MHz, $CDCl_3$)** δ = 167.0, 151.4, 129.9, 129.1, 125.0, 77.0, 52.2, 37.3, 13.2; **HRMS** (EI^+) [$C_{12}H_{13}O_3$] requires [M-H] 205.0865, found 205.0863.

4-(1-Hydroxycyclobutyl)benzamide (43)

To a stirred solution of **41** (400 mg, 2.08 mmol, 1.0 eq.) in THF (10 ml) was added SOCl_2 (0.36 mL, 4.8 mmol, 2.3 eq.) at 0 °C and the reaction mixture was stirred at rt for 1 h. Upon cooling to 0 °C the reaction mixture was poured into an ice-cold solution of NH_4OH (2.40 mL, 35% in water) and stirred for 5 min. The reaction mixture was extracted with CH_2Cl_2 (3×15 mL) and the organic layers were dried (MgSO_4), filtered and concentrated under reduced pressure. The residue obtained was purified by flash column chromatography (70% EtOAc/hexanes, silica gel) to afford **43** (56 mg, 15%) as a white amorphous solid.

R_f = 0.32 (100% EtOAc); **M.p.:** 156-158 °C; **FTIR** (ν_{max} cm^{-1} , thin film) 3267 (br), 3169 (br), 1665, 1607, 1557, 1420, 1290, 1138, 1117, 891, 808, 650; **¹H NMR (500 MHz, DMSO)** δ = 7.93 (br, 1H), 7.86 – 7.77 (m, 2H), 7.57 – 7.49 (m, 2H), 7.30 (br, 1H), 5.59 (s, 1H), 2.43 – 2.33 (m, 2H), 2.33 – 2.22 (m, 2H), 1.99 – 1.86 (m, 1H), 1.73 – 1.60 (m, 1H); **¹³C NMR (126 MHz, DMSO)** δ = 167.8, 151.0, 132.3, 127.2, 124.6, 75.0, 37.3, 12.7; **HRMS (EI⁺)** [$\text{C}_{11}\text{H}_{13}\text{NO}_2$] requires [M+H] 192.1025, found 192.1026.

4-(1-Hydroxycyclobutyl)benzonitrile (**44**)

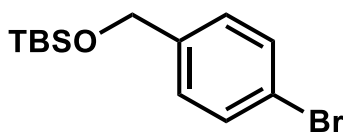


Preparation of Turbo-Grignard (*i*-PrMgCl.LiCl): To a flame-dried RBF was added dry LiCl (1.75 g, 38.0 mmol, 1.00 eq.), magnesium turnings (1.20 g, 50.0 mmol, 1.30 eq.) and a crystal of iodine followed by THF (20 mL). The mixture was cooled to 0 °C and 2-chloropropane (3.5 mL, 38.0 mmol, 1.00 eq.) was added dropwise maintaining the temperature of the bath at 0 °C. After the addition was complete, the reaction mixture was brought to rt and stirred for 12 h. The resulting black reaction mixture (1.1 M) was kept under nitrogen and used as such in the following reaction.

Preparation of 31: In a flame-dried RBF was added 4-bromobenzonitrile (2.18 g, 12.0 mmol, 1.2 eq.) and THF (20 mL) and cooled to -7 °C. The pre-formed Turbo-Grignard reagent (13.63 mL, 1.1 M, 15.0 mmol, 1.5 eq.) was added dropwise and the resulting mixture was stirred for 4 h at -7 °C. Cyclobutanone (747 μ L, 10.0 mmol, 1.0 eq.) was added dropwise and the resulting mixture was stirred for 1 h at -7 °C and then stirred at rt for an additional 2 h. The reaction was quenched with sat. NH_4Cl (20 mL) and extracted with EtOAc (3 \times 25 mL). The combined organic layers were dried (MgSO_4), filtered and concentrated under reduced pressure. The crude residue was purified by flash column chromatography (5 \rightarrow 20% EtOAc/Petrol, silica gel) to afford **44** (700 mg, 40%) as a colourless liquid.

R_f = 0.20 (15% EtOAc/Petrol); **FTIR** (ν_{max} cm^{-1} , thin film) 3333 (br), 2984, 2934, 2361, 2340, 1487, 1456, 1377, 1277, 1231, 1123, 1024, 887, 758, 727; **^1H NMR (500 MHz, CDCl_3)** δ = 7.74 – 7.56 (m, 4H), 2.60 – 2.48 (m, 2H), 2.46 – 2.35 (m, 5H), 2.15 – 2.05 (m, 2H), 1.84 – 1.71 (m, 1H); **^{13}C NMR (126 MHz, CDCl_3)** δ = 151.6, 132.5, 125.8, 119.1, 111.1, 76.8, 37.5, 13.1; **HRMS** (EI^+) [$\text{C}_{11}\text{H}_{11}\text{NO}$] requires $[M]$ 173.0841, found 173.0841.

((4-Bromophenyl)oxy)(*tert*-butyl)dimethylsilane (2-C)

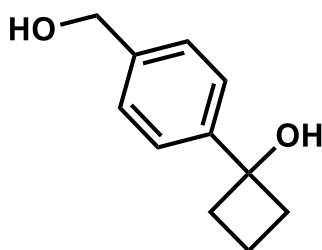


To a solution of (4-bromophenyl)methanol (4.00 g, 21.3 mmol 1.0 eq.) in CH_2Cl_2 was added imidazole (2.91 g, 42.7 mmol, 2.0 eq.) and *tert*-butylchlorodimethylsilane (6.44 g, 42.7 mmol, 2.0 eq.). The resulting mixture was stirred for 14 h at rt, then poured into water (50 mL) and extracted with CH_2Cl_2 (3 \times 30 mL). The combined organics were dried (MgSO_4), filtered and concentrated *in vacuo*. The crude residue was purified by flash column chromatography (5% EtOAc/Petrol) to afford **2-C** (5.8 g, 94%) as a colourless liquid.

R_f = 0.18 (10% EtOAc/Petrol); ^1H NMR (300 MHz, CDCl_3) δ = 7.51 – 7.39 (m, 2H), 7.25 – 7.14 (m, 2H), 4.69 (s, 2H), 0.94 (s, 9H), 0.09 (s, 6H); ^{13}C NMR (75 MHz, CDCl_3) δ = 140.4, 131.2, 127.7, 120.5, 64.3, 25.9, 18.5, -5.3.

These data are consistent with those previously reported in the literature.⁶⁴

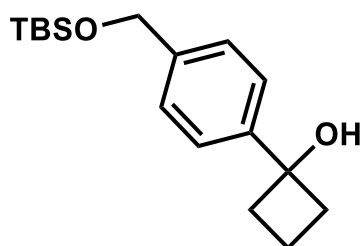
1-(4-(Hydroxymethyl)phenyl)cyclobutan-1-ol (**45**)



To a solution of **46** (2.00 g, 6.8 mmol, 1.0 eq.) in dry THF (20 mL, 0.34 M) at 0 °C was added TBAF (13.6 mL, 1 M in THF, 13.6 mmol, 2.0 eq.). The reaction mixture was stirred for 2 h at rt. Water (15 mL) was added and the mixture was extracted with EtOAc (3 × 30 mL). The combined organics were dried (MgSO_4), filtered and concentrated *in vacuo*. The crude residue was purified by flash column chromatography (30 % EtOAc/Petrol, silica gel) to afford **45** (800 mg, 66%) as a white solid.

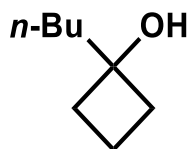
R_f = 0.20 (30% EtOAc/Petrol); **M.p.:** 64-66 °C (lit.^[9] 63-66 °C); ^1H NMR (500 MHz, CDCl_3) δ = 7.53 – 7.47 (m, 2H), 7.40-7.34 (m, 2H), 4.69 (s, 2H), 2.61 – 2.51 (m, 2H), 2.42 – 2.32 (m, 2H), 2.08 (s, 1H), 2.06 – 1.97 (m, 1H), 1.79 (s, 1H) 1.75 – 1.62 (m, 1H); ^{13}C NMR (126 MHz, CDCl_3) δ = 145.9, 140.0, 127.3, 125.4, 77.0, 65.2, 37.1, 13.1.

These data are consistent with those previously reported in the literature.⁶⁵

1-(4-(((*Tert*-butyldimethylsilyl)oxy)methyl)phenyl)cyclobutan-1-ol (46)

Prepared according to General Procedure C using compound **2-C** (1.80 g, 6.00 mmol, 1.2 eq.), *n*-butyllithium (4.10 mL, 2.2 M in hexanes, 9.00 mmol, 1.5 eq.) and cyclobutanone (374 μ L, 5.00 mmol, 1.0 eq.). The crude residue was purified by flash column chromatography (5 \rightarrow 10% EtOAc/Petrol, silica gel) to afford **46** (0.99 g, 57%) as a colourless oil.

R_f = 0.20 (15% EtOAc/Petrol); **FTIR** (ν_{max} cm⁻¹, thin film) 3354 (br), 2866, 2934, 1460, 1367, 1251, 1089, 833, 771, 667; **¹H NMR** (500 MHz, CDCl₃) δ = 7.51 – 7.43 (m, 2H), 7.36–7.31 (m, 2H), 4.75 (s, 2H), 2.62 – 2.51 (m, 2H), 2.43 – 2.31 (m, 2H), 2.06 – 1.95 (m, 2H), 1.74 – 1.63 (m, 1H), 0.95 (s, 9H), 0.11 (s, 6H); **¹³C NMR** (126 MHz, CDCl₃) δ = 145.0, 140.7, 126.3, 125.0, 77.1, 64.9, 37.0, 26.1, 18.6, 13.1, -5.1; **HRMS** (EI⁺) [C₁₇H₂₈O₂Si] requires [M-H] 291.1780, found 291.1779.

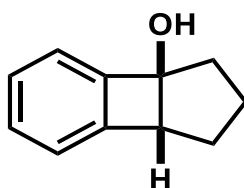
1-Butylcyclobutan-1-ol (62)

Prepared according to General Procedure A using *n*-butylmagnesium chloride (2.00 mL, 20% w/v in THF/Toluene, 3.75 mmol) and cyclobutanone (187 μ L, 2.50 mmol). The crude residue was purified by flash column chromatography (10% Et₂O/Petrol, silica gel) to afford **62** (268 mg, 84%) as a colourless liquid.

$R_f = 0.31$ (10% EtOAc/Petrol); $^1\text{H NMR}$ (500 MHz, CDCl_3) $\delta = 2.09 - 1.93$ (m, 4H), 1.79 – 1.69 (m, 1H), 1.63 – 1.45 (m, 4H), 1.40 – 1.30 (m, 4H), 0.97 – 0.89 (m, 3H); $^{13}\text{C NMR}$ (126 MHz, CDCl_3) $\delta = 75.6, 39.4, 36.1, 25.7, 23.3, 14.3, 12.3$.

These data are consistent with those previously reported in the literature.⁶¹

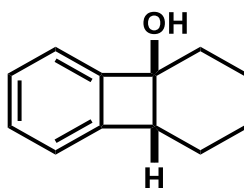
1,2,3,7b-Tetrahydro-3aH-cyclopenta[3,4]cyclobuta[1,2]benzen-3a-ol (64)



Prepared according to General Procedure F using 2,2,6,6-tetramethylpiperidine (4.21 mL, 25.0 mmol), *n*-butyllithium (11.9 mL, 2.1 M in hexanes, 25.0 mmol), cyclopentanone (0.88 mL, 10.0 mmol) and bromobenzene (1.05 mL, 10.0 mmol). The crude residue was purified by flash column chromatography (5→10% EtOAc/Petrol, silica gel) to afford **64** (550 mg, 34%) as a white solid.

$R_f = 0.50$ (15% EtOAc/Petrol); **M.p.:** 55-57 °C; **FTIR** (ν_{max} cm^{-1} , thin film) 3321 (br), 2945, 2855, 1452, 1292, 1221, 1165, 1094, 1038, 756, 737, 658; $^1\text{H NMR}$ (500 MHz, CDCl_3) $\delta = 7.33 - 7.23$ (m, 2H), 7.17 (d, $J = 7.0$ Hz, 1H), 7.10 (d, $J = 7.0$ Hz, 1H), 3.51 (d, $J = 6.0$ Hz, 1H), 2.40 (s, 1H), 2.12 – 2.04 (m, 1H), 1.89 – 1.63 (m, 4H), 1.22 – 1.07 (m, 1H); $^{13}\text{C NMR}$ (126 MHz, CDCl_3) $\delta = 147.8, 144.0, 129.8, 128.1, 123.2, 121.0, 89.5, 57.2, 35.9, 28.7, 24.7$; **HRMS** (EI^+) [$\text{C}_{11}\text{H}_{12}\text{O}$] requires $[M]$ 160.0888, found 160.0888.

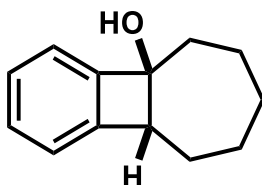
1,3,4,8b-Tetrahydrobiphenylen-4a(2H)-ol (65)



Prepared according to General Procedure F using 2,2,6,6-tetramethylpiperidine (4.21 mL, 25.0 mmol), *n*-butyllithium (11.90 mL, 2.1 M in hexanes, 25.0 mmol), cyclohexanone (1.03 mL, 10.0 mmol) and iodobenzene (2.24 mL, 20.0 mmol). The crude residue was purified by flash column chromatography (5→10 % EtOAc/Petrol, silica gel) to afford **65** (1.40 g, 80%) as a white solid.

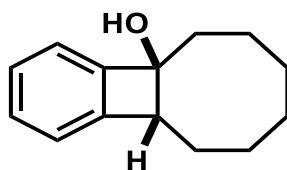
R_f = 0.52 (15% EtOAc/Petrol); **M.p.:** 107-109 °C; **FTIR** (ν_{max} cm⁻¹, thin film) 3231 (br), 2938, 2862, 1456, 1356, 1165, 1076, 1007, 745, 696, 654; **¹H NMR (500 MHz, CDCl₃)** δ = 7.31 – 7.21 (m, 2H), 7.19 – 7.13 (m, 2H), 3.39 (t, *J* = 5.0 Hz, 1H), 2.27 (s, 1H), 2.08 – 1.92 (m, 3H), 1.86 – 1.76 (m, 1H), 1.64 – 1.42 (m, 2H), 1.37 – 1.08 (m, 2H); **¹³C NMR (126 MHz, CDCl₃)** δ = 149.5, 145.7, 129.3, 127.7, 123.3, 121.2, 79.2, 53.8, 31.7, 23.9, 17.9, 17.6; **HRMS** (EI⁺) [C₁₂H₁₄O] requires [M] 174.1045, found 174.1042.

5,6,7,8,9,9a-Hexahydro-4bH-benzo[3,4]cyclobuta[1,2][7]annulen-4b-ol (66)



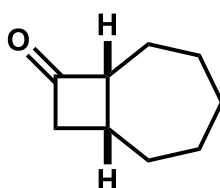
Prepared according to General Procedure F using 2,2,6,6-tetramethylpiperidine (4.21 mL, 25.0 mmol), *n*-butyllithium (11.9 mL, 2.1 M in hexanes, 25.0 mmol), cycloheptanone (1.17 mL, 10.0 mmol) and iodobenzene (1.12 mL, 10.0 mmol). The crude residue was purified by flash column chromatography (5→10% EtOAc/Petrol, silica gel) to afford **66** (829 mg, 44%) as a white solid.

R_f = 0.48 (15% EtOAc/Petrol); **M.p.:** 96-98 °C; **FTIR** (ν_{max} cm⁻¹, thin film) 3302 (br), 2918, 2843, 1456, 1395, 1333, 1182, 1047, 754, 735; **¹H NMR (500 MHz, CDCl₃)** δ = 7.31 – 7.19 (m, 2H), 7.18 – 7.10 (m, 2H), 3.56 – 3.37 (m, 1H), 2.31 – 2.21 (m, 1H), 2.20 – 2.07 (m, 2H), 1.99 – 1.86 (m, 1H), 1.84 – 1.30 (m, 7H); **¹³C NMR (126 MHz, CDCl₃)** δ = 149.3, 145.9, 129.3, 127.7, 123.1, 120.9, 83.8, 60.6, 36.4, 32.2, 31.0, 27.7, 24.4; **HRMS** (EI⁺) [C₁₃H₁₆O] requires M 188.1201, found 188.1204.

6,7,8,9,10,10a-Hexahydrobenzo[3,4]cyclobuta[1,2][8]annulen-4b(5H)-ol (67)

Prepared according to General Procedure F using 2,2,6,6-tetramethylpiperidine (4.21 mL, 25.0 mmol), *n*-butyllithium (11.9 mL, 2.1 M in hexanes, 25.0 mmol), cyclooctanone (1.26 g, 10.0 mmol) and iodobenzene (1.12 mL, 10.0 mmol). The crude residue was purified by flash column chromatography (5→10 % EtOAc/Petrol, silica gel) to afford **67** (1.19 g, 59%) as a colourless liquid.

R_f = 0.72 (15% EtOAc/Petrol); **FTIR** (ν_{max} cm⁻¹, thin film) 3397 (br), 2926, 2855, 1462, 1445, 1217, 1184, 1115, 1034, 993, 756, 731; **¹H NMR (500 MHz, CDCl₃)** δ = 7.30 – 7.20 (m, 2H), 7.18 – 7.12 (m, 2H), 3.16 (dd, *J* = 12.0, 1.5 Hz, 1H), 2.23 (s, 1H), 2.18 – 2.11 (m, 1H), 2.06 – 1.95 (m, 1H), 1.91 – 1.48 (m, 9H), 1.34 – 1.24 (m, 1H); **¹³C NMR (126 MHz, CDCl₃)** δ = 150.1, 146.3, 129.4, 127.8, 122.8, 120.4, 81.8, 59.9, 33.2, 29.3, 28.2, 26.1, 25.7, 25.1; **HRMS** (EI⁺) [C₁₄H₁₈O] requires [M] 202.1358, found 202.1359.

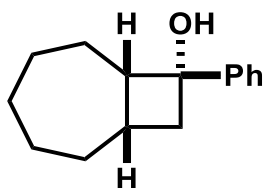
Bicyclo[5.2.0]nonan-8-one (74)

Following a literature procedure:⁶⁶ To a solution of cycloheptene (2.33 mL, 20.0 mmol) in hexane (60 mL) was added dichloroacetyl chloride (2.89 mL, 30.0 mmol) and the resulting mixture was heated at reflux for 20 minutes, followed by slow addition of a solution of triethylamine (4.21 mL, 30.2 mmol) in hexane (30 mL). The reaction mixture was stirred at reflux overnight. Upon cooling, the formed precipitate was removed by filtration and the resultant filtrate was washed with sat. NaHCO₃ (2 × 100 mL).

The organic layer was dried (MgSO_4), filtered and the hexane was removed under vacuum to give a yellow oil.

The material from the previous step was taken up in MeOH (140 mL) and stirred at 0 °C. Zinc powder (14.4 g, 220 mmol) was added, followed by NH_4Cl (7.90 g, 148 mmol) and the reaction mixture was allowed to stir at rt overnight. The unreacted zinc was removed by filtration and the filtrate was concentrated *in vacuo*. The residue was taken up in Et_2O (100 mL) and washed with sat. NaHCO_3 (2×100 mL). The combined aqueous layers were extracted with Et_2O (2×100 mL). The combined organic layers were dried (MgSO_4), filtered and concentrated under reduced pressure. The crude residue was purified by flash column chromatography (2% Et_2O /Pentane, silica gel) afforded **62** (1.10 g, 40% over 2 steps) as a yellow oil which was used in the next step without further purification.

8-Phenylbicyclo[5.2.0]nonan-8-ol (**75**)



To a solution of **S33** (346 mg, 2.50 mmol) in dry THF (10 mL) at -78 °C was added phenyllithium (1.97 mL, 1.9 M in dibutyl ether, 3.25 mmol) dropwise and the reaction mixture was stirred for 5 h, gradually warming to rt. The reaction was quenched by the addition of sat. NH_4Cl (15 mL) and the aqueous layer was extracted with EtOAc (2×15 mL). The combined organic layers were dried (MgSO_4), filtered and concentrated *in vacuo*. The crude residue was purified by flash column chromatography (5→10% EtOAc /Petrol, silica gel) to afford **75** (280 mg, 53%) as a colourless oil.

R_f = 0.41 (10% EtOAc /Petrol); **FTIR** (ν_{max} cm^{-1} , thin film) 3435 (br), 2922, 2847, 1445, 1223, 1132, 1049, 762, 696; **^1H NMR (500 MHz, CDCl_3)** δ = 7.50 – 7.47 (m, 2H), 7.38 – 7.34 (m, 2H), 7.28 – 7.24 (m, 1H), 2.79 – 2.70 (m, 2H), 2.33 – 2.22 (m, 1H), 2.02 – 1.75 (m, 8H), 1.65 – 1.55 (m, 1H), 1.32 – 1.02 (m, 3H); **^{13}C NMR (126 MHz, CDCl_3)** δ = 148.2, 128.5, 127.1, 124.8, 74.3, 50.5, 41.6, 34.2, 32.3, 32.3, 29.8, 29.4, 25.5; **HRMS** (ES^+) [$\text{C}_{15}\text{H}_{20}\text{O}$] requires [M-OH] 199.1487, found 199.1480.

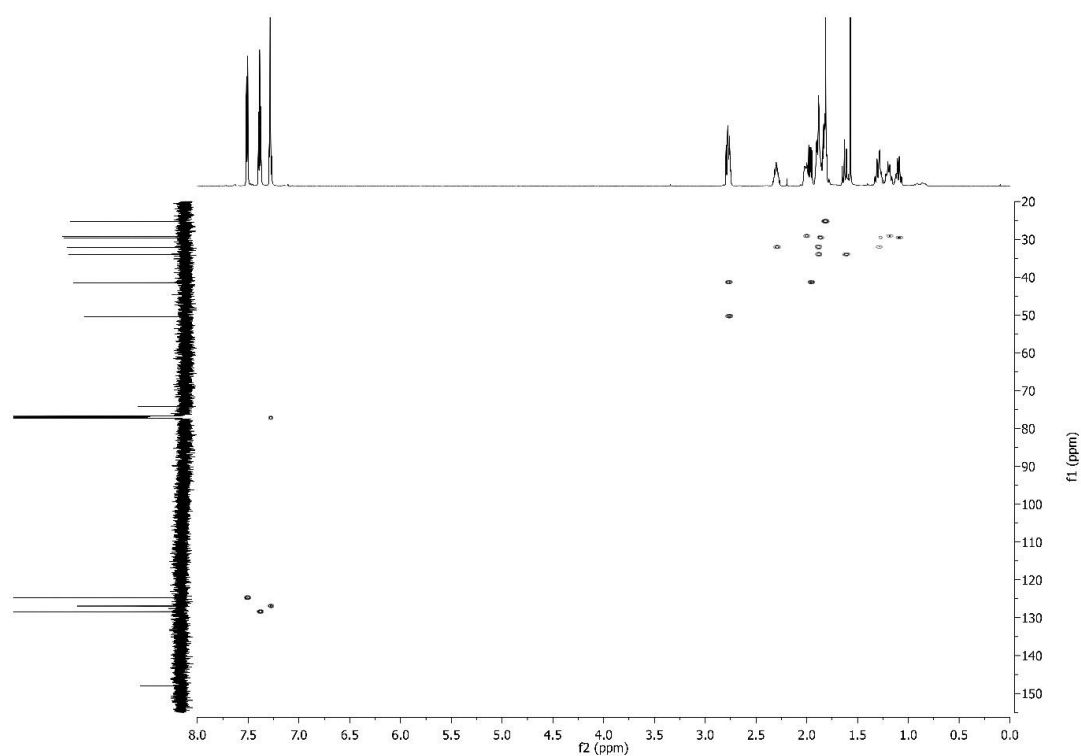


Figure 3 – HSQC spectrum of 63

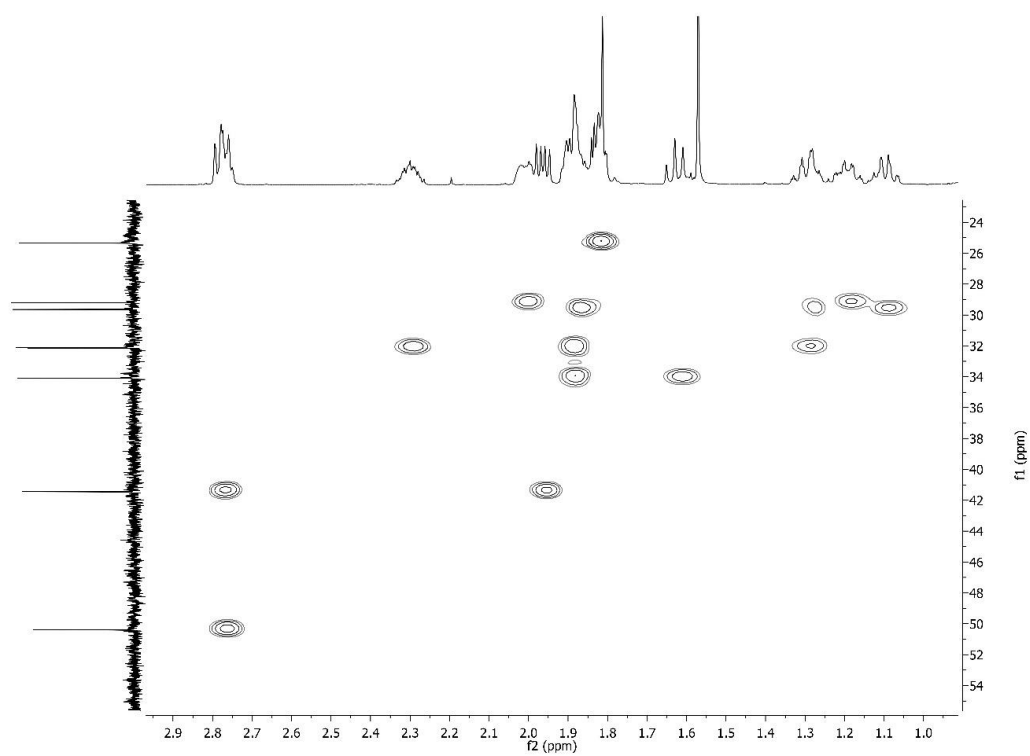


Figure 4 - Figure 5 – HSQC spectrum expansion of 63

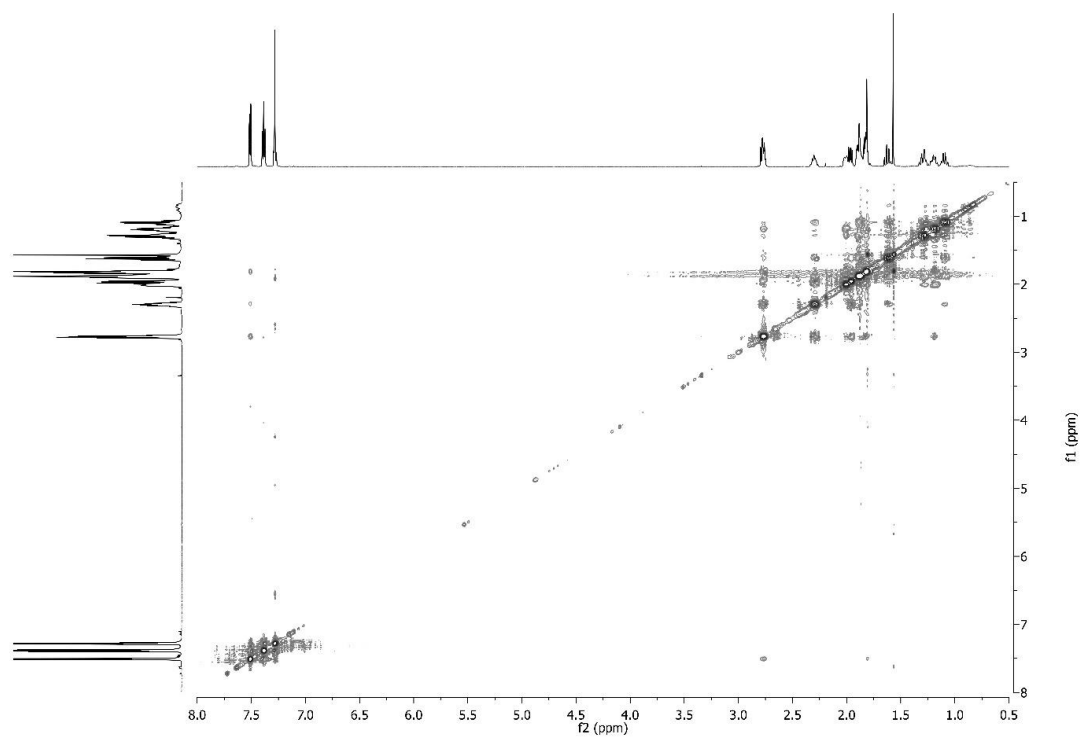


Figure 6 – nOesy spectrum of 64

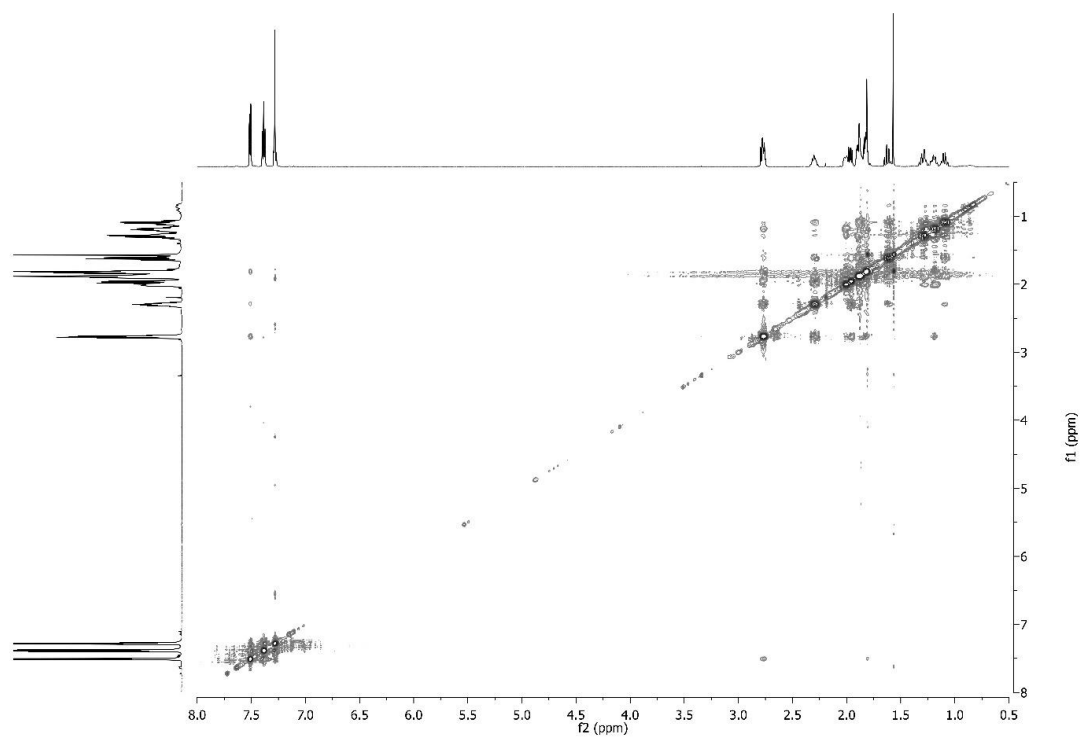


Figure 7 – nOesy spectrum expansion of 64

5.3. General Procedures – Electrochemical Deconstructive-Chlorination of Cycloalkanols

5.3.1. General Procedure G – Standard Procedure

To an oven-dried 10 mL ElectraSyn vial equipped with a magnetic stirrer bar, was added substrate (0.30 mmol), Mn(OTf)₂ (11 mg, 0.03 mmol), MgCl₂ (143 mg, 1.50 mmol) and LiClO₄ (64 mg, 0.60 mmol). The threaded glass was wrapped with PTFE tape and connected to the ElectraSyn cap, which was fitted with a graphite anode and a graphite cathode. The vial was purged with N₂ gas *via* evacuate-refill cycles (\times 3). MeCN (5.25 mL) was added, followed by AcOH (0.75 mL) and the mixture was stirred for a minute to ensure solvation of the MgCl₂. The mixture was then purged *via* bubbling with N₂ gas for 10 minutes. During this time, the vial was connected to an ElectraSyn GoGo module and submerged in a 25 °C water bath mounted on a magnetic stirrer. Electrolysis at 10 mA was conducted for 3 h under N₂ with continuous stirring. After electrolysis was complete, the reaction mixture was left to stir at 25 °C for an additional 30 minutes. The crude reaction mixture was diluted with Et₂O (10 mL) and washed with sat. NaHCO₃ (2 \times 15 mL). The aqueous layer was extracted with Et₂O (3 \times 10 mL) and the combined extracts were dried (MgSO₄), filtered and concentrated under reduced pressure. The crude residue was purified by flash column chromatography on silica gel to afford the pure product. ***N.B.***: If the substrate is an oil, it is weighed directly into the ElectraSyn vial before addition of solid reactants.

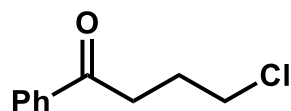
5.3.2. General Procedure H – Syringe Pump Addition of Substrate

To an oven-dried 10 mL ElectraSyn vial equipped with a magnetic stirrer bar, was added Mn(OTf)₂ (11 mg, 0.03 mmol), MgCl₂ (143 mg, 1.50 mmol) and TBAOAc (181 mg, 0.60 mmol). The threaded glass was wrapped with PTFE tape and connected to the ElectraSyn cap, which was fitted with a graphite anode and a graphite cathode. The vial was purged with N₂ gas *via* evacuate-refill cycles (× 3). MeCN (3.25 mL) was added, followed by AcOH (0.75 mL) and the mixture was stirred for one minute to ensure solvation of the MgCl₂.

The mixture was then purged *via* bubbling with N₂ gas for 10 minutes. During this time, the vial was connected to an ElectraSyn GoGo module and submerged in a 25 °C water bath mounted on a magnetic stirrer. In a separate 5 mL vial, substrate (0.30 mmol) and MeCN (2 mL) was added, and the mixture was purged *via* bubbling with N₂ gas for 2 minutes before it was transferred into a 3 mL disposable syringe and connected to a syringe pump. Electrolysis at 10 mA was conducted for 3 h under N₂ with continuous stirring, while syringe pump addition of the tertiary alcohol solution in MeCN (1 mL/h) was started after 2 minutes of electrolysis. After electrolysis was complete, the reaction mixture was left to stir at 25 °C for an additional 30 minutes. The crude reaction mixture was diluted with Et₂O (10 mL) and washed with sat. aq. NaHCO₃ (2 × 15 mL). The aqueous layer was further extracted with Et₂O (3 × 10 mL) and the combined organic extracts were dried (MgSO₄), filtered and concentrated under reduced pressure. The crude residue was purified by flash column chromatography on silica gel to afford the pure product.

5.4. Characterization of Products

4-Chloro-1-phenylbutan-1-one (28)

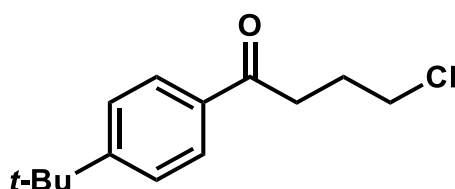


Prepared following General Procedure G using **26** (44 mg). The crude residue was purified by flash column chromatography (5% EtOAc/Petrol, silica gel) to afford **28** (43 mg, 78%) as a colourless oil.

R_f = 0.30 (5% EtOAc/Petrol); ^1H NMR (500 MHz, CDCl_3) δ = 8.01 – 7.95 (m, 2H, (ArH (2,6)), 7.60 – 7.55 (m, 1H (ArH (4))), 7.50 – 7.45 (m, 2H (ArH (3,5))), 3.68 (t, J = 6.0 Hz, 2H, (CH_2 (Cl))), 3.19 (t, J = 7.0 Hz, 2H, (CH_2 (C=O))), 2.27 – 2.20 (m, 2H, (CH_2)); ^{13}C NMR (126 MHz, CDCl_3) δ = 199.1 (C=O), 136.9 (ArC (C=O)), 133.4 (ArC (4)), 128.8 (ArC (2,6)), 128.2 (ArC (3,5)), 44.8 (CH_2 (Cl)), 35.4 (CH_2 (C=O)), 26.9 (CH_2).

These data are consistent with those previously reported in the literature.⁶⁷

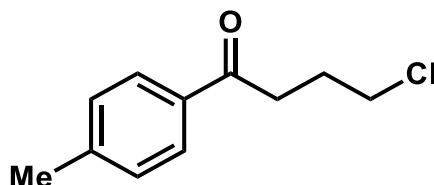
1-(4-(tert-butyl)phenyl)-4-chlorobutan-1-one (30)



Prepared following General Procedure H using **29** (61 mg). The crude residue was purified by flash column chromatography (5% Et₂O/Pentane, silica gel) to afford **30** (57 mg, 80%) as a colourless oil.

R_f = 0.87 (15% EtOAc/Petrol); ^1H NMR (500 MHz, CDCl_3) δ = 7.94 – 7.90 (m, 2H), 7.50 – 7.46 (m, 2H), 3.68 (t, J = 6.0 Hz, 2H), 3.16 (t, J = 7.0 Hz, 2H), 2.26 – 2.20 (m, 1H), 1.35 (s, 9H); ^{13}C NMR (126 MHz, CDCl_3) δ = 198.8, 157.1, 134.4, 128.2, 125.7, 44.9, 35.3, 35.3, 31.1, 26.8.

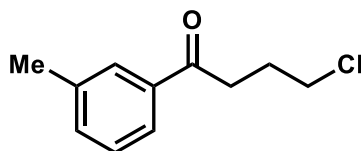
These data are consistent with those previously reported in the literature.⁶⁸

4-Chloro-1-(*p*-tolyl)butan-1-one (47)

Prepared following General Procedure H using **32** (49 mg). The crude residue was purified by flash column chromatography (6% Et₂O/Pentane, silica gel) to afford **47** (45 mg, 76%) as a white solid.

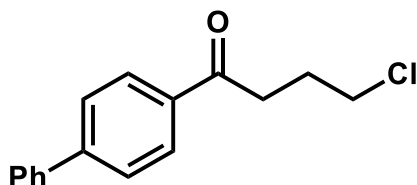
R_f = 0.75 (15% EtOAc/Petrol); **M.p.**: 28-31 °C; **¹H NMR (500 MHz, CDCl₃)** δ = 7.90 – 7.85 (m, 2H), 7.29 – 7.24 (m, 2H), 3.68 (t, *J* = 6.5 Hz, 2H), 3.15 (t, *J* = 7.0 Hz, 2H), 2.42 (s, 3H), 2.25 – 2.19 (m, 2H); **¹³C NMR (126 MHz, CDCl₃)** δ = 198.7, 144.2, 134.4, 129.5, 128.3, 44.9, 35.3, 27.0, 21.8.

These data are consistent with those previously reported in the literature.⁶⁹

4-chloro-1-(*m*-tolyl)butan-1-one (48)

Prepared following General Procedure G using **33** (48 mg). The crude residue was purified by flash column chromatography (5% Et₂O/Pentane, silica gel) to afford **48** (26 mg, 44%) as a colourless oil.

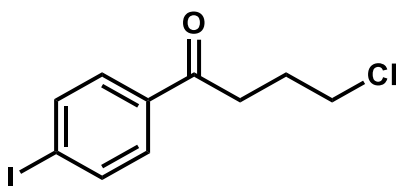
R_f = 0.78 (15% EtOAc/Petrol); **FTIR** (ν_{max} cm⁻¹, thin film) 2358, 1681, 1558, 1539, 1506, 1460, 738, 692; **¹H NMR (500 MHz, CDCl₃)** δ = 7.80 – 7.75 (m, 2H), 7.41 – 7.33 (m, 2H), 3.68 (t, *J* = 6.0 Hz, 2H), 3.17 (t, *J* = 7.0 Hz, 2H), 2.42 (s, 3H), 2.26 – 2.20 (m, 2H); **¹³C NMR (126 MHz, CDCl₃)** δ = 199.1, 138.4, 136.7, 133.9, 128.5, 128.5, 125.2, 44.7, 35.3, 26.7, 21.3; **HRMS** (EI⁺) [C₁₁H₁₄ClO] requires [M+H] 197.0733, found 197.0727.

1-([1,1'-Biphenyl]-4-yl)-4-chlorobutan-1-one (49)

Prepared following General Procedure H using **34** (67 mg). The crude residue was purified by flash column chromatography (8% EtOAc/Petrol, silica gel) to afford **49** (32 mg, 41%) as a white solid.

R_f = 0.82 (15% EtOAc/Petrol); **M.p.**: 120-122 °C (lit.^[18] 119-121 °C); **¹H NMR (500 MHz, CDCl₃)** δ = 8.09 – 8.03 (m, 2H), 7.74 – 7.67 (m, 2H), 7.66 – 7.60 (m, 2H), 7.51 – 7.45 (m, 2H), 7.43 – 7.39 (m, 1H), 3.70 (t, *J* = 6.0 Hz, 2H), 3.22 (t, *J* = 7.0 Hz, 2H), 2.31 – 2.22 (m, 2H); **¹³C NMR (126 MHz, CDCl₃)** δ = 198.7, 146.0, 139.9, 135.6, 129.1, 128.8, 128.4, 127.4, 127.4, 44.9, 35.5, 26.9.

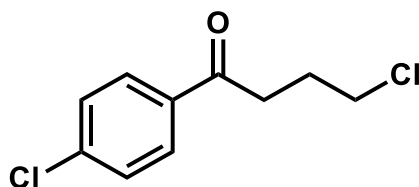
These data are consistent with those previously reported in the literature.⁶⁷

4-Chloro-1-(4-iodophenyl)butan-1-one (50)

Prepared following General Procedure G using **35** (82 mg) and tetra-*n*-butylammonium acetate (181 mg, 0.60 mmol) instead of LiClO₄. The crude residue was purified by flash column chromatography (5% Et₂O/Hexane, silica gel) to afford **50** (58 mg, 62%) as an amorphous white solid.

R_f = 0.69 (15% EtOAc/Petrol); **FTIR** (ν_{max} cm⁻¹, thin film) 2926, 2899, 1685, 1577, 1560, 1481, 1452, 1388, 1354, 1300, 1215, 1178, 1149, 1056, 1001, 983; **¹H NMR (500 MHz, CDCl₃)** δ = 7.88 – 7.80 (m, 2H), 7.72 – 7.63 (m, 2H), 3.67 (t, J = 6.0 Hz, 2H), 3.13 (t, J = 7.0 Hz, 2H), 2.27 – 2.18 (m, 2H); **¹³C NMR (101 MHz, CDCl₃)** δ 198.4, 138.1, 136.1, 129.5, 101.3, 44.7, 35.3, 26.7; **HRMS** (EI⁺) [C₁₀H₁₀ClO] requires [M+H] 308.9543, found 308.9538.

4-Chloro-1-(4-chlorophenyl)butan-1-one (51)

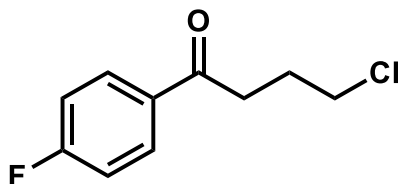


Prepared following General Procedure G using **36** (55 mg). The crude residue was purified by flash column chromatography (5% Et₂O/Pentane, silica gel) to afford **51** (59 mg, 90%) as a colourless oil.

R_f = 0.75 (15% EtOAc/Petrol); **¹H NMR (400 MHz, CDCl₃)** δ = 7.96 – 7.88 (m, 2H), 7.48 – 7.41 (m, 2H), 3.73 – 3.61 (m, 2H), 3.15 (t, J = 7.0 Hz, 2H), 2.27 – 2.17 (m, 2H); **¹³C NMR (101 MHz, CDCl₃)** δ = 197.8, 139.8, 135.2, 129.6, 129.1, 44.7, 35.4, 26.8.

These data are in agreement with those previously reported in the literature.⁶⁷

4-Chloro-1-(4-fluorophenyl)butan-1-one (52)

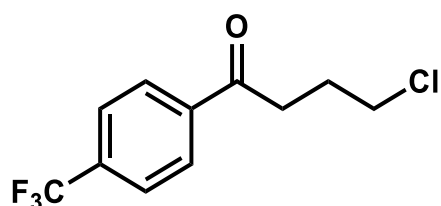


Prepared following General Procedure H using **37** (50 mg). The crude residue was purified by flash column chromatography (5% EtOAc/Petrol, silica gel) to afford **52** (51 mg, 84%) as a colourless oil.

R_f = 0.32 (5% EtOAc/Petrol); ^1H NMR (500 MHz, CDCl_3) δ = 8.04 – 7.98 (m, 2H), 7.17 – 7.11 (m, 2H), 3.68 (t, J = 6.0 Hz, 2H), 3.16 (t, J = 7.0 Hz, 2H), 2.26 – 2.20 (m, 2H); ^{13}C NMR (126 MHz, CDCl_3) δ = 197.5, 166.0 (d, J = 255.0 Hz), 133.3 (d, J = 3.0 Hz), 130.80 (d, J = 9.5 Hz), 115.90 (d, J = 22.0 Hz), 44.8, 35.3, 26.8; ^{19}F NMR (471 MHz, CDCl_3) δ = -105.00.

These data are in agreement with those previously reported in the literature.⁸

4-Chloro-1-(4-(trifluoromethyl)phenyl)butan-1-one (53)

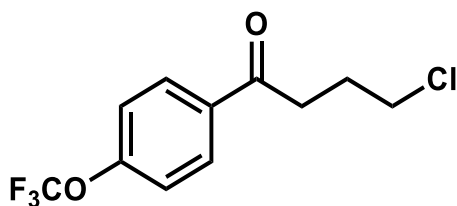


Prepared following General Procedure G using **38** (65 mg). The crude residue was purified by flash column chromatography (5% Et₂O/Pentane, silica gel) to afford **53** (49 mg, 67%) as a colourless oil.

R_f = 0.71 (15% EtOAc/Petrol); ^1H NMR (500 MHz, CDCl_3) δ = 8.09 – 8.07 (m, 2H), 7.77 – 7.71 (m, 2H), 3.69 (t, J = 6.0 Hz, 2H), 3.20 (t, J = 7.0 Hz, 2H), 2.28 – 2.22 (m, 2H); ^{13}C NMR (126 MHz, CDCl_3) δ = 198.1, 139.5 (q, J = 1.0 Hz), 134.7 (q, J = 32.5 Hz), 128.5, 125.9 (q, J = 3.5 Hz), 123.7 (q, J = 272.5 Hz), 44.4, 35.6, 26.5; ^{19}F NMR (471 MHz, CDCl_3) δ = -63.1.

These data are in agreement with those previously reported in the literature.^[15]

4-Chloro-1-(4-(trifluoromethoxy)phenyl)butan-1-one (54)

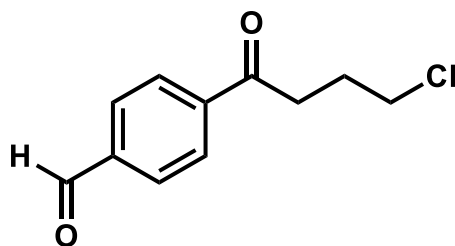


Prepared following General Procedure G using **39** (70 mg). The crude residue was purified by flash column chromatography (5% Et₂O/Pentane, silica gel) to afford **54** (49 mg, 61%) as a colourless oil.

R_f = 0.78 (15% EtOAc/Petrol); **¹H NMR (500 MHz, CDCl₃)** δ = 8.07 – 8.00 (m, 2H), 7.33 – 7.27 (m, 2H), 3.68 (t, *J* = 6.0 Hz, 2H), 3.18 (t, *J* = 7.0 Hz, 2H), 2.29 – 2.19 (m, 2H); **¹³C NMR (126 MHz, CDCl₃)** δ = 197.5, 152.9 (q, *J* = 1.5 Hz), 135.1, 130.2, 120.6, 120.4 (q, *J* = 259.0 Hz), 44.7, 35.4, 26.8; **¹⁹F NMR (376 MHz, CDCl₃)** δ -57.6.

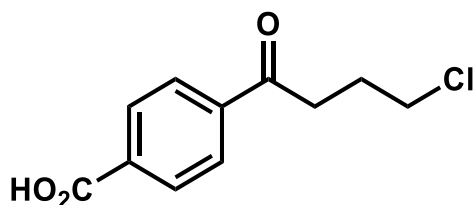
These data are consistent with those previously reported in the literature.⁷⁰

4-(4-Chlorobutanoyl)benzaldehyde (**55**)



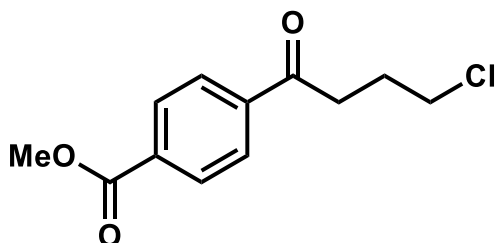
Prepared following General Procedure G using **40** (53 mg). The crude residue was purified by flash column chromatography (15% EtOAc/Hexane, silica gel) to afford **55** (22 mg, 35%) as a colourless liquid.

R_f = 0.36 (15% EtOAc/Petrol); **FTIR** (ν_{max} cm⁻¹, thin film) 2938, 2843, 1705, 1688, 1572, 1499, 1387, 1227, 1200, 997, 835; **¹H NMR (500 MHz, CDCl₃)** δ = 10.12 (s, 1H), 8.15 – 8.10 (m, 2H), 8.02 – 7.97 (m, 2H), 3.70 (t, *J* = 6.0 Hz, 2H), 3.23 (t, *J* = 7.0 Hz, 2H), 2.30 – 2.22 (m, 2H); **¹³C NMR (126 MHz, CDCl₃)** δ = 198.5, 191.7, 141.0, 139.3, 130.0, 128.7, 44.6, 35.9, 26.7; **HRMS** (EI⁺) [C₁₁H₁₁O₂Cl] requires [*M*] 210.0448, found 210.0446.

4-(4-Chlorobutanoyl)benzoic acid (56)

Prepared following General Procedure G using **41** (58 mg). For this example, the reaction mixture was washed with distilled water instead of sat. NaHCO₃. The crude residue was purified by flash column chromatography (70% EtOAc/Petrol, silica gel) to afford **56** (30 mg, 47%) as a white solid.

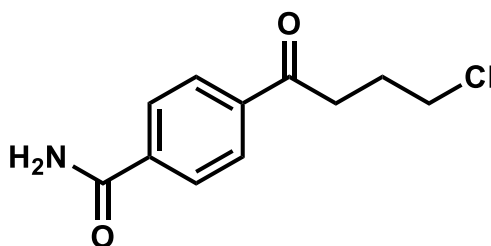
R_f = 0.29 (50% EtOAc); **M.p.:** 137-139 °C; **FTIR** (ν_{max} cm⁻¹, thin film) 2888, 2865, 1699, 1676, 1574, 1431, 1412, 1290, 1223, 934, 772, 735; **¹H NMR (500 MHz, CDCl₃)** δ = 8.24 – 8.19 (m, 2H), 8.10 – 8.04 (m, 2H), 3.70 (t, J = 6.0 Hz, 2H), 3.23 (t, J = 7.0 Hz, 2H), 2.30 – 2.21 (m, 2H); **¹³C NMR (126 MHz, CDCl₃)** δ = 198.58, 170.5, 140.7, 133.1, 130.7, 128.2, 44.6, 35.9, 26.7; **HRMS** (EI⁺) [C₁₁H₁₁ClO₃] requires [M+H] 225.0323, found 225.0318.

Methyl 4-(4-chlorobutanoyl)benzoate (57)

Prepared following General Procedure G using **42** (62 mg). The crude residue was purified by flash column chromatography (10% Et₂O/Pentane, silica gel) to afford **57** (41 mg, 57%) as a colourless oil.

R_f = 0.36 (10% EtOAc/Petrol); **FTIR** (ν_{max} cm⁻¹, thin film) 2949, 1726, 1688, 1506, 1435, 1410, 1278, 1221, 1107, 758, 694; **¹H NMR (500 MHz, CDCl₃)** δ = 8.16 – 8.11 (m, 2H), 8.05 – 8.00 (m, 2H), 3.95 (s, 3H), 3.69 (t, J = 6.0 Hz, 2H), 3.22 (t, J = 7.0 Hz, 2H), 2.29 – 2.20 (m, 2H); **¹³C NMR (126 MHz, CDCl₃)** δ = 198.6, 166.3, 140.0, 134.2, 130.0, 128.0, 52.6, 44.7, 35.8, 26.7; **HRMS** (EI⁺) [C₁₂H₁₃ClO₃] requires [M+H] 241.0628, found 241.0631.

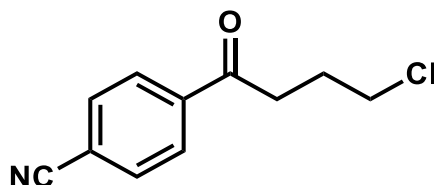
4-(4-Chlorobutanoyl)benzamide (**58**)



Prepared following General Procedure G using **43** (57 mg). The crude residue was purified by flash column chromatography (80% EtOAc/Petrol, silica gel) to afford **58** (41 mg, 61%) as a white solid.

R_f = 0.60 (100% EtOAc/Hexanes); **M.p.:** 173-175 °C; **FTIR** (ν_{max} cm⁻¹, thin film) 3408 (br), 3157 (br), 1674, 1653, 1618, 1562, 1506, 1411, 1379, 1224, 1188, 1143, 1112, 997, 777; **¹H NMR (400 MHz, DMSO)** δ = 8.14 (s, 1H), 8.07 – 7.94 (m, 4H), 7.57 (s, 1H), 3.72 (t, J = 6.5 Hz, 2H), 3.22 (t, J = 7.0 Hz, 2H), 2.16 – 2.01 (m, 2H); **¹³C NMR (101 MHz, DMSO)** δ = 198.8, 167.1, 138.3, 138.1, 127.8, 127.8, 44.8, 35.5, 26.8; **HRMS** (EI⁺) [C₁₁H₁₂ClNO₂] requires [M+H] 226.0638, found 226.0635.

4-(4-Chlorobutanoyl)benzonitrile (59)

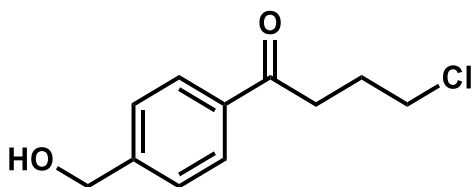


Prepared following General Procedure G using **44** (52 mg). The crude residue was purified by flash column chromatography (5% Et₂O/Pentane, silica gel) to afford **59** (25 mg, 40%) as a white solid.

R_f = 0.27 (10% EtOAc/Petrol); **M.p.:** 84-86 °C; **FTIR** (ν_{max} cm⁻¹, thin film) 3090, 2965, 2934, 2236, 1688, 1603, 1404, 1315, 1229, 997, 853, 779, 646, 577; **¹H NMR (500 MHz, CDCl₃)** δ = 8.09 – 8.04 (m, 2H), 7.81 – 7.75 (m, 2H), 3.69 (t, *J* = 6.5 Hz, 2H), 3.20 (t, *J* = 7.0 Hz, 2H), 2.25 – 2.22 (m, 2H); **¹³C NMR (126 MHz, CDCl₃)** δ = 197.6, 139.6, 132.6,

128.4, 117.9, 116.5, 44.3, 35.6, 26.4; **HRMS** (EI⁺) [C₁₁H₁₀ClNO] requires [M+H] 208.0529, found 208.0535.

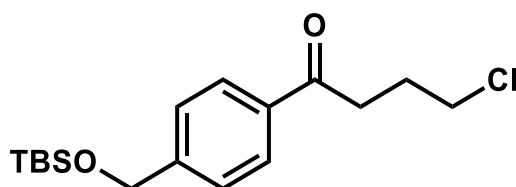
4-Chloro-1-(4-(hydroxymethyl)phenyl)butan-1-one (60)



Prepared following General Procedure H using **45** (54 mg). The crude residue was purified by flash column chromatography (50% EtOAc/Petrol, silica gel) to afford **60** (37 mg, 58%) as a colourless oil.

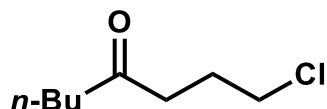
R_f = 0.48 (50% EtOAc/Petrol); **FTIR** (ν_{max} cm⁻¹, thin film) = 3415 (br), 2929, 2858, 1705, 1606, 1570, 1413, 1319, 1228, 1045, 810, 779, 648, 569; **¹H NMR (500 MHz, CDCl₃)** δ = 7.99 – 7.94 (m, 2H), 7.50 – 7.42 (m, 2H), 4.78 (s, 2H), 3.68 (t, J = 6.0 Hz, 2H), 3.18 (t, J = 7.0 Hz, 2H), 2.28 – 2.19 (m, 2H), 1.85 (s, 1H); **¹³C NMR (126 MHz, CDCl₃)** δ = 198.8, 146.4, 136.1, 128.5, 126.8, 64.8, 44.8, 35.5, 26.9; **HRMS** (EI⁺) [C₁₁H₁₃O₂Cl] requires [M+H] 213.0682, found 213.0687.

1-(4-(((*Tert*-butyldimethylsilyl)oxy)methyl)phenyl)-4-chlorobutan-1-one (61)



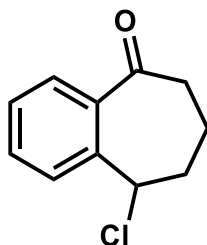
Prepared following General Procedure H using **46** (88 mg). The crude residue was purified by flash column chromatography (5% Et₂O/Pentane, silica gel) to afford **61** (46 mg, 47%) as a colourless oil.

R_f = 0.15 (10% EtOAc/Petrol); **FTIR** (ν_{max} cm⁻¹, thin film) 2930, 1688, 1607, 1410, 1227, 1047, 810; **¹H NMR (500 MHz, CDCl₃)** δ = 7.98 – 7.93 (m, 2H), 7.45 – 7.39 (m, 2H), 4.80 (s, 2H), 3.68 (t, J = 6.0 Hz, 2H), 3.18 (t, J = 7.0 Hz, 2H), 2.29 – 2.18 (m, 2H), 0.95 (s, 9H), 0.11 (s, 6H); **¹³C NMR (126 MHz, CDCl₃)** δ = 198.8, 147.3, 135.7, 128.3, 126.1, 64.6, 44.9, 35.4, 27.0, 26.1, 18.5, -5.2; **HRMS** (EI⁺) [C₁₇H₂₇ClO₂Si] requires [M+H] 327.1547, found 327.1543.

1-Chlorooctan-4-one (63)

Prepared following General Procedure G using **62** (38 mg). The crude residue was purified by flash column chromatography (4% Et₂O/Pentane, silica gel) to afford **63** (29 mg, 60%) as a colourless oil.

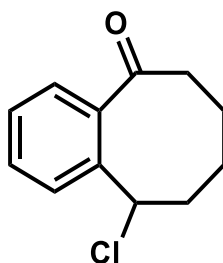
R_f = 0.60 (10% EtOAc/Petrol); **FTIR** (ν_{max} cm⁻¹, thin film) 2972, 2895, 1714, 1384, 1251, 1157, 958; **¹H NMR (500 MHz, CDCl₃)** δ = 3.58 (t, *J* = 6.0 Hz, 2H), 2.61 (t, *J* = 7.0 Hz, 2H), 2.42 (t, *J* = 7.5 Hz, 2H), 2.09 – 2.00 (m, 2H), 1.61 – 1.54 (m, 2H), 1.37 – 1.27 (m, 2H), 0.91 (t, *J* = 7.5 Hz, 3H); **¹³C NMR (126 MHz, CDCl₃)** δ = 210.2, 44.7, 42.9, 39.4, 26.4, 26.1, 22.5, 13.9; **HRMS** (EI⁺) [C₈H₁₅OCl] requires [*M*] 162.0811, found 162.0807.

9-Chloro-6,7,8,9-tetrahydro-5H-benzo[7]annulen-5-one (68)

Prepared following General Procedure G using **64** (48 mg). The crude residue was purified by flash column chromatography (5% Et₂O/Pentane, silica gel) to afford **68** (32 mg, 54%) as a colourless oil.

R_f = 0.47 (10% EtOAc/Petrol); **¹H NMR (500 MHz, CDCl₃)** δ = 7.64 – 7.58 (m, 1H), 7.52 – 7.36 (m, 3H), 5.40 – 5.35 (m, 1H), 3.17 – 3.07 (m, 1H), 2.76 – 2.66 (m, 1H), 2.45 – 2.31 (m, 2H), 2.22 – 2.10 (m, 1H), 2.02 – 1.91 (m, 1H); **¹³C NMR (126 MHz, CDCl₃)** δ = 205.5, 139.1, 139.1, 132.0, 129.0, 129.0, 128.8, 62.1, 41.9, 34.6, 20.3.

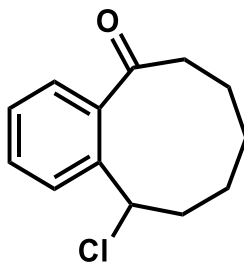
These data are consistent with those previously reported in the literature.⁶⁹

10-Chloro-7,8,9,10-tetrahydrobenzo[8]annulen-5(6H)-one (69)

Prepared following General Procedure H using **65** (52 mg). The crude residue was purified by flash column chromatography (5% Et₂O/Pentane, silica gel) to afford **69** (26 mg, 42%) as a colourless oil.

R_f = 0.50 (10% EtOAc/Petrol); **¹H NMR (500 MHz, CDCl₃)** δ = 7.68 – 7.62 (m, 1H), 7.48 – 7.41 (m, 1H), 7.38 – 7.31 (m, 1H), 7.21 – 7.16 (m, 1H), 5.29 (dd, *J* = 11.0, 4.0 Hz, 1H), 2.76 – 2.70 (m, 2H), 2.42 – 2.31 (m, 1H), 2.25 – 2.13 (m, 1H), 1.87 – 1.60 (m, 4H); **¹³C NMR (126 MHz, CDCl₃)** δ = 210.2, 139.3, 137.6, 130.3, 129.0, 128.5, 125.8, 60.9, 45.8, 37.0, 25.7, 22.2.

These data are consistent with those previously reported in the literature.⁶⁷

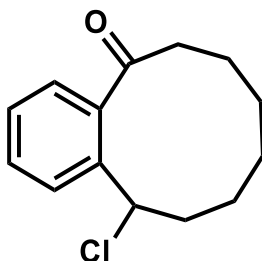
11-chloro-6,7,8,9,10,11-hexahydro-5H-benzo[9]annulen-5-one (70)

Prepared following General Procedure G using **66** (57 mg). The crude residue was purified by flash column chromatography (5% Et₂O/Pentane, silica gel) to afford **70** (35 mg, 53%) as a yellow solid.

R_f = 0.45 (10% EtOAc/Petrol); **M.p.:** 63-65 °C; **¹H NMR (500 MHz, CDCl₃)** δ = 7.67 – 7.61 (m, 1H), 7.49 – 7.42 (m, 1H), 7.38 – 7.31 (m, 1H), 7.20 – 7.14 (m, 1H), 5.24 (dd, *J* = 11.5, 5.0 Hz, 1H), 2.89 (ddd, *J* = 14.5, 8.5, 3.5 Hz, 1H), 2.80 (ddd, *J* = 14.5, 9.0, 4.0 Hz, 1H), 2.24 (dddd, *J* = 14.0, 11.5, 5.0, 4.0 Hz, 1H), 2.09 – 2.00 (m, 1H), 1.97 – 1.85 (m, 1H), 1.81 – 1.69 (m, 1H), 1.69 – 1.49 (m, 2H), 1.49 – 1.37 (m, 1H), 1.17 – 1.05 (m, 1H); **¹³C NMR (126 MHz, CDCl₃)** δ = 210.9, 141.8, 136.7, 130.2, 128.3, 128.1, 124.4, 58.6, 43.5, 40.4, 26.1, 25.4, 24.5.

These data are consistent with those previously reported in the literature.¹⁰

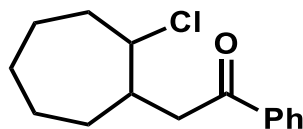
12-chloro-7,8,9,10,11,12-hexahydrobenzo[10]annulen-5(6H)-one (71)



Prepared following General Procedure G using **67** (60 mg). The crude residue was purified by flash column chromatography (5% Et₂O/Pentane, silica gel) to afford **71** (36 mg, 51%) as a white solid.

R_f = 0.52 (10% EtOAc/Petrol); **M.p.:** 85-87 °C; **¹H NMR (500 MHz, CDCl₃)** δ = 7.81 – 7.74 (m, 1H), 7.55 – 7.47 (m, 1H), 7.37 – 7.24 (m, 2H), 5.63 (dd, *J* = 12.0, 5.0 Hz, 1H), 3.25 – 3.15 (m, 1H), 2.58 – 2.45 (m, 1H), 2.18 – 2.07 (m, 1H), 1.90 – 1.67 (m, 3H), 1.56 – 1.14 (m, 5H), 0.62 – 0.49 (m, 1H); **¹³C NMR (126 MHz, CDCl₃)** δ = 210.1, 139.6, 138.9, 131.3, 128.6, 127.5, 125.1, 55.8, 44.2, 40.9, 28.0, 22.8, 22.3, 21.8.

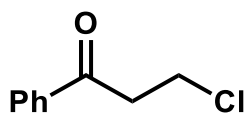
These data are consistent with those previously reported in the literature.⁶⁷

2-(2-Chlorocycloheptyl)-1-phenylethan-1-one (76)

Prepared following General Procedure H using **75** (65 mg). The crude residue was purified by flash column chromatography (4% Et₂O/Pentane, silica gel) to afford **76** (58 mg, 77%) as a colourless oil. The compound was obtained as a 1:1 inseparable mixture of diastereoisomers.

R_f = 0.56 (10% EtOAc/Petrol); **FTIR** (ν_{max} cm⁻¹, thin film) 2929, 2862, 1683, 1598, 1579, 1450, 1361, 1282, 1211, 985, 752, 690; **HRMS** (ES⁺) [C₁₅H₁₉OCl] requires [M+H] 251.1203, found 251.1203.

Data for both diastereoisomers: **¹H NMR (500 MHz, CDCl₃)** δ = 8.03 – 7.94 (m, 4H), 7.60 – 7.53 (m, 2H), 7.50 – 7.44 (m, 4H), 4.52 – 4.41 (m, 1H), 4.07 – 3.96 (m, 1H), 3.47 (dd, J = 16.5, 3.0 Hz, 1H), 3.25 (dd, J = 17.5, 6.5 Hz, 1H), 2.97 (ddd, J = 16.5, 11.0, 8.0 Hz, 2H), 2.69 – 2.58 (m, 1H), 2.54 – 2.42 (m, 1H), 2.21 – 2.00 (m, 4H), 1.86 – 1.31 (m, 16H); **¹³C NMR (126 MHz, CDCl₃)** δ = 199.5, 199.5, 137.3, 137.2, 133.3, 133.2, 128.8, 128.8, 128.3, 128.2, 68.4, 68.3, 45.5, 44.4, 43.8, 40.8, 37.6, 37.2, 30.5, 29.2, 28.6, 27.3, 27.1, 26.2, 23.3, 23.0.

3-Chloro-1-phenylpropan-1-one (77)

Prepared following General Procedure H using **1** (40 mg). For this example, the reaction mixture was washed with distilled water instead of sat. NaHCO₃. The crude residue was purified by flash column chromatography (5% Et₂O/Pentane, silica gel) to afford **77** (27 mg, 54%) as a colourless oil.

R_f = 0.69 (10% EtOAc/Petrol); **¹H NMR (500 MHz, CDCl₃)** δ = 8.00 – 7.93 (m, 2H), 7.63–7.57 (m, 1H), 7.52 – 7.45 (m, 2H), 3.93 (t, *J* = 7.0 Hz, 2H), 3.47 (t, *J* = 7.0 Hz, 2H); **¹³C NMR (126 MHz, CDCl₃)** δ = 196.7, 136.5, 133.7, 128.9, 128.2, 41.4, 38.8.

These data are consistent with those previously reported in the literature.⁷¹

5.5. References

- 1 M. Schmittl and A. Burghart, *ChemInform*, 2010, **29**, 2550–2589.
- 2 K. Uneyama, H. Asai, Y. Dan-Oh and H. Matta, *Electrochim. Acta*, 1997, **42**, 2005–2007.
- 3 S. Torii, K. Uneyama and M. Ono, *Tetrahedron Lett.*, 1980, **21**, 2741–2744.
- 4 Tung Siu, and Christine J. Picard and A. K. Yudin*, *J. Org. Chem.*, 2005, **70**, 932–937.
- 5 A. Guirado, A. Zapata, J. L. Gómez, L. Trabalón and J. Gálvez, *Tetrahedron*, 1999, **55**, 9631–9640.
- 6 L.-J. Li, Y.-Y. Jiang, C. M. Lam, C.-C. Zeng, L.-M. Hu and R. D. Little, *J. Org. Chem.*, 2015, **80**, 11021–11030.
- 7 F. Kakiuchi, T. Kochi, H. Mutsutani, N. Kobayashi, S. Urano, M. Sato, S. Nishiyama and T. Tanabe, *J. Am. Chem. Soc.*, 2009, **131**, 11310–11311.
- 8 J. Yoshida, R. Hayashi and A. Shimizu, *Green Oxid. Org. Synth.*, 2019, 409–437.
- 9 T. Sunaga, M. Atobe, S. Inagi and T. Fuchigami, *Chem. Commun.*, 2009, 956–958.
- 10 F. Bu, L. Lu, X. Hu, S. Wang, H. Zhang and A. Lei, *Chem. Sci.*, 2020, **11**, 10000–10004.
- 11 T. Morofuji, A. Shimizu and J. Yoshida, *J. Am. Chem. Soc.*, 2013, **135**, 5000–5003.
- 12 L. D. Pachón, C. J. Elsevier and G. Rothenberg, *Adv. Synth. Catal.*, 2006, **348**, 1705–1710.
- 13 Y. Yuan and A. Lei, *Acc. Chem. Res.*, 2019, **52**, 3309–3324.
- 14 Y. Gao, Y. Wang, J. Zhou, H. Mei and J. Han, *Green Chem.*, 2018, **20**, 583–587.
- 15 H. Takakura and S. Yamamura, *Tetrahedron Lett.*, 1999, **40**, 299–302.
- 16 C. Zhu, N. W. J. Ang, T. H. Meyer, Y. Qiu and L. Ackermann, *ACS Cent. Sci.*, 2021, **7**, 415–431.
- 17 B. A. Frontana-Urbe, R. D. Little, J. G. Ibanez, A. Palma and R. Vasquez-Medrano, *Green Chem.*, 2010, **12**, 2099–2119.
- 18 M. Yan, Y. Kawamata and P. S. Baran, *Chem. Rev.*, 2017, **117**, 13230–13319.

- 19 V. Alessandro, *Philos. Trans. R. Soc. London*, 1800, **90**, 403–431.
- 20 F. Michael, *Philos. Trans. R. Soc. London*, 1834, **124**, 77–122.
- 21 F. Joschka Holzhäuser, J. B. Mensah and Regina Palkovits, *Green Chem.*, 2020, **22**, 286–301.
- 22 A. Hickling, *Trans. Faraday Soc.*, 1942, **38**, 27–33.
- 23 *Nat.* 1959 1844695, 1959, **184**, 1271–1271.
- 24 J. E. B. Randles, *Trans. Faraday Soc.*, 1948, **44**, 327–338.
- 25 C. Kingston, M. D. Palkowitz, Y. Takahira, J. C. Vantourout, B. K. Peters, Y. Kawamata and P. S. Baran, *Acc. Chem. Res.*, 2019, **53**, 72–83.
- 26 H. Kunkely, A. Merz and A. Vogler, *J. Am. Chem. Soc.*, 2002, **105**, 7241–7243.
- 27 B. Lee, H. Naito, M. Nagao and T. Hibino, *Angew. Chemie Int. Ed.*, 2012, **51**, 6961–6965.
- 28 L. E. Sattler, C. J. Otten and G. Hilt, *Chem. – A Eur. J.*, 2020, **26**, 3129–3136.
- 29 S. Rodrigo, C. Um, J. C. Mixdorf, D. Gunasekera, H. M. Nguyen and L. Luo, *Org. Lett.*, 2020, **22**, 2021.
- 30 L. Schulz, S. R. Waldvogel, L. Schulz and S. R. Waldvogel, , DOI:10.1055/s-0037-1610303.
- 31 T. Shono, *Compr. Org. Synth.*, 1991, 789–813.
- 32 J. M. Friedrich, C. Ponce-de-León, G. W. Reade and F. C. Walsh, *J. Electroanal. Chem.*, 2004, **561**, 203–217.
- 33 T. X. Huong Le, M. Bechelany and M. Cretin, *Carbon N. Y.*, 2017, **122**, 564–591.
- 34 D. M. Heard and A. J. J. Lennox, *Angew. Chemie Int. Ed.*, 2020, **59**, 18866–18884.
- 35 G. Hilt, *ChemElectroChem*, 2020, **7**, 395–405.
- 36 M. Rafiee, M. N. Mayer, B. T. Punchihewa and M. R. Mumau, *J. Org. Chem.*, , DOI:10.1021/ACS.JOC.1C01391.
- 37 R. Francke and R. D. Little, *Chem. Soc. Rev.*, 2014, **43**, 2492–2521.
- 38 J. Simmonet and J. F. Pilard, *organic electrochemistry*, 2001.
- 39 R. Francke and R. D. Little, *Chem. Soc. Rev.*, 2014, **43**, 2492–2521.
- 40 C. C. Zeng, N. T. Zhang, C. M. Lam and R. D. Little, *Org. Lett.*, 2012, **14**, 1314–1317.
- 41 J. A. Miranda, C. J. Wade and R. Daniel Little, , DOI:10.1021/jo051148.
- 42 R. D. Little, *Chem. Rev.*, 2002, **96**, 93–114.
- 43 N. Elgrishi, K. J. Rountree, B. D. McCarthy, E. S. Rountree, T. T. Eisenhart and J. L. Dempsey, *J. Chem. Educ.*, 2017, **95**, 197–206.
- 44 C. Sandford, M. A. Edwards, K. J. Klunder, D. P. Hickey, M. Li, K. Barman, M. S. Sigman, H. S. White and S. D. Minter, *Chem. Sci.*, 2019, **10**, 6404–6422.

- 45 M. M. Baizer, *Pure Appl. Chem.*, 1986, **58**, 889–894.
- 46 B. R. Rosen, E. W. Werner, A. G. O'Brien and P. S. Baran, *J. Am. Chem. Soc.*, 2014, **136**, 5571–5574.
- 47 P. S. B. and J. M. Richter, *J. Am. Chem. Soc.*, 2004, **126**, 7450–7451.
- 48 W. H. Perkin and S. H. Tucker, *J. Chem. Soc. Trans.*, 1921, **119**, 216–225.
- 49 J. F. Ambrose, L. L. Carpenter and R. F. Nelson, *J. Electrochem. Soc.*, 1975, **122**, 876.
- 50 W. E. Geiger†, *Organometallics*, 2007, **26**, 5738–5765.
- 51 P. Gandeepan and L. Ackermann, *Chem*, 2018, **4**, 199–222.
- 52 K. M. Engle, T.-S. Mei, X. Wang and J.-Q. Yu, *Angew. Chemie Int. Ed.*, 2011, **50**, 1478–1491.
- 53 F. Xu, Y.-J. Li, C. Huang and H.-C. Xu, *ACS Catal.*, 2018, **8**, 3820–3824.
- 54 N. Chen and H.-C. Xu, *Green Synth. Catal.*, 2021, **2**, 165–178.
- 55 M. D. Kärkäs, *Chem. Soc. Rev.*, 2018, **47**, 5786–5865.
- 56 M. D. Kärkäs, *ACS Catal.*, 2017, **7**, 4999–5022.
- 57 Z.-W. Hou, Z.-Y. Mao, H.-B. Zhao, Y. Y. Melcamu, X. Lu, J. Song and H.-C. Xu, *Angew. Chemie Int. Ed.*, 2016, **55**, 9168–9172.
- 58 A. Hu, J.-J. Guo, H. Pan, H. Tang, Z. Gao and Z. Zuo, *J. Am. Chem. Soc.*, 2018, **140**, 1612–1616.
- 59 J. J. Guo, A. Hu and Z. Zuo, *Tetrahedron Lett.*, 2018, **59**, 2103–2111.
- 60 J.-F. Zhao, B.-H. Tan and T.-P. Loh, *Chem. Sci.*, 2011, **2**, 349–352.
- 61 H. Zeng, P. Pan, J. Chen, H. Gong and C.-J. Li, *European J. Org. Chem.*, 2017, **2017**, 1070–1073.
- 62 W. J. Leigh and J. A. Postigo, <https://doi.org/10.1139/v95-028>, 2011, **73**, 191–203.
- 63 V. Dhayalan, C. Sämann and P. Knochel, *Chem. Commun.*, 2015, **51**, 3239–3242.
- 64 V. L. van Zyl, A. Muller and D. B. G. Williams, *Tetrahedron Lett.*, 2018, **59**, 918–921.
- 65 Y. Sun, X. Huang, X. Li, F. Luo, L. Zhang, M. Chen, S. Zheng and B. Peng, *Adv. Synth. Catal.*, 2018, **360**, 1082–1087.
- 66 E. Lee-Ruff and D. Wells, <http://dx.doi.org/10.1080/15257770802088886>, 2008, **27**, 484–494.
- 67 L. Huan and C. Zhu, *Org. Chem. Front.*, 2016, **3**, 1467–1471.
- 68 M. S. Gowda, S. S. Pande, R. A. Ramakrishna and K. R. Prabhu, *Org. Biomol. Chem.*, 2011, **9**, 5365–5368.
- 69 W. Schliemann, A. Buege and L. Reppel, *Pharmazie*, 1980, **35**, 140–143.
- 70 R. L. Zhai, Y. S. Xue, T. Liang, J. J. Mi and Z. Xu, *J. Org. Chem.*, 2018, **83**, 10051–10059.

- 71 X. Fan, H. Zhao, J. Yu, X. Bao and C. Zhu, *Org. Chem. Front.*, 2016, **3**, 227–232.
- 72 Y. Wen, G. Chen, S. Huang, Y. Tang, J. Yang and Y. Zhang, *Adv. Synth. Catal.*, 2016, **358**, 947–957.
- 73 K. Jia, F. Zhang, H. Huang and Y. Chen, *J. Am. Chem. Soc.*, 2016, **138**, 1514–1517.
- 74 J. Wang, B. Huang, C. Shi, C. Yang and W. Xia, *J. Org. Chem.*, 2018, **83**, 9696–9706.
- 75 L. Schnaubelt, H. Petzold, E. Dmitrieva, M. Rosenkranz and H. Lang, *Dalt. Trans.*, 2018, **47**, 13180–13189.
- 76 L. Huang, T. Ji and M. Rueping, *J. Am. Chem. Soc.*, 2020, **0**, 3–10.
- 77 P. Thamaraiselvi, E. Varathan, V. Subramanian and S. Easwaramoorthi, *Dye. Pigment.*, 2020, **172**, 107838.
- 78 X. Fan, H. Zhao, J. Yu, X. Bao and C. Zhu, *Org. Chem. Front.*, 2016, **3**, 227–232.
- 79 H. G. Yayla, H. Wang, K. T. Tarantino, H. S. Orbe and R. R. Knowles, *J. Am. Chem. Soc.*, 2016, **138**, 10794–10797.
- 80 J. Wang, Y.-B. Pang, N. Tao, R.-S. Zeng and Y. Zhao, *J. Org. Chem.*, 2019, **84**, 15315–15322.
- 81 X. Wu, M. Wang, L. Huan, D. Wang, J. Wang and C. Zhu, *Angew. Chemie*, 2018, **130**, 1656–1660.
- 82 M. Zhang, X. Ding, A. Lu, J. Kang, Y. Gao, Z. Wang, H. Li and Q. Wang, *Org. Chem. Front.*, 2021, **8**, 961–967.
- 83 J. Barluenga, F. J. Fañanás, R. Sanz, C. Marcos and J. M. Ignacio, , DOI:10.1039/b414966a.

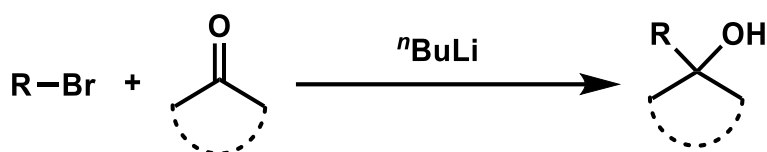
Gradatim Ferociter
(Step-by-step ferociously)

**Chapter 6: Experimental – Electrochemical
Deconstructive Bromination of Cycloalkanols via
Alkoxy Radicals Enabled by Proton Coupled Electron
Transfer (PCET)**

6. Experimental and Characterization Data

6.1. General Procedures – Substrate Synthesis (PCET-Bromination)

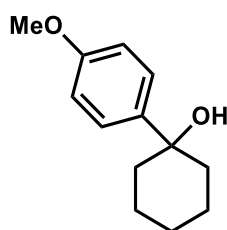
6.1.1. General Procedure A – Generation and Addition of Organolithium Reagents to Cycloalkanones



To a flame-dried RBF fitted with a septum seal was added a solution of alkyl or aryl halide (1.3 eq.) in THF (0.3 M). The mixture was cooled to $-78\text{ }^{\circ}\text{C}$, and a solution of *n*-butyllithium (solution in hexanes, 1.3 eq.) was added dropwise. The solution was left to stir for 1-3 h before adding a solution of the cycloalkanone (1.0 eq.) in THF (1.0 M) dropwise. The reaction mixture was left to stir for 1-3 h, whilst warming to rt. Water was added dropwise, followed by extraction with EtOAc ($\times 3$). The combined organics were dried (MgSO_4), filtered, and concentrated under reduced pressure. The resultant crude material was purified by flash column chromatography to afford the desired compound.

6.2. Characterization of Substrates

1-(4-methoxyphenyl)cyclohexan-1-ol (1)

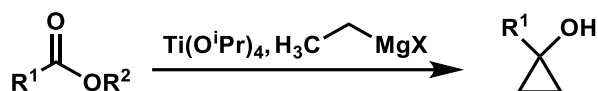


Prepared according to General Procedure A using 1-bromo-4-methoxybenzene (3.75 g, 20.0 mmol, 1.0 eq.), *n*-butyllithium (12.0 mL, 2.5 M in hexanes, 30.0 mmol, 1.5 eq.) and cyclohexanone (2.3 mL, 22.0 mmol, 1.1 eq.). The crude residue was purified by flash column chromatography (5→10% EtOAc/Petrol, silica gel) to afford **1** (3.45 g, 54%) as a white solid.

R_f = 0.15 (10% EtOAc/Petrol); **M.p.**: 37-39 °C; **¹H NMR (500 MHz, CDCl₃)** δ = 7.43 (d, J = 8.8 Hz, 2H, (ArH (2,6))), 6.88 (d, J = 8.9 Hz, 2H, (ArH (3,5))), 3.81 (s, 3H), 1.86 – 1.70 (m, 7H), 1.66 – 1.58 (m, 3H), 1.31 – 1.23 (m, 1H); **¹³C NMR (126 MHz, CDCl₃)** δ = 158.4 (ArC(4)OMe), 141.7 (ArC(1)O), 125.9 (ArC(2,6)H), 113.6 (ArC(3,5)H), 72.8, 55.4 (CH₃O), 39.1, 25.6, 22.4

These data are consistent with those previously reported in the literature.⁷²

1-(4-methoxyphenyl)cyclopropan-1-ol (**9**)

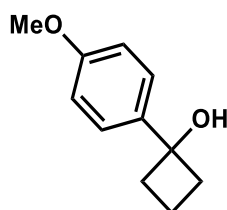


To a flame-dried RBF fitted with a septum seal was added the ester (0.83 g, 5.0 mmol, 1.0 eq.), Ti(O^{*i*}Pr)₄ (2.13 mL, 7.0 mmol, 1.4 eq.), and THF (0.16 M with respect to the ester). The mixture was cooled to 0 °C and a solution of ethylmagnesium bromide (4.65 mL, 14.0 mmol, 2.8 eq.) was added dropwise. After complete addition, the resulting mixture was left to warm to rt and stirred overnight. After completion water was added and the resulting precipitate was filtered under vacuum through celite and washed with EtOAc. The layers of the filtrate were separated, and the aqueous layer was further extracted with EtOAc (× 2). The combined organics were dried (MgSO₄), filtered, and concentrated under reduced pressure. The resultant crude material was purified by flash column chromatography to afford **9** (560 mg, 68%) as a colourless oil.

R_f = 0.17 (10% EtOAc/Petrol); $^1\text{H NMR}$ (500 MHz, CDCl_3) δ = 7.29 – 7.24 (m, 2H, (ArH (2,6))), 6.88 – 6.83 (m, 2H, (ArH (3,5))), 3.81 (s, 3H), 2.43 (s, 1H, OH), 1.21 – 1.16 (m, 2H), 1.0 – 0.94 (m, 2H); $^{13}\text{C NMR}$ (126 MHz, CDCl_3) δ = 158.4 (ArC(4)OMe), 136.4 (ArC(1)O), 125.9 (ArC(2,6)H), 113.6 (ArC(3,5)H), 56.6, 55.4(CH_3O), 16.66

These data are consistent with those previously reported in the literature.⁷³

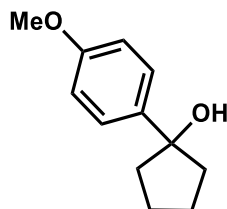
1-(4-methoxyphenyl)cyclobutan-1-ol (**10**)



Prepared according to General Procedure A using 1-bromo-4-methoxybenzene (0.62 mL, 5.0 mmol, 1.0 eq.), *n*-butyllithium (3.16 mL, 2.5 M in hexanes, 6.0 mmol, 1.5 eq.) and cyclobutanone (0.56 mL, 5.5 mmol, 1.1 eq.). The crude residue was purified by flash column chromatography (5→10% EtOAc/Petrol, silica gel) to afford **10** (0.79 g, 95%) as a colourless liquid.

R_f = 0.12 (10% EtOAc/Petrol); $^1\text{H NMR}$ (500 MHz, CDCl_3) δ = 7.43 (d, J = 8.9 Hz, 2H, (ArH (2,6))), 6.91 (d, J = 8.9 Hz, 2H, (ArH (3,5))), 3.82 (s, 3H), 2.64 – 2.44 (m, 2H), 2.39 – 2.31 (m, 2H), 2.02 – 1.92 (m, 2H), 1.69 – 1.56 (m, 1H); $^{13}\text{C NMR}$ (126 MHz, CDCl_3) δ = 158.90, 138.56, 126.49, 113.87, 76.83, 55.44, 36.99, 13.02.

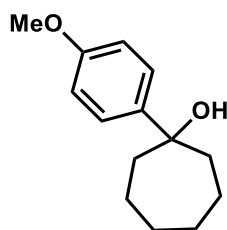
These data are consistent with those previously reported in the literature.⁷³

1-(4-methoxyphenyl)cyclopentan-1-ol (11)

Prepared according to General Procedure A using 1-bromo-4-methoxybenzene (0.62 mL, 5.0 mmol, 1.0 eq.), *n*-butyllithium (3.16 mL, 2.5 M in hexanes, 6.0 mmol, 1.5 eq.) and cyclopentanone (0.66 mL, 5.5 mmol, 1.1 eq.). The crude residue was purified by flash column chromatography (5→10% EtOAc/Petrol, silica gel) to afford **11** (0.765 g, 77%) as a colourless liquid.

R_f = 0.16 (10% EtOAc/Petrol); $^1\text{H NMR}$ (300 MHz, CDCl_3) δ = 7.42 (d, J = 8.8 Hz, 2H), 6.88 (d, J = 8.8 Hz, 2H), 3.81 (s, 3H), 2.12 – 1.86 (m, 6H), 1.89 – 1.75 (m, 2H), 1.51 (s, 1H).; $^{13}\text{C NMR}$ (75 MHz, CDCl_3) δ = 158.6, 139.3, 126.5, 113.7, 83.3, 55.4, 41.64, 23.8.

These data are consistent with those previously reported in the literature.⁷⁴

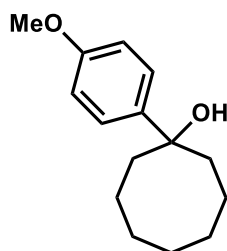
1-(4-methoxyphenyl)cycloheptan-1-ol (12)

Prepared according to General Procedure A using 1-bromo-4-methoxybenzene (0.62 mL, 5.0 mmol, 1.0 eq.), *n*-butyllithium (3.16 mL, 2.5 M in hexanes, 6.0 mmol, 1.5 eq.) and cycloheptanone (0.7 mL, 5.5 mmol, 1.1 eq.). The crude residue was purified by flash column chromatography (5→10% EtOAc/Petrol, silica gel) to afford **12** (0.980 g, 70%) as a colourless liquid.

R_f = 0.19 (10% EtOAc/Petrol); **¹H NMR (300 MHz, CDCl₃)** δ = 7.42 (d, *J* = 8.9 Hz, 2H), 6.87 (d, *J* = 8.9 Hz, 2H), 3.80 (s, 3H), 2.16 – 1.66 (m, 8H), 1.55 – 1.50 (m, 4H), 0.99 – 0.82 (m, 1H); **¹³C NMR (75 MHz, CDCl₃)** δ = 158.3, 142.9, 125.9, 113.5, 55.4, 43.4, 29.3, 22.6.

These data are consistent with those previously reported in the literature.⁷⁴

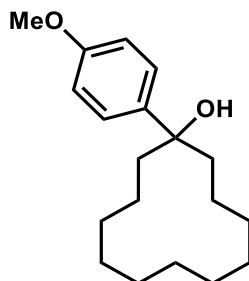
1-(4-methoxyphenyl)cyclooctan-1-ol (**13**)



Prepared according to General Procedure A using 1-bromo-4-methoxybenzene (0.62 mL, 5.0 mmol, 1.0 eq.), *n*-butyllithium (3.16 mL, 2.5 M in hexanes, 6.0 mmol, 1.5 eq.) and cyclooctanone (0.7 mL, 5.5 mmol, 1.1 eq.). The crude residue was purified by flash column chromatography (5→10% EtOAc/Petrol, silica gel) to afford **13** (1.2 g, 88%) as a colourless liquid.

R_f = 0.2 (10% EtOAc/Petrol); **¹H NMR (300 MHz, CDCl₃)** δ = 7.44 (d, *J* = 8.9 Hz, 2H), 6.87 (d, *J* = 8.8 Hz, 2H), 3.81 (s, 3H), 2.03 – 1.96 (m, 5H), 1.73 – 1.70 (m, 5H), 1.52 – 1.50 (m, 4H), 1.05 – 0.83 (m, 1H); **¹³C NMR (75 MHz, CDCl₃)** δ = 158.4, 141.3, 126.4, 113.5, 76.5, 55.4, 37.8, 28.5, 24.6, 22.2.

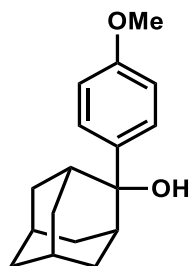
These data are consistent with those previously reported in the literature.⁷⁴

1-(4-methoxyphenyl)cyclododecan-1-ol (14)

Prepared according to General Procedure A using 1-bromo-4-methoxybenzene (0.62 mL, 5.0 mmol, 1.0 eq.), *n*-butyllithium (3.16 mL, 2.5 M in hexanes, 6.0 mmol, 1.5 eq.) and cyclododecanone (1.3 g, 5.5 mmol, 1.1 eq.). The crude residue was purified by flash column chromatography (5→10% EtOAc/Petrol, silica gel) to afford **14** (0.7 g, 45%) as a colourless liquid.

R_f = 0.2 (10% EtOAc/Petrol); **¹H NMR (500 MHz, CDCl₃)** δ = 7.40 (d, *J* = 8.9 Hz, 2H), 6.86 (d, *J* = 8.8 Hz, 2H), 3.80 (s, 3H), 1.85 (t, *J* = 7.5 Hz, 4H), 1.55 (d, *J* = 1.3 Hz, 1H) 1.46 – 1.16 (m, 18H); **¹³C NMR (75 MHz, CDCl₃)** δ = 158.4, 140.7, 126.5, 113.3, 76.3, 55.4, 35.6, 26.5, 26.2, 22.6, 22.3, 20.1.

These data are consistent with those previously reported in the literature.⁷⁴

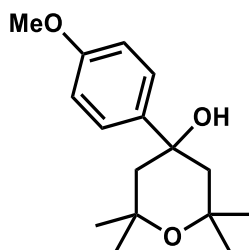
(1r,3r,5r,7r)-2-(4-methoxyphenyl)adamantan-2-ol (21)

Prepared according to General Procedure A using 1-bromo-4-methoxybenzene (0.62 mL, 5.0 mmol, 1.0 eq.), *n*-butyllithium (3.16 mL, 2.5 M in hexanes, 6.0 mmol, 1.5 eq.) and adamantanonone (1.08 g, 7.18 mmol, 1.2 eq.). The crude residue was purified by flash column chromatography (5→10% EtOAc/Petrol, silica gel) to afford **21** (1.08 g, 78%) as a white solid.

R_f = 0.16 (10% EtOAc/Petrol); $^1\text{H NMR}$ (500 MHz, CDCl_3) δ = 7.47 (d, J = 8.9 Hz, 2H), 6.90 (d, J = 8.9 Hz, 2H), 3.81 (s, 3H), 2.54 (s, 2H), 2.43 – 2.36 (m, 2H), 1.90 (s, 1H), 1.77 – 1.66 (m, 9H), 1.45 (s, 1H); $^{13}\text{C NMR}$ (75 MHz, CDCl_3) δ = 158.6, 137.7, 126.6, 114.1, 75.5, 55.4, 37.8, 35.9, 35.1, 33.1, 27.6, 27.01.

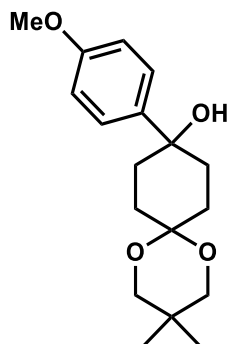
These data are consistent with those previously reported in the literature.⁷⁴

4-(4-methoxyphenyl)-2,2,6,6-tetramethyltetrahydro-2H-pyran-4-ol (**22**)



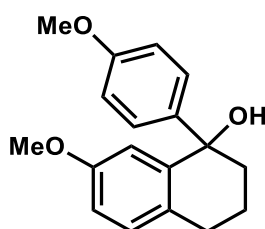
Prepared according to General Procedure A using 1-bromo-4-methoxybenzene (0.62 mL, 5.0 mmol, 1.0 eq.), *n*-butyllithium (3.16 mL, 2.5 M in hexanes, 6.0 mmol, 1.5 eq.) and 2,2,6,6-tetramethyltetrahydro-4H-pyran-4-one (0.85 g, 5.5 mmol, 1.1 eq.). The crude residue was purified by flash column chromatography (5→10% EtOAc/Petrol, silica gel) to afford **22** (0.90 g, 68%).

R_f = 0.41 (15% EtOAc/Petrol); **FTIR** (ν_{max} cm^{-1} , thin film) = 3486 (bs), 2971, 2873, 1610, 1514, 1466, 1365, 1249, 1233, 1186, 1162, 1033, 1014, 835; $^1\text{H NMR}$ (500 MHz, CDCl_3) δ = 7.42 (d, J = 8.9 Hz, 2H), 6.89 (d, J = 8.9 Hz, 2H), 3.81 (s, 3H), 1.90 – 1.82 (m, 4H), 1.71 (s, 1H), 1.54 (s, 6H), 1.27 (s, 6H); $^{13}\text{C NMR}$ (126 MHz, CDCl_3) δ = 158.6, 141.6, 125.7, 113.7, 73.1, 71.9, 55.4, 47.3, 34.8, 30.0; **HRMS** (EI) [$\text{C}_{16}\text{H}_{24}\text{O}_3$] requires $[M]$ 264.1725, found 264.1722.

9-(4-methoxyphenyl)-3,3-dimethyl-1,5-dioxaspiro[5.5]undecan-9-ol (23)

Prepared according to General Procedure A using 1-bromo-4-methoxybenzene (0.62 mL, 5.0 mmol, 1.0 eq.), *n*-butyllithium (3.16 mL, 2.5 M in hexanes, 6.0 mmol, 1.5 eq.) and 3,3-dimethyl-1,5-dioxaspiro[5.5]undecan-9-one (1.18 g, 5.5 mmol, 1.1 eq.). The crude residue was purified by flash column chromatography (5→10% EtOAc/Petrol, silica gel) to afford **23** (1.05 g, 70%).

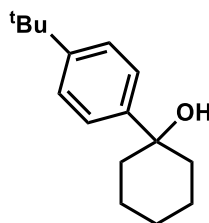
R_f = 0.39 (15% EtOAc/Petrol); **FTIR** (ν_{max} cm⁻¹, thin film) = 3448 (bs), 2951, 2868, 1698, 1512, 1470, 1389, 1365, 1249, 1178, 1037, 985, 830; **¹H NMR (500 MHz, CDCl₃)** δ = 7.43 (d, *J* = 9.0 Hz, 2H), 6.87 (d, *J* = 8.8 Hz, 2H), 3.80 (s, 3H), 3.58 (s, 2H), 3.51 (s, 2H), 2.22 – 2.13 (m, 2H), 2.06 (m, Hz, 2H), 1.90 (Hz, 2H), 1.76 – 1.68 (m, 2H), 1.47 (s, 1H), 0.99 (s, 6H); **¹³C NMR (126 MHz, CDCl₃)** δ = 158.6, 140.8, 125.9, 113.63, 97.3, 72.6, 70.2, 55.4, 35.5, 30.4, 28.3, 22.9 ; **HRMS (ES⁺)** [C₁₈H₂₂O₃] requires [M-H₂O] 289.1804, found 289.1815.

7-methoxy-1-(4-methoxyphenyl)-1,2,3,4-tetrahydronaphthalen-1-ol (24)

Prepared according to General Procedure A using 1-bromo-4-methoxybenzene (0.62 mL, 5.0 mmol, 1.0 eq.), *n*-butyllithium (3.16 mL, 2.5 M in hexanes, 6.0 mmol, 1.5 eq.) and 3,3,7-methoxy-3,4-dihydronaphthalen-1(2H)-one (1.05 g, 5.5 mmol, 1.1 eq.). The crude residue was purified by flash column chromatography (5→10% EtOAc/Petrol, silica gel) to afford **23** (1.1 g, 66%) as a colourless liquid.

R_f = 0.2 (10% EtOAc/Petrol); **FTIR** (ν_{\max} cm⁻¹, thin film) = 3478 (bs), 2973, 2837, 1606, 1508, 1463, 1437, 1271, 1233, 1174, 1085, 856; **¹H NMR (500 MHz, CDCl₃)** δ = 7.22 (d, J = 9.0 Hz, 2H), 7.09 – 7.06 (m, 1H), 6.82 (d, J = 8.9 Hz, 2H), 6.79 (dd, J = 8.4, 2.8 Hz, 1H), 6.64 (d, J = 2.7 Hz, 1H), 3.80 (s, 3H), 3.67 (s, 3H), 2.88 – 2.70 (m, 2H), 2.20 (s, 1H), 2.13 – 2.07 (m, 2H), 1.98 – 1.86 (m, 1H), 1.77 – 1.66 (m, 1H); **¹³C NMR (75 MHz, CDCl₃)** δ = 158.4, 158.1, 143.2, 140.9, 129.1, 129.8, 114.4, 113.1, 112.9, 75.5, 55.4, 41.6, 29.1, 19.9 **HRMS** (ES⁺) [C₁₈H₂₀O₃] requires [M-H₂O] 267.1385, found 267.1383.

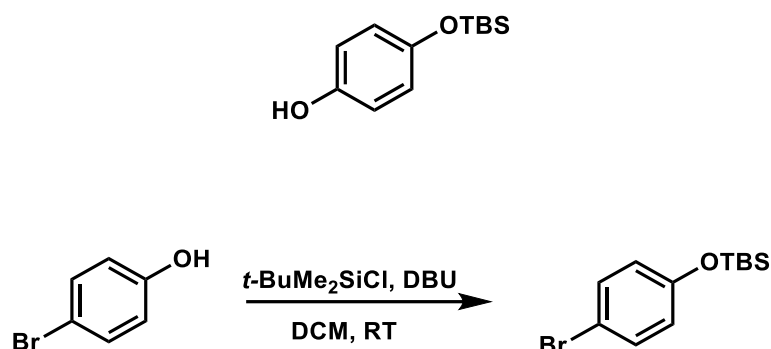
1-(4-(*tert*-butyl)phenyl)cyclohexan-1-ol (**28**)



Prepared according to General Procedure A using 1-bromo-4-(*tert*-butyl)benzene (2.16 g, 10 mmol, 1.0 eq.), *n*-butyllithium (4.4 mL, 2.5 M in hexanes, 6.0 mmol, 1.5 eq.) and 3,3-cyclohexanone (1.24 mL, 11 mmol, 1.1 eq.). The crude residue was purified by flash column chromatography (5→10% EtOAc/Petrol, silica gel) to afford **28** (1.4 g, 60%) as a white solid.

R_f = 0.2 (10% EtOAc/Petrol); **¹H NMR (500 MHz, CDCl₃)** δ = 7.50 – 7.31 (m, 4H), 1.90 – 1.60 (m, 10H), 1.55 (s, 1H), 1.33 (s, 9H); **¹³C NMR (125 MHz, CDCl₃)** δ = 149.4, 146.5, 125.2, 124.4, 73.0, 39.0, 34.5, 31.5, 25.7, 22.3

4-((tert-butyldimethylsilyl)oxy)phenol (3-A)

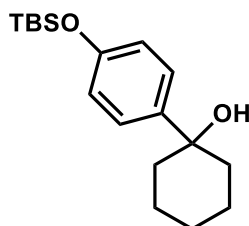


Prepared according to the reported procedure using 4-bromophenol (1 g, 5.78 mmol) and *tert*-butyldimethylsilyl chloride (1.74 g, 11.6 mmol) dissolved in DCM (30 mL). To this solution was added 1,8-diazabicyclo[5.4.0]undec-7-ene (DBU) (2.27 mL, 15 mmol) dropwise and the reaction mixture was stirred for 2 h at room temperature. After completion by TLC, the reaction was quenched by aq. NaHCO₃ and extracted with DCM X2, dried over MgSO₄ and concentrated under reduced pressure to afford 3-A (1.68 g, 100%) as colourless oil.

R_f = 0.9 (10% EtOAc/Petrol); **¹H NMR (400 MHz, CDCl₃)** δ = 7.35 – 7.26 (m, 2H), 6.80 – 6.67 (m, 2H), 0.97 (s, 9H), 0.18 (s, 6H); **¹³C NMR (101MHz, CDCl₃)** δ = 155.0, 132.4, 122.1, 113.7, 25.8, 18.3, -4.32

These data are consistent with those previously reported in the literature.⁷⁵

1-(4-((tert-butyldimethylsilyl)oxy)phenyl)cyclohexan-1-ol (29)

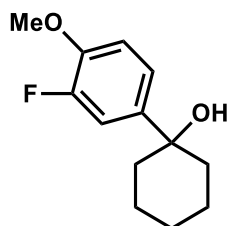


Prepared according to General Procedure A using 1-bromo-4-(tert-butyl)benzene (1.43 g, 5.0 mmol, 1.0 eq.), *n*-butyllithium (2.4 mL, 2.5 M in hexanes, 6.0 mmol, 1.5 eq.) and 3,3-cyclohexanone (0.62 mL, 6 mmol, 1.1 eq.). The crude residue was purified by flash column chromatography (5→10% EtOAc/Petrol, silica gel) to afford **29** (0.96 g, 63%) as a colourless oil.

R_f = 0.62 (10% EtOAc/Petrol); **¹H NMR (500 MHz, CDCl₃)** δ = 7.38 – 7.33 (m, 2H), 6.83 – 6.75 (m, 2H), 1.86 – 1.68 (m, 7H), 1.64 – 1.56 (m, 2H), 1.52 (s, 1H), 1.32 – 1.23 (m, 1H), 0.98 (s, 9H), 0.19 (s, 6H).; **¹³C NMR (125 MHz, CDCl₃)** δ = 154.4, 142.2, 126.0, 120.0 72.9, 39.0, 25.8, 25.7, 22.4, -4.3.

These data are consistent with those previously reported in the literature.⁷⁶

1-(3-fluoro-4-methoxyphenyl)cyclohexan-1-ol (**30**)



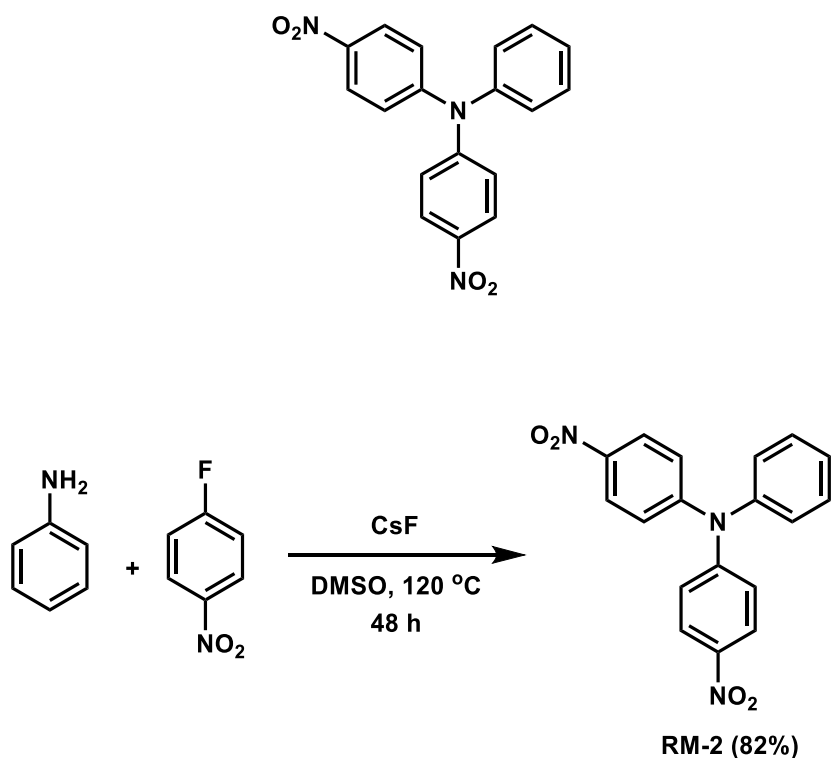
Prepared according to General Procedure A using 4-bromo-2-fluoro-1-methoxybenzene (0.65 mL, 5.0 mmol, 1.0 eq.), *n*-butyllithium (2.4 mL, 2.5 M in hexanes, 6.0 mmol, 1.5 eq.) and 3,3-cyclohexanone (0.62 mL, 6 mmol, 1.1 eq.). The crude residue was purified by flash column chromatography (5→10% EtOAc/Petrol, silica gel) to afford **30** (0.70 g, 62%) as a colourless oil.

R_f = 0.21 (10% EtOAc/Petrol); **¹H NMR (500 MHz, CDCl₃)** δ = 7.23 – 7.17 (m, 1H), 7.15 (ddd, *J* = 8.5, 2.3, 1.2 Hz, 1H), 6.88 (t, *J* = 8.7 Hz, 1H), 3.84 (s, 3H), 1.76 – 1.65 (m, 9H), 1.61 – 1.58 (m, 2H); **¹³C NMR (125 MHz, CDCl₃)** δ = 152.9 (s), 146.8 (s), 143.9 (s), 120.4 (d), 113.5(d), 113.5(d), 72.3(s), 55.9 (q), 39.1 (t), 25.8 (t), 22.4 (t); **¹⁹F (471 MHz, CDCl₃)** δ = -135.37

These data are consistent with those previously reported in the literature.⁷⁶

6.3. Synthesis of Redox Mediators

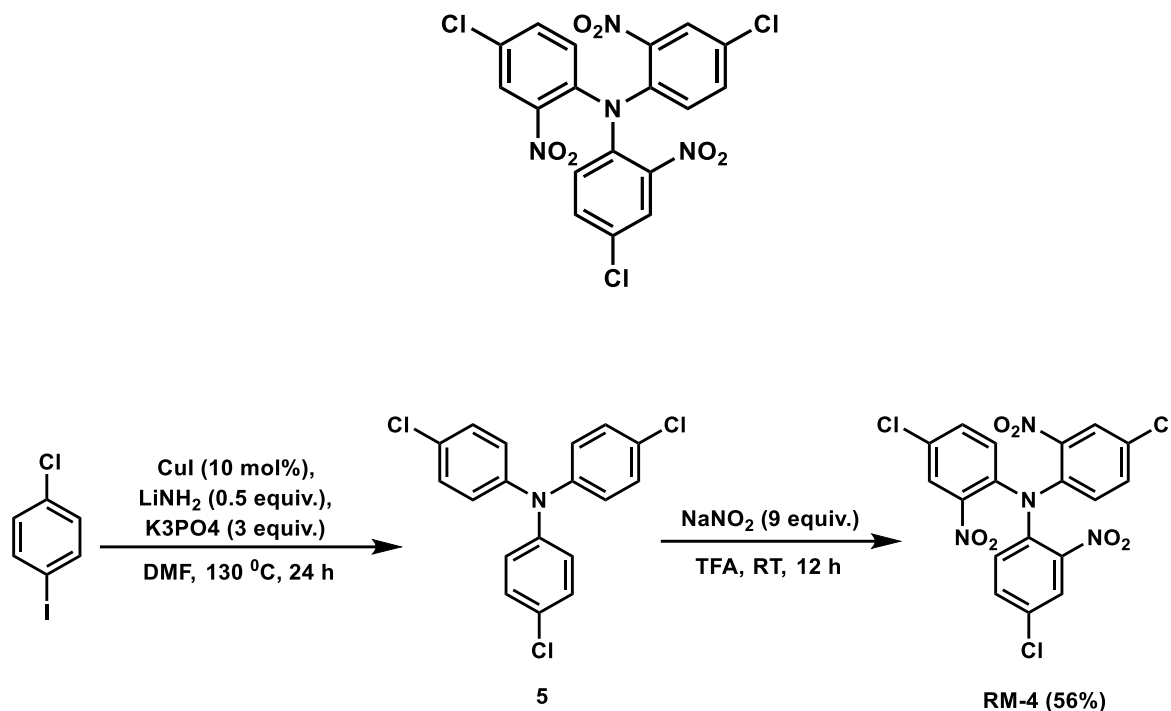
4-nitro-N-(4-nitrophenyl)-N-phenylaniline (RM-2)



Synthetic Procedure – Aniline (2.15 g, 23.1 mmol), 4-fluoronitrobenzene (7.24 g, 51.3 mmol) and cesium fluoride (7.79 g, 51.3 mmol) were dissolved in dried 100 ml DMSO, and the reactant mixture was stirred at 120 °C for 48 h. The reaction mixture was cooled to room temperature, poured into 500 ml of cold water and the precipitated orange solid was then collected by filtration and washed with methanol to afford **RM-2** (6.73 g, 82%) as a yellow solid.

¹H NMR (500 MHz, DMSO-*d*₆) δ = 8.19 (d, *J* = 9.1 Hz, 4H), 7.51 (t, *J* = 7.7 Hz, 2H), 7.38 (dd, *J* = 8.5, 6.2 Hz, 1H), 7.30 – 7.26 (m, 2H), 7.20 (d, *J* = 9.0 Hz, 4H).; **¹³C NMR (101 MHz, DMSO-*d*₆)** δ = 151.6, 144.5, 142.0, 130.6, 127.4, 127.2, 125.6, 122.4

These data are consistent with those previously reported in the literature.⁷⁷

Tris(4-chloro-2-nitrophenyl)amine (RM-4)

Synthetic Procedure of 5 – In an oven dried seal-tube, was transferred 4-chloroiodobenzene (1.17 g, 5 mmol), LiNH_2 (60 mg, 0.5 mmol), CuI (95 mg, 10 mol%), K_3PO_4 (3.18 g, 15 mmol, 3 equiv.) and the tube was backfilled with N_2 3 times. Then anhydrous DMF (10 mL) was added under N_2 . The tube was sealed and heated to 130°C for 24 h. After cooling to room temperature, water was added to the reaction mixture and extracted with DCM X3. Combined organic layers were dried over MgSO_4 and distilled under reduced pressure. The obtained crude residue was purified by flash column chromatography (100% petrol, silica gel) to afford **5** (0.98 g, 41%) as a white solid.

Synthetic Procedure of RM-4 – To a solution of 5 (349 mg, 1mmol) in TFA (100 mL) was added sodium nitrite (625 mg, 9 mmol). The reaction turned first deep blue then green in colour. After stirring the reaction mixture for overnight, water was added, and the reaction mixture was then cooled to 0 °C. While stirring, NaOH pellets (50 g) were added slowly (*exothermic*) until the solution was alkaline. The product was extracted with DCM (10 mL X 3) and washed with cold water and dried under vacuum over night to afford RM-4 (290 mg, 60%) as yellow amorphous solid.

¹H NMR (500 MHz, DMSO-*d*₆) δ = 8.15 (d, *J* = 2.5 Hz, 3H), 7.76 (dd, *J* = 8.8, 2.5 Hz, 3H), 7.29 (d, *J* = 8.8 Hz, 3H); **¹³C NMR (126 MHz, DMSO-*d*₆)** δ = 143.8, 136.5, 134.5, 130.5, 129.7, 126.1.

These data are consistent with those previously reported in the literature.⁷⁷

6.4. Cyclic Voltammetry

General Information: Cyclic Voltammetry (CV) experiments were conducted with in a 10 mL glass vial fitted with a glassy carbon working electrode (3 mm dia., BASi), a Ag/AgCl reference electrode and a platinum wire counter electrode. The solution of interest was purged with N₂ for 5 minutes before data collection. After data collection, ferrocene (5 mM) was added, and an additional scan was run.

6.4.1. Cyclic Voltammogram of Substrates

1-(4-methoxyphenyl)cyclohexan-1-ol (1)

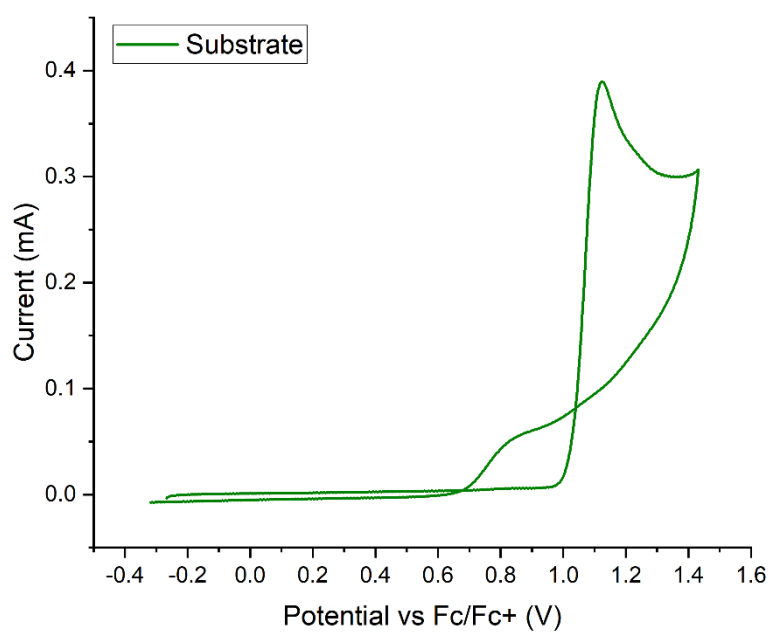
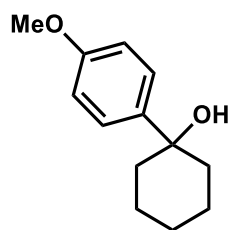


Figure 6.1 – Cyclic voltammogram of parent substrate (4.0 mM) MeCN (4 mM), LiClO₄ (0.1 M).
Scan rate: 100 mV/s

$E_{p/2} = 1.10 \text{ V vs Fc/Fc}^+$

1-(4-(tert-butyl)phenyl)cyclohexan-1-ol (28)

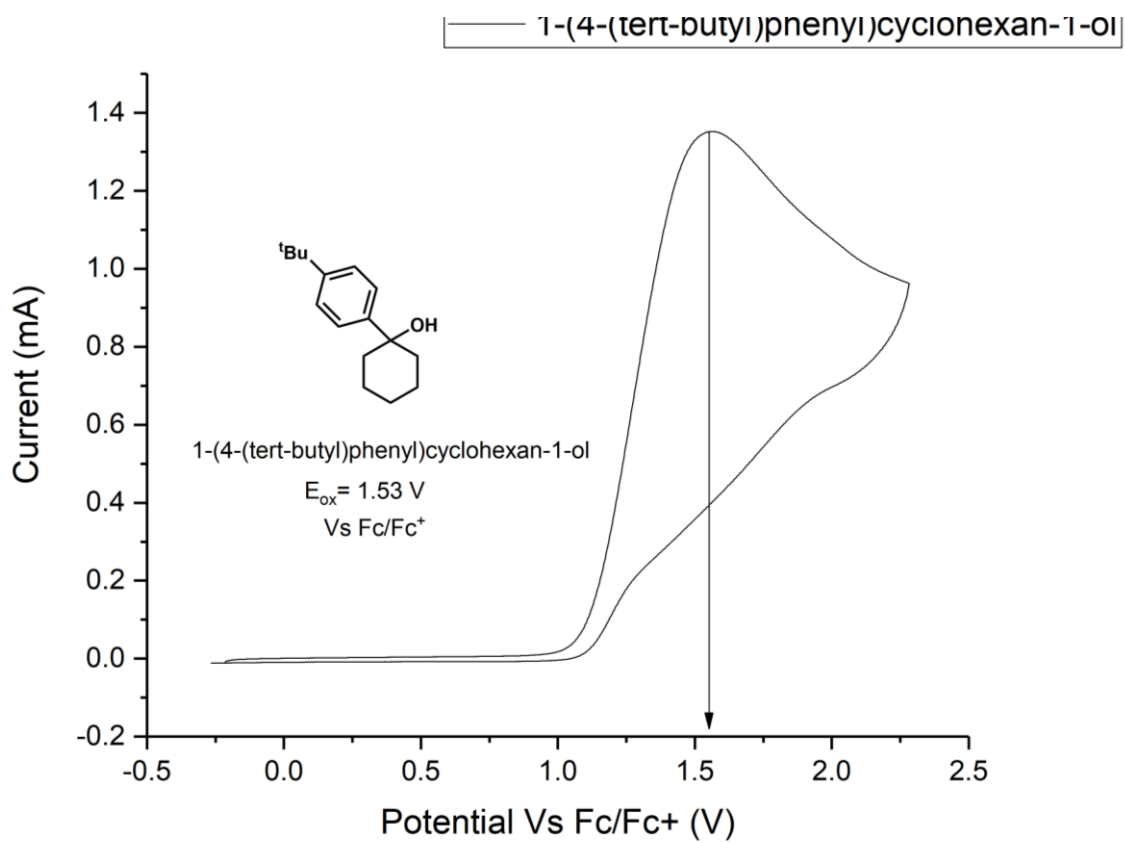
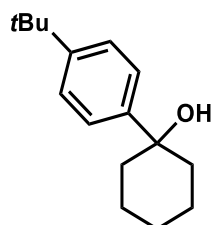


Figure 6.2– Cyclic voltammogram of substrate 28 (4.0 mM) MeCN (4 mM), LiClO_4 (0.1 M).
Scan rate: 100 mV/s

$$E_{p/2} = 1.53 \text{ V vs Fc/Fc}^+$$

1-(4-((tert-butyldimethylsilyl)oxy)phenyl)cyclohexan-1-ol (29)

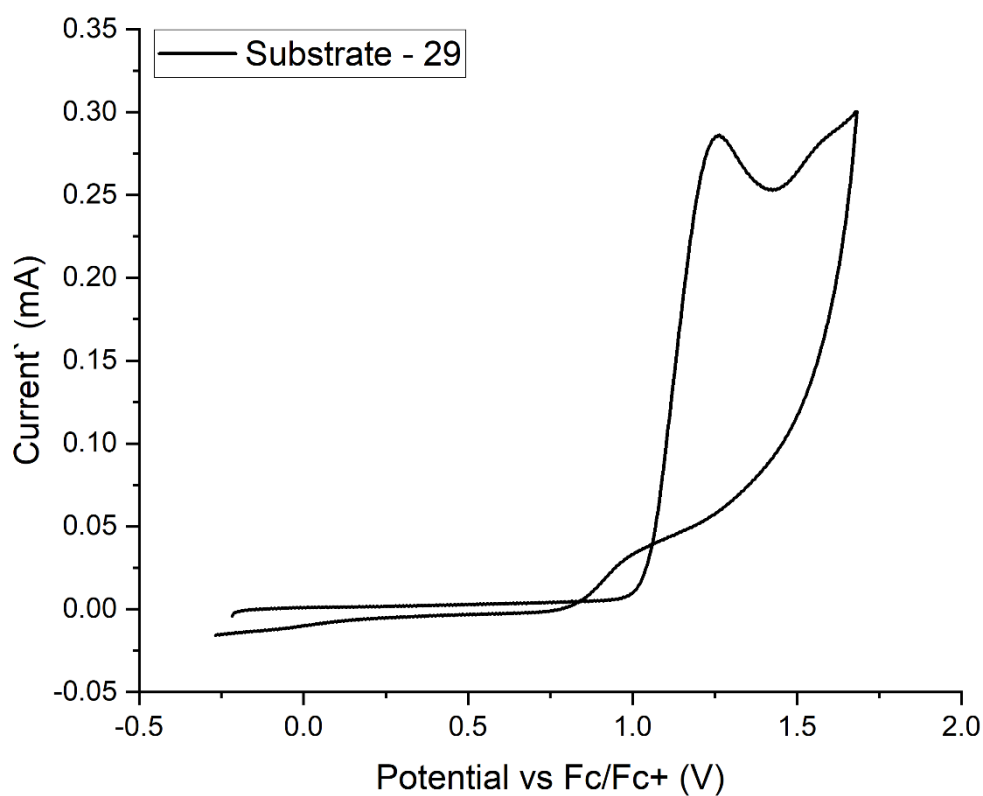
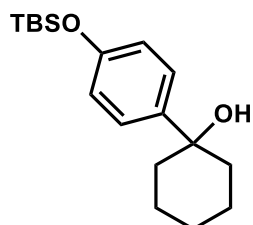


Figure 6.3 – Cyclic voltammogram of substrate 29 (4.0 mM) MeCN (4 mM), LiClO₄ (0.1 M).
Scan rate: 100 mV/s

$E_{p/2} = 1.20 \text{ V vs Fc/Fc}^+$

1-(3-fluoro-4-methoxyphenyl)cyclohexan-1-ol (30)

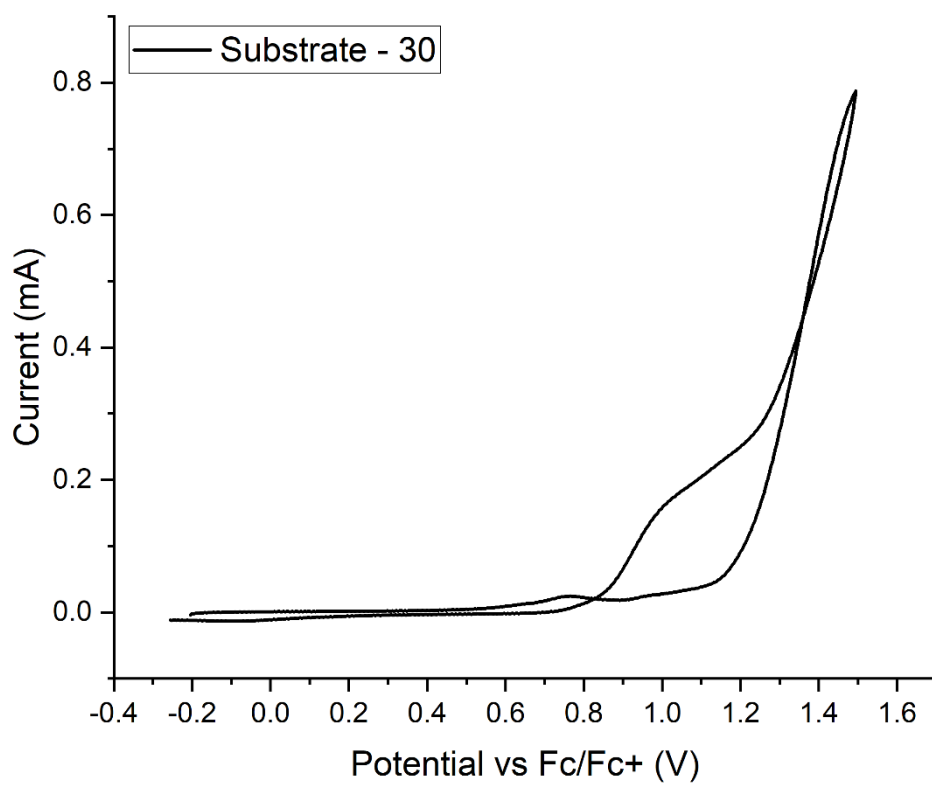
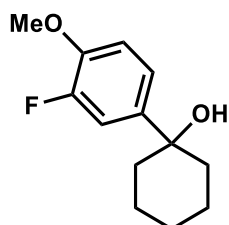


Figure 6.4 – Cyclic voltammogram of substrate 30 (4.0 mM) MeCN (4 mM), LiClO₄ (0.1 M).
Scan rate: 100 mV/s

$E_{p/2} = 1.19 \text{ V vs Fc/Fc}^+$

6.4.2. Cyclic Voltammetry of Redox Mediators

RM-2

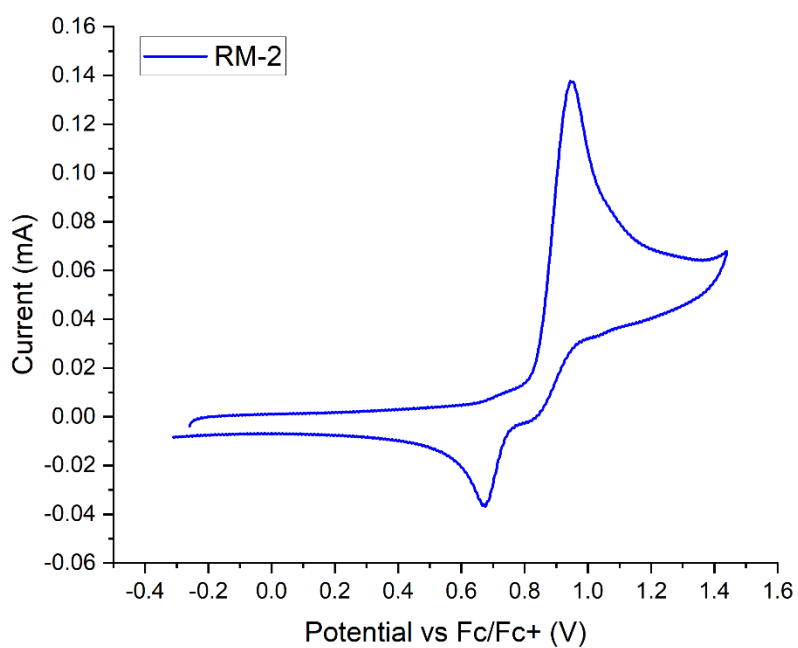
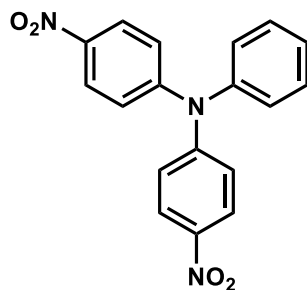


Figure 6.5 – Cyclic voltammogram of RM-2 (4.0 mM) MeCN (4 mM), LiClO₄ (0.1 M).
Scan rate: 100 mV/s

$E_{p/2} = 0.98 \text{ V vs Fc/Fc}^+$

RM-4

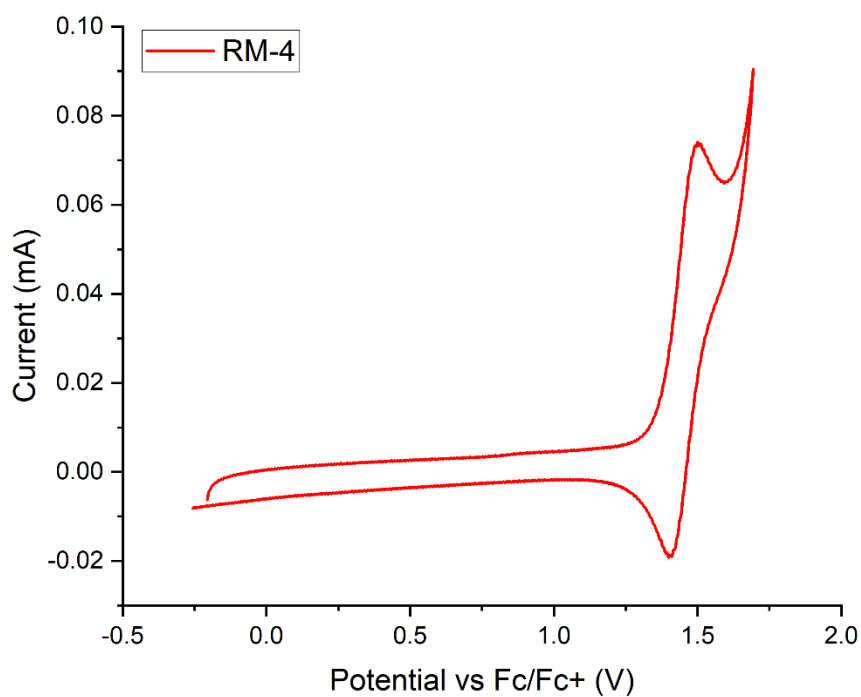
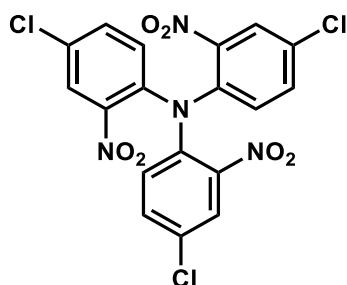
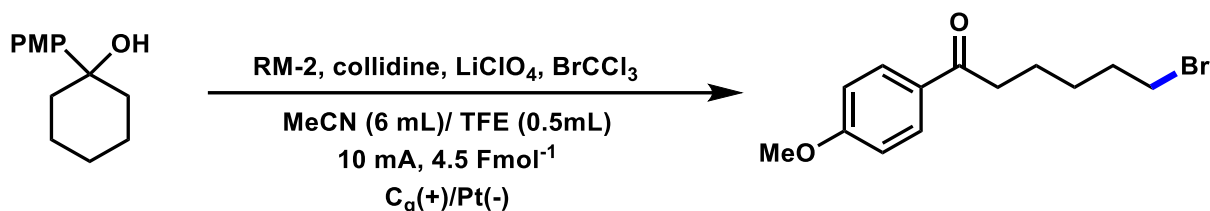


Figure 6.6 – Cyclic voltammogram of RM-4 (4.0 mM) MeCN (4 mM), LiClO₄ (0.1 M).
Scan rate: 100 mV/s

$E_{p/2} = 1.48 \text{ V vs Fc/Fc}^+$

6.4. General Procedure for Electrochemical Deconstructive Bromination of Cycloalkanols

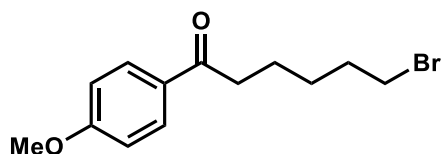


Experimental Procedure: To an oven dried 10 mL electrasyn vial, cycloalkanol (0.30 mmol), redox-mediator (5 mol%), collidine dried over molecular sieves (3.0 equiv), lithium perchlorate (2 equiv) was taken, and the vial was sealed with electrasyn cap comprised of a graphite (anode) and platinum (cathode). The vial was back filled with nitrogen (three cycles) and dry acetonitrile (6 mL) and trifluoroethanol dried over molecular sieves (0.5 mL) was added under nitrogen atmosphere. The vial was then purged with nitrogen for 10 minutes and bromotrichloromethane (2 equiv) was added and the reaction mixture was then electrolysed using electrasyn 2.0 at constant current of 10mA until 4.5 Fmol⁻¹ of charge (3.37 hours) has been passed at ambient temperature. To the reaction mixture was then added 0.1 mmol of trimethoxybenzene as an internal standard to get the crude NMR yield.

The reaction was quenched with aq. NH₄Cl, washed with aq. CuSO₄ solution, and extracted with EtOAc (10 mL X 2). The organic layer was dried over MgSO₄ and distilled under reduced pressure. The crude residue obtained was purified flash column chromatography (5→10 % EtOAc/Petrol, silica gel) to afford the brominated ketones.

6.4.1. Characterization of Products

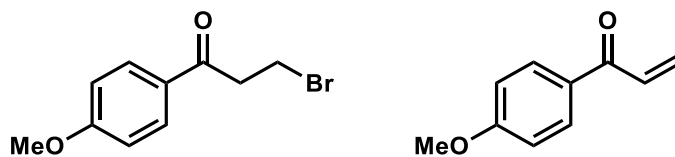
6-bromo-1-(4-methoxyphenyl)hexan-1-one (8)



Prepared according to General Procedure using **1** (62 mg). The crude was purified by flash column chromatography (5→10 % EtOAc/Petrol, silica gel) to afford **8** (80.4 mg, 94%) as a low melting solid.

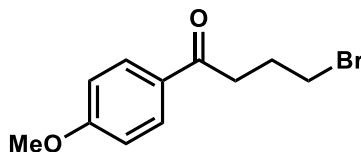
R_f = 0.54 (15% EtOAc/Petrol); **FTIR** (ν_{max} cm⁻¹, thin film) = 2939, 2841, 1675, 1600, 1572, 1509, 1456, 1383, 1345, 1254, 1173, 920, 837, 807; **¹H NMR (500 MHz, CDCl₃)** δ = 7.94 (d, J = 9.0 Hz, 2H (ArH(2,6))), 6.93 (d, J = 8.9 Hz, 2H, (ArH(3,5))), 3.87 (s, 3H (OCH₃)), 3.43 (t, J = 6.8 Hz, 2H (CH₂-Br)), 2.97 – 2.89 (m, 2H (CH₂-C=O)), 2.01 – 1.87 (m, 2H (al)), 1.80 – 1.70 (m, 2H (al)), 1.59 – 1.49 (m, 2H (al)).; **¹³C NMR (126 MHz, CDCl₃)** δ = 198.8 (C=O), 163.6 (ArC(OMe)), 130.4 (ArC (2,6)), 130.2 (ArC (C=O)), 113.9 (ArC (3,5)), 55.6 (OCH₃), 38.1 (CH₂ (C=O)), 33.8 (CH₂-Br), 32.8 (al), 28.1(al), 23.7 (al); **HRMS (ES⁺)** [C₁₃H₁₈O₂Br] requires 285.0490, found 285.0484.

3-bromo-1-(4-methoxyphenyl)propan-1-one (15)



Product **15** could not be isolated as β -bromo ketones are unstable and alkene peaks were observed in the NMR.

4-bromo-1-(4-methoxyphenyl)butan-1-one (16)

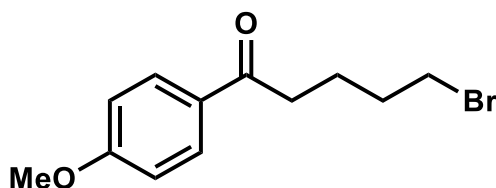


Prepared according to General Procedure using **10** (54 mg). The crude was purified by flash column chromatography (5 \rightarrow 10 % EtOAc/Petrol, silica gel) to afford **16** (65 mg, 83%) as a colourless oil.

R_f = 0.48 (15% EtOAc/Petrol); $^1\text{H NMR}$ (500 MHz, CDCl_3) δ = 7.97 (d, J = 9.0 Hz, 2H), 6.94 (d, J = 9.0 Hz, 2H), 3.88 (s, 3H), 3.55 (t, J = 6.3 Hz, 2H), 3.13 (t, J = 7.0 Hz, 2H), 2.44 – 2.06 (m, 2H); $^{13}\text{C NMR}$ (126 MHz, CDCl_3) δ = 197.5, 163.7, 130.4, 130.0, 114.0, 55.6, 36.3, 34.0, 27.1

These data are consistent with those previously reported in the literature.⁷⁸

5-bromo-1-(4-methoxyphenyl)pentan-1-one (17)

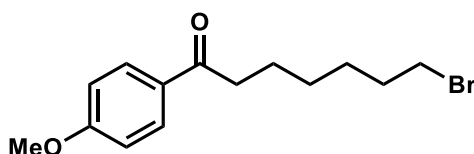


Prepared according to General Procedure using **11** (58 mg). The crude was purified by flash column chromatography (5 \rightarrow 10 % EtOAc/Petrol, silica gel) to afford **17** (68 mg, 82%) as a colourless oil.

R_f = 0.41 (15% EtOAc/Petrol); $^1\text{H NMR}$ (500 MHz, CDCl_3) δ = 7.94 (d, J = 9.0 Hz, 2H), 6.94 (d, J = 8.9 Hz, 2H), 3.87 (s, 3H), 3.45 (t, J = 6.6 Hz, 2H), 2.96 (t, J = 7.0 Hz, 2H), 2.17 – 1.68 (m, 4H); $^{13}\text{C NMR}$ (126 MHz, CDCl_3) δ = 198.3, 163.6, 130.4, 130.1, 113.9, 55.6, 37.2, 33.6, 32.4, 23.1

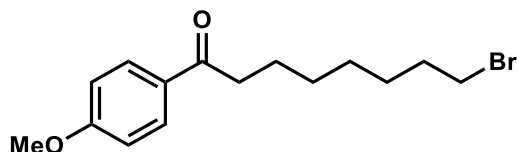
These data are consistent with those previously reported in the literature.⁷⁹

7-bromo-1-(4-methoxyphenyl)heptan-1-one (18)



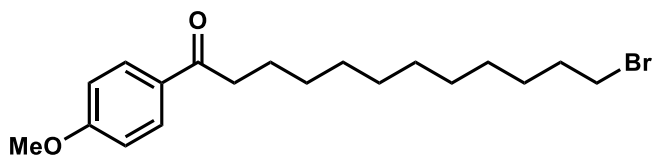
Prepared according to General Procedure using **12** (66 mg). The crude was purified by flash column chromatography (5→10 % EtOAc/Petrol, silica gel) to afford **18** (57 mg, 64%) as a colourless oil.

R_f = 0.59 (15% EtOAc/Petrol); **FTIR** (ν_{max} cm^{-1} , thin film) = 2937, 2848, 1676, 1602, 1574, 1512, 1465, 1417, 1310, 1255, 1216, 1170, 1112, 1026, 830; $^1\text{H NMR}$ (500 MHz, CDCl_3) δ = 7.94 (d, J = 9.0 Hz, 2H), 6.93 (d, J = 9.0 Hz, 2H), 3.87 (s, 3H), 3.41 (t, J = 6.8 Hz, 2H), 2.96 – 2.88 (m, 2H), 1.95 – 1.82 (m, 2H), 1.79 – 1.70 (m, 2H), 1.53 – 1.35 (m, 4H); $^{13}\text{C NMR}$ (126 MHz, CDCl_3) δ = 199.1, 163.5, 130.5, 130.3, 113.8, 55.6, 38.2, 34.1, 32.7, 28.6, 28.2, 24.4; **HRMS** (ES^+) [$\text{C}_{14}\text{H}_{20}\text{O}_2\text{Br}$] requires 299.0647, found 299.0644.

8-bromo-1-(4-methoxyphenyl)octan-1-one (19)

Prepared according to General Procedure using **13** (70 mg). The crude was purified by flash column chromatography (5→10 % EtOAc/Petrol, silica gel) to afford **19** (38 mg, 40%) as a colourless oil.

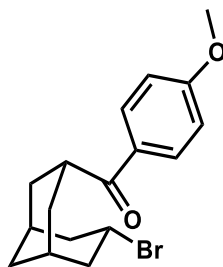
R_f = 0.55 (15% EtOAc/Petrol); **FTIR** (ν_{\max} cm^{-1} , thin film) = 2935, 2848, 1676, 1595, 1510, 1459, 1421, 1310, 1257, 1231, 1168, 1129, 1030, 841, 805; **^1H NMR (500 MHz, CDCl_3)** δ = 7.94 (d, J = 8.9 Hz, 2H), 6.93 (d, J = 8.9 Hz, 2H), 3.87 (s, 3H), 3.40 (t, J = 6.8 Hz, 2H), 2.91 (t, J = 7.4 Hz, 2H), 1.94 – 1.82 (m, 2H), 1.77 – 1.69 (m, 2H), 1.50 – 1.28 (m, 6H); **^{13}C NMR (126 MHz, CDCl_3)** δ = 199.2, 163.5, 130.5, 130.3, 113.8, 55.6, 38.3, 34.1, 32.9, 29.3, 28.9, 28.2, 24.6; **HRMS** (ES^+) [$\text{C}_{15}\text{H}_{22}\text{O}_2\text{Br}$] requires 313.0803, found 313.0790.

12-bromo-1-(4-methoxyphenyl)dodecan-1-one (20)

Prepared according to General Procedure using **14** (87 mg). The crude was purified by flash column chromatography (5→10 % EtOAc/Petrol, silica gel) to afford **20** (105 mg, 95%) as a colourless oil.

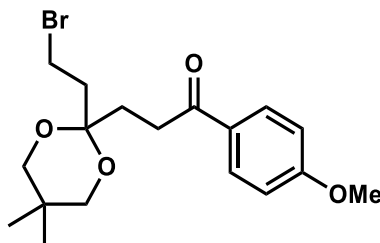
R_f = 0.58 (15% EtOAc/Petrol); **FTIR** (ν_{max} cm⁻¹, thin film) = 2915, 2850, 1680, 1606, 1510, 1472, 1263, 1168, 1114, 1031, 971, 832; **¹H NMR (500 MHz, CDCl₃)** δ = 7.94 (d, *J* = 8.9 Hz, 2H), 6.93 (d, *J* = 8.9 Hz, 2H), 3.87 (s, 3H), 3.41 (t, *J* = 6.9 Hz, 2H), 3.04 – 2.80 (m, 2H), 1.88 – 1.82 (m, 2H), 1.74 – 1.67 (m, 2H), 1.44 – 1.23 (m, 14H); **¹³C NMR (126 MHz, CDCl₃)** δ = 199.4, 163.4, 130.5, 130.3, 113.8, 55.6, 38.5, 34.3, 33.0, 29.6, 29.5, 29.5, 28.9, 28.3, 25.0; **HRMS** (ES⁺) [C₁₉H₂₉O₂Br] requires 368.1345, found 368.1341.

((1R,3s,5S,7s)-7-bromobicyclo[3.3.1]nonan-3-yl)(4-methoxyphenyl)methanone
(25)



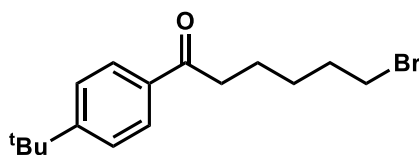
Prepared according to General Procedure using **21** (78 mg). The crude was purified by flash column chromatography (5→10 % EtOAc/Petrol, silica gel) to afford **25** (85 mg, 84%) as a colourless oil.

R_f = 0.58 (15% EtOAc/Petrol); **FTIR** (ν_{max} cm⁻¹, thin film) = 2933, 1674, 1599, 1512, 1459, 1248, 1210, 1165, 1131, 1030, 839, 752; **¹H NMR (500 MHz, CDCl₃)** δ = 7.93 (d, *J* = 8.9 Hz, 2H), 6.94 (d, *J* = 8.9 Hz, 2H), 4.58 (tt, *J* = 12.2, 4.8 Hz, 1H), 3.87 (s, 3H), 3.49 (tt, *J* = 12.6, 6.1 Hz, 1H), 2.34 – 2.16 (m, 4H), 2.13 – 2.02 (m, 2H), 1.96 – 1.81 (m, 3H), 1.64 – 1.48 (m, 2H), 1.31 (dt, *J* = 13.2, 2.6 Hz, 1H); **¹³C NMR (126 MHz, CDCl₃)** δ = 202.4, 163.6, 130.6, 129.6, 113.9, 55.6, 47.8, 45.3, 36.9, 29.7, 28.3, 28.1; **HRMS** (ES⁺) [C₁₇H₂₂O₂Br] requires 337.0803, found 337.810.

3-(2-(2-bromoethyl)-5,5-dimethyl-1,3-dioxan-2-yl)-1-(4-methoxyphenyl)propan-1-one (26)

Prepared according to General Procedure using **23** (92 mg) passing 6 F/mol of charge. The crude was purified by flash column chromatography (5→10 % EtOAc/Petrol, silica gel) to afford **26** (106 mg, 93%) as a colourless oil.

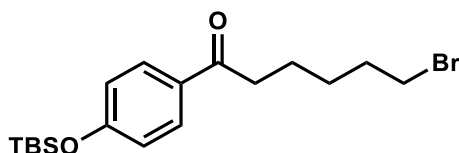
R_f = 0.48 (15% EtOAc/Petrol); **FTIR** (ν_{max} cm⁻¹, thin film) = 2951, 2870, 1678, 1599, 1512, 1465, 1320, 1259, 1172, 1122, 1028, 837; **¹H NMR (500 MHz, CDCl₃)** δ = 7.96 (d, *J* = 8.9 Hz, 2H), 6.94 (d, *J* = 8.9 Hz, 2H), 3.87 (s, 3H), 3.63 – 3.39 (m, 6H), 3.13 – 2.96 (m, 2H), 2.41 – 2.28 (m, 2H), 2.21 – 2.12 (m, 2H), 0.98 (s, 3H), 0.93 (s, 3H); **¹³C NMR (126 MHz, CDCl₃)** δ = 198.2, 163.6, 130.4, 130.1, 99.5, 70.3, 55.6, 39.2, 32.3, 29.7, 27.8, 27.4, 22.9, 22.74; **HRMS** (ES⁺) [C₁₈H₂₆O₂Br] requires 385.1014, found 385.1016.

6-bromo-1-(4-(tert-butyl)phenyl)hexan-1-one (32)

Prepared according to General Procedure using **28** (70 mg) at 20 mA, using RM-4 (10 mol%) passing 9 F/mol of charge. The crude was purified by flash column chromatography (5→10 % EtOAc/Petrol, silica gel) to afford **32** (45 mg, 48%) as a colourless oil.

R_f = 0.31 (15% EtOAc/Petrol); **FTIR** (ν_{max} cm⁻¹, thin film) = 2965, 2868, 1682, 1604, 1465, 1403, 1361, 1265, 1203, 1193, 1148, 1107, 980, 828; **¹H NMR (500 MHz, CDCl₃)** δ = 7.97 – 7.85 (m, 2H), 7.57 – 7.41 (m, 2H), 3.44 (t, J = 6.8 Hz, 2H), 3.13 – 2.85 (m, 2H), 2.02 – 1.85 (m, 2H), 1.83 – 1.70 (m, 2H), 1.61 – 1.46 (m, 2H), 1.35 (s, 9H); **¹³C NMR (126 MHz, CDCl₃)** δ = 200.0, 156.6, 134.5, 128.1, 125.7, 38.3, 33.9, 32.8, 31.2, 28.0, 23.5; **HRMS** (ES⁺) [C₁₆H₂₄O₂Br] requires 311.1011, found 311.1016.

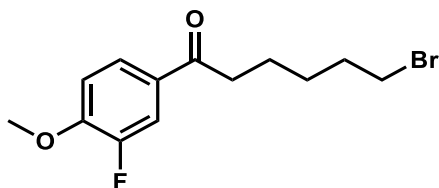
6-bromo-1-(4-((tert-butyldimethylsilyl)oxy)phenyl)hexan-1-one (33)



Prepared according to General Procedure using **30** (67 mg) passing 6 F/mol of charge. The crude was purified by flash column chromatography (5→10 % EtOAc/Petrol, silica gel) to afford **32** (89 mg, 51%) as a colourless oil.

R_f = 0.61 (15% EtOAc/Petrol); **FTIR** (ν_{max} cm⁻¹, thin film) = 2935, 2862, 1676, 1595, 1510, 1463, 1417, 1363, 1255, 1203, 1148, 1069, 969, 835; **¹H NMR (500 MHz, CDCl₃)** δ = 7.92 – 7.85 (m, 2H), 6.92 – 6.82 (m, 2H), 3.43 (t, J = 6.8 Hz, 2H), 2.93 (t, J = 6.9 Hz, 2H), 2.00 – 1.86 (m, 2H), 1.81 – 1.71 (m, 2H), 1.58 – 1.47 (m, 2H), 0.99 (s, 9H), 0.23 (s, 6H); **¹³C NMR (126 MHz, CDCl₃)** δ = 198.9, 160.3, 130.7, 130.3, 120.1, 38.1, 33.8, 32.8, 28.1, 25.7, 23.6, 18.4, -4.22; **HRMS** = (ES⁺) [C₁₈H₃₀O₂SiBr] requires 385.1198, found 385.1207.

6-bromo-1-(3-fluoro-4-methoxyphenyl)hexan-1-one (34)



Prepared according to General Procedure using **30** (67 mg) passing 6 F/mol of charge. The crude was purified by flash column chromatography (5→10 % EtOAc/Petrol, silica gel) to afford **34** (46 mg, 51%) as a colourless oil.

R_f = 0.39 (15% EtOAc/Petrol); **FTIR** (ν_{max} cm⁻¹, thin film) = 2930, 2857, 1678, 1599, 1505, 1464, 1411, 1263, 1166, 911, 842, 781; **¹H NMR (500 MHz, CDCl₃)** δ = 7.74 (ddd, J = 8.5, 2.1, 1.1 Hz, 1H), 7.70 (dd, J = 11.9, 2.1 Hz, 1H), 7.00 (t, J = 8.3 Hz, 1H), 3.96 (s, 3H), 3.43 (t, J = 6.7 Hz, 2H), 2.92 (t, J = 7.3 Hz, 2H), 2.00 – 1.85 (m, 2H), 1.76 (dt, J = 15.1, 7.4 Hz, 2H), 1.54 – 1.49 (m, 2H); **¹³C NMR (126 MHz, CDCl₃)** δ = 197.8, 152.0, 130.4, 125.4, 115.9, 112.5, 56.4, 38.1, 33.8, 32.6, 28.0, 23.5; **HRMS (ES⁺)** [C₁₃H₁₇O₂FBr] requires 303.0396, found 303.0406.

6.5. Experimental for Flow Electrochemical Scale Up

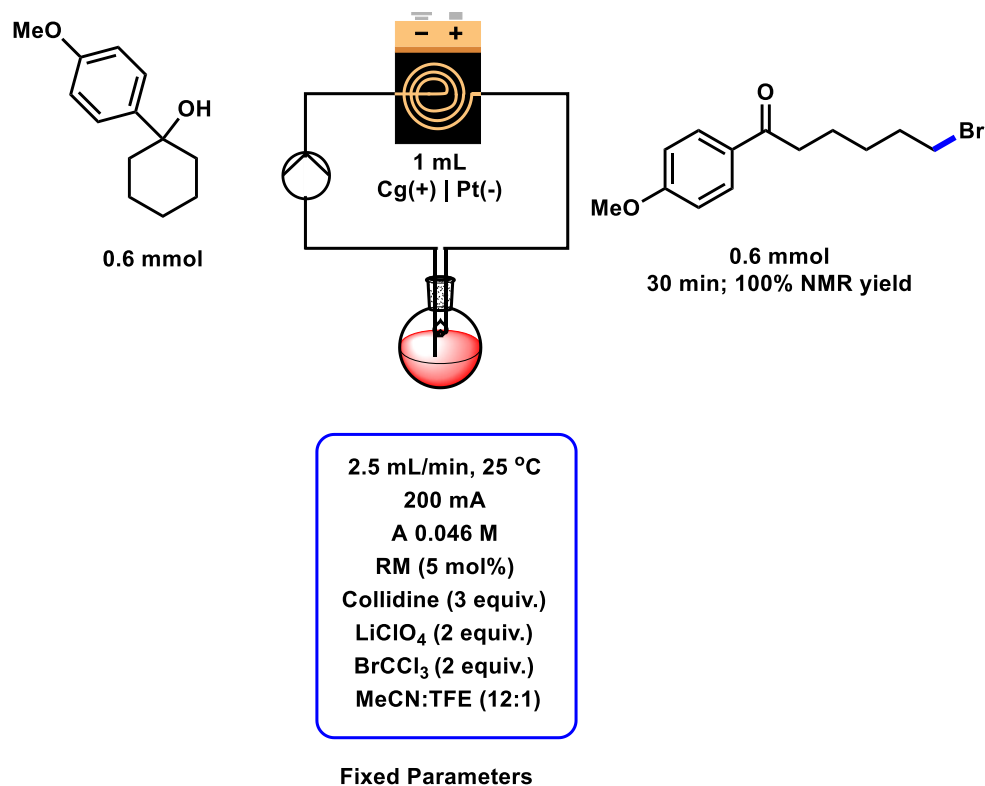
General Methods for Flow Processes

The flow setup used PFA tubing with a 0.79 ± 0.1 mm internal diameter and 1.58 ± 0.1 mm outer diameter supplied by Polyflon. All flow fittings and connections were purchased from Kinesis (Gripper fitting nuts, part number: 002103; Adapters, part number: P-618; Omnilok type-p fitting ferrule, part number: 008FT16; Y-Connector, part number: P-512; Threaded union, part number: P-623; 40 psi Back pressure regulator (used as check valve for DCM pump, Scheme S3) part number: P-785). Pumps used was Knauer P4.1S and P2.1S Azura HPLC pumps. Pumps were calibrated by pumping solvent into a measuring cylinder, recording the time taken for the desired volume to be dispensed and then adjusting the pump's flow rate to the correct value, if required. The power supply used was a Voltcraft LRP-1205 that supplied DC to the electrochemical system. The electrochemical flow cell was purchased from Cambridge Reactor Design, the Ammonite 8 (part number: 74660). The electrochemical flow cell consists of carbon/platinum electrodes that are fixed either side of a FFKM gasket with a channel groove length of 1000 mm and an internal volume of 2.5 mL, of which 1 mL is exposed to the electrodes. The inlet and outlet fittings of the ammonite 8 cell were modified from 1/16" ID to accommodate 1/32" ID PFA tubing using Swagelok reducers, nuts and ferrules.

The electrochemical cell was dismantled after 3 runs, and electrodes were washed with IPA and MeCN. Graphite electrode was polished using silica 230-400 particle size with cotton. Platinum electrode was washed with IPA and MeCN and prior to use was burned on Bunsen burner to remove any organic/ inorganic impurities.

The electrochemical reactor was used in three modes of operation, **mode 1** for exploring recirculating parameters, **mode 2** for single pass experiments.

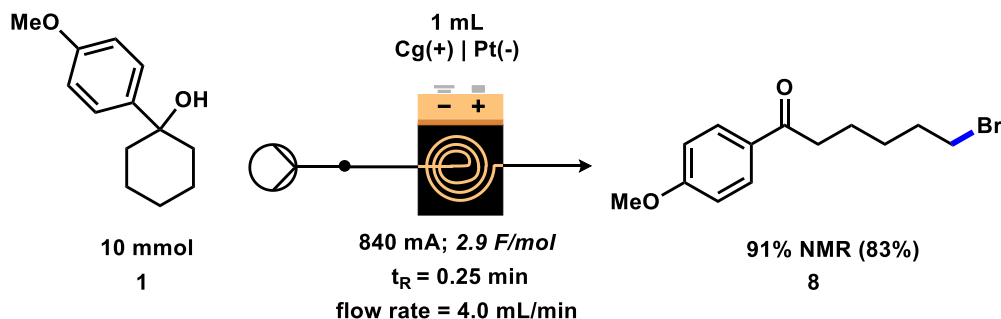
6.5.1. Recirculating Flow



A 25 mL round-bottom flask and stirrer bar was flame dried and charged with **1** (0.6 mmol, 0.125 g), RM-2 (0.06 mmol, 10 mg), collidine (1.8 mmol, 240 μ L) and sealed with a Suba-seal and parafilm. The reagent flask was evacuated on a Schlenk line and back filled with nitrogen gas for three cycles. Both the inlet and outlet tubing of the electrochemical flow system were pushed through the Suba-seal and the reagents dissolved with dry degassed MeCN (12 mL) and trifluoroethanol (1 mL). The reaction mixture was then purged with N₂ for 10 min. BrCCl₃ (120 μ L) was then added under N₂. The HPLC pump was primed with the reaction mixture and set to recirculate at 2.5 mL/min. The electrolysis was then commenced and conducted at a constant current of 400 mA, the recirculated reaction was monitored by TLC until completion, which, at this scale required 30 min.

Upon completion, electrolysis was turned off and 0.2 mmol of trimethoxy benzene was added as an internal standard. The crude reaction mixture was then analyzed by ¹H NMR spectroscopy, which showed quantitative yield.

6.5.2. Single Pass Flow



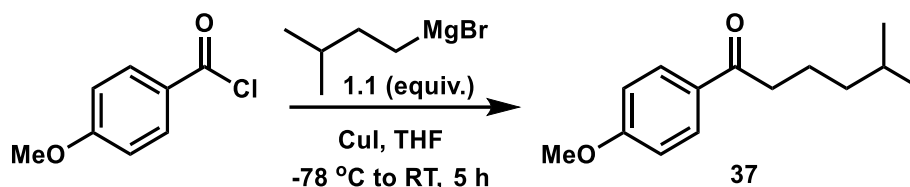
A 500 mL round-bottom flask and stirrer bar was flame dried and charged with **1** (10.0 mmol, 2.06 g), RM-2 (0.5 mmol, 168 mg), collidine (4.0 mL) and sealed with a Suba-seal and parafilm. The reagent flask was evacuated on a Schlenk line and back filled with nitrogen gas for three cycles. Both the inlet and outlet tubing of the electrochemical flow system were pushed through the Suba-seal and the reagents dissolved with dry degassed MeCN (200 mL) and trifluoroethanol (16.6 mL). The reaction mixture was then purged with N₂ for 10 min. BrCCl₃ (1.9 mL) was then added under N₂.

The HPLC pump was primed with the reaction mixture and flow was set to 4.0 mL/min at constant current of 840 mA. HPLC pumping was initiated, and the outlet of the flow system was set to waste for the first 3.46 mL (representing 1 whole flow path volume, inclusive of tubing, connectors and reactor) of reaction mixture to allow the flow system to be filled. After this initial priming, the power supply was switched on and the electrolysis commenced at a constant current with the system outlet still set to waste for a further 2.5 mL (representing a total volume from 'in' to 'out' of the electrochemical reactor; exposed electrochemical path = 1 mL). The outlet stream of the flow system was then collected for 205 mL.

After the end of electrolysis, to the collected volume was added sat. NH₄Cl (50 mL) and extracted with EtOAc (100 mL). The organic layer was then washed with aq. CuSO₄ (25 mL x 2). The organic layer was then dried over MgSO₄ and concentrated under reduced pressure. The crude residue this obtained was purified by flash column chromatography (5→10 % EtOAc/Petrol, silica gel) to afford **8** (2.3 g, 83%) as off white solid.

6.6. Substrate Synthesis (PCET-HAT-FG Migration)

1-(4-methoxyphenyl)-5-methylhexan-1-one (37)

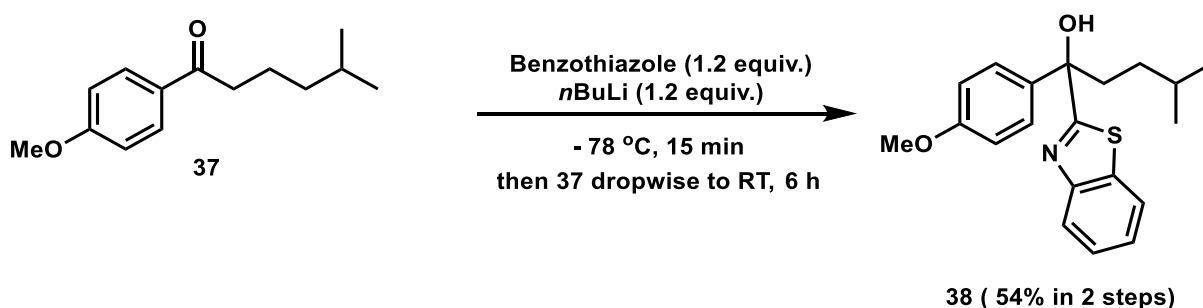


Synthesis of Grignard: To an oven dried three-neck equipped with air condenser 100 mL RBF was added Mg (1.4 g, 58 mmol, 1.5 equiv.) was heated with Bunsen burner under vacuum. Upon cooling to ambient temperature, the flask was brought under N₂ atmosphere and added a crystal of I₂. To this was then added dry THF (20 mL) and the mixture was stirred. 1-Bromo-3-methylbutane (4.8 mL, 40 mmol) was added initially 1.45 mL to initiate the reaction once initiated, the rest of alkyl bromide was added dropwise. The reaction was then stirred for 3 hours at 40 °C. After 4 hours the resulting solution was cooled to room temperature and used as such.

Synthesis of ketone 37: To an oven 500 mL flask was added *p*-anisoyl chloride (4.7 mL, 35 mmol), CuI (666 mg, 10 mol%) and THF (150 mL). The flask was cooled to -78 °C keeping under the N₂ atmosphere. Freshly prepared Grignard (20 mL, 2 M appx, 1.1 equiv.) was then added dropwise to the reaction mixture at -78 °C. The resulting reaction mixture was then allowed to warm slowly to room temperature and stirred for 5 h. The reaction mixture was then quenched with water, extracted with ether, combined organic layers were dried over MgSO₄ and concentrated under reduced pressure. The crude residue was purified by flash column chromatography (100 % Petrol, silica gel) to afford **37** (4.1 g, 52%) as a colourless liquid.

R_f = 0.7 (10% EtOAc/Petrol); **¹H NMR (400 MHz, CDCl₃)** δ = 7.94 (d, *J* = 9.0 Hz, 2H), 6.93 (d, *J* = 8.9 Hz, 2H), 3.86 (s, 3H), 2.94 – 2.87 (m, 2H), 1.69 – 1.53 (m, 3H), 0.94 (d, *J* = 6.3 Hz, 6H); **¹³C NMR (101 MHz, CDCl₃)** δ = 199.5, 163.4, 130.5, 130.3, 113.8, 55.6, 36.5, 33.7, 28.1, 22.6

These data are consistent with those previously reported in the literature.⁸⁰

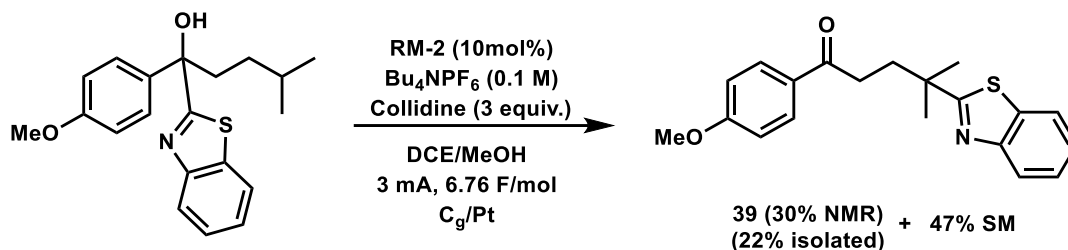
1-(benzo[d]thiazol-2-yl)-1-(4-methoxyphenyl)-4-methylpentan-1-ol (38)

Synthesis of 38: To an oven dried 250 mL RBF was added benzothiazole (1.3 mL, 12 mmol, 1.2 equiv.), THF (20 mL) and cooled to -78 °C. *n*BuLi (5.75 mL, 2.5 M in THF, 1.2 equiv.) was added dropwise to the above solution at -78 °C ab stirred and the resulting yellow solution was then stirred for 15 min. at -78 °C. After 15 min. ketone **37** (1.76 g, 10 mmol, 1 equiv.) was added dropwise maintain temperature of -78 °C. After the addition of ketone **37**, the reaction the reaction mixture was allowed to warm to room temperature and stirred for additional 6 h. The reaction mixture was quenched with aq. NH₄Cl, extracted with EtOAc, combined organic layers were dried over MgSO₄ and concentrated under reduced pressure. The crude residue was purified by flash column chromatography (5 → 10 % EtOAc/Petrol, silica gel) to afford **38** (1.5 g, 45%) as a yellow solid.

R_f = 0.21 (15% EtOAc/Petrol); **¹H NMR (400 MHz, CDCl₃)** δ = 7.99 (dd, *J* = 8.2, 0.5 Hz, 1H), 7.85 – 7.77 (m, 1H), 7.58 (d, *J* = 8.9 Hz, 2H), 7.45 (ddd, *J* = 8.3, 7.2, 1.2 Hz, 1H), 7.34 (ddd, *J* = 8.3, 7.2, 1.2 Hz, 1H), 6.88 (d, *J* = 8.9 Hz, 1H), 3.79 (s, 3H), 2.48 – 2.37 (m, 2H), 1.58 (dt, *J* = 13.3, 6.7 Hz, 1H), 1.38 – 1.15 (m, 2H), 0.89 (d, *J* = 1.0 Hz, 6H); **¹³C NMR (126 MHz, CDCl₃)** δ = 178.94, 159.08, 152.77, 136.42, 135.89, 127.01, 126.08, 125.05, 123.21, 121.82, 113.84, 78.79, 55.37, 40.63, 32.47, 28.38, 22.73, 22.67

These data are consistent with those previously reported in the literature.⁸¹

6.7. Electrochemical Reaction (PCET-HAT-FG Migration)



Experimental Procedure: To an oven dried 10 mL electrosyn vial, tertiary alcohol 38 (102 mg, 0.30 mmol), redox-mediator (5 mol%), collidine dried over molecular sieves (3.0 equiv), Bu_4NPF_6 (2 equiv) was taken, and the vial was sealed with electrosyn cap comprised of a graphite (anode) and platinum (cathode). The vial was back filled with nitrogen (three cycles) and dry DCE (6 mL) and MeOH dried over molecular sieves (0.5 mL) was added under nitrogen atmosphere. The vial was then purged with nitrogen for 10 minutes. The reaction mixture was electrolysed using electrosyn 2.0 at constant current of 3.0 mA until 6.76 Fmol^{-1} of charge (3.37 hours) has been passed at ambient temperature. To the reaction mixture was then added 0.1 mmol of trimethoxybenzene as an internal standard to get the crude NMR yield.

The reaction was quenched with aq. NH_4Cl , washed with aq. CuSO_4 solution, and extracted with EtOAc (10 mL X 2). The organic layer was dried over MgSO_4 and distilled under reduced pressure. The crude residue obtained was purified flash column chromatography (5→10 % EtOAc/Petrol, silica gel) to afford 39 (22 mg, 22%) as yellow oil.

R_f = 0.17 (15% EtOAc/Petrol); $^1\text{H NMR}$ (400 MHz, CDCl_3) δ = 8.01 (d, J = 8.2 Hz, 1H), 7.91 – 7.83 (m, 3H), 7.46 (ddd, J = 8.3, 7.2, 1.3 Hz, 1H), 7.36 (ddd, J = 8.2, 7.2, 1.2 Hz, 1H), 6.87 (d, J = 8.9 Hz, 2H), 3.84 (s, 3H), 3.03 – 2.74 (m, 2H), 2.38 – 2.15 (m, 2H), 1.57 (s, 6H); $^{13}\text{C NMR}$ (126 MHz, CDCl_3) δ = 198.5, 180.7, 163.5, 152.7, 134.8, 130.5, 130.0, 126.2, 125.1, 122.7, 121.7, 113.7, 55.5, 41.3, 38.3, 34.1, 28.9; ; **HRMS** (ES^+) [$\text{C}_{20}\text{H}_{22}\text{NO}_2\text{S}$] requires 340.1371, found 340.1371.

These data are consistent with those previously reported in the literature.⁸¹

6.8. References

- 1 M. Schmittl and A. Burghart, *ChemInform*, 2010, **29**, 2550–2589.
- 2 K. Uneyama, H. Asai, Y. Dan-Oh and H. Matta, *Electrochim. Acta*, 1997, **42**, 2005–2007.
- 3 S. Torii, K. Uneyama and M. Ono, *Tetrahedron Lett.*, 1980, **21**, 2741–2744.
- 4 Tung Siu, and Christine J. Picard and A. K. Yudin*, *J. Org. Chem.*, 2005, **70**, 932–937.
- 5 A. Guirado, A. Zapata, J. L. Gómez, L. Trabalón and J. Gálvez, *Tetrahedron*, 1999, **55**, 9631–9640.
- 6 L.-J. Li, Y.-Y. Jiang, C. M. Lam, C.-C. Zeng, L.-M. Hu and R. D. Little, *J. Org. Chem.*, 2015, **80**, 11021–11030.
- 7 F. Kakiuchi, T. Kochi, H. Mutsutani, N. Kobayashi, S. Urano, M. Sato, S. Nishiyama and T. Tanabe, *J. Am. Chem. Soc.*, 2009, **131**, 11310–11311.
- 8 J. Yoshida, R. Hayashi and A. Shimizu, *Green Oxid. Org. Synth.*, 2019, 409–437.
- 9 T. Sunaga, M. Atobe, S. Inagi and T. Fuchigami, *Chem. Commun.*, 2009, 956–958.
- 10 F. Bu, L. Lu, X. Hu, S. Wang, H. Zhang and A. Lei, *Chem. Sci.*, 2020, **11**, 10000–10004.
- 11 T. Morofuji, A. Shimizu and J. Yoshida, *J. Am. Chem. Soc.*, 2013, **135**, 5000–5003.
- 12 L. D. Pachón, C. J. Elsevier and G. Rothenberg, *Adv. Synth. Catal.*, 2006, **348**, 1705–1710.
- 13 Y. Yuan and A. Lei, *Acc. Chem. Res.*, 2019, **52**, 3309–3324.
- 14 Y. Gao, Y. Wang, J. Zhou, H. Mei and J. Han, *Green Chem.*, 2018, **20**, 583–587.
- 15 H. Takakura and S. Yamamura, *Tetrahedron Lett.*, 1999, **40**, 299–302.
- 16 C. Zhu, N. W. J. Ang, T. H. Meyer, Y. Qiu and L. Ackermann, *ACS Cent. Sci.*, 2021, **7**, 415–431.
- 17 B. A. Frontana-Urbe, R. D. Little, J. G. Ibanez, A. Palma and R. Vasquez-Medrano, *Green Chem.*, 2010, **12**, 2099–2119.
- 18 M. Yan, Y. Kawamata and P. S. Baran, *Chem. Rev.*, 2017, **117**, 13230–13319.
- 19 V. Alessandro, *Philos. Trans. R. Soc. London*, 1800, **90**, 403–431.
- 20 F. Michael, *Philos. Trans. R. Soc. London*, 1834, **124**, 77–122.
- 21 F. Joschka Holzhäuser, J. B. Mensah and Regina Palkovits, *Green Chem.*, 2020, **22**, 286–301.
- 22 A. Hickling, *Trans. Faraday Soc.*, 1942, **38**, 27–33.

- 23 *Nat.* 1959 1844695, 1959, **184**, 1271–1271.
- 24 J. E. B. Randles, *Trans. Faraday Soc.*, 1948, **44**, 327–338.
- 25 C. Kingston, M. D. Palkowitz, Y. Takahira, J. C. Vantourout, B. K. Peters, Y. Kawamata and P. S. Baran, *Acc. Chem. Res.*, 2019, **53**, 72–83.
- 26 H. Kunkely, A. Merz and A. Vogler, *J. Am. Chem. Soc.*, 2002, **105**, 7241–7243.
- 27 B. Lee, H. Naito, M. Nagao and T. Hibino, *Angew. Chemie Int. Ed.*, 2012, **51**, 6961–6965.
- 28 L. E. Sattler, C. J. Otten and G. Hilt, *Chem. – A Eur. J.*, 2020, **26**, 3129–3136.
- 29 S. Rodrigo, C. Um, J. C. Mixdorf, D. Gunasekera, H. M. Nguyen and L. Luo, *Org. Lett.*, 2020, **22**, 2021.
- 30 L. Schulz, S. R. Waldvogel, L. Schulz and S. R. Waldvogel, , DOI:10.1055/s-0037-1610303.
- 31 T. Shono, *Compr. Org. Synth.*, 1991, 789–813.
- 32 J. M. Friedrich, C. Ponce-de-León, G. W. Reade and F. C. Walsh, *J. Electroanal. Chem.*, 2004, **561**, 203–217.
- 33 T. X. Huong Le, M. Bechelany and M. Cretin, *Carbon N. Y.*, 2017, **122**, 564–591.
- 34 D. M. Heard and A. J. J. Lennox, *Angew. Chemie Int. Ed.*, 2020, **59**, 18866–18884.
- 35 G. Hilt, *ChemElectroChem*, 2020, **7**, 395–405.
- 36 M. Rafiee, M. N. Mayer, B. T. Punchihewa and M. R. Mumau, *J. Org. Chem.*, , DOI:10.1021/ACS.JOC.1C01391.
- 37 R. Francke and R. D. Little, *Chem. Soc. Rev.*, 2014, **43**, 2492–2521.
- 38 J. Simmonet and J. F. Pilard, *organic electrochemistry*, 2001.
- 39 R. Francke and R. D. Little, *Chem. Soc. Rev.*, 2014, **43**, 2492–2521.
- 40 C. C. Zeng, N. T. Zhang, C. M. Lam and R. D. Little, *Org. Lett.*, 2012, **14**, 1314–1317.
- 41 J. A. Miranda, C. J. Wade and R. Daniel Little, , DOI:10.1021/jo051148.
- 42 R. D. Little, *Chem. Rev.*, 2002, **96**, 93–114.
- 43 N. Elgrishi, K. J. Rountree, B. D. McCarthy, E. S. Rountree, T. T. Eisenhart and J. L. Dempsey, *J. Chem. Educ.*, 2017, **95**, 197–206.
- 44 C. Sandford, M. A. Edwards, K. J. Klunder, D. P. Hickey, M. Li, K. Barman, M. S. Sigman, H. S. White and S. D. Minter, *Chem. Sci.*, 2019, **10**, 6404–6422.
- 45 M. M. Baizer, *Pure Appl. Chem.*, 1986, **58**, 889–894.
- 46 B. R. Rosen, E. W. Werner, A. G. O'Brien and P. S. Baran, *J. Am. Chem. Soc.*, 2014, **136**, 5571–5574.
- 47 P. S. B. and and J. M. Richter, *J. Am. Chem. Soc.*, 2004, **126**, 7450–7451.
- 48 W. H. Perkin and S. H. Tucker, *J. Chem. Soc. Trans.*, 1921, **119**, 216–225.

- 49 J. F. Ambrose, L. L. Carpenter and R. F. Nelson, *J. Electrochem. Soc.*, 1975, **122**, 876.
- 50 W. E. Geiger†, *Organometallics*, 2007, **26**, 5738–5765.
- 51 P. Gandeepan and L. Ackermann, *Chem*, 2018, **4**, 199–222.
- 52 K. M. Engle, T.-S. Mei, X. Wang and J.-Q. Yu, *Angew. Chemie Int. Ed.*, 2011, **50**, 1478–1491.
- 53 F. Xu, Y.-J. Li, C. Huang and H.-C. Xu, *ACS Catal.*, 2018, **8**, 3820–3824.
- 54 N. Chen and H.-C. Xu, *Green Synth. Catal.*, 2021, **2**, 165–178.
- 55 M. D. Kärkäs, *Chem. Soc. Rev.*, 2018, **47**, 5786–5865.
- 56 M. D. Kärkäs, *ACS Catal.*, 2017, **7**, 4999–5022.
- 57 Z.-W. Hou, Z.-Y. Mao, H.-B. Zhao, Y. Y. Melcamu, X. Lu, J. Song and H.-C. Xu, *Angew. Chemie Int. Ed.*, 2016, **55**, 9168–9172.
- 58 A. Hu, J.-J. Guo, H. Pan, H. Tang, Z. Gao and Z. Zuo, *J. Am. Chem. Soc.*, 2018, **140**, 1612–1616.
- 59 J. J. Guo, A. Hu and Z. Zuo, *Tetrahedron Lett.*, 2018, **59**, 2103–2111.
- 60 J.-F. Zhao, B.-H. Tan and T.-P. Loh, *Chem. Sci.*, 2011, **2**, 349–352.
- 61 H. Zeng, P. Pan, J. Chen, H. Gong and C.-J. Li, *European J. Org. Chem.*, 2017, **2017**, 1070–1073.
- 62 W. J. Leigh and J. A. Postigo, <https://doi.org/10.1139/v95-028>, 2011, **73**, 191–203.
- 63 V. Dhayalan, C. Sämann and P. Knochel, *Chem. Commun.*, 2015, **51**, 3239–3242.
- 64 V. L. van Zyl, A. Muller and D. B. G. Williams, *Tetrahedron Lett.*, 2018, **59**, 918–921.
- 65 Y. Sun, X. Huang, X. Li, F. Luo, L. Zhang, M. Chen, S. Zheng and B. Peng, *Adv. Synth. Catal.*, 2018, **360**, 1082–1087.
- 66 E. Lee-Ruff and D. Wells, <http://dx.doi.org/10.1080/15257770802088886>, 2008, **27**, 484–494.
- 67 L. Huan and C. Zhu, *Org. Chem. Front.*, 2016, **3**, 1467–1471.
- 68 M. S. Gowda, S. S. Pande, R. A. Ramakrishna and K. R. Prabhu, *Org. Biomol. Chem.*, 2011, **9**, 5365–5368.
- 69 W. Schliemann, A. Buege and L. Reppel, *Pharmazie*, 1980, **35**, 140–143.
- 70 R. L. Zhai, Y. S. Xue, T. Liang, J. J. Mi and Z. Xu, *J. Org. Chem.*, 2018, **83**, 10051–10059.
- 71 X. Fan, H. Zhao, J. Yu, X. Bao and C. Zhu, *Org. Chem. Front.*, 2016, **3**, 227–232.
- 72 Y. Wen, G. Chen, S. Huang, Y. Tang, J. Yang and Y. Zhang, *Adv. Synth. Catal.*, 2016, **358**, 947–957.
- 73 K. Jia, F. Zhang, H. Huang and Y. Chen, *J. Am. Chem. Soc.*, 2016, **138**, 1514–1517.
- 74 J. Wang, B. Huang, C. Shi, C. Yang and W. Xia, *J. Org. Chem.*, 2018, **83**, 9696–9706.

- 75 L. Schnaubelt, H. Petzold, E. Dmitrieva, M. Rosenkranz and H. Lang, *Dalt. Trans.*, 2018, **47**, 13180–13189.
- 76 L. Huang, T. Ji and M. Rueping, *J. Am. Chem. Soc.*, 2020, **0**, 3–10.
- 77 P. Thamaraiselvi, E. Varathan, V. Subramanian and S. Easwaramoorthi, *Dye. Pigment.*, 2020, **172**, 107838.
- 78 X. Fan, H. Zhao, J. Yu, X. Bao and C. Zhu, *Org. Chem. Front.*, 2016, **3**, 227–232.
- 79 H. G. Yayla, H. Wang, K. T. Tarantino, H. S. Orbe and R. R. Knowles, *J. Am. Chem. Soc.*, 2016, **138**, 10794–10797.
- 80 J. Wang, Y.-B. Pang, N. Tao, R.-S. Zeng and Y. Zhao, *J. Org. Chem.*, 2019, **84**, 15315–15322.
- 81 X. Wu, M. Wang, L. Huan, D. Wang, J. Wang and C. Zhu, *Angew. Chemie*, 2018, **130**, 1656–1660.
- 82 M. Zhang, X. Ding, A. Lu, J. Kang, Y. Gao, Z. Wang, H. Li and Q. Wang, *Org. Chem. Front.*, 2021, **8**, 961–967.
- 83 J. Barluenga, F. J. Fañanás, R. Sanz, C. Marcos and J. M. Ignacio, , DOI:10.1039/b414966a.

ॐ सर्वे भवन्तु सुखिनः
सर्वे सन्तु निरामयाः ।
सर्वे भद्राणि पश्यन्तु
मा कश्चिद्दुःखभाग्भवेत् ।
ॐ शान्तिः शान्तिः शान्तिः ॥

Om Sarve Bhavantu Sukhinah
Sarve Santu Niraamayaah |
Sarve Bhadraanni Pashyantu
Maa Kashcid-Duhkha-Bhaag-Bhavet |
Om Shaantih Shaantih Shaantih ||

Meaning:

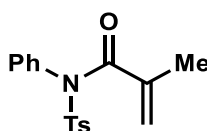
- 1: Om, May All be Happy,
- 2: May All be Free from Illness.
- 3: May All See what is Auspicious,
- 4: May no one Suffer.
- 5: Om Peace, Peace, Peace.

Chapter 7: Experimental – Electrochemical Alkene Functionalization

7. Experimental and Characterization Data

7.1 Substrate Synthesis (Electrochemical Alkene Trifluoromethylation)

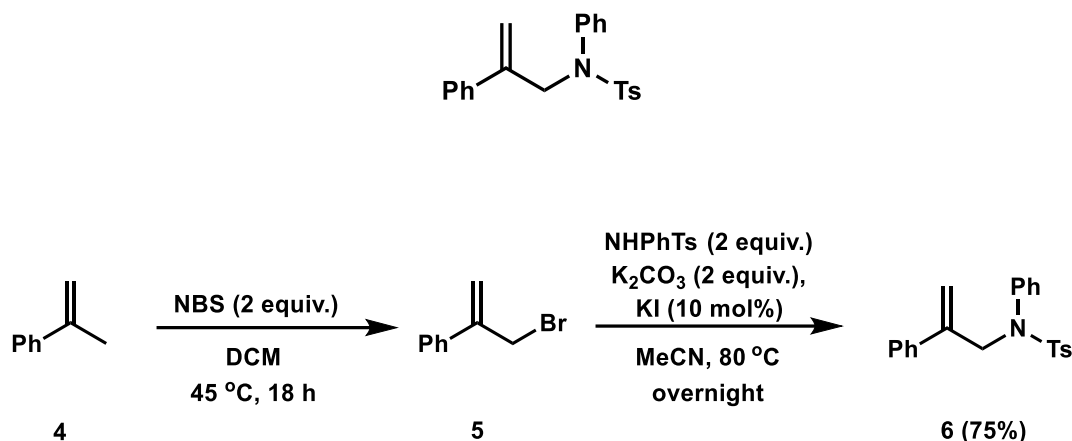
N-phenyl-N-tosylmethacrylamide (**3**)



To a 250 mL round bottom was added amine (2.47 g, 10 mmol, 1 equiv.), 4-dimethylaminopyridine (122 mg, 10 mol %), triethylamine (2.8 mL, 2 eq.) and CH₂Cl₂ (50 mL). The solution was stirred then cooled to 0 °C using an ice bath. Methacryloyl chloride (1.9 mL, 20 mmol, 2 eq.) was added dropwise by syringe over 15 minutes turning the solution bright yellow. The mixture was stirred at 0 °C for 30 mins before being allowed to warm to room temperature and stir overnight. The mixture was quenched with saturated sodium bicarbonate solution (50 mL), layers separated, and organics washed with saturated sodium bicarbonate solution (2 x 50 mL). The aqueous was extracted CH₂Cl₂ (2 x 50 mL) and organics combined. The organics were washed with water (50 mL), dried over MgSO₄ and concentrated *in vacuo* to crude product. Purification by flash column chromatography (10% EtOAc/Petrol, silica gel) to afford **3** (2.06 g, 66%) as white solid.

R_f = 0.19 (15% EtOAc/Petrol); **¹H NMR (500 MHz, CDCl₃)** δ = 7.87 – 7.64 (m, 2H, ArH), 7.49 – 7.35 (m, 3H, ArH), 7.29 (dt, *J* = 8.0, 0.7 Hz, 2H, ArH), 7.19 – 7.08 (m, 2H, ArH), 5.38 – 5.36 (m, 1H, =CH₂), 5.25 – 5.23 (m, 1H, =CH₂), 2.44 (s, 3H, N-CH₃), 1.67 (s, 3H, CH₃); **¹³C NMR (126 MHz, CDCl₃)** δ = 171.1, 144.9, 139.5, 137.3, 135.4, 130.1, 129.5, 129.4, 129.3, 124.5, 21.8, 19.3.

These data are consistent with those previously reported in the literature.⁸²

4-Methyl-N-phenyl-N-(2-phenylallyl)benzenesulfonamide (6)

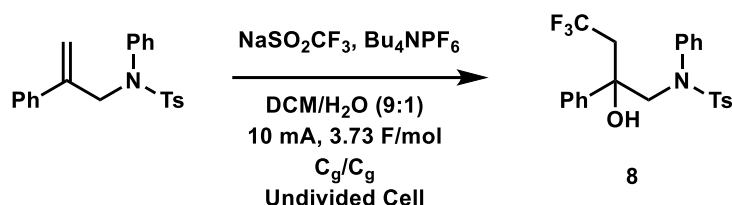
To a solution of alpha methyl styrene (2.6 mL, 20 mmol) in DCM (70 mL) was added NBS (7.11 g, 40 mmol) and the reaction was stirred for 18 h at 45 °C. The reaction was quenched with water, extracted with DCM, dried over MgSO_4 , and concentrated under reduced pressure to afford crude **5** as a colourless oil which was used without purification.

In a 100 mL RBF fitted with air condenser was charged **5** (1.0 g, 5 mmol, 1 equiv.), NhPhTs (2.56 g, 10 mmol, 2 equiv.), K_2CO_3 (1.4 g, 10 mmol, 2 equiv.), and KI (83 mg, 10 mol%). To this MeCN (16 mL) was added and the reaction mixture was stirred overnight at 80 °C. After that, the reaction was cooled to room temperature and filtered through a celite pad. The resulting solution was concentrated under reduced pressure. The crude mixture was purified by flash column chromatography (10% EtOAc/Petrol, silica gel) to afford **6** (1.02 g, 55%) as off white solid.

R_f = 0.21 (15% EtOAc/Petrol); $^1\text{H NMR}$ (500 MHz, CDCl_3) δ = 7.51 – 7.44 (m, 2H), 7.41 – 7.28 (m, 5H), 7.25 – 7.15 (m, 4H), 6.84 – 6.76 (m, 2H), 5.27 (t, J = 0.8 Hz, 1H), 5.04 (q, J = 1.2 Hz, 1H), 4.67 – 4.56 (m, 2H), 2.43 (s, 3H); $^{13}\text{C NMR}$ (126 MHz, CDCl_3) δ 143.6, 142.5, 138.6, 138.3, 135.1, 129.5, 129.1, 128.7, 128.3, 128.1, 127.9, 127.9, 126.7, 117.1, 54.4, 21.7.

These data are consistent with those previously reported in the literature.⁸³

7.2 Electrochemical Reaction (Electrochemical Alkene Trifluoromethylation)



In a 10 mL oven dried electrasyn vial was added **6** (109 mg, 0.30 mmol, 1 equiv.), Bu₄NPF₆ (232 mg, 0.6 mmol, 2 equiv.), NaSO₂CF₃ (94 mg, 0.6 mmol, 2 equiv.), DCM (5 mL), water (1.0 mL). Electrasyn cap fitted with graphite as the anode and cathode was put on the vial. Electrolysis was carried out at constant current of 10 mA until 3.73 F/mol of charge has been passed at ambient temperature. At the end of the electrolysis, the reaction mixture was washed with water (10 mL x 2), combined organic layers were dried over MgSO₄, and concentrated under reduced pressure. The crude mixture was purified by column chromatography (15% EtOAc/Petrol, silica gel) to afford **8** (94 mg, 70%) as a white solid.

R_f = 0.14 (15% EtOAc/Petrol); **M.p.**: 119-121 °C; **FTIR** (ν_{max} cm⁻¹, thin film) = 3491, 1598, 1494, 1448, 1375, 1336, 1261, 1228, 1157, 1114; **¹H NMR (500 MHz, CDCl₃)** δ = 7.41 – 7.36 (m, 2H, ArH), 7.32 – 7.27 (m, 2H, ArH), 7.25 – 7.12 (m, 8H, ArH), 6.75 – 6.66 (m, 2H, ArH), 4.12 (d, J = 15.0 Hz, 1H, CH₂), 3.90 (s, 1H, O-H), 3.75 (d, J = 15.1 Hz, 1H, CH₂), 2.85 (dq, J = 15.5, 10.4 Hz, 1H, CF₃-CH₂), 2.70 (dq, J = 15.5, 10.9 Hz, 1H, CF₃-CH₂), 2.41 (s, 3H, Ts-CH₃); **¹³C NMR (126 MHz, CDCl₃)** δ = 144.3 (ArC), 142.1 (ArC), 141.3 (ArC), 134.3 (ArC), 129.7 (ArC), 129.1 (ArC), 128.9 (ArC), 128.2 (ArC), 128.1 (ArC), 128.1 (ArC), 127.5 (ArC), 125.1 (ArC), 74.6 (d, J = 2.1 Hz), 61.96 (d, J = 1.9 Hz), 43.3 (q, J = 26.3 Hz, CF₃), 21.7; **¹⁹F NMR (471 MHz, Chloroform-*d*)** δ = -58.78. **HRMS (ES⁺)** [C₂₃H₂₁NO₂F₃S] requires [M-H₂O] 432.1245, found 432.1245.

7.3 X-ray: Oxytrifluoromethylated Product 8 (Electrochemical Alkene Trifluoromethylation)

$R_1=7.84\%$

Crystal Data and Experimental

Experimental. Single colourless block-shaped crystals of **2020ncs0004z** were supplied. A suitable crystal $0.12 \times 0.05 \times 0.03 \text{ mm}^3$ was selected and mounted on a MITIGEN holder in perfluoroether oil on a Rigaku FRE+ equipped with VHF Varimax confocal mirrors and an AFC12 goniometer and HyPix 6000 detector. The crystal was kept at a steady $T = 100(2) \text{ K}$ during data collection. The structure was solved with the **ShelXT** (Sheldrick, 2015) structure solution program using the dual methods solution method and by using **Olex2** (Dolomanov et al., 2009) as the graphical interface. The model was refined with **ShelXL** 2018/3 (Sheldrick, 2015) using full matrix least squares minimisation on F^2 minimisation.

Crystal Data. $\text{C}_{23}\text{H}_{22}\text{F}_3\text{NO}_3\text{S}$, $M_r = 449.47$, orthorhombic, $Pna2_1$ (No. 33), $a = 28.3981(13) \text{ \AA}$, $b = 12.1431(5) \text{ \AA}$, $c = 6.0697(2) \text{ \AA}$, $\alpha = \beta = \gamma = 90^\circ$, $V = 2093.08(15) \text{ \AA}^3$, $T = 100(2) \text{ K}$, $Z = 4$, $Z' = 1$, $\mu(\text{Mo K}\alpha) = 0.207 \text{ mm}^{-1}$, 28341 reflections measured, 5816 unique ($R_{\text{int}} = 0.0755$) which were used in all calculations. The final wR_2 was 0.1672 (all data) and R_1 was 0.0784 ($I > 2(I)$).

Structure Quality Indicators

Reflections:	d min (Mo)	0.72	I/σ	21.0	Rint	7.55%	complete 100% (IUCr)	100%		
Refinement:	Shift	0.000	Max Peak	0.4	Min Peak	-0.4	Goof	1.173	Flack	.01(7)

A colourless block-shaped crystal with dimensions $0.12 \times 0.05 \times 0.03 \text{ mm}^3$ was mounted on a MITIGEN holder in perfluoroether oil. X-ray diffraction data were collected using a Rigaku FRE+ equipped with VHF Varimax confocal mirrors and an AFC12 goniometer and HyPix 6000 detector equipped with an Oxford Cryosystems low-temperature device, operating at $T = 100(2) \text{ K}$.

Data were measured using profile data from ω -scans of 0.2° per frame for 35.0 s using $\text{Mo K}\alpha$ radiation (Rotating Anode, 45.0 kV, 55.0 mA). The total number of runs and images was based on the strategy calculation from the program **CrysAlisPro** (Rigaku, V1.171.40.69a, 2020). The maximum resolution achieved was $\Theta = 29.574^\circ$.

Cell parameters were retrieved using the **CrysAlisPro** (Rigaku, V1.171.40.69a, 2020) software and refined using **CrysAlisPro** (Rigaku, V1.171.40.69a, 2020) on 7508 reflections, 26 % of the observed reflections. Data reduction was performed using the **CrysAlisPro** (Rigaku, V1.171.40.69a, 2020) software which corrects for Lorentz polarisation. The final completeness is 100.00 % out to 29.574° in Θ .

A multi-scan absorption correction was performed using **CrysAlisPro** (Rigaku, V1.171.40.69a, 2020) Empirical absorption correction using spherical harmonics, implemented in SCALE3 ABSPACK scaling algorithm.. The absorption coefficient μ of this material is 0.207 mm^{-1} at this wavelength ($\lambda = 0.71075 \text{ \AA}$) and the minimum and maximum transmissions are 0.910 and 1.000.

The structure was solved in the space group $Pna2_1$ (# 33) by using dual methods using the **ShelXT** (Sheldrick, 2015) structure solution program and refined by full matrix least squares minimisation on F^2 using **ShelXL** 2018/3 (Sheldrick, 2015). All non-hydrogen atoms were refined anisotropically. Hydrogen atom positions were calculated geometrically and refined using the riding model.

_diffn_special_details: Please note, the R enantiomer of the chiral structure is shown but the crystal is a racemic mixture containing both enantiomers in equal proportions.

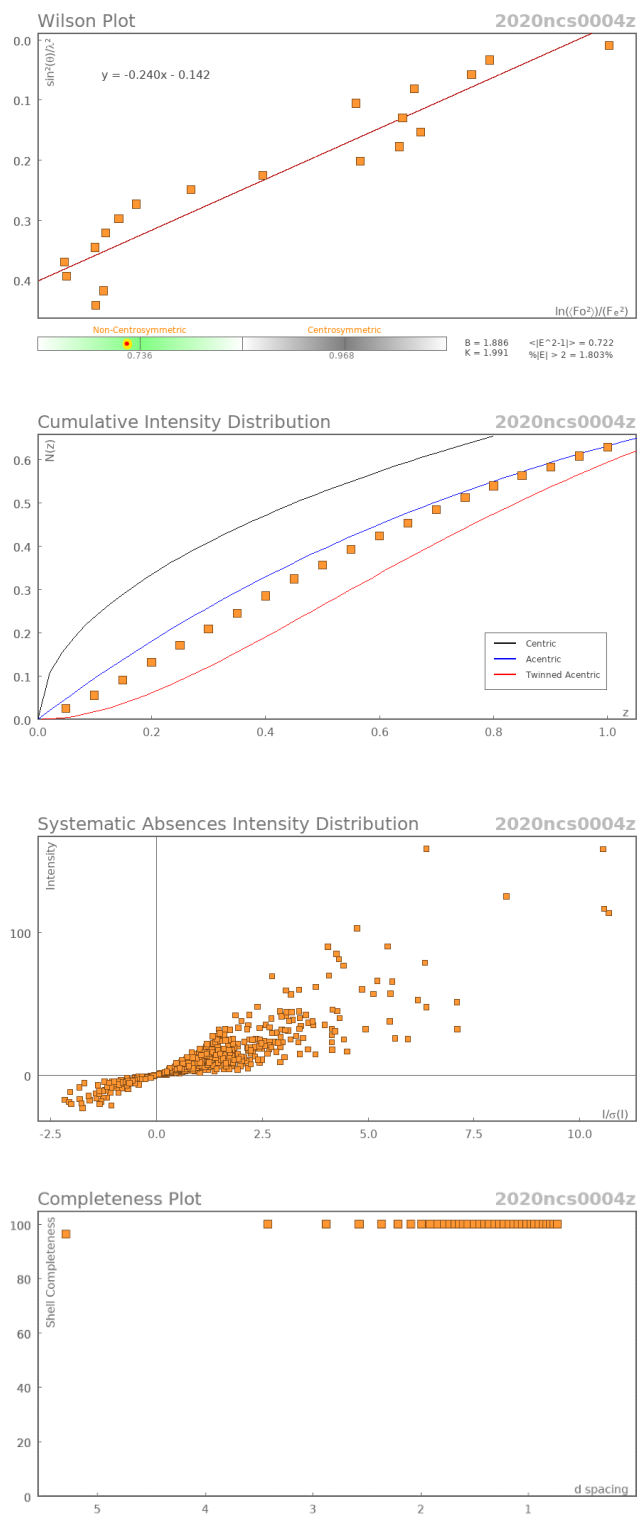
_refine_special_details: The CF_3 group is positionally disordered (ca.56:44). The disorder components were refined with 1,2 and 1,3 geometrical restraints and thermal restraints.

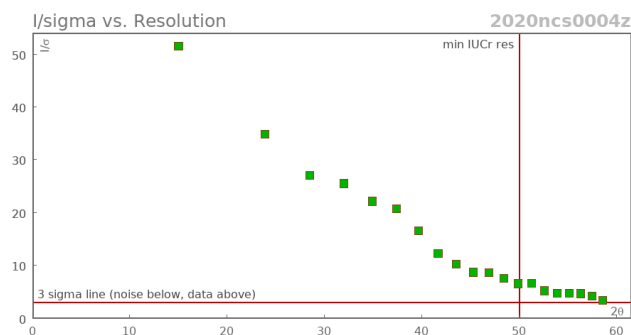
_exptl_absorpt_process_details: **CrysAlisPro** (Rigaku, V1.171.40.69a, 2020) using spherical harmonics as implemented in SCALE3 ABSPACK.

There is a single molecule in the asymmetric unit, which is represented by the reported sum formula. In other words: Z is 4 and Z' is 1.

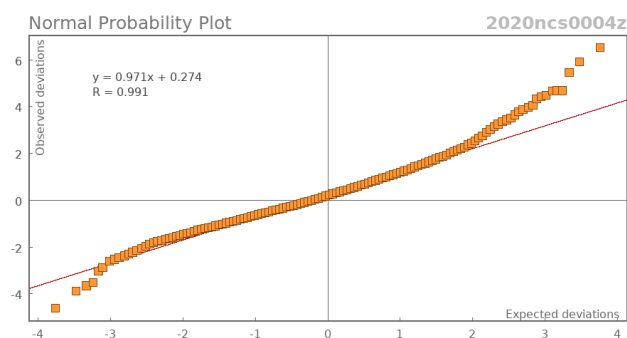
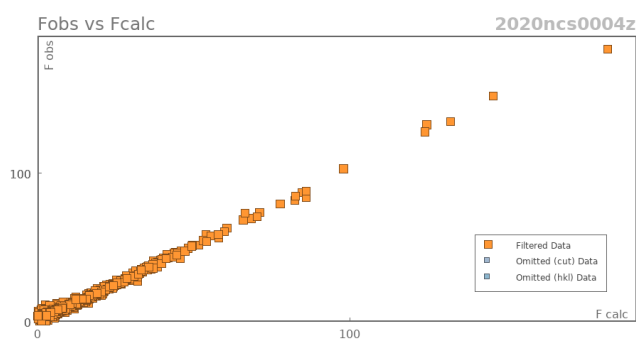
The Flack parameter was refined to 0.01(7). Determination of absolute structure using Bayesian statistics on Bijvoet differences using the Olex2 results in 0.09(4). Note: The Flack parameter is used to determine chirality of the crystal studied, the value should be near 0, a value of 1 means that the stereochemistry is wrong, and the model should be inverted. A value of 0.5 means that the crystal consists of a racemic mixture of the two enantiomers. N.B. in this instance, the Flack parameter indicates the polarity rather than chirality of the crystal. As mentioned above, the crystal is a racemic mixture containing both enantiomers in equal proportions.

Data Plots: Diffraction Data





Data Plots: Refinement and Data



Reflection Statistics

Total reflections (after filtering)	29319
Completeness	0.989
hkl _{max} collected	(33, 16, 8)
hkl _{max} used	(39, 16, 8)
Lim d _{max} collected	100.0
d _{max} used	11.17
Friedel pairs	6565
Inconsistent equivalents	23
R _{sigma}	0.0476
Omitted reflections	0
Multiplicity	(9106, 6256, 2159, 296, 8)
Removed systematic absences	978
Unique reflections	5816
Mean I/ σ	14.31
hkl _{min} collected	(-39, -16, -8)

hklmin used	(0, 0, -8)
Lim dmin collected	0.36
dmin used	0.72
Friedel pairs merged	0
Rint	0.0755
Intensity transformed	0
Omitted by user (OMIT hkl)	0
Maximum multiplicity	14
Filtered off (Shel/OMIT)	0

Table 1: Fractional Atomic Coordinates ($\times 10^4$) and Equivalent Isotropic Displacement Parameters ($\text{\AA}^2 \times 10^3$) for **2020ncs0004z**. U_{eq} is defined as $1/3$ of the trace of the orthogonalised U_{ij} .

Atom	x	y	z	U_{eq}
S1	4560.7(4)	6573.1(9)	2949(2)	26.7(2)
O1	4401.4(14)	7100(3)	957(6)	36.6(9)
O2	4775.7(13)	5508(3)	2822(7)	36.3(8)
O3	3768.1(14)	4284(3)	3765(6)	37.3(9)
N1	4102.4(13)	6428(3)	4562(7)	22.6(8)
C1	4949.8(16)	7487(4)	4230(8)	22.8(9)
C2	5148(2)	7190(4)	6254(9)	34.8(12)
C3	5449(2)	7923(5)	7281(9)	39.9(13)
C4	5558.4(18)	8937(4)	6337(10)	33.3(11)
C5	5356.9(19)	9205(4)	4343(10)	36.4(12)
C6	5052.7(17)	8488(4)	3276(9)	32.9(11)
C7	5904(2)	9699(5)	7466(13)	50.5(17)
C8	3797.9(16)	7379(4)	4848(8)	24.2(9)
C9	3461.4(17)	7604(4)	3236(9)	28.4(10)
C10	3151.8(17)	8477(4)	3518(9)	33.5(12)
C11	3174(2)	9109(5)	5393(10)	39.3(13)
C12	3514(2)	8907(5)	6993(10)	39.5(13)
C13	3826.9(19)	8037(4)	6684(8)	29.3(10)
C14	4114.7(16)	5594(4)	6319(9)	24.9(9)
C15	3726.0(17)	4721(4)	5928(8)	24.6(9)
C16	3815.9(18)	3784(4)	7618(10)	33.6(12)
C17	3482(2)	2809(5)	7464(13)	48.8(15)
C18	3238.0(17)	5227(4)	6241(8)	25.9(9)
C19	2897.7(18)	5209(4)	4583(9)	30.7(10)
C20	2467.7(19)	5730(4)	4922(10)	36.7(13)
C21	2372.3(19)	6285(5)	6861(11)	39.4(13)
C22	2702(2)	6283(5)	8518(9)	38.5(13)
C23	3131.3(18)	5757(4)	8213(10)	35.1(11)
F1A	3598(11)	2000(20)	8810(50)	69(6)
F2A	3404(13)	2440(20)	5490(20)	94(7)
F3A	3066(6)	3150(20)	8260(60)	82(7)
F1B	3589(11)	2160(30)	9200(60)	70(8)
F2B	3608(15)	2176(18)	5810(50)	89(8)
F3B	3033(6)	3000(30)	7390(60)	67(6)

Table 2: Anisotropic Displacement Parameters ($\times 10^4$) for **2020ncs0004z**. The anisotropic displacement factor exponent takes the form: $-2\pi^2[h^2a^{*2} \times U_{11} + \dots + 2hka^* \times b^* \times U_{12}]$

Atom	U_{11}	U_{22}	U_{33}	U_{23}	U_{13}	U_{12}
S1	32.1(5)	27.5(5)	20.4(4)	-5.0(5)	-0.8(5)	1.9(5)
O1	45(2)	47(2)	17.9(16)	1.5(16)	-2.4(15)	2.1(18)
O2	46.0(19)	31.0(17)	31.8(18)	-12.0(17)	1.0(19)	6.2(15)
O3	39(2)	37(2)	36(2)	-16.9(17)	2.8(16)	-2.3(17)
N1	26.8(18)	14.4(16)	26.6(19)	2.9(15)	-1.1(15)	1.4(14)
C1	26(2)	21(2)	21(2)	-4.1(17)	0.7(17)	0.0(17)
C2	48(3)	26(2)	30(3)	6(2)	-6(2)	-8(2)
C3	41(3)	46(3)	33(3)	6(2)	-12(2)	-11(3)
C4	29(2)	31(3)	40(3)	-9(2)	4(2)	-1.6(19)
C5	37(3)	24(2)	48(3)	5(2)	6(2)	-1(2)
C6	34(2)	30(2)	34(3)	8(2)	0(2)	4(2)
C7	42(3)	41(3)	69(5)	-14(3)	-2(3)	-9(3)
C8	25(2)	16(2)	32(2)	5.3(18)	-0.2(19)	0.4(16)
C9	32(2)	22(2)	31(3)	1.5(19)	-10(2)	-1.9(17)
C10	29(2)	29(2)	42(3)	12(2)	-7(2)	1.9(19)
C11	40(3)	30(3)	47(3)	6(2)	6(2)	13(2)
C12	59(4)	31(3)	28(2)	-2(2)	6(3)	10(2)
C13	38(3)	26(2)	23(2)	6.1(19)	-4.1(19)	2(2)
C14	26(2)	21(2)	28(2)	1.8(18)	-6.5(19)	1.9(16)
C15	32(2)	20(2)	22(2)	-1.3(18)	-1.8(18)	-1.2(18)
C16	32(2)	24(2)	44(3)	15(2)	-2(2)	4.7(18)
C17	41(3)	35(3)	71(4)	24(3)	5(3)	-5(2)
C18	27(2)	21(2)	30(2)	10.2(19)	-5.9(19)	-6.1(17)
C19	36(3)	24(2)	32(3)	2(2)	-5(2)	-6(2)
C20	28(2)	33(3)	49(4)	15(2)	-11(2)	-5(2)
C21	27(3)	34(3)	57(4)	11(3)	2(2)	1(2)
C22	38(3)	41(3)	36(3)	0(2)	5(2)	1(2)
C23	32(2)	39(3)	35(3)	1(2)	-1(2)	4(2)
F1A	58(10)	32(5)	115(12)	24(6)	-27(9)	-2(5)
F2A	136(18)	63(11)	85(6)	13(5)	-35(8)	-60(10)
F3A	27(5)	69(11)	150(18)	60(11)	2(7)	-3(5)
F1B	35(8)	53(15)	122(14)	59(14)	10(9)	2(8)
F2B	121(18)	30(7)	115(12)	-7(8)	39(12)	-22(9)
F3B	37(5)	43(8)	121(17)	42(10)	-20(6)	-13(4)

Table 3: Bond Lengths in Å for **2020ncs0004z**.

Atom	Atom	Length/Å
S1	O1	1.441(4)
S1	O2	1.433(3)
S1	N1	1.638(4)
S1	C1	1.749(5)
O3	C15	1.421(6)
N1	C8	1.453(6)
N1	C14	1.471(6)
C1	C2	1.399(7)
C1	C6	1.377(7)
C2	C3	1.382(7)

Atom	Atom	Length/Å
C3	C4	1.392(8)
C4	C5	1.378(8)
C4	C7	1.513(8)
C5	C6	1.387(8)
C8	C9	1.395(6)
C8	C13	1.374(7)
C9	C10	1.388(7)
C10	C11	1.374(8)
C11	C12	1.392(9)
C12	C13	1.393(7)
C14	C15	1.548(6)
C15	C16	1.554(7)
C15	C18	1.528(7)
C16	C17	1.519(8)
C17	F1A	1.322(15)
C17	F2A	1.297(15)
C17	F3A	1.342(14)
C17	F1B	1.350(17)
C17	F2B	1.315(16)
C17	F3B	1.294(17)
C18	C19	1.395(7)
C18	C23	1.392(8)
C19	C20	1.390(8)
C20	C21	1.383(9)
C21	C22	1.374(8)
C22	C23	1.390(7)

Table 4: Bond Angles in ° for **2020ncs0004z**.

Atom	Atom	Atom	Angle/°
O1	S1	N1	107.4(2)
O1	S1	C1	106.8(2)
O2	S1	O1	119.3(3)
O2	S1	N1	105.9(2)
O2	S1	C1	109.2(2)
N1	S1	C1	107.7(2)
C8	N1	S1	117.3(3)
C8	N1	C14	118.4(4)
C14	N1	S1	119.2(3)
C2	C1	S1	118.8(4)
C6	C1	S1	120.5(4)
C6	C1	C2	120.7(4)
C3	C2	C1	118.6(5)
C2	C3	C4	121.4(5)
C3	C4	C7	119.9(5)
C5	C4	C3	118.5(5)
C5	C4	C7	121.5(5)
C4	C5	C6	121.3(5)
C1	C6	C5	119.3(5)
C9	C8	N1	118.7(4)
C13	C8	N1	121.6(4)
C13	C8	C9	119.8(4)
C10	C9	C8	119.8(5)
C11	C10	C9	120.0(5)
C10	C11	C12	120.7(5)
C11	C12	C13	118.8(5)
C8	C13	C12	120.8(5)
N1	C14	C15	110.1(4)

Atom	Atom	Atom	Angle/°
O3	C15	C14	109.7(4)
O3	C15	C16	108.8(4)
O3	C15	C18	110.0(4)
C14	C15	C16	106.5(4)
C18	C15	C14	110.6(4)
C18	C15	C16	111.2(4)
C17	C16	C15	115.3(5)
F1A	C17	C16	112.7(14)
F1A	C17	F3A	103.1(19)
F2A	C17	C16	115.8(10)
F2A	C17	F1A	110.6(18)
F2A	C17	F3A	106.9(13)
F3A	C17	C16	106.6(15)
F1B	C17	C16	105.4(17)
F2B	C17	C16	109.4(13)
F2B	C17	F1B	101(2)
F3B	C17	C16	118.7(15)
F3B	C17	F1B	110(2)
F3B	C17	F2B	110.2(16)
C19	C18	C15	122.2(5)
C23	C18	C15	119.3(4)
C23	C18	C19	118.5(5)
C20	C19	C18	119.6(5)
C21	C20	C19	121.3(5)
C22	C21	C20	119.3(5)
C21	C22	C23	120.1(5)
C22	C23	C18	121.2(5)

Table 5: Torsion Angles in ° for 2020ncs0004z.

Atom	Atom	Atom	Atom	Angle/°
S1	N1	C8	C9	81.4(5)
S1	N1	C8	C13	-100.2(5)
S1	N1	C14	C15	-117.7(4)
S1	C1	C2	C3	-178.8(4)
S1	C1	C6	C5	179.0(4)
O1	S1	N1	C8	-47.1(4)
O1	S1	N1	C14	158.6(3)
O1	S1	C1	C2	178.2(4)
O1	S1	C1	C6	-0.9(5)
O2	S1	N1	C8	-175.6(3)
O2	S1	N1	C14	30.0(4)
O2	S1	C1	C2	-51.5(5)
O2	S1	C1	C6	129.4(4)
O3	C15	C16	C17	-59.6(6)
O3	C15	C18	C19	1.3(6)
O3	C15	C18	C23	-176.6(4)
N1	S1	C1	C2	63.0(4)
N1	S1	C1	C6	-116.0(4)
N1	C8	C9	C10	177.0(4)
N1	C8	C13	C12	-176.2(5)
N1	C14	C15	O3	53.5(5)
N1	C14	C15	C16	171.1(4)
N1	C14	C15	C18	-68.0(5)
C1	S1	N1	C8	67.7(4)
C1	S1	N1	C14	-86.6(4)

Atom	Atom	Atom	Atom	Angle/°
C1	C2	C3	C4	-0.5(9)
C2	C1	C6	C5	0.0(7)
C2	C3	C4	C5	0.5(9)
C2	C3	C4	C7	-177.6(6)
C3	C4	C5	C6	-0.3(8)
C4	C5	C6	C1	0.0(8)
C6	C1	C2	C3	0.2(8)
C7	C4	C5	C6	177.8(5)
C8	N1	C14	C15	88.3(5)
C8	C9	C10	C11	-0.7(8)
C9	C8	C13	C12	2.1(7)
C9	C10	C11	C12	2.0(8)
C10	C11	C12	C13	-1.3(9)
C11	C12	C13	C8	-0.8(8)
C13	C8	C9	C10	-1.3(7)
C14	N1	C8	C9	-124.0(5)
C14	N1	C8	C13	54.3(6)
C14	C15	C16	C17	-177.8(5)
C14	C15	C18	C19	122.6(5)
C14	C15	C18	C23	-55.2(5)
C15	C16	C17	F1A	174.7(18)
C15	C16	C17	F2A	46(2)
C15	C16	C17	F3A	-72.9(17)
C15	C16	C17	F1B	-174(2)
C15	C16	C17	F2B	78(2)
C15	C16	C17	F3B	-49(2)
C15	C18	C19	C20	-176.8(4)
C15	C18	C23	C22	176.2(5)
C16	C15	C18	C19	-119.3(5)
C16	C15	C18	C23	62.9(5)
C18	C15	C16	C17	61.7(6)
C18	C19	C20	C21	1.1(8)
C19	C18	C23	C22	-1.7(7)
C19	C20	C21	C22	-2.7(8)
C20	C21	C22	C23	2.0(8)
C21	C22	C23	C18	0.2(8)
C23	C18	C19	C20	1.0(7)

Table 6: Hydrogen Fractional Atomic Coordinates ($\times 10^4$) and Equivalent Isotropic Displacement Parameters ($\text{\AA}^2 \times 10^3$) for **2020ncs0004z**. U_{eq} is defined as 1/3 of the trace of the orthogonalised U_{ij} .

Atom	x	y	z	U_{eq}
H3	4042.06	4394.08	3292.93	56
H2	5078.13	6499.04	6908.07	42
H3A	5583.57	7731.86	8661.2	48
H5	5427.77	9895.53	3685.35	44
H6	4916.79	8685.05	1901.2	40
H7A	6220.71	9380.12	7393.17	76
H7B	5812.45	9793.53	9011.5	76
H7C	5902.73	10415.8	6726.04	76
H9	3444.27	7161.01	1948.01	34
H10	2924.64	8637.25	2414.75	40
H11	2954.41	9690.53	5599.31	47
H12	3532.67	9354.81	8274.05	47

Atom	x	y	z	U_{eq}
H13	4063.18	7897.13	7755.51	35
H14A	4065.34	5952.66	7764.89	30
H14B	4426.92	5231.5	6338.32	30
H16A	4141.74	3511.89	7417.55	40
H16B	3793.9	4096.87	9120.81	40
H19	2959.39	4842.91	3230.68	37
H20	2234.87	5704.07	3799.29	44
H21	2082.17	6663.3	7045.05	47
H22	2635.78	6641.7	9874.7	46
H23	3356.27	5758.14	9371.17	42

Table 7: Atomic Occupancies for all atoms that are not fully occupied in **2020ncs0004z**.

Atom	Occupancy
F1A	0.56(6)
F2A	0.56(6)
F3A	0.56(6)
F1B	0.44(6)
F2B	0.44(6)
F3B	0.44(6)

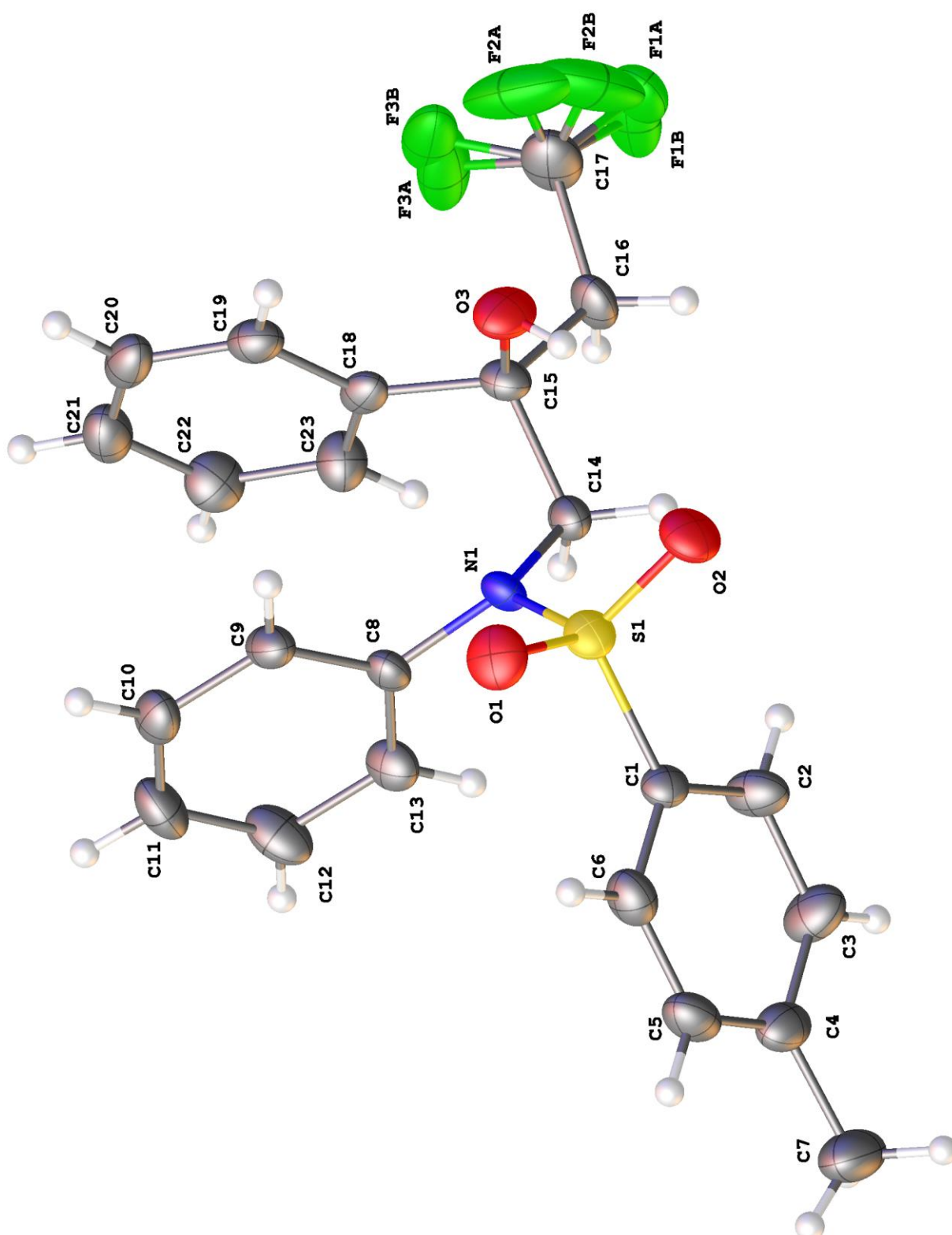
Citations

CrysAlisPro Software System, Rigaku Oxford Diffraction, (2020).

O.V. Dolomanov and L.J. Bourhis and R.J. Gildea and J.A.K. Howard and H. Puschmann, Olex2: A complete structure solution, refinement and analysis program, *J. Appl. Cryst.*, (2009), **42**, 339-341.

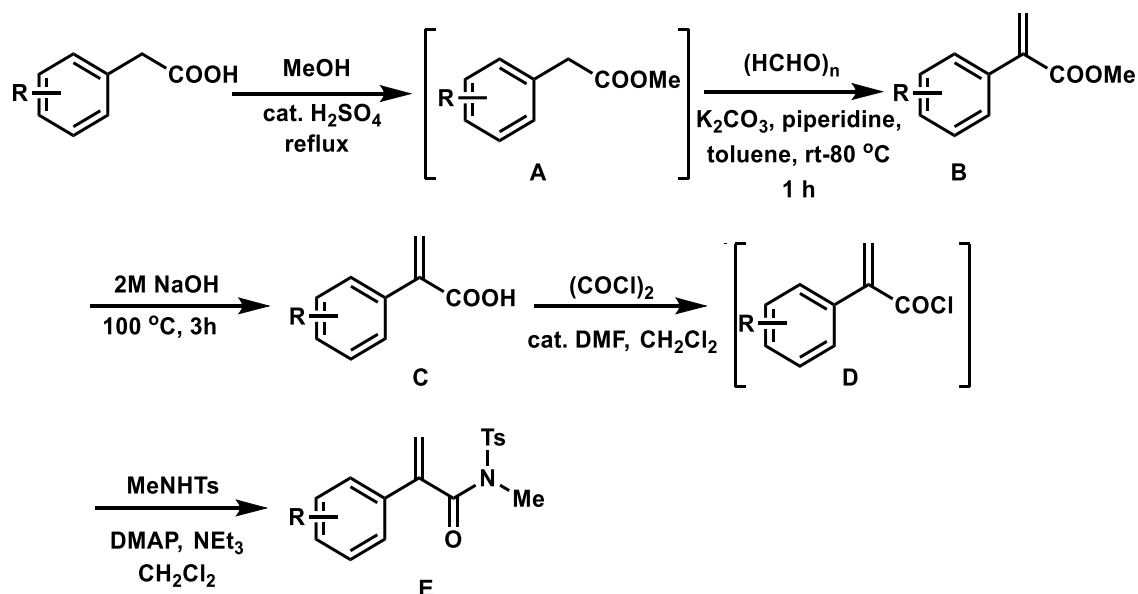
Sheldrick, G.M., Crystal structure refinement with ShelXL, *Acta Cryst.*, (2015), **C27**, 3-8.

Sheldrick, G.M., ShelXT-Integrated space-group and crystal-structure determination, *Acta Cryst.*, (2015), **A71**, 3-8.



7.4 Substrate Synthesis (Electrochemical oxidative Z-selective C(sp²)-H chlorination of acrylamide)

General Procedure



Step 1:

To a solution of 2-aryl acetic acid (20 mmol) in MeOH (25 mL) was added 5 drops of concentrated H₂SO₄. The solution was then heated at reflux for 16 h. Upon completion of the mixture was concentrated *in vacuo*. The residue was diluted with EtOAc (50 mL) and then neutralized with saturated sodium bicarbonate solution (50 mL). The organic phase was dried over MgSO₄, filtered, and concentrated under reduced pressure to afford the corresponding methyl ester, which was used for the next step without further purification.

Step 2:

Methyl ester (20 mmol), paraformaldehyde (40 mmol, 2 eq.), TBAI (4 mmol, 0.2 eq.) and K₂CO₃ (40 mmol, 2 eq.) in toluene (30 mL) was heated to 80 °C overnight as a viscous suspension. Upon cooling the mixture was diluted with EtOAc (120 mL) and quenched with water (120 mL). The layers were separated and the aqueous re-extracted with EtOAc (120 mL). The organics were combined and dried over MgSO₄ and concentrated

yielding crude methyl acrylate. The residue was purified by flash column chromatography unless stated otherwise (eluent = 3 to 8 % EtOAc in hexanes, silica gel) to yield pure methyl acrylate products.

Step 3:

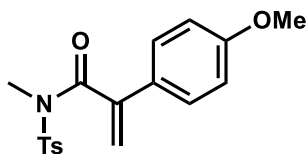
To a clean 50 mL round bottom flask was added prepared methyl acrylates and a 2M NaOH solution (3 mL/ mmol). The mixture was heated at reflux for 2 h before being cooled to room temperature. The aqueous was extracted with Et₂O (3 mL/ mmol) then acidified to pH 1 using 2M HCl. The acidified aqueous suspension was then extracted with CH₂Cl₂ (3 x 30 mL), organics combined and dried over MgSO₄, filtered and concentrated to afford crude acrylic acids.

Step 4, part A:

A solution of the 2-acrylacrylic acid derivatives (1.1 eq.) in CH₂Cl₂ (3 mL/ mmol) and DMF (3 drops) was prepared. Oxalyl chloride (1.5 eq.) was added dropwise at room temperature and the mixture was allowed to stir for 3 h until no gas evolution was observed. The solution was concentrated *in vacuo* and redissolved in CH₂Cl₂ (1 mL/mmol).

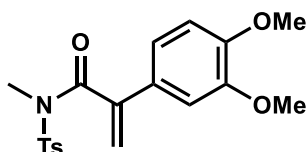
Step 4, part B:

A solution of N-methyl-N-tosylamine (0.9 eq.), DMAP (10 mol %) and triethylamine (2 eq.) in CH₂Cl₂ (8 mL/mmol) was prepared and cooled to 0 °C using an salt/ice bath. The crude acyl chloride solution prepared in **Step 4, part A** was added dropwise and the mixture was stirred at 0 °C for 15 mins before being allowed to warm to room temperature and stir overnight. The reaction mixture was quenched with a saturated sodium bicarbonate solution (8 mL/mmol), layers separated and aqueous phase extracted with CH₂Cl₂ (2 x 40 mL). The organics were combined and dried over MgSO₄, filtered and concentrated *in vacuo* yielding crude product. The crude residue was purified by flash column chromatography (silica gel) to yield pure product.

2-(4-methoxyphenyl)-N-methyl-N-tosylacrylamide (13)

Prepared according to General procedure using 4-methoxyphenylacetic acid (3.32 g, 20.0 mmol). Step 4B was carried out using N-methyl-p-toluenesulfonamide (460 mg, 2.50 mmol), dimethylaminopyridine (30.0 mg, 0.25 mmol), triethylamine (0.80 mL, 5.00 mmol), CH₂Cl₂ (25 mL) and acyl chloride (2.80 mmol). The crude residue was purified by flash column chromatography (eluent = 15 to 25 % EtOAc in hexanes, silica gel) to afford product **13** as a white solid (480 mg, 50 % yield), (Step 1- 4B overall yield = 7 %).

Mp.: 67-69 °C **R_f** = 0.14 (eluent = 15 % EtOAc in hexanes); **v_{max}** / **cm⁻¹** (thin film) 1686, 1606, 1512, 1355, 1290, 1251, 1168, 1056; **¹H NMR (500 MHz, CDCl₃)** δ_H = 7.83 (2H, d, *J* 8.5 Hz, Ar*H*), 7.28-7.35 (2H, m, Ar*H*), 7.19 (2H, d, *J* 8.7 Hz, Ar*H*), 6.84 (2H, d, *J* 8.7 Hz, Ar*H*), 5.63 (1H, m, =CH), 3.81 (3H, s, O-CH₃), 5.30 (1H, m, =CH), 3.18-3.20 (3H, m, N-CH₃), 2.45 (3H, s, Ts-CH₃); **¹³C NMR (126 MHz, CDCl₃)** δ_C = 170.6 (N-C=O), 160.3 (ArC-OCH₃), 145.1 (=C), 144.3(ArC), 135.8 (ArC), 129.6 (ArC), 128.6 (ArC), 127.3(ArC), 127.2 (=CH), 115.5(ArC), 114.4 (ArC), 55.5 (O-CH₃), 34.4 (N-CH₃), 21.8 (Ts-CH₃); **HRMS (ES⁺)** [C₁₈H₁₉NO₄S] requires [M⁺ + H⁺] 346.1113 found 346.1118.

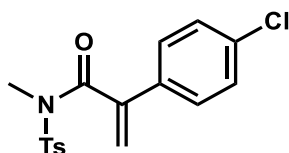
2-(3,4-dimethoxyphenyl)-N-methyl-N-tosylacrylamide (14)

Prepared according to General procedure using 3,4-dimethoxyphenylacetic acid (3.92 g, 20.0 mmol). Step 4B was carried out using N-methyl-p-toluenesulfonamide (386 mg, 2.10 mmol), dimethylaminopyridine (25.2 mg, 0.21 mmol), triethylamine (0.70 mL, 4.20 mmol), CH₂Cl₂ (20 mL) and acyl chloride (2.35 mmol). The crude residue was purified by

flash column chromatography (eluent = 15 to 25 % EtOAc in hexanes, silica gel) to afford product **14** as a white solid (450 mg, 49 % yield), (Step 1- 4B overall yield = 6.0 %).

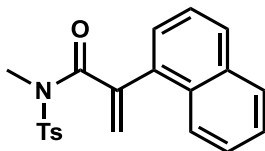
Mp.: 88-90 °C; **R_f** = 0.13 (eluent = 15 % EtOAc in hexanes); **v_{max}** / **cm⁻¹** (thin film) 1681, 1597, 1517, 1463, 1344, 1255, 1169, 1022; **¹H NMR (500 MHz, CDCl₃)** δ_H = 7.83-7.86 (2H, m), 7.30-7.34 (2H, m), 6.78-6.83 (3H, m), 5.65 (1H, s), 5.33 (1H, s), 3.89 (3H, s), 3.81 (3H, s), 3.21 (3H, s), 2.45 (3H, s); **¹³C NMR (126 MHz, CDCl₃)** δ_C = 170.5, 149.3, 145.1, 144.5, 135.9, 129.6, 128.6, 127.5, 119.0, 115.7, 111.4, 108.9, 56.1, 56.0, 34.5, 21.8; **HRMS (ES⁺)** [C₁₉H₂₁NO₅S] requires [M⁺⁺ H⁺] 376.1219 found 376.1218.

2-(4-chlorophenyl)-N-methyl-N-tosylacrylamide (**15**)



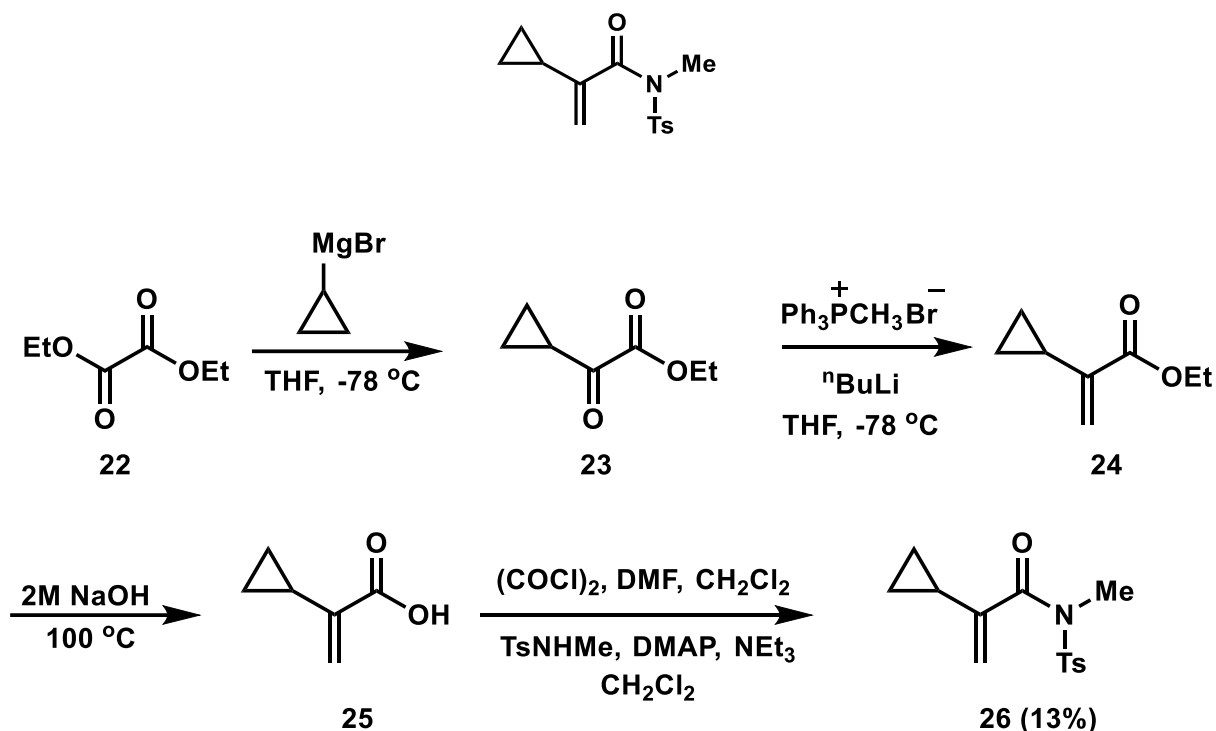
Prepared according to General procedure using 4-chlorophenylacetic acid (3.41 g, 20.0 mmol). Step 4B was carried out using N-methyl-p-toluenesulfonamide (960 mg, 5.20 mmol), dimethylaminopyridine (64.0 mg, 0.52 mmol), triethylamine (1.44 mL, 10.4 mmol), CH₂Cl₂ (40 mL) and acyl chloride (5.7 mmol). The crude residue was purified by flash column chromatography (eluent = 15 to 25 % EtOAc in hexanes, silica gel) to afford product **15** as a white solid (1.28 g, 63 % yield), (Step 1- 4B overall yield = 18 %).

Mp.: 96-98 °C; **R_f** = 0.27 (eluent = 15 % EtOAc in hexanes); **v_{max}** / **cm⁻¹** (thin film) 1685, 1595, 1492, 1355, 1163, 1088; **¹H NMR (500 MHz, CDCl₃)** δ_H = 7.76 (2H, d, *J* 8.3 Hz), 7.27-7.34 (4H, m), 7.18-7.22 (2H, m), 5.73 (1H, s), 5.41 (1H, s), 3.21 (3H, s), 2.45 (3H, s); **¹³C NMR (126 MHz, CDCl₃)** δ_C = 169.9, 145.3, 143.9, 135.6, 135.0, 133.4, 129.7, 129.2, 128.4, 127.4, 117.9, 34.2, 21.8; **HRMS (ES⁺)** [C₁₇H₁₆NO₃SCl] requires [M⁺⁺ H⁺] 350.0618 found 350.0614.

N-methyl-2-(naphthalen-1-yl)-N-tosylacrylamide (16)

Prepared according to General procedure using 1-naphthaleneacetic acid (3.72 g, 20.0 mmol). Step 4B was carried out using N-methyl-p-toluenesulfonamide (894 mg, 4.84 mmol), dimethylaminopyridine (59.0 mg, 0.48 mmol), triethylamine (1.35 mL, 9.70 mmol), CH₂Cl₂ (37 mL) and acyl chloride (5.30 mmol). The crude residue was purified by flash column chromatography (eluent = 15 to 25 % EtOAc in hexanes, silica gel) to afford product **16** as a white solid (1.24 g, 64 % yield), (Step 1- 4B overall yield = 17 %).

Mp.: 90-92 °C **R_f** = 0.26 (eluent = 15 % EtOAc in hexanes); **v_{max}** / **cm⁻¹** (thin film) 1678, 1595, 1498, 1354, 1305, 1170, 1066; **¹H NMR (500 MHz, CDCl₃)** δ_H = 7.92 (1H, d, *J* 8.5 Hz), 7.83-7.88 (2H, m), 7.74 (2H, d, *J* 8.3 Hz), 7.46-7.52 (1H, m), 7.37-7.45 (2H, m), 7.32 (1H, dd, *J* 7.1, 1.0 Hz), 7.25-7.28 (2H, m), 6.15 (1H, s), 5.85 (1H, s), 3.02 (3H, s), 2.44 (3H, s); **¹³C NMR (126 MHz, CDCl₃)** δ_C = 170.6, 144.9, 144.1, 135.5, 134.0, 133.6, 130.8, 129.5, 129.5, 128.8, 128.7, 127.1, 127.0, 126.9, 126.3, 125.4, 124.7, 34.6, 21.8; **HRMS (ES⁺)** [C₂₁H₁₉NO₃S] requires [M⁺⁺ H⁺] 366.1164 found 366.1168.

2-Cyclopropyl-N-methyl-N-tosylacrylamide (26)

Experimental Procedure:

Step 1:

To a solution of diethyl oxalate (50 mmol) in THF (50 mL) at -78 °C was dropwise added freshly prepared cyclopropylmagnesium bromide (54 mmol, 0.9M) over 1 h with the help of syringe pump. After stirring for 1 h at -78 °C, the mixture was warmed to room temperature and quenched with 2N HCl (10 mL). The aqueous layer was extracted with ethyl acetate (3×10 mL) and the combined organic layers were dried over MgSO_4 and then filtered. The volatile compounds were removed *in vacuo* and the crude α -ketoester was directly used in the next step without further purification.

Step 2:

A stirred solution of methyl triphenylphosphonium bromide (35 mmol) in dry THF (70 mL) was cooled to -78 °C and *n*-butyllithium (35 mmol, 2.5M in THF) was dropwise added to the solution under N_2 atmosphere. After stirring 15 minutes, the resulting yellow reaction mixture was warmed up to room temperature and stirred for 1 hour, once the

reaction mixture became transparent yellow, it was again cooled to -78 °C followed with the addition of crude α -ketoester obtained in last step. After stirring for 1 hour at -78 °C, the mixture was warmed up to room temperature and the progress of the reaction was monitored using TLC. Once the reaction was complete, 2N HCl (10 mL) was added followed by extraction with ethyl acetate (3 x 100 mL) and drying over MgSO₄. After filtration the organic solvent was removed *in vacuo*, and the residue was subjected to column chromatography on silica gel to deliver the α -substituted ethyl acrylate derivatives.

Step 3:

To a clean 50 mL round bottom flask was added prepared methyl acrylates and a 2M NaOH solution (3 mL/ mmol). The mixture was heated at reflux for 2 h before being cooled to room temperature. The aqueous was extracted with Et₂O (3 mL/ mmol) then acidified to pH 1 using 2M HCl. The acidified aqueous suspension was then extracted with CH₂Cl₂ (3 x 30 mL), organics combined and dried over MgSO₄, filtered and concentrated to afford crude acrylic acid.

Step 4, part A:

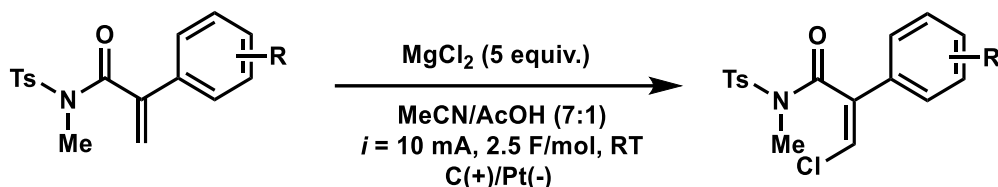
A solution of the 2-acrylacrylic acid derivative (1.1 equiv.) in CH₂Cl₂ (3 mL/ mmol) and DMF (3 drops) was prepared. Oxalyl chloride (1.5 equiv.) was added dropwise at room temperature and the mixture was allowed to stir for 3 h until no gas evolution was observed. The solution was concentrated *in vacuo* and redissolved in CH₂Cl₂ (1 mL/mmol).

Step 4, part B:

A solution of N-methyl-N-tosylamine (0.82 g, 4.42 mmol, 0.9 equiv.), DMAP (54 mg, 10 mol %) and triethylamine (1.2 mL, 2 equiv.) in CH₂Cl₂ (8 mL/mmol) was prepared and cooled to 0 °C using an salt/ice bath. The crude acyl chloride solution (0.58 g, 4.45 mmol) prepared in **Step 4, part A** was added dropwise, and the mixture was stirred at 0 °C for 15 mins before being allowed to warm to room temperature and stir overnight. The reaction mixture was quenched with a saturated sodium bicarbonate solution (8 mL/mmol), layers separated, and aqueous phase extracted with CH₂Cl₂ (2 x 40 mL). The organics were combined and dried over MgSO₄, filtered and concentrated *in vacuo* yielding crude product. The crude residue was purified by flash column chromatography (silica gel) to yield pure product **26** as a white solid (166 mg, 13%).

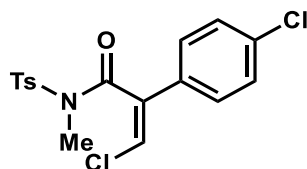
Mp.: 56-58 °C; **R_f** = 0.28 (eluent = 15% EtOAc in hexanes); **v_{max}** / **cm⁻¹** (thin film) 3020, 1686, 1595, 1354, 1285, 1188, 1167, 1086, 1047 ; **¹H NMR (300 MHz, CDCl₃)** δ_H = 7.82-7.87 (2H, m), 7.30-7.35 (2H, m), 5.14 (1H, d, *J* 1.0 Hz), 5.08 (1H, s), 3.29 (3H, s), 2.44 (3H, s), 1.54-1.62 (1H, m), 0.72-0.82 (2H, m), 0.54-0.57 (2H, m); **¹³C NMR (126 MHz, CDCl₃)** δ_C = 21.8, 171.4, 146.7, 145.0, 135.8, 129.7, 128.4, 115.2, 34.6, 13.7, 7.3; **HRMS (ES⁺)** [C₁₄H₁₈NO₃S] requires [M+H]⁺ 280.1007, found 280.1009.

7.5. Electrochemical Reactions (Electrochemical oxidative Z-selective C(sp²)-H chlorination of acrylamide



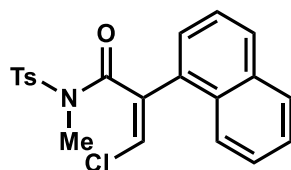
Experimental Procedure:

To an oven-dried 10 mL ElectraSyn vial equipped with a magnetic stirrer bar, was added substrate alkene (0.30 mmol) and MgCl₂ (143 mg, 1.50 mmol). The threaded glass of the vial was wrapped with PTFE tape and connected to the ElectraSyn cap, which was fitted with a graphite anode and a platinum foil cathode. The vial was purged with N₂ gas via evacuate-refill cycles (\times 3). MeCN (5.25 mL) was added, followed by AcOH (0.75 mL) and the mixture was stirred for a minute to ensure solvation of the MgCl₂. The mixture was then purged via bubbling with N₂ gas for 10 minutes. The vial was then connected to an ElectraSyn. Electrolysis at 10 mA was conducted for 2 h under N₂ with continuous stirring. After electrolysis was complete, the reaction mixture was quenched with a saturated solution of aqueous NaHCO₃ (8 mL) and diluted with EtOAc (4 mL). Mesitylene internal standard (42 μ L, 0.30 mmol) was added to the organic phase and the organic layer was sampled for crude ¹H NMR analysis. The aqueous and organic phases were separated and the aqueous extracted with EtOAc (2 \times 10 mL), the combined extracts were dried over MgSO₄, filtered and concentrated *in vacuo*. The crude residue was purified by flash column chromatography on silica gel.

(Z)-3-chloro-2-(4-chlorophenyl)-N-methyl-N-tosylacrylamide (18)

Prepared according to the General Procedure using 2-(4-chlorophenyl)-N-methyl-N-tosylacrylamide (105 mg, 0.30 mmol, 1 equiv.), magnesium chloride (143 mg, 1.50 mmol, 5 equiv.), acetonitrile (5.25 mL) and acetic acid (0.75 mL). Purification by flash column chromatography (eluent = 5 to 15% EtOAc in hexanes, silica gel) to afford product as a white solid **18** (96.4 mg, 84% yield).

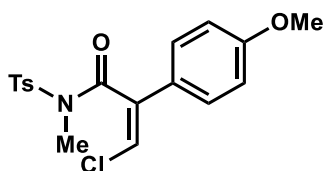
Mp.: 151-152 °C; **R_f** = 0.27 (eluent = 15% EtOAc in hexanes); **v_{max}** / **cm⁻¹** (thin film) = 3050, 1680, 1595, 1494, 1350, 1323, 1271, 1165, 1083, 952; **¹H NMR (500 MHz, CDCl₃)** δ_{H} = 7.75 (2H, d, *J* 8.1 Hz, Ar*H*), 7.28-7.34 (4H, m, Ar*H*), 7.16-7.22 (2H, m, Ar*H*), 6.53 (1H, s, =CH), 3.30 (3H, s, N-CH₃), 2.45 (3H, s, Ts-CH₃); **¹³C NMR (126 MHz, CDCl₃)** δ_{C} = 166.1, 145.5, 139.1, 135.6, 135.1, 131.2, 129.7, 129.6, 128.5, 127.2, 118.1, 33.1, 21.9; **HRMS (ES⁺)** [C₁₇H₁₅NO₃SCl₂] requires 384.0228 [M+H]⁺ found 384.0231.

(Z)-3-chloro-N-methyl-2-(naphthalen-1-yl)-N-tosylacrylamide (19)

Prepared according to the General Procedure using N-methyl-2-(naphthalen-1-yl)-N-tosylacrylamide (110 mg, 0.30 mmol, 1 equiv.), magnesium chloride (143 mg, 1.50 mmol, 5 equiv.), acetonitrile (5.25 mL) and acetic acid (0.75 mL). Purification by flash column chromatography (eluent = 5 to 15% EtOAc in hexanes, silica gel) to afford product **19** as a colourless oil (88.0 mg, 74% yield).

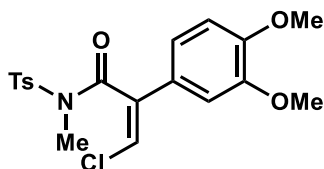
R_f = 0.27 (eluent = 15% EtOAc in hexanes); ν_{\max} / cm^{-1} (thin film) = 3040, 1688, 1594, 1358, 1317, 1188, 1168, 1087, 932; ^1H NMR (500 MHz, CDCl_3) δ_{H} = 8.15-8.24 (1H, m), 7.82-7.89 (2H, m), 7.73 (2H, d, J 8.2 Hz), 7.48-7.53 (2H, m), 7.38-7.45 (2H, m), 7.23 (2H, d, J 8.1 Hz), 6.56 (1H, s), 3.36 (3H, s), 2.41 (3H, s); ^{13}C NMR (126 MHz, CDCl_3) δ_{C} = 166.6, 145.1, 138.2, 135.2, 134.2, 131.2, 130.4, 130.0, 129.5, 128.8, 128.5, 127.3, 126.9, 126.5, 125.3, 124.8, 122.6, 33.5, 21.8; HRMS (ES^+) [$\text{C}_{21}\text{H}_{18}\text{NO}_3\text{SCl}$] requires $[\text{M}+\text{H}]^+$ 400.0774 found 400.0768.

(Z)-3-chloro-2-(4-methoxyphenyl)-N-methyl-N-tosylacrylamide (20)



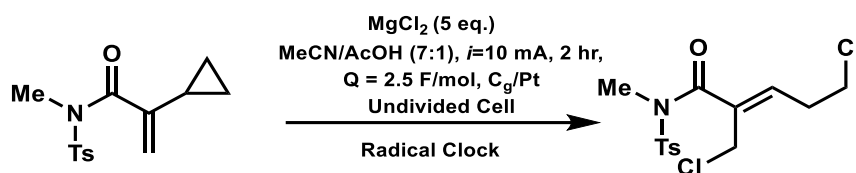
Prepared according to the General Procedure using 2-(4-methoxyphenyl)-N-methyl-N-tosylacrylamide (104 mg, 0.30 mmol, 1 equiv.), magnesium chloride (143 mg, 1.50 mmol, 5 equiv.), acetonitrile (5.25 mL) and acetic acid (0.75 mL). Purification by flash column chromatography (eluent = 5 to 15% EtOAc in hexanes, silica gel) to afford product **20** as a colourless oil (52.1 mg, 46% yield).

R_f = 0.21 (eluent = 15% EtOAc in hexanes); ν_{\max} / cm^{-1} (thin film) 3076, 1692, 1606, 1514, 1464, 1358, 1186, 1168, 1084, 952; ^1H NMR (500 MHz, CDCl_3) δ_{H} = 7.81 (2H, d, J 8.0 Hz), 7.31 (2H, d, J 8.0 Hz), 7.14-7.19 (2H, m), 6.82-6.88 (2H, m), 6.42 (1H, s), 3.81 (3H, s), 3.31 (3H, s), 2.44 (3H, s); ^{13}C NMR (126 MHz, CDCl_3) δ_{C} = 166.8, 160.6, 145.2, 139.4, 135.4, 129.6, 128.6, 127.2, 125.0, 115.5, 114.8, 55.5, 33.2, 21.8; HRMS (ES^+) [$\text{C}_{18}\text{H}_{18}\text{NO}_4\text{SCl}$] requires $[\text{M}+\text{H}]^+$ 380.0723 found 380.0720.

(Z)-3-chloro-2-(3,4-dimethoxyphenyl)-N-methyl-N-tosylacrylamide (21)

Prepared according to the General Procedure using 2-(3,4-dimethoxyphenyl)-N-methyl-N-tosylacrylamide (113 mg, 0.30 mmol, 1 equiv.), magnesium chloride (143 mg, 1.50 mmol, 5 equiv.), acetonitrile (5.25 mL) and acetic acid (0.75 mL). Purification by flash column chromatography (eluent = 5 to 15% EtOAc in hexanes, silica gel) to afford product **21** as a colourless oil (42.0 mg, 34% yield).

R_f = 0.17 (eluent = 15% EtOAc in hexanes); **v_{max}** / **cm⁻¹** (thin film) 3080, 1692, 1597, 1516, 1463, 1357, 1263, 1167, 1083; **¹H NMR (500 MHz, CDCl₃)** δ_{H} = 7.82 (2H, d, *J* 8.0 Hz), 7.28-7.33 (2H, m), 6.81 (2H, d, *J* 1.3 Hz), 6.73 (1H, s), 6.44 (1H, s), 3.89 (3H, s), 3.80 (3H, s), 3.31 (3H, s), 2.44 (3H, s); **¹³C NMR (126 MHz, CDCl₃)** δ_{C} = 166.7, 150.3, 149.5, 145.2, 139.6, 135.4, 129.6, 128.7, 125.2, 119.0, 115.8, 111.5, 108.6, 56.1, 56.0, 33.2, 21.8; **HRMS (ES⁺)** [C₁₉H₂₀NO₅SCl] requires [M+H]⁺ 410.0829 found 410.0837.

(Z)-5-chloro-2-(chloromethyl)-N-methyl-N-tosylpent-2-enamide (26)

Prepared according to General Procedure using 2-cyclopropyl-N-methyl-N-tosylacrylamide (84.0 mg, 0.30 mmol, 1 equiv.), magnesium chloride (143 mg, 1.50 mmol, 5 equiv.), acetonitrile (5.25 mL) and acetic acid (0.75 mL). Purification by flash column chromatography (eluent = 5 to 15% EtOAc in hexanes, silica gel) to afford product **26** as a 1:1 mixture of E/Z stereoisomers as a colourless oil (21.1 mg, 20% yield).

$R_f = 0.27$ (eluent = 15% EtOAc in hexanes); $\nu_{\text{max}} / \text{cm}^{-1}$ (thin film) 1685, 1355, 1168, 545; $^1\text{H NMR}$ (500 MHz, CDCl_3) $\delta_{\text{H}} = 7.75\text{--}7.93$ (4H, m), 7.33–7.36 (4H, m), 6.25 (1H, t, J 7.3 Hz), 5.94 (1H, t, J 7.3, 1.1 Hz), 4.34 (2H, s), 4.27 (2H, s), 3.67 (2H, t, J 6.4 Hz), 3.51 (2H, t, J 6.5 Hz), 3.34 (3H, s), 3.22 (3H, s), 2.78 (2H, m), 2.33–2.53 (8H, m); $^{13}\text{C NMR}$ (126 MHz, CDCl_3) $\delta_{\text{C}} = 170.5, 168.3, 145.5, 145.2, 138.2, 135.4, 135.4, 135.2, 134.9, 132.0, 129.9, 129.9, 128.4, 128.3, 53.6, 45.8, 42.8, 42.6, 38.7, 35.1, 34.0, 32.2, 31.3, 21.9, 21.8$; HRMS (ES^+) [$\text{C}_{14}\text{H}_{17}\text{Cl}_2\text{NO}_3\text{S}$] requires $[\text{M}+\text{H}]^+ 350.0385$, found 350.0384.

7.6. X-ray: Z-Chlorinated Product 9 (Electrochemical oxidative Z-selective C(sp²)-H chlorination of acrylamide)

$R_1=7.67\%$

Crystal Data and Experimental

Experimental. Single colourless block crystals of **2020ncs0348z** were supplied.. A suitable crystal with dimensions $0.20 \times 0.10 \times 0.08 \text{ mm}^3$ was selected and mounted on a Rigaku FRE+ equipped with VHF Varimax confocal mirrors and an AFC12 goniometer and HyPix 6000 detector diffractometer. The crystal was kept at a steady $T = 100(2) \text{ K}$ during data collection. The structure was solved with the **ShelXT** (Sheldrick, 2015) solution program using dual methods and by using **Olex2** 1.3 (Dolomanov et al., 2009) as the graphical interface. The model was refined with **ShelXL** 2018/3 (Sheldrick, 2015) using full matrix least squares minimisation on F^2 .

Crystal Data. $\text{C}_{17}\text{H}_{16}\text{ClNO}_3\text{S}$, $M_r = 349.82$, monoclinic, $P2_1/c$ (No. 14), $a = 15.9785(5) \text{ \AA}$, $b = 6.87810(10) \text{ \AA}$, $c = 14.9093(4) \text{ \AA}$, $\beta = 91.666(2)^\circ$, $\alpha = \gamma = 90^\circ$, $V = 1637.87(7) \text{ \AA}^3$, $T = 100(2) \text{ K}$, $Z = 4$, $Z' = 1$, $\mu(\text{Mo K}\alpha) = 0.374$, 20204 reflections measured, 4652 unique ($R_{\text{int}} = 0.0639$) which were used in all calculations. The final wR_2 was 0.1992 (all data) and R_1 was 0.0767 ($I \geq 2 \sigma(I)$).

Structure Quality Indicators

Reflections:

d min (Mo)	0.68	I/ $\sigma(I)$	22.4	R _{int}	6.39%	complete 100% (IUCr)	100%
------------	------	----------------	------	------------------	-------	-------------------------	------

Refinement:

Shift	-0.001	Max Peak	1.2	Min Peak	-0.8	Goof	1.129
-------	--------	----------	-----	----------	------	------	-------

Compound	2020ncs0348z
Formula	C ₁₇ H ₁₆ ClNO ₃ S
$D_{calc.}/\text{g cm}^{-3}$	1.419
μ/mm^{-1}	0.374
Formula Weight	349.82
Colour	colourless
Shape	(cut) block
Size/mm ³	0.20×0.10×0.08
T/K	100(2)
Crystal System	monoclinic
Space Group	$P2_1/c$
$a/\text{\AA}$	15.9785(5)
$b/\text{\AA}$	6.87810(10)
$c/\text{\AA}$	14.9093(4)
$\alpha/^\circ$	90
$\beta/^\circ$	91.666(2)
$\gamma/^\circ$	90
$V/\text{\AA}^3$	1637.87(7)
Z	4
Z'	1
Wavelength/ \AA	0.71073
Radiation type	Mo K α
$\theta_{min}/^\circ$	2.550
$\theta_{max}/^\circ$	31.337
Measured Refl's.	20204
Indep't Refl's	4652
Refl's $I \geq 2 \sigma(I)$	4041
R_{int}	0.0639
Parameters	210
Restraints	0
Largest Peak	1.161
Deepest Hole	-0.806
GooF	1.129
wR_2 (all data)	0.1992
wR_2	0.1922
R_1 (all data)	0.0880
R_1	0.0767

A colourless (cut) block-shaped crystal with dimensions $0.20 \times 0.10 \times 0.08 \text{ mm}^3$ was mounted. Data were collected using a Rigaku FRE+ equipped with VHF Varimax confocal

mirrors and an AFC12 goniometer and HyPix 6000 detector diffractometer equipped with an Oxford Cryosystems low-temperature device operating at $T = 100(2)$ K.

Data were measured using profile data from ω -scans using Mo K_α radiation. The diffraction pattern was indexed and the total number of runs and images was based on the strategy calculation from the program **CrysAlisPro** (Rigaku, V1.171.40.82a, 2020). The maximum resolution that was achieved was $\Theta = 31.337^\circ$ (0.68 Å).

The unit cell was refined using **CrysAlisPro** (Rigaku, V1.171.40.82a, 2020) on 8609 reflections, 43% of the observed reflections.

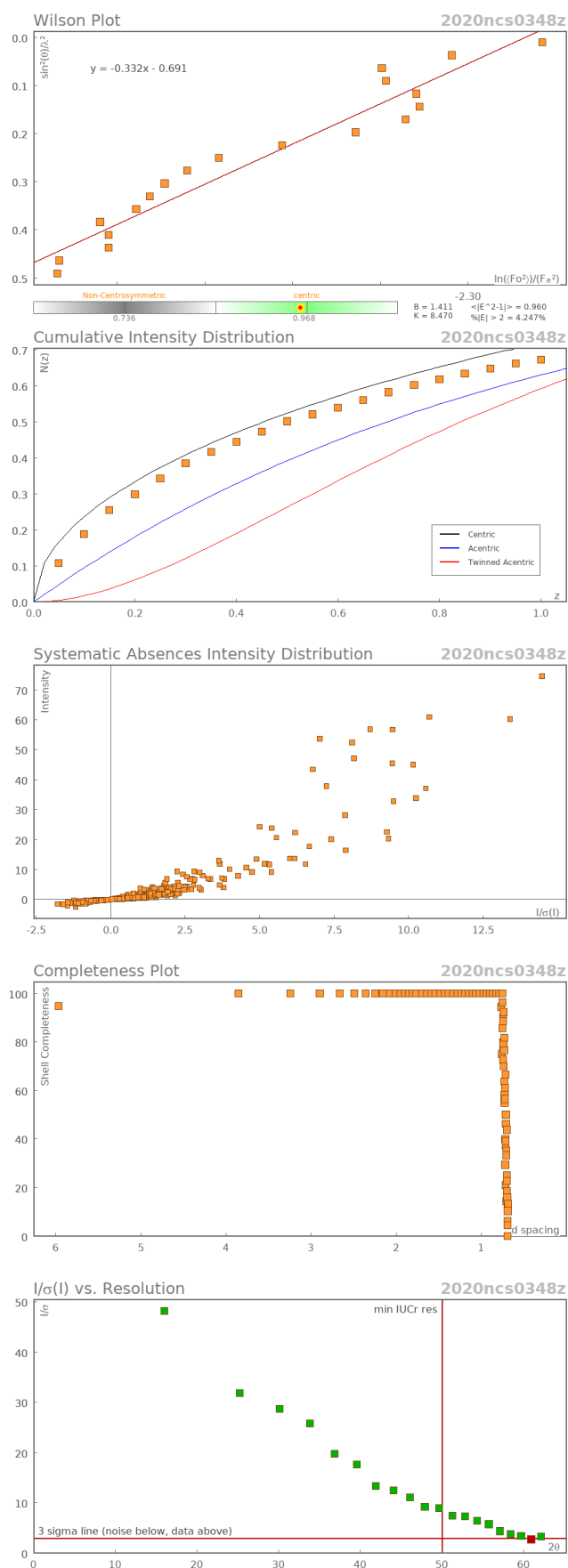
Data reduction, scaling and absorption corrections were performed using **CrysAlisPro** (Rigaku, V1.171.40.82a, 2020). The final completeness is 100.00 % out to 31.337° in Θ . A multi-scan absorption correction was performed using **CrysAlisPro** (Rigaku, V1.171.40.82a, 2020) with empirical absorption correction using spherical harmonics, as implemented in SCALE3 ABSPACK scaling algorithm. The absorption coefficient μ of this material is 0.374 mm^{-1} at this wavelength ($\lambda = 0.71075 \text{ Å}$) and the minimum and maximum transmissions are 0.669 and 1.000.

The structure was solved and the space group $P2_1/c$ (# 14) determined by the **ShelXT** (Sheldrick, 2015) structure solution program using dual methods and refined by full matrix least squares minimisation on F^2 using **ShelXL** 2018/3 (Sheldrick, 2015). All non-hydrogen atoms were refined anisotropically. Hydrogen atom positions were calculated geometrically and refined using the riding model.

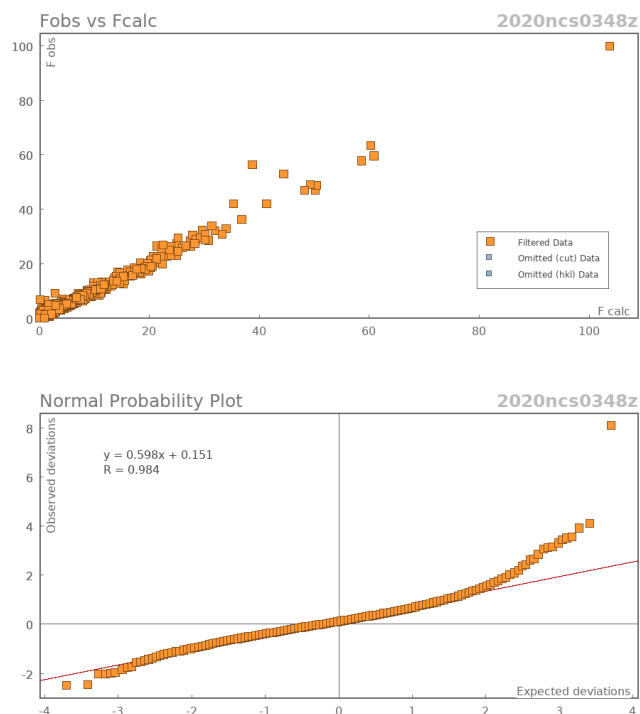
_exptl_absorpt_process_details: **CrysAlisPro** (Rigaku, V1.171.40.82a, 2020) using spherical harmonics as implemented in SCALE3 ABSPACK scaling algorithm.

There is a single molecule in the asymmetric unit, which is represented by the reported sum formula. In other words: Z is 4 and Z' is 1.

Data Plots: Diffraction Data



Data Plots: Refinement and Data



Reflection Statistics

Total reflections (after filtering)	21244	Unique reflections	4652
Completeness	0.869	Mean I/σ	15.17
hkl_{\max} collected	(22, 9, 21)	hkl_{\min} collected	(-22, -9, -20)
hkl_{\max} used	(22, 9, 21)	hkl_{\min} used	(-22, 0, 0)
Lim d_{\max} collected	100.0	Lim d_{\min} collected	0.36
d_{\max} used	10.74	d_{\min} used	0.68
Friedel pairs	5678	Friedel pairs merged	1
Inconsistent equivalents	50	R_{int}	0.0639
R_{sigma}	0.0446	Intensity transformed	0
Omitted reflections	0	Omitted by user (OMIT hkl)	0
Multiplicity	(8316, 4221, 1339, 101, 13)	Maximum multiplicity	12
Removed systematic absences	1040	Filtered off (Shel/OMIT)	0

Table 8: Fractional Atomic Coordinates ($\times 10^4$) and Equivalent Isotropic Displacement Parameters ($\text{\AA}^2 \times 10^3$) for **2020ncs0348z**. U_{eq} is defined as 1/3 of the trace of the orthogonalised U_{ij} .

Atom	x	y	z	U_{eq}
Cl1	5421.6(5)	8166.9(13)	5457.9(6)	35.3(2)
S1	8101.2(4)	7237.7(9)	6422.6(4)	14.72(17)
O1	6673.4(13)	6703(3)	7573.3(13)	21.5(4)
O2	7926.0(13)	9130(3)	6765.5(14)	21.3(4)
O3	8565.3(13)	7031(3)	5618.2(13)	20.2(4)
N1	7166.2(14)	6131(3)	6167.2(15)	14.8(4)
C1	6554.6(17)	6075(4)	6820.6(18)	17.3(5)
C2	5730.3(18)	5148(5)	6553(2)	24.2(6)
C3	5519(2)	3189(6)	7068(2)	37.4(9)
C4	5210(2)	6006(5)	5989(2)	28.0(6)
C5	7126.1(15)	4843(4)	5400.9(17)	13.6(5)
C6	7161.8(17)	2844(4)	5553.9(19)	17.7(5)
C7	7133.1(19)	1590(4)	4824(2)	22.0(6)
C8	7082.0(18)	2312(4)	3954(2)	21.1(6)
C9	7059.3(17)	4309(4)	3807.6(17)	18.4(5)
C10	7073.8(16)	5582(4)	4533.7(17)	15.7(5)
C11	8560.6(16)	5790(4)	7269.7(16)	14.0(5)
C12	8603.3(17)	6452(4)	8150.4(18)	18.0(5)
C13	8922.7(17)	5225(4)	8819.1(18)	19.7(5)
C14	9175.0(17)	3332(4)	8619.6(18)	18.7(5)
C15	9153.7(18)	2720(4)	7722.1(19)	19.3(5)
C16	8850.9(17)	3936(4)	7045.1(18)	17.9(5)
C17	9417(2)	1938(5)	9363(2)	27.1(6)

Table 9: Anisotropic Displacement Parameters ($\times 10^4$) for **2020ncs0348z**. The anisotropic displacement factor exponent takes the form: $-2\pi^2[h^2a^{*2} \times U_{11} + \dots + 2hka^* \times b^* \times U_{12}]$

Atom	U_{11}	U_{22}	U_{33}	U_{23}	U_{13}	U_{12}
Cl1	35.9(5)	30.9(4)	39.1(5)	6.3(3)	-2.4(3)	10.5(3)
S1	19.4(3)	8.5(3)	16.2(3)	1.0(2)	0.4(2)	-2.2(2)
O1	25.7(10)	20.7(10)	18.4(9)	-5.3(8)	4.1(7)	-1.5(8)
O2	31.1(11)	7.1(8)	25.7(10)	-1.0(7)	-3.1(8)	-2.1(7)
O3	23.1(10)	20.2(10)	17.5(9)	3.5(8)	2.4(7)	-4.0(8)
N1	16.5(10)	11.3(9)	16.7(10)	-3.7(8)	1.3(8)	-1.0(8)
C1	18.5(12)	13.5(11)	20.0(12)	-3.0(10)	3.2(9)	-0.7(9)
C2	22.0(14)	27.3(14)	23.7(13)	-9.4(12)	6.0(10)	-4.1(11)
C3	30.4(17)	65(2)	16.8(13)	-4.1(15)	6.7(11)	-35.6(17)
C4	28.7(16)	28.2(15)	27.4(14)	-7.0(13)	5.6(12)	-0.3(12)
C5	16.2(11)	8.8(10)	15.9(11)	-2.5(9)	1.9(9)	0.9(8)
C6	22.1(13)	10.7(11)	20.5(12)	1.9(10)	2.1(10)	-0.1(9)
C7	27.5(14)	8.7(11)	29.9(15)	-2.6(10)	2.6(11)	0.9(10)
C8	22.6(13)	15.7(12)	24.9(13)	-10.1(11)	-0.3(10)	2.2(10)
C9	21.2(13)	18.3(12)	15.6(11)	-3.0(10)	0.4(9)	0.6(10)
C10	18.5(12)	10.1(10)	18.4(12)	-0.4(9)	0.7(9)	0.4(9)
C11	16.5(11)	11.2(10)	14.5(11)	0.4(9)	-0.1(8)	0.2(9)
C12	20.0(13)	15.3(11)	18.7(12)	-3.3(10)	1.5(9)	-1.2(9)
C13	21.4(13)	23.0(13)	14.7(11)	-0.9(10)	0.8(9)	-2.2(10)
C14	17.0(12)	21.2(13)	17.8(12)	3.5(10)	-0.2(9)	-1.9(10)
C15	22.8(13)	13.6(11)	21.4(13)	0.9(10)	-0.4(10)	1.2(10)
C16	23.3(13)	13.2(11)	17.3(11)	-2.8(10)	0.3(9)	0.4(10)
C17	25.0(15)	31.6(16)	24.6(14)	12.0(13)	-1.2(11)	1.7(12)

Table 10: Bond Lengths in Å for **2020ncs0348z**.

Atom	Atom	Length/Å
Cl1	C4	1.722(4)
S1	O2	1.4289(19)
S1	O3	1.435(2)
S1	N1	1.710(2)
S1	C11	1.753(3)
O1	C1	1.212(3)
N1	C1	1.400(3)
N1	C5	1.446(3)
C1	C2	1.507(4)
C2	C3	1.592(5)
C2	C4	1.306(5)
C5	C6	1.394(3)
C5	C10	1.389(3)
C6	C7	1.388(4)
C7	C8	1.389(4)
C8	C9	1.391(4)
C9	C10	1.392(4)
C11	C12	1.389(4)
C11	C16	1.401(3)
C12	C13	1.392(4)
C13	C14	1.397(4)
C14	C15	1.402(4)
C14	C17	1.508(4)
C15	C16	1.387(4)

Table 11: Bond Angles in ° for 2020ncs0348z

Atom	Atom	Atom	Angle/°
O2	S1	O3	120.04(12)
O2	S1	N1	107.83(12)
O2	S1	C11	109.99(12)
O3	S1	N1	103.83(11)
O3	S1	C11	109.26(12)
N1	S1	C11	104.64(11)
C1	N1	S1	118.70(17)
C1	N1	C5	121.1(2)
C5	N1	S1	117.85(17)
O1	C1	N1	122.7(2)
O1	C1	C2	120.5(2)
N1	C1	C2	116.7(2)
C1	C2	C3	115.2(3)
C4	C2	C1	121.0(3)
C4	C2	C3	123.6(3)
C2	C4	C11	123.8(3)
C6	C5	N1	118.3(2)
C10	C5	N1	120.8(2)
C10	C5	C6	120.9(2)
C7	C6	C5	119.0(3)
C6	C7	C8	120.6(2)
C7	C8	C9	120.0(2)
C8	C9	C10	120.0(3)
C5	C10	C9	119.5(2)
C12	C11	S1	120.2(2)
C12	C11	C16	121.1(2)
C16	C11	S1	118.66(19)
C11	C12	C13	119.0(2)
C12	C13	C14	121.0(2)
C13	C14	C15	118.9(2)
C13	C14	C17	120.4(3)
C15	C14	C17	120.6(3)
C16	C15	C14	120.8(3)
C15	C16	C11	119.1(2)

Table 12: Torsion Angles in ° for 2020ncs0348z.

Atom	Atom	Atom	Atom	Angle/°
S1	N1	C1	O1	-3.3(4)
S1	N1	C1	C2	177.9(2)
S1	N1	C5	C6	101.1(2)
S1	N1	C5	C10	-77.4(3)
S1	C11	C12	C13	176.0(2)
S1	C11	C16	C15	-174.9(2)
O1	C1	C2	C3	-64.8(4)
O1	C1	C2	C4	110.0(3)
O2	S1	N1	C1	-51.6(2)
O2	S1	N1	C5	145.45(18)
O2	S1	C11	C12	8.3(3)
O2	S1	C11	C16	-174.1(2)
O3	S1	N1	C1	-180.0(2)
O3	S1	N1	C5	17.1(2)
O3	S1	C11	C12	142.1(2)
O3	S1	C11	C16	-40.4(2)
N1	S1	C11	C12	-107.2(2)
N1	S1	C11	C16	70.3(2)
N1	C1	C2	C3	114.1(3)
N1	C1	C2	C4	-71.1(4)
N1	C5	C6	C7	-179.3(2)
N1	C5	C10	C9	178.2(2)
C1	N1	C5	C6	-61.4(3)
C1	N1	C5	C10	120.1(3)
C1	C2	C4	Cl1	3.4(4)
C3	C2	C4	Cl1	177.8(2)
C5	N1	C1	O1	159.0(3)
C5	N1	C1	C2	-19.7(4)
C5	C6	C7	C8	0.9(4)
C6	C5	C10	C9	-0.2(4)
C6	C7	C8	C9	0.0(4)
C7	C8	C9	C10	-1.1(4)
C8	C9	C10	C5	1.1(4)
C10	C5	C6	C7	-0.9(4)
C11	S1	N1	C1	65.5(2)
C11	S1	N1	C5	-97.5(2)
C11	C12	C13	C14	-1.9(4)
C12	C11	C16	C15	2.6(4)
C12	C13	C14	C15	4.2(4)
C12	C13	C14	C17	-172.3(3)
C13	C14	C15	C16	-3.0(4)
C14	C15	C16	C11	-0.3(4)
C16	C11	C12	C13	-1.5(4)
C17	C14	C15	C16	173.4(3)

Table 13: Hydrogen Fractional Atomic Coordinates ($\times 10^4$) and Equivalent Isotropic Displacement Parameters ($\text{\AA}^2 \times 10^3$) for **2020ncs0348z**. U_{eq} is defined as 1/3 of the trace of the orthogonalised U_{ij} .

Atom	x	y	z	U_{eq}
H3A	5899.02	2156.88	6880.06	56
H3B	4939.67	2808.18	6925.44	56
H3C	5589.59	3395.77	7716.35	56
H4	4684.25	5403.44	5864.38	34
H6	7205.13	2348.84	6148.24	21
H7	7148.6	225.05	4920.76	26
H8	7062.54	1441.73	3458.85	25
H9	7033.82	4803.34	3212.57	22
H10	7048.2	6945.72	4436.93	19
H12	8417.17	7722.84	8293.95	22
H13	8969.91	5681.13	9419.86	24
H15	9349.11	1458.1	7576.06	23
H16	8840.42	3516.84	6437.65	22
H17A	8915.3	1274.99	9570.52	41
H17B	9681.24	2657.46	9862.93	41
H17C	9811.59	974.52	9139.08	41

Citations

CrysAlisPro Software System, v.1.171.40.82a, Rigaku Oxford Diffraction, (2020).

O.V. Dolomanov and L.J. Bourhis and R.J. Gildea and J.A.K. Howard and H. Puschmann, Olex2: A complete structure solution, refinement and analysis program, *J. Appl. Cryst.*, (2009), **42**, 339-341.

Sheldrick, G.M., Crystal structure refinement with ShelXL, *Acta Cryst.*, (2015), **C27**, 3-8.

Sheldrick, G.M., ShelXT-Integrated space-group and crystal-structure determination, *Acta Cryst.*, (2015), **A71**, 3-8

7.7. References

- 1 M. Zhang, X. Ding, A. Lu, J. Kang, Y. Gao, Z. Wang, H. Li and Q. Wang, *Org. Chem. Front.*, 2021, **8**, 961–967.
- 2 J. Barluenga, F. J. Fañanás, R. Sanz, C. Marcos and J. M. Ignacio, *Chem. Commun.*, 2005, 933–935.

